

N-Heterocyclic Bisphosphine Ligands For Use In Nickel-Catalyzed
C(*sp*²)-N Cross-Coupling

by

Alexandre V. Gatien

Submitted in partial fulfilment of the requirements
for the degree of Master of Science

at

Dalhousie University
Halifax, Nova Scotia
June 2018

© Copyright by Alexandre V. Gatien, 2018

Table of Contents

List of Figures	v
List of Schemes	vi
Abstract	vii
List of Abbreviations and Symbols Used	viii
Acknowledgements	x
Chapter 1 - Introduction	1
1.1 Introduction to Catalysis	1
1.1.1 Overview	1
1.2 Concepts in Ligand Design	1
1.3 Evolution of Transition Metal-Catalyzed C(<i>sp</i> ²)-N Cross-Coupling	2
1.3.1 Development of Buchwald-Hartwig Amination	3
1.3.2 Mechanistic Considerations	4
1.3.3 Premier Ligands for BHA	6
1.3.4 Development of Nickel-Catalyzed C(<i>sp</i> ²)-N Cross-Coupling	7
1.3.5 Mechanistic Considerations for Nickel-Catalyzed C(<i>sp</i> ²)-N Cross-Coupling	7
1.3.6 Highly Effective Ligands for Nickel-Catalyzed C(<i>sp</i> ²)-N Cross-Coupling	8
1.4 A New Approach to Ligand Design for Nickel-Catalyzed Aminations	9
1.5 Overview of Thesis Work	11
Chapter 2 - Application of NHP-Based Bisphosphines in Nickel-Catalyzed C(<i>sp</i> ²)-N Cross-Couplings	13
2.1 Contributions	13
2.2 Introduction	13
2.3 Results and Discussion	15
2.3.1 Ligand Synthesis and Characterization	15
2.3.2 Screening of Ligands L1-L6 in Nickel-Catalyzed C(<i>sp</i> ²)-N Cross-Couplings	16
2.3.3 Nickel Coordination Chemistry	18
2.3.3.1 Coordination Chemistry of Nickel Dichlorides	18
2.3.3.2 Coordination Chemistry of Nickel Pre-catalysts	20
2.3.4 Scope of Reactivity Employing Precatalyst C1	22

2.3.4.1 Challenging Substrates Employing Precatalyst C1	24
2.3.4.2 Electrophile Selectivity Employing Precatalyst C1	26
2.3.5 Comparison of Different L2 and L7 Containing Nickel Precatalyst Systems	27
2.3.6 Computational Comparison of NHP-DalPhos (L2) and PAd-DalPhos (L7)	28
2.3.7 Experimental Investigation into the Reactivity of C3	30
2.3.8 Computational Investigation into the Reactivity of C3	33
2.3.9 Conclusions	34
2.4 Experimental Section	35
2.4.1 General Considerations	35
Chapter 3 - Development of 1,1-Bisdiazaphosphenyl Ferrocene Ligands for Nickel-Catalyzed C(<i>sp</i> ²)-N Cross-Couplings	46
3.1 Contributions	46
3.2 Introduction	46
3.2 Results and Discussion	47
3.2.1 Ligand Synthesis	47
3.2.2 Solid State Structures of Ligands	49
3.3 Conclusions	49
3.4 Experimental Section	50
3.4.1 General Considerations	50
Chapter 4 – Conclusions and Future Work	52
4.1 General Conclusions	52
4.2 Future Work	52
4.2.2 Chapter 2	52
4.2.3 Chapter 3	53
References	55
Appendix A – Supplementary Information	1
Catalytic Screening Results	1
Characterization of Cross-Coupling Products	5
Computational Data	11
Appendix References	73
Crystallographic Solutions and Refinement Details	74

NMR Spectra	87
Appendix B	132
Copyright Permission.....	132

List of Figures

Figure 1: Blockbuster pharmaceuticals which can be made utilizing BHA methods.....	3
Figure 2: Premier ligands for palladium-catalyzed C-N cross-coupling reactions.....	6
Figure 3: Premier ligands for nickel-catalyzed C(<i>sp</i> ²)-N cross-coupling reactions	9
Figure 4: Previously reported bidentate NHP-type ancillary ligands	14
Figure 5: Crystallographically determined structures of L1 , L2 , and L4	16
Figure 6: Single-crystal X-ray structures of (L2)NiCl ₂ and C1	20
Figure 7: Single-crystal X-ray structures of C2 and C3	22
Figure 8: ³¹ P{ ¹ H} NMR data for the stoichiometric experiments on the activation of C3 employing toluene and 1 equivalent of COD.	32
Figure 9: ³¹ P{ ¹ H} NMR data for the stoichiometric experiments on the activation of C3 employing d ₈ -toluene and no COD.	32
Figure 10: Previously reported ferrocene containing ancillary ligands	47
Figure 11: Single-crystal X-ray structures of L9 and L10	49

List of Schemes

Scheme 1: General catalytic cycle for palladium-catalyzed C(<i>sp</i> ²)-N cross-coupling reaction.....	5
Scheme 2: Synthesis of the NHP-bisphosphines L1-L6	15
Scheme 3: Screening of ligands in nickel-catalyzed C(<i>sp</i> ²)-N cross-couplings.....	17
Scheme 4: Nickel coordination complexes derived from L2	19
Scheme 5: Substrate scope for the cross-coupling of primary alkylamines and (hetero)aryl halides employing C1 as a pre-catalyst	23
Scheme 6: Small nucleophilic amine substrates employing C1 as a catalyst	24
Scheme 7: Bulky primary amine substrates employing C1 as a catalyst	25
Scheme 8: Primary amide substrates employing C1 as a catalyst.	26
Scheme 9: (Pseudo)halide competition study employing C1	27
Scheme 10: DFT study comparing (L2/L7)Ni species	30
Scheme 11: Activation of C3	34
Scheme 12: Synthesis of L9 and L10 via lithiation of ferrocene.....	48
Scheme 13: Synthesis of L10 via P-cyclopentadienyl-substituted route	48

Abstract

Notwithstanding the utility of Buchwald-Hartwig Amination (BHA) technology, the cost and scarcity of palladium has prompted a move to base metal catalysis in recent years. Nickel has emerged as a prime candidate in this chemistry to compete with palladium, being both cheap and abundant. Amination chemistry with nickel is relatively unexplored, and the distinct electronic properties of nickel offer reactivity benefits over palladium when employing challenging phenol derived electrophiles. While ligand design requirements for BHA chemistry are well-understood, structure-reactivity trends for nickel counterparts are ill-defined, with few ligands capable of promoting these nickel-catalyzed cross-couplings. Following the establishment of PAd-DalPhos as the state-of-the-art ligand in challenging nickel-catalyzed amination reactions, we sought to build on this *ortho* phenylene bridged motif and explore new architectures encompassing a bulky, modestly electron-donating bisphosphine framework which would favour reductive elimination, the presumed rate-limiting step in the catalytic cycle.

My thesis work aims to explore the incorporation of N-heterocyclic phosphine fragments into bisphosphine ligand frameworks for application in nickel-catalyzed C(*sp*²)-N cross-coupling reactions. Notably, this thesis reports on the synthesis and catalytic application of a new family of *ortho*-phenylene bridged bisphosphine ancillary ligands featuring a sterically demanding NHP donor fragment paired with an adjacent PR₂ donor group (R = alkyl or aryl), whereby the incorporation of phosphorus into either a saturated or unsaturated heterocyclic ring serves as a means of modulating the donicity of the NHP fragment. Screening the new ligands in representative nickel-catalyzed C(*sp*²)-N cross-coupling test reactions allowed for the identification of one variant, featuring a saturated NHP structure and an adjacent diphenylphosphino donor group (i.e., NHP-DalPhos), as being particularly effective in transformations of primary alkylamines. Application of the derived pre-catalyst (NHP-DalPhos)NiCl(*o*-tolyl) enabled the typically challenging monoarylation of structurally diverse primary alkylamines with (hetero)aryl chlorides or bromides at room temperature. Within this thesis is also reported the synthesis and characterization of two 1,1-bisdiazaphospholenyl ferrocene ligands, featuring the privileged ferrocene backbone, for application in the nickel-catalyzed amination of secondary amines and challenging N-heterocyclic nucleophiles.

List of Abbreviations and Symbols Used

α alpha position – first carbon adjacent to a carbonyl group in this thesis

β beta position – second carbon adjacent to a carbonyl group in this thesis

δ chemical shift

η hapticity - eta (contiguous donor atoms)

1-Ad 1-adamantyl

Å angstrom

Ar aryl

BHA Buchwald-Hartwig amination

BINAP 2,2'-bis(diphenylphosphino)-1,1'-binaphthalene

COD 1,5-cyclooctadiene

Cy cyclohexyl

cat. catalytic or catalyst

d doublet

DCM dichloromethane

DFT density functional theory

DME dimethoxyethane

DPPF 1,1'-ferrocenediyl-bis(diphenylphosphine)

Equiv equivalent

ESI electrospray ionization

GC gas chromatography

GP General Procedure

h hour(s)

HRMS high-resolution mass spectrometry

Hz hertz

IN intermediate

$J_{XX'}$ coupling constant between atom X and atom X'

L ligand

M mega or mol/L or molecular ion

m multiplet

Mes mesityl
NHC N-heterocyclic carbene
NHP N-heterocyclic phosphine
NMR nuclear magnetic resonance
O.A. oxidative addition
o-tol *ortho* tolyl
Ph phenyl
PhBPin phenylboronic acid pinacol ester
PTFE poly(tetrafluoroethylene)
q quartet
R.E. reductive elimination
rt room temperature
s singlet
t triplet
THF tetrahydrofuran
TLC thin layer chromatography
TMEDA tetramethylethylenediamine
TS transition state
X halide substituent or anionic ligand

Acknowledgements

I would like to express my deepest gratitude to my graduate supervisors, Dr. Mark Stradiotto and Dr. Alex Speed, who have been invaluable resources to me throughout my studies, providing wisdom, supportive insight, and perspective on both life and chemistry. I would also like to thank past and present Stradiotto group members Preston MacQueen, Nicholas Rotta-Loria, Ryan Sawatzky, Chris Lavoie, Joseph Tassone, Jillian Clark and Ryan McGuire for their advice, input and comradery. As well, I would like to thank my summer student Raymond Bennett who contributed to the substrate screen of Chapter 2 and who allowed me to develop my teaching and mentoring skills. I am grateful to have had the opportunity to work with such a cohesive and enjoyable group of people mentioned above.

I would like to thank Dr. Mike Lumsden (NMR3) for assistance in setting up and interpreting NMR experiments, Mr. Xiao Feng for his expertise in collecting mass-spectrometry data, and Dr. Robert McDonald and Dr. Michael Ferguson (University of Alberta) for their high-quality X-ray crystallographic analysis, all of whom have contributed to the work reported herein. I would also like to thank my thesis committee member, Dr. Laura Turculet, for her advice and guidance of my thesis progress. The Natural Sciences and Engineering Council (NSERC) of Canada, the Chemistry Graduate Student Society (CGSS), the Department of Chemistry, and Dalhousie University are thanked for providing funding.

I would like to thank my partner Ainsley Lofstedt for her support and patience during the more stressful and challenging periods of my graduate studies, as well as my family and friends for their love and support over the past two years.

Chapter 1 - Introduction

1.1 Introduction to Catalysis

1.1.1 Overview

Transition metal-catalyzed cross-coupling reactions are ubiquitous in modern synthetic chemistry, enabling the assembly of complex molecular structures from easily procured starting materials.¹ The activity of a metal catalyst is greatly influenced by its coordination sphere. In the majority of cases, the success of such metal catalysts hinges on the identification of an appropriate supporting ancillary ligand, an organic or main-group molecule which binds to the metal and alters the coordination sphere. When bound to a reactive metal of interest, the ancillary ligand can engender desired catalytic properties (e.g., activity, selectivity, *etc.*).² Ancillary ligands help to control the steric and electronic properties of a metal complex and therefore its reactivity. Hence, the establishment of new ligands has enabled once challenging or inconceivable transformations, opening doors to alternative synthetic pathways with far-reaching applications in pharmaceutical, agrochemical and material sciences.³ For example, the industrial synthesis of the Parkinson's drug L-DOPA was enabled through the use of chiral DIPAMP phosphine ligands allowing for the key rhodium-catalyzed enantioselective hydrogenation step to be achieved.⁴ Indeed, the importance of transition metal-catalyzed cross-coupling reactions was highlighted in the 2010 Nobel Prize to Richard F. Heck, Akira Suzuki, Ei-ichi Negishi for the development of palladium-catalyzed methodologies for carbon-carbon bond formation.

1.2 Concepts in Ligand Design

A key parameter for controlling the metal coordination sphere is steric bulk. The size of a ligand has an impact on metal complex stability as well as reactivity. Ligands with appropriate steric hindrance can, for example, prevent unwanted dimerization of reactive low-coordinate intermediates, as well as increase selectivity by limiting access to the active metal site to specific substrates or geometric orientations.⁵ The importance of steric bulk is also well-established in cross-coupling reactions, whereby ligands with large steric encumbrance can aid in reductive elimination (R.E.), regenerating the active catalyst and turning over product.⁶ The most common methods for quantification of ligand steric parameters are ligand cone angles, whereby the angle between ligand substituents protruding from the metal at a fixed metal-donor atom length is determined. This metric provides a useful means of comparing the steric effect of substituents on

tertiary phosphine ligands.⁷ As well, percent buried volume ($\%V_{\text{bur}}$), where the percent volume of a sphere of fixed radius occupied by the ligand is determined, offers an alternative description of the steric environment for non-conical ligands, such as *N*-heterocyclic carbene (NHC) ligands or Buchwald biaryl phosphines.⁸ Related to the notion of steric bulk is that of ligand bite angle, the angle between two donor atoms and the metal center. In a bidentate ligand, the backbone steric and geometric constraints may prevent binding at an ideal angle of 90° , which can have an impact on reactivity. For example, the larger than anticipated bite angle of XantPhos enables enhanced reactivity in Rh-catalyzed hydroformylation reactions.⁹

Ligands can also influence the electronic properties of a metal by interacting with metal *d*-orbitals of appropriate symmetry and changing the electron density at the metal centre. For example, donation of electron density from a filled ligand orbital to an empty metal *d*-orbital to form a metal-ligand σ -bond will increase the electron density at the metal centre, thereby leading to more nucleophilic characteristics. Conversely, ligands with empty *p*-orbitals or π^* orbitals can also accept electron density from a filled metal *d*-orbital of appropriate symmetry. This donation of electron density from metal to ligand orbitals, or π backbonding, leads to an increase in electrophilic character at the metal centre. The relative electronic effects of a ligand can be determined by comparing bond lengths in crystallographic data of structurally related complexes, as backbonding lengthens the bond *trans* to the metal-ligand bond. As well, the CO stretching frequency of metal carbonyl complexes of type $L_nM(\text{CO})_m$, determined experimentally or computationally, can be used to quantify ligand electronic properties, and is referred to as the Tolman Electronic Parameter (TEP).⁷

Evidently, an appropriate balance of steric and electronic parameters is required to obtain desired catalytic reactivity from a transition metal complexes. This challenge lies at the core of ligand design in transition metal-mediated cross-coupling reactions. Of particular relevance to this thesis is the evolution of ligands for palladium catalyzed $C(sp^2)$ -N cross-coupling reactions, known as the Buchwald-Hartwig Amination (BHA).

1.3 Evolution of Transition Metal-Catalyzed $C(sp^2)$ -N Cross-Coupling

The synthetic power of BHA technology lies in the ability to form arylamine $C(sp^2)$ -N bonds from widely available and inexpensive aryl (pseudo)halides and a broad range of nitrogen nucleophiles under mild conditions (e.g. room temperature, low catalyst loadings, *etc.*). Such protocols have found widespread academic and industrial applications in the development of

pharmaceuticals, materials and natural products.^{3, 5, 10} Traditional methods for the synthesis of arylamine C(*sp*²)-N bonds involved the nitration of arenes followed by reduction of the corresponding nitroarene to form the desired aniline, typically occurring under highly acidic conditions and thus severely limiting the substrate scope.¹¹ Copper was the first transition metal used at the turn of the 20th century to catalyze C(*sp*²)-N bond formation and has a well-established history in C(*sp*²)-N cross-coupling chemistry, however the requirement of elevated reaction temperatures, in combination with relatively activated (hetero)aryl electrophiles (commonly bromides and iodides), can render such protocols less desirable relative to BHA.¹²

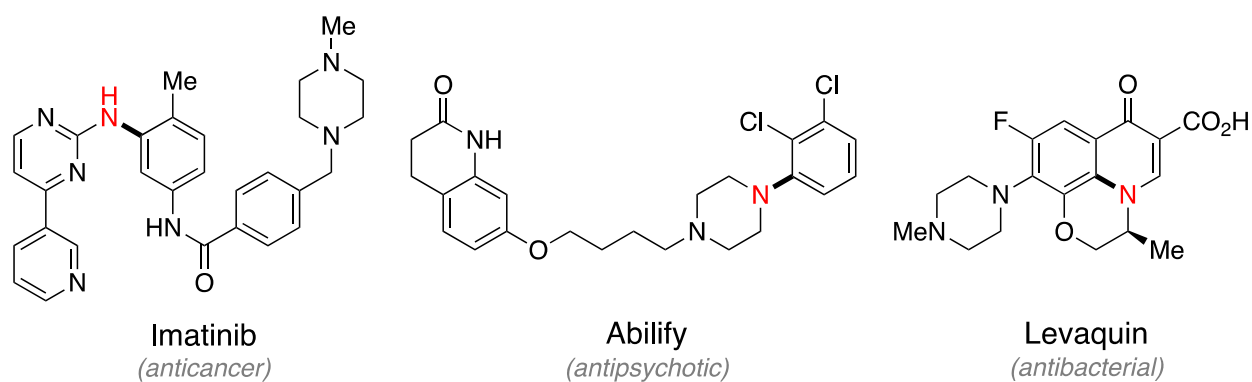


Figure 1: Selection of blockbuster pharmaceuticals which can be made utilizing BHA methods.¹³

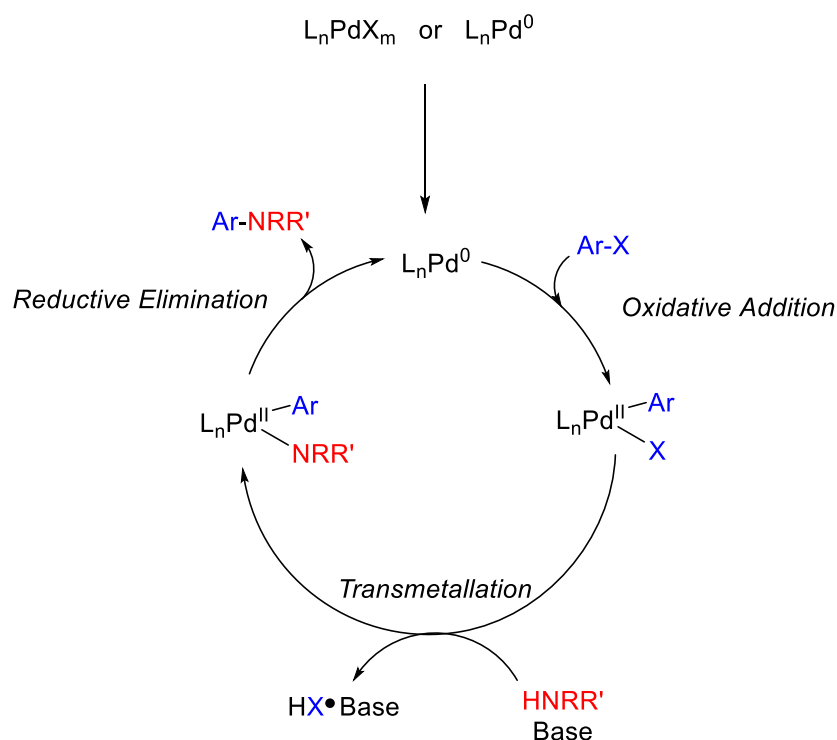
1.3.1 Development of Buchwald-Hartwig Amination

Initial developments in modern palladium catalyzed C(*sp*²)-N cross-coupling reactions began in 1995 with independent reports from the Buchwald and Hartwig groups on the coupling of aryl bromides and secondary dialkyl and arylalkyl amines using P(*o*-tol)₃ and other bulky triarylmonophosphines.¹⁴ Shortly thereafter, both groups independently reported the application of chelating bisphosphine ligands, DPPF and *rac*-BINAP, for use in second-generation catalysts for this chemistry, allowing a significant decrease in catalyst loadings and the ability to couple a small scope of primary alkylamines.¹⁵ Chelating bisphosphine ligands offer enhanced stability compared to their monophosphine counterparts, referred to as the chelate effect, and can enforce a *cis* geometry at the metal center, favouring productive elementary catalytic steps. Continued development of ligands for BHA led to the third generation of ligands, hindered monodentate phosphines, such as P(*t*-Bu)₃¹⁶ and biaryl dialkylphosphines,^{5, 17} and *N*-heterocyclic carbenes (NHCs),¹⁸ in which the steric bulk prevents unwanted side-reactions and whose electron-rich donor

atoms facilitate the oxidative addition of unactivated aryl electrophiles. This allowed for coupling of cheaper and more abundant aryl chlorides (*cf.* aryl bromides, iodides) as well as the use of milder conditions (e.g. room temperature, < 1 mol% loadings). Further advances in ligand design led to bulky and electron-donating species which aimed to stabilize the active low-coordinate palladium centre through a second donor atom,¹⁹ by blocking reactive sites with extreme steric bulk,²⁰ or through interaction of the metal centre with the ligand arene backbone.²¹ This latest fourth generation of ancillary ligands combines the chelation benefits of the second generation ligands with the steric bulk and strong σ -donation abilities of the encumbered alkylphosphine ligands of the third generation,²² allowing for the broadest scope of electrophilic and nucleophilic partners to date under the mildest conditions thus far. These ligands include variants of the JosiPhos family,²²⁻²³ Buchwald biarylmonophosphines,^{3,5} Mor-DalPhos¹⁰ and BippyPhos^{20,24} (for ligand-specific reactions, *vide infra*).

1.3.2 Mechanistic Considerations

Throughout the course of ligand development for BHA, mechanistic insights into the catalytic cycle have guided improvements in ligand design, allowing for new and ever more challenging transformations to be accomplished. Though the exact nature of elementary steps and their order can vary somewhat depending on the substrates and conditions involved, a general mechanistic picture has emerged involving a Pd(0)/Pd(II) cycle, as outlined in **Scheme 1**.^{14a} Following the generation of a ligand-bound Pd(0) species, oxidative addition of the aryl halide substrate occurs, cleaving the carbon-halogen bond and generating a Pd(II) oxidative addition intermediate. A combination of amine binding and dehydrohalogenation by base affords a palladium (aryl)amido intermediate. From this intermediate, reductive elimination of the aryl and amido ligands leads to the formation of the C(sp^2)-N bond and regenerates the ligand bound Pd(0) species.



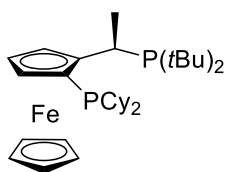
Scheme 1: General catalytic cycle for palladium-catalyzed C(sp^2)-N cross-coupling reaction

The ligands used in these transformations have a direct impact on the reaction. Mechanistic studies have established that the rate-limiting step in BHA chemistry is often the oxidative addition of the aryl (pseudo)halide bond, especially in the case of aryl chlorides.²⁵ As such, electron-rich ligands, which enhance the electron density at the metal centre and increase the propensity for backbonding into the σ^*_{C-X} orbital, make the cleavage of the carbon-halide bond more facile. Indeed, the more electron-rich alkylphosphine and NHC ligands have found the most success in this chemistry.²² As well, steric bulk helps prevent unwanted side reactions, such as dimerization, in low-coordinate Pd^0 species and has the additional benefit of promoting reductive elimination by pushing the aryl and amide ligands closer together.^{3, 5} It is worth noting that the electronic requirements for oxidative addition and reductive elimination are orthogonal; ligands can only be designed to favour one process or the other. Due to the rate-limiting oxidative addition (O.A.) step in BHA, electron-rich and sterically encumbered ligands have had the most success, which is clearly highlighted in the newest generation of ligands.

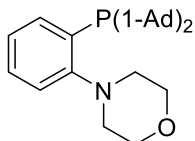
1.3.3 Premier Ligands for BHA

The current state-of-the-art ligands for palladium catalyzed C(*sp*²)-N cross-coupling reactions all incorporate steric bulk and electron rich alkylphosphine donor atoms. A selection of these are shown below in **Figure 2**. The JosiPhos ligand family, initially developed for enantioselective hydrogenations, has found widespread applicability in numerous cross-coupling reactions.^{22, 26} Notably, the CyPF-*t*Bu variant has been used successfully as a fourth generation ligand for palladium catalyzed C(*sp*²)-N cross-couplings, enabling the monoarylation of ammonia in 2006,²⁷ a challenging and highly desirable transformation, as well as the monoarylation of hydrazones, and a broad range of primary and secondary amines with < 50 ppm catalyst loadings in certain instances.²² Another highly successful bisphosphine ligand for this chemistry has been Mor-DalPhos, an electronic intermediate between the well-established JosiPhos and Buchwald monophosphine ligand families. Along with the monoarylation of ammonia and hydrazine, this ligand has enabled challenging oxidative additions, permitting the use of aryl tosylates electrophiles, and facilitates room temperature reactivity.^{10, 19} The highly modular bulky biaryl monophosphines developed by Buchwald make up an important segment of ligands developed for BHA. Varying the backbone has allowed for reaction-specific ligand tailoring. For example, the larger steric bulk of AdBrettPhos over BrettPhos allows for the monoarylation of ammonia, and can accommodate the coupling of weakly nucleophilic amides.^{3, 28} BippyPhos shares similar characteristics to the Buchwald ligand class and has been touted as an excellent ligand with general applicability in BHA. Indeed, its broad nucleophile scope includes monoarylation of ammonia and hydrazine, a range of primary and secondary amines, amides and derived sulfonamides, as well as the medicinally relevant indole motif.²⁰

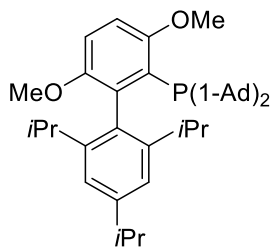
JosiPhos (CyPF-*t*Bu)



Mor-DalPhos



AdBrettPhos



BippyPhos

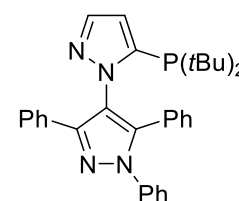


Figure 2: Selection of premier ligands for palladium-catalyzed C-N cross-coupling reactions

1.3.4 Development of Nickel-Catalyzed C(sp²)-N Cross-Coupling

Notwithstanding the utility of BHA, the relative scarcity and high cost of precious metals, including palladium, provides motivation for the development of alternative protocols employing base metal catalysis.²⁹ From an industrial perspective, the challenges in obtaining bulk quantities of palladium provide further incentive for transitioning towards base metals. Though copper is well-established in C(sp²)-N cross-couplings (*vide supra*), limitations with respect to scope (e.g. aryl chlorides are typically ineffective) and harsh conditions make this a less attractive route relative to BHA. Conversely, nickel catalysis has emerged as a competitive alternative to palladium-based methods,^{26, 30} being significantly more abundant and less expensive than palladium. In addition, the enhanced propensity of nickel to engage in C(sp²)-X bond oxidative additions in typically less reactive (hetero)aryl chlorides³¹ or related phenol-derived electrophiles³² makes nickel particularly well-suited to supplant palladium in C(sp²)-N cross-coupling applications, given the rate-limiting nature of oxidative additions in palladium cross-couplings. Nickel also has an established track-record in other cross-coupling reactions, such as Negishi,³³ Kumada,³⁴ Mizoroki-Heck,^{26, 35} photoredox cross-couplings³⁶ as well as shuttle catalysis.³⁷

The use of nickel catalysis in amination reactions had its debut in the 1950s, whereby the coupling of methylamine and chlorobenzene was examined briefly.³⁸ The investigation of various nickel sources for amination reactions remained a relatively quiet field until the emergence of palladium aminations around the turn of the 21st century. In 1997 Wolfe and Buchwald reported the use of DPPF or 1,10-phenanthroline along with Ni(cod)₂ to couple aryl chlorides with primary and secondary amines at elevated temperatures.³⁹ Air-stable pre-catalyst variants were made, allowing for convenient *in situ* generation of the active metal species. This seminal work set the stage for modern developments in nickel catalyzed C(sp²)-N cross-coupling reactions, with a range of bisphosphine and NHC ligands allowing for mild reaction conditions, low catalyst loadings and challenging electrophiles such as electron-rich aryl chlorides and phenol derivatives to be successfully applied in cross-coupling reactions, competing with and in many cases surpassing the abilities of analogous palladium based catalyst systems.^{26, 40}

1.3.5 Mechanistic Considerations for Nickel-Catalyzed C(sp²)-N Cross-Coupling

As with the development of BHA, mechanistic studies for nickel-catalyzed amination initially lagged behind empirical advances in ligand application. A 2014 study by Hartwig on the

amination of aryl chlorides using a (BINAP)Ni(η^2 -NCPH) complex found that a similar mechanism to that invoked for BHA (**Scheme 1**) was operational, supporting a Ni(0)/Ni(II) catalytic cycle.⁴¹ Kinetic experiments with activated aryl chlorides and alkylamines led to the conclusion that the oxidative addition step was rate limiting in this system. The lack of observed cyclized product using a radical clock experiment in a similar (JosiPhos)Ni(η^2 -NCPH) species was used to discount the possibility for a Ni(I)/Ni(III) cycle.⁴² Conversely, a 2015 mechanism study by Stewart on a related (BINAP)Ni[P(OPh)₃]₂ complex for C(sp^2)-N cross-coupling of aryl halides and primary alkylamines found O.A. to be rapid and either transmetallation or R.E. to be the rate-limiting-step.⁴³ A more recent study by Nicasio on the amination of chloropyridines and indoles using the NHC precatalyst (IPr)Ni(η^6 -toluene) concluded that reductive elimination was rate-limiting in their system,⁴⁴ highlighting the challenges in mechanism determination where changes in substrate and ligand can have a significant impact. Furthermore, the propensity for nickel to mediate single electron redox chemistry cannot be neglected, and there is growing evidence for parallel Ni(I)/Ni(III) cycle involving a rate-limiting oxidative addition step.⁴⁵ Currently, the broadly accepted predominant mechanism is a Ni(0)/Ni(II) catalytic cycle similar to the BHA mechanism, with reductive elimination being the rate limiting step in the majority of studied cases.^{26, 34, 40, 46}

1.3.6 Highly Effective Ligands for Nickel-Catalyzed C(sp^2)-N Cross-Coupling

Though the mechanism of nickel and palladium catalyzed C(sp^2)-N cross-coupling reactions differ in certain respects, little effort has been put into designing ligands tailored to nickel catalysis. Indeed, the general research method for nickel catalyzed C(sp^2)-N cross-couplings has been to repurpose ligands designed for analogous palladium chemistry, with inconsistent results. This is in part due to the smaller atomic radius and higher electropositive nature of nickel versus palladium.^{26, 30} Currently, bisphosphines such as DPPF^{39, 47} and JosiPhos CyPF-Cy^{32, 46, 47b} as well as the NHC IPr^{40c, 48} represent top-tier ligands in nickel-catalyzed transformations (**Figure 3**). DPPF was used in the 1997 seminal report on nickel-catalyzed C(sp^2)-N cross-coupling by Wolfe and Buchwald, allowing for the coupling of aryl chlorides with secondary alkylarylamines and alkylamines.³⁹ Since then, DPPF has become a premier ligand for use with secondary cyclic and acyclic alkylamines as well as N-H containing heterocycles such as indole,^{47c} a sought after substrate for its biological activity.⁴⁹ The electrophile scope has also since been expanded to allow for the use of sulfamates, mesylates and triflates.^{47a} The JosiPhos variant CyPF-Cy was used in the first monoarylation of ammonia with nickel in 2015,⁴⁶ and can be used to couple a broad range of

primary alkylamines, including heterocyclic variants, at ambient temperatures.^{46, 47b} Phenol-derived carboxylate electrophiles such as sulfamates, carbamates and pivalates are also accommodated, increasing the versatility of this catalyst system.³² NHC ligands were first used in nickel amination reactions in 2001, with SIPr enabling the cross-coupling of aryl chlorides with secondary alkyl and arylamines as well as anilines at elevated temperatures.⁵⁰ Since then, the substrate scope has been expanded to include ammonia surrogates, cyclic and acyclic amines, medicinally relevant *N*-heterocyclic motifs such as indole, as well as various pseudohalide electrophiles with the IPr^{40c, 48, 51} ligand framework. The use of π -allyl complexes as pre-catalysts have since allowed for room temperature reactivity using NHCs.^{51c}

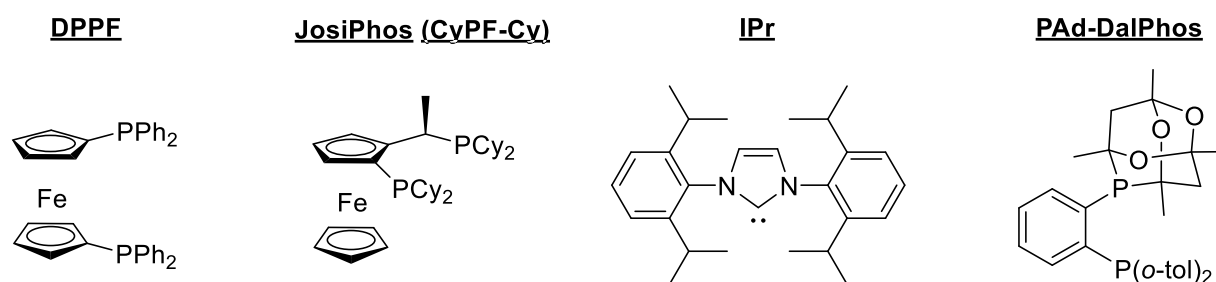


Figure 3: Premier ligands for nickel-catalyzed C(sp²)-N cross-coupling reactions

1.4 A New Approach to Ligand Design for Nickel-Catalyzed Aminations

Despite the success of these ligands, ‘repurposing’ ligands developed for use with palladium in nickel chemistry has proven inconsistent. No clear ligand design trends for nickel C(sp²)-N cross-couplings have emerged thus far, in contrast to the general trend of bulky and electron-rich ligands developed for palladium aminations (*vide supra*). Furthermore, no ancillary ligand design targeting nickel C(sp²)-N cross-couplings specifically had yet been reported by 2016. To address this deficiency, the Stradiotto group aimed to design ligands tailored to nickel, leading to the development of PAd-DalPhos^{40b} for use more broadly in nickel-catalyzed C(sp²)-N cross-couplings. Unlike the bulky and electron-rich ancillary ligands that are optimal in palladium-catalyzed C(sp²)-N cross-couplings, it was envisioned that a sterically demanding but more modestly electron-donating ligand would be well-suited, given the propensity of nickel for oxidative addition of aryl halide bonds compared to palladium. Such ligands would also facilitate the presumptive turnover-limiting C(sp²)-N bond reductive elimination within a Ni(0)/Ni(II) catalytic cycle – an assertion which recently gained computational support.⁴⁴⁻⁴⁵ Therefore, a

phosphaadamantane fragment was strategically incorporated into the ligand framework to accomplish these goals, having the σ -donation ability comparable to that of a phosphite, yet the large steric bulk similar to that of $P(tBu)_2$.⁵²

PAd-DalPhos (**Figure 3**) has proven to be a highly effective ligand design for nickel amination chemistry. When complexed to nickel to form an air-stable pre-catalyst of type $LNiCl(o-tol)$, it has enabled a number of reactivity breakthroughs in challenging $C(sp^2)$ -N cross-couplings.^{40b} This ligand facilitated the first nickel-catalyzed room-temperature monoarylation of ammonia with aryl halides and pseudohalides, including sought-after mesylate electrophiles. The ability to use gaseous ammonia in these reactions makes this system attractive for scaling up to industrial needs. The room-temperature amination of challenging primary amines, such as methyl and ethylamine, was accomplished, as well as the first nickel catalyzed $C(sp^2)$ -N cross-coupling of primary amides and lactams using activated aryl electrophiles.⁵³ A recent PAd-DalPhos variant, CyPAd-DalPhos, substituting cyclohexyl groups for the original *ortho*-tolyl substituents excelled in the nickel-catalyzed $C(sp^2)$ -N cross-coupling of cyclopropylamine at room-temperature,⁵⁴ a pharmaceutically relevant motif for which few catalyst systems exist. Previous systems were limited to palladium catalysis of aryl bromides at room-temperature or aryl chlorides at elevated temperatures.⁵⁵ These significant advances in the field enabled by the PAd-DalPhos motif highlights the benefit of designing ligands tailored to the specific needs of nickel in $C(sp^2)$ -N cross-coupling reactions.

Since the development of the PAd-DalPhos ligand family, other notable advances in the field of ligand design for nickel have occurred. Though not directly related to $C(sp^2)$ -N cross-coupling, the Doyle group reported in 2017 the development of new ligands for nickel-catalyzed Suzuki cross-coupling reactions.⁵⁶ Motivated by the failure of repurposing ligands designed for analogous palladium chemistry, they used statistical models to quantify ligand steric and electronic properties, leading to the identification of new and successful ligands for nickel catalysis. A key metric developed was remote steric hindrance, whereby a large cone angle combined with low percent buried volume can be used in conjunction as a predictor for ligand success in Suzuki cross-couplings. The idea of remote steric hindrance has the potential for far-reaching applications in ligand design for a broad range of nickel cross-coupling reactions, including $C(sp^2)$ -N cross-coupling. Another method of ligand development for nickel, identified by the Weix group, involved screening a pharmaceutical compound library to find new nitrogen and oxygen

containing heterocycles for use in nickel-catalyzed cross-electrophile coupling.⁵⁷ From an initial library of 2.8 million compounds, 31 new heterocyclic ligands were identified, vastly expanding the repertoire of known ligands for cross-electrophile couplings with minimal time and effort compared to traditional modular ligand design methodologies. Together, these studies highlight the success that tailored ligand design can have on nickel cross-couplings.

1.5 Overview of Thesis Work

Transition metal-catalyzed cross-coupling reactions have revolutionized synthetic chemistry, enabling the facile generation of complex products under mild conditions. Among these cross-coupling reactions, the palladium-catalyzed Buchwald-Hartwig Amination has had a profound impact on the pharmaceutical industry, facilitating the formation of medicinally relevant C(*sp*²)-N bonds.³ Notwithstanding its utility, the cost and scarcity of palladium has motivated the development of cheap and abundant base metals as alternative catalysts for this chemistry. As outlined in the previous section, nickel has surged to the forefront as a viable replacement, allowing for competitive if not superior reactivity in C(*sp*²)-N cross-coupling reactions compared to palladium.^{26, 33, 40b, c, 46, 57-58} However, the mixed results from repurposing ligands designed for palladium in analogous nickel chemistry has prompted a drive to develop ligands tailored to the unique properties of nickel. Indeed, due to the well-established propensity of nickel to mediate challenging oxidative addition reactions,³¹ and the strong likelihood for reductive elimination to be the rate limiting step,⁴³⁻⁴⁵ bulky and modestly electron-donating ligands should be successful in this chemistry. To this point, the first ligand developed specifically for nickel, PAd-DalPhos, enabled the monoarylation of ammonia at room temperature, a first for the field.^{40b}

It is obvious that continued advances in nickel-catalyzed C(*sp*²)-N cross-coupling chemistry relies on the development of new ligands to address challenges in the field. With this in mind and encouraged by the success of PAd-DalPhos, we turned our attention toward developing complementary and modular new classes of bisphosphines, so as to diversify the ancillary ligand ‘toolkit’. Building on the successful use of diaminophosphine oxide-derived, saturated *N*-heterocyclic phosphine (NHP) ancillary ligands in nickel-catalyzed C(*sp*²)-C(*sp*²) cross-couplings by Ackermann and co-workers,⁵⁹ I became interested in developing *ortho*-phenylene bridged bisphosphine ancillary ligands in which a sterically demanding neutral NHP donor fragment is paired with an easily varied PR₂ donor group (R = alkyl or aryl) for use in nickel-catalyzed C(*sp*²)-N cross-coupling. These fragments are not widely explored, and so we became curious as to how

the donicity of this NHP moiety would compare to a traditional phosphine donor. The synthesis and characterization of these ligands and their nickel-bound pre-catalyst variants are described at the beginning of Chapter 2. The scope of C(*sp*²)-N cross-coupling reactions enabled by the pre-catalyst system is described, and an experimental and computational comparison to the state-of-the-art system PAd-DalPhos is discussed in the second half of Chapter 2.

In building on this work, I next turned my attention to developing an NHP variant of 1,1'-bis(diphenylphosphino)ferrocene (DPPF), which has a well-established track record in nickel-catalyzed C(*sp*²)-N cross-coupling chemistry.^{15b, 47b, c} My next focus was to build on this motif and develop a bis-NHP containing variant in an attempt to address shortcomings in current C(*sp*²)-N cross-couplings mediated by DPPF. The synthesis and characterization of these new ligands are described in Chapter 3. As well, proposals for future work are detailed in Chapter 4, with concluding remarks provided in Chapter 5.

Chapter 2 - Application of NHP-Based Bisphosphines in Nickel-Catalyzed C(*sp*²)-N Cross-Couplings

2.1 Contributions

This chapter describes the development of a new class of neutral NHP containing bisphosphines for use in the nickel-catalyzed C(*sp*²)-N cross-coupling of aryl halides with primary aryl and alkylamines at room-temperature. This project was completed in collaboration with Christopher Lavoie and Dr. Erin Johnson, who performed all the computational experiments found herein, Raymond Bennett, who assisted in the isolation of the substrate scope, and Dr. Robert McDonald and Dr. Michael Ferguson who conducted the crystallographic solutions and refinements. The author's contributions consist of the synthesis and characterization of the new ligands, selection of a lead candidate through reaction screening, development and characterization of pre-catalysts, isolation and characterization of the substrate scope, stoichiometric experiments to probe catalyst activation, preparing the supplementary information and drafting the manuscript. This work is published in ACS Catalysis (DOI: 10.1021/acscatal.8b01005)

2.2 Introduction

As outlined in Chapter 1 (*vide supra*), we aimed to build on the success of the PAd-DalPhos ligand framework through the incorporation of *N*-heterocyclic phosphine (NHP) fragments to generate sterically demanding bisphosphine ancillary ligands. This modular framework allows for the incorporation of phosphorus into either a saturated or unsaturated heterocyclic ring which could serve as a means of modulating the donicity of the NHP fragment, in keeping with *N*-heterocyclic carbene⁶⁰ ancillary ligands.⁶¹ As well, the easily varied PR₂ donor group (R = alkyl or aryl) allow for further tuning of the ligand steric and electronic parameters. The incorporation of bulky mesityl groups prevent dimerization while promoting reductive elimination, a common feature utilized in both NHP⁶¹⁻⁶² and NHC^{48, 63} ligands. To the best of our knowledge, no ancillary ligands of this type exist in the literature.

The NHP motif has featured prominently in other chemistry, such as the bidentate *N*-heterocyclic phosphonium ligand (**A**) developed by Thomas and co-workers, for which the coordination chemistry with nickel is explored, though no catalytic applications are discussed.⁶⁴ An NHP-benzenesulfonato ancillary ligand (**B**) was utilized by Caporaso, Mecking, Göttker-Schnetmann, and co-workers in palladium-catalyzed Mizoroki-Heck reactions involving acrylates,⁶⁵ allowing for regioselective control to form the regioirregular 1,2-insertion product.

The air-stable diaminophosphine oxide-derived, saturated *N*-heterocyclic phosphine ligand framework (C) has also been successfully utilized by Ackermann in palladium-catalyzed $C(sp^2)$ - $C(sp^2)$ Kumada couplings, enabling the use of aryl chlorides, fluorides and (a)cyclic alkenyl tosylates.⁵⁹ As well, NHPs have previously been used for hydroboration,⁶⁶ hydrophosphination,⁶⁷ and stoichiometric reductions,⁶⁸ such as in the recent use of chiral diazaphospholenes for the asymmetric hydroboration of imines reported by Speed and co-workers in 2017.⁶⁹

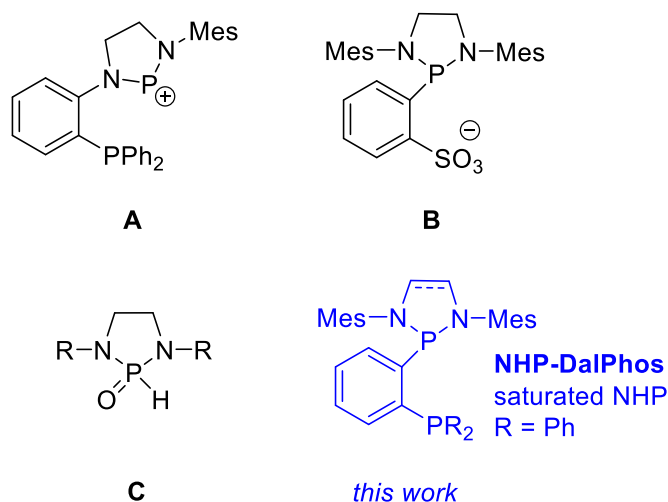


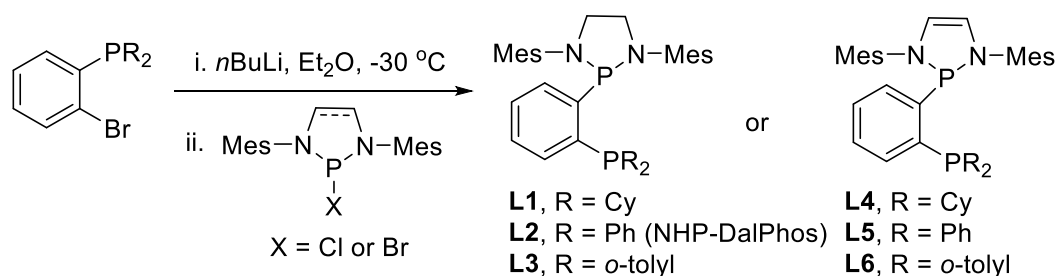
Figure 4: Some previously reported bidentate NHP-type ancillary ligands, and the new NHP-DalPhos ancillary ligand developed herein

Described below are the results of our synthetic and catalytic investigations of new *ortho*-phenylene bridged NHP-bisphosphine ancillary ligands in the context of nickel-catalyzed $C(sp^2)$ -N cross-coupling chemistry. This work establishes that the use of (NHP-DalPhos)NiCl(*o*-tolyl) (**C1**), featuring the new NHP-DalPhos ancillary ligand (**Figure 4**), enables the monoarylation of primary alkylamines and related ammonium salts with (hetero)aryl chlorides or bromides at room temperature – a reaction for which few effective nickel catalyst systems are known.^{40b, 41, 47b, 54} To complement this experimental work, the results of our comparative DFT analysis of nickel-catalyzed primary alkylamine $C(sp^2)$ -N cross-coupling employing PAd-DalPhos or NHP-DalPhos are also presented.

2.3 Results and Discussion

2.3.1 Ligand Synthesis and Characterization

The targeted series of new saturated and unsaturated *ortho*-phenylene bridged NHP-bisphosphines (**L1-L6**) was prepared as outlined in **Scheme 2**. In all cases ligands featuring sterically demanding *N*-mesityl groups on the NHP fragment were pursued in an effort to promote C(*sp*²)-N bond reductive elimination at nickel in cross-coupling applications. Cyclohexyl, phenyl, and *ortho*-tolyl substituents were incorporated as substituents on the adjacent phosphine donor fragment, to allow for the steric and electronic properties of the NHP-bisphosphine structure to be varied further (**Scheme 2**).



Scheme 2: Synthesis of the NHP-bisphosphines **L1-L6**

The new ligands **L1-L6** were fully characterized on the basis of NMR spectroscopic and mass spectrometric data; restricted rotation of the bulky *N*-Mes groups is evident to various extents in the ¹H and ¹³C{¹H} spectra of **L1-L6** at 300 K. In the case of **L1**, **L2**, and **L4**, the connectivity was confirmed on the basis of single-crystal X-ray data (**Figure 5**). Comparison of the geometrical parameters in these three structures revealed no systematic variation of either the P-N or P-C distances, or the angles at phosphorus, within the NHP fragment. While the heterocyclic C-N distances in **L1** and **L2** (~1.47 Å) are only modestly longer than those in **L4** (~1.42 Å), as expected a much longer heterocyclic C7-C8 linkage is found in the saturated diazaphospholidine ligands (**L1**: 1.505(3) Å; **L2**: 1.517(3) Å) versus the unsaturated diazaphospholene (**L4**: 1.3307(18) Å).

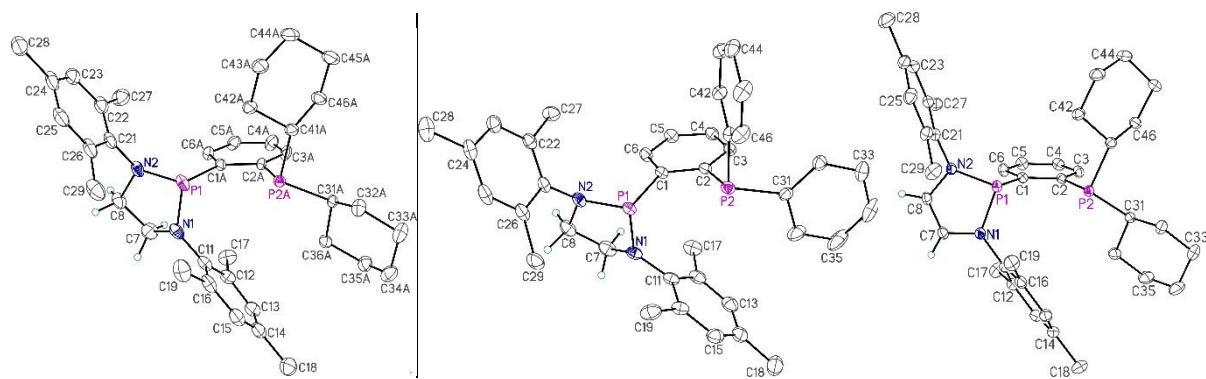
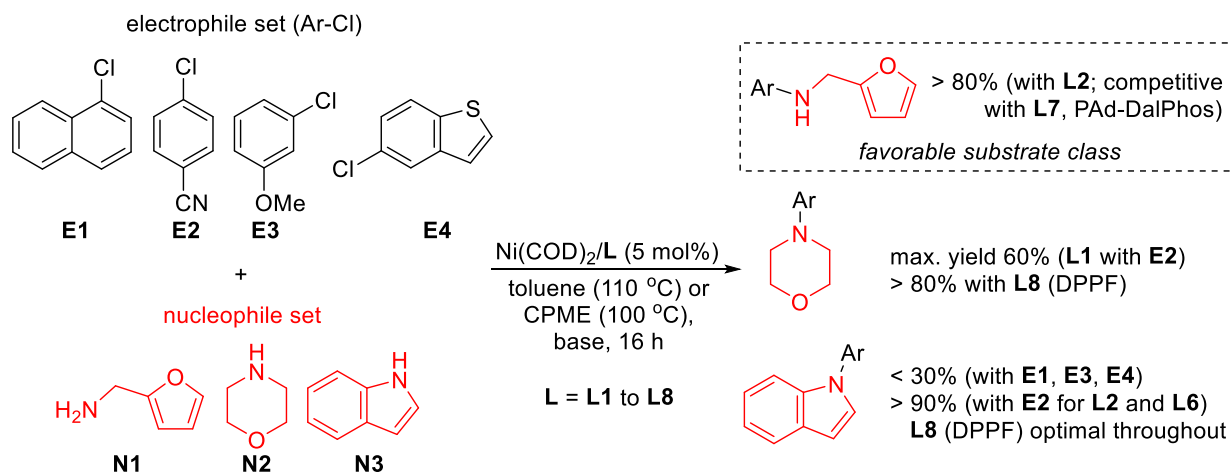


Figure 5: Crystallographically determined structures of **L1** (left), **L2** (middle), and **L4** (right), represented with thermal ellipsoids at the 30% probability level. Selected hydrogen atoms are omitted for clarity.

2.3.2 Screening of Ligands **L1-L6** in Nickel-Catalyzed $C(sp^2)$ -N Cross-Couplings

With the NHP-bisphosphines **L1-L6** in hand, their utility in promoting the nickel-catalyzed $C(sp^2)$ -N cross-coupling of (hetero)aryl chlorides was evaluated in a preliminary screen employing $Ni(COD)_2/L$ precatalyst mixtures. In this regard, 1-chloronaphthalene (**E1**), 4-chlorobenzonitrile (**E2**), 3-chloroanisole (**E3**), and 5-chlorobenzo[*b*]thiophene (**E4**) were employed as representative *ortho*-substituted, *para*-substituted electron-poor, *meta*-substituted electron-poor, and heterocyclic test electrophiles, respectively, while furfurylamine (**N1**), morpholine (**N2**), and indole (**N3**) were employed as representative primary alkylamine, secondary cyclic dialkylamine, and heterocyclic NH reaction partners, respectively. Both PAd-DalPhos (**L7**)^{40b} and DPPF (**L8**)^{39, 47a} were screened alongside **L1-L6**, so as to provide a direct comparison to state-of-the-art ligands in nickel-catalyzed $C(sp^2)$ -N cross-coupling. The reaction preferences exhibited by **L1-L6** are summarized in **Scheme 3**; for full tabulated catalytic results, see Appendix Figures A1-A4.



Scheme 3: Screening of NHP-bisphosphine ligands in nickel-catalyzed C(*sp*²)-N cross-couplings. Results are estimated on the basis of calibrated GC data using dodecane as an internal standard.

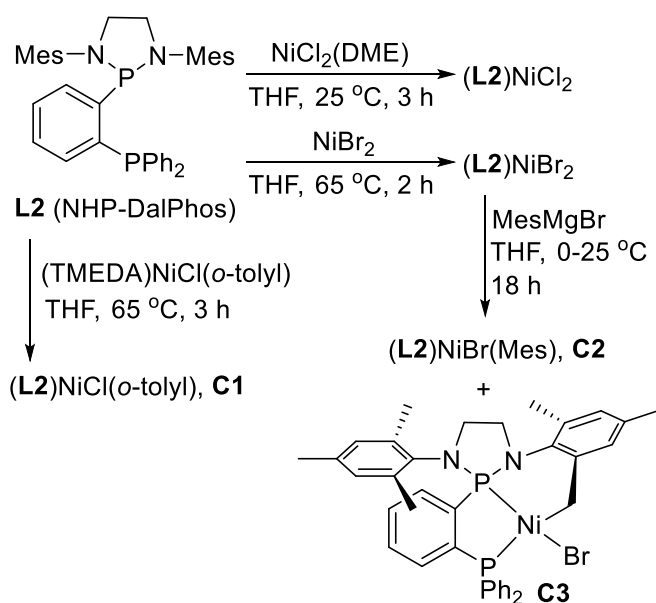
The results of the screen employing **L1-L6** in the nickel-catalyzed C(*sp*²)-N cross-coupling of (hetero)aryl chlorides with furfurylamine (**N1**) suggests that these new NHP-bisphosphine ligands hold promise in such cross-couplings of primary alkylamines. Under the conditions employed, the performance of **L2** (NHP-DalPhos) in particular was consistently competitive with, or superior to, both the other NHP-bisphosphines surveyed, as well as the highly effective PAd-DalPhos (**L7**).^{40b} In many but not all cases, structurally analogous ancillary ligands featuring a saturated NHP moiety (**L1-L3**) out-performed analogous unsaturated variants (**L4-L6**) in the cross-coupling of **E1-E4** with **N1**.⁷⁰ Unlike **L7**, NHP-bisphosphines bearing a P(*o*-tolyl)₂ donor fragment (i.e., **L3** and **L6**) performed consistently worse than the other NHP-bisphosphine ligands examined herein as well as **L7** in the monoarylation of **N1**, including generating the highest percentage of by-products resulting from dehydrohalogenation and other undesired off-cycle events. Such reactivity differences are likely the result of steric rather than electronic factors, given the similar σ -donor properties of PPh₃ and P(*o*-tolyl)₃.⁷ In turning our attention to cross-couplings involving morpholine or indole, the performance of DPPF (**L8**) was found to be superior to that of **L1-L6** in all of the transformations examined; only in the particular pairing of 4-chlorobenzonitrile (**E2**) and indole (**N3**) did **L2** and **L6** offer competitive performance relative to **L8**. Collectively, the reactivity profile displayed by the NHP-bisphosphines reported herein, and **L2** (NHP-DalPhos) in particular, in the nickel-catalyzed C(*sp*²)-N cross-coupling of amines is analogous to that of **L7** (PAd-DalPhos).^{47b}

2.3.3 Nickel Coordination Chemistry

Having identified **L2** as being a suitably effective ancillary ligand for use in the nickel-catalyzed C(*sp*²)-N cross-coupling of primary alkylamines, we turned our attention to preparing derived nickel precatalysts of the type (**L2**)NiX(aryl). Such precatalysts are attractive in that they can provide direct access to (**L2**)Ni⁰ species under standard amination conditions in the absence of potential inhibition by COD,⁷¹ thereby enabling more mild reaction conditions (e.g. low loadings, room temperature, *etc*) to be employed.^{40a} Given that the choice of X and aryl within L_nNiX(aryl) can impact the stability and reactivity of such precatalysts,⁷² the synthesis of two variants was targeted: (**L2**)NiCl(*o*-tolyl) (**C1**) and (**L2**)NiBr(Mes) (**C2**).

2.3.3.1 Coordination Chemistry of Nickel Dichlorides

Initial synthetic efforts were directed toward the preparation of (**L2**)NiCl₂ as a precursor to **C1**. Treatment of NiCl₂(DME) with **L2** afforded (**L2**)NiCl₂ as an analytically pure orange solid in 85% isolated yield (**Scheme 4**). The crystallographically determined structure of (**L2**)NiCl₂ (**Figure 6**) features a distorted square planar geometry at nickel, whereby the observed Ni-Cl interatomic distances of 2.2487(10) Å (*trans* to NHP) and 2.2073(10) Å (*trans* to the PPh₂) suggest that the NHP is a stronger *trans*-directing group relative to the triarylphosphine moiety. Both of the Ni-P distances in (**L2**)NiCl₂ are shorter than those in (**L7**)NiCl₂, whereas the corresponding Ni-Cl distances in (**L2**)NiCl₂ are modestly longer than those in (**L7**)NiCl₂,^{40b} this observation would appear to suggest that **L2** binds nickel more tightly than does **L7**, despite the considerable steric demands of the NHP group in the former. With this in mind, and given the negligible difference in the Ni-P distances (Ni-NHP 2.1373(11) Å, Ni-PPh₂ 2.1263(10) Å), it is plausible that a shorter than expected Ni-NHP interaction in (**L2**)NiCl₂ arises in part due to π -backbonding phenomena. While the crystal structure of a conceptually related (κ^2 -P,P)NiCl₂ complex comprising a chelated neutral variant of **A** (**Figure 4**) featuring a P-Cl linkage has been reported by Thomas and co-workers,⁶⁴ the bonding in this complex varies significantly from that observed in (**L2**)NiCl₂.



Scheme 4: Nickel coordination complexes derived from **L2**

With the goal of comparing the effect of backbone saturation and phosphine substituent on the nickel coordination chemistry, we were able to synthesize nickel dichloride complexes of **L1**, **L4**, and **L6** through analogous methods to those employed for **(L2)NiCl₂**. All three complexes exhibited a distorted square planar geometry at nickel, in keeping with **(L2)NiCl₂**. In the saturated NHP backbone complexes, the Ni-Cl bond distance *trans* to the NHP was approximately the same in both **(L1)NiCl₂** (2.2366(5) Å) and **(L2)NiCl₂**, whereas the Ni-Cl bond distance *trans* to the PR₂ moiety was slightly longer for **(L1)NiCl₂** (2.2334(5) Å), in keeping with the stronger donicity of the alkyl phosphine relative to the aryl phosphine substituent. The Ni-P distances for **(L1)NiCl₂** (Ni-NHP 2.1380(6) Å, Ni-PCy₂ 2.1473(5) Å) were similar to those seen in **(L2)NiCl₂**, albeit with a slight elongation in the Ni-PR₂ bond rationalized by the increased steric bulk of the cyclohexyl substituent.⁷ In general, the unsaturated dichloride complexes, **(L4)NiCl₂** and **(L6)NiCl₂**, exhibited slightly shorter Ni-Cl bonds *trans* to the NHP, at 2.2011(14) Å and 2.2193(9) Å, respectively. It is likely that this shortened Ni-Cl bond is caused by reduced σ -donation character of the unsaturated NHP, relative to the saturated variant. As well, both **L4** and **L6** bound dichlorides demonstrated an elongated Ni-PR₂ bond compared to their saturated analogues, which may be caused by the reduced flexibility in the unsaturated NHP backbone preventing tighter binding to the nickel center. It is worthwhile to note that the Ni-NHP distance remains nearly constant in all nickel

dichloride complexes, with a slight elongation in the case of **(L6)NiCl₂** likely caused by the larger steric bulk of the *ortho*-tolyl substituents.

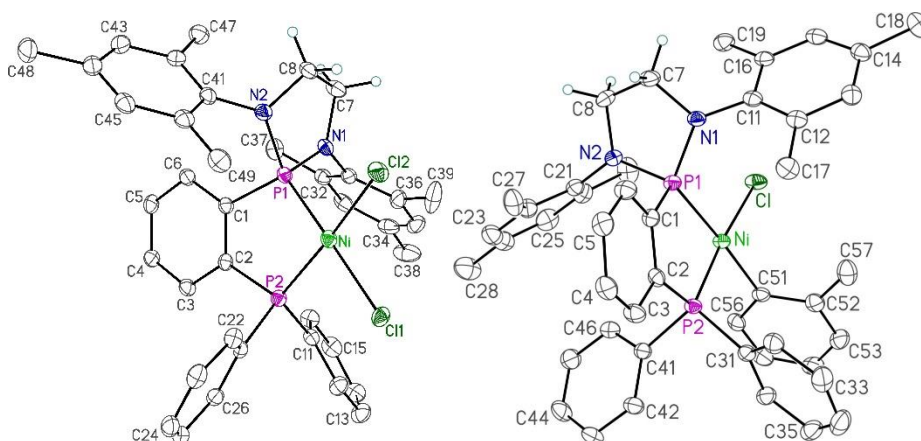


Figure 6: Single-crystal X-ray structures of **(L2)NiCl₂** (left) and **C1** (right), represented with thermal ellipsoids at the 30% probability level. Selected hydrogen atoms are omitted for clarity. Selected interatomic distances (Å) for **(L2)NiCl₂**: Ni-P1 2.1373(11); Ni-P2 2.1263(10); Ni-Cl1 2.2487(10); Ni-Cl2 2.2073(10). Selected interatomic distances (Å) for **C1**: Ni-P1 2.2010(7); Ni-P2 2.1217(7); Ni-Cl 2.1886(7); Ni-C51 1.949(3).

2.3.3.2 Coordination Chemistry of Nickel Pre-catalysts

While treatment of **(L2)NiCl₂** with (*o*-tolyl)MgCl under various conditions afforded the target complex **C1** as the major product on the basis of ³¹P NMR data, the quantitative formation of **C1** was achieved upon combination of **L2** with (TMEDA)NiCl(*o*-tolyl),⁷³ as outlined in **Scheme 4**. Precatalyst **C1** was thus obtained as an analytically pure yellow solid (98% yield), and was characterized by use of spectroscopic and X-ray crystallographic techniques (**Figure 6**). The solution ³¹P{¹H} NMR spectrum of **C1** (THF-*d*₈, 300 K) features only two doublets (120.3 and 57.0 ppm) in keeping with the existence of a single diastereomer in solution, while the ¹H NMR spectrum of this complex features signals consistent with a *C*₁-symmetric structure whereby Ni-C(*o*-tolyl) bond rotation is apparently slow on the NMR timescale. A distorted square planar geometry is observed about nickel in the crystal structure of **C1**, with chloride positioned *trans* to the triarylphosphine moiety. While it is likely that a combination of steric and electronic factors contribute the observed *cis*-disposed NHP and chloride donors in **C1**, it is worth noting that in the corresponding PAd-DalPhos complex **(L7)NiCl(*o*-tolyl)**, chloride is preferentially positioned *trans* to the phosphadamantane group. In keeping with the stronger *trans*-directing character of an aryl group relative to chloride, the Ni-NHP distance in **C1** (2.2010(7) Å) is significantly longer

than the related distance in (L2)NiCl₂ (*vide supra*), whereas the Ni-PPh₂ contact in C1 (2.1217(7) Å) is indistinguishable from that found in (L2)NiCl₂.

In the pursuit of C2, L2 was treated with NiBr₂ as outlined in Scheme 4, thereby affording (L2)NiBr₂ as an analytically pure red solid in 90% isolated yield. Subsequent exposure of (L2)NiBr₂ to MesMgBr employing literature methods^{72b} afforded what is tentatively assigned as a mixture (~10:1) of diastereomers of the target complex C2, along with approximately 10% of an additional by-product (C3), on the basis of ³¹P NMR data obtained from a sample of the crude reaction mixture. Although I have thus far been unable to obtain useful quantities of analytically pure C2 free of contamination by C3, X-ray crystallographic analysis (Figure 7) of a minute quantity of crystalline C2 confirmed the identity of this species as the distorted square planar complex (L2)NiBr(Mes), whereby the mesityl group is *trans* to the NHP fragment, and the Ni-P and Ni-C(aryl) distances are comparable to those found in C1. In one instance I was also fortuitously able to isolate a small quantity of crystalline C3, which was characterized on the basis of data obtained from ³¹P NMR, elemental analysis, and X-ray crystallographic experiments. Whereas the ³¹P NMR data allowed us to confirm the identity of this material as being the same as that formed as a by-product in the synthesis of C2 (i.e., C3, *vide supra*), the X-ray data obtained for C3 (corroborated by elemental analysis data) allowed for the identification of this species as a distorted square planar complex as arising from cyclometallation of an *ortho*-methyl of an NHP-mesityl group, with net loss of mesitylene (Figure 7). The tridentate nature of the cyclometallated ancillary ligand in C3, along with the presence of a weakly *trans*-directing bromide ligand, results in C3 having the shortest Ni-NHP distance (2.0929(5) Å) amongst the complexes reported herein. Given the apparent complexities associated with the synthesis of C2, in moving forward we opted to employ C1 exclusively as a pre-catalyst.

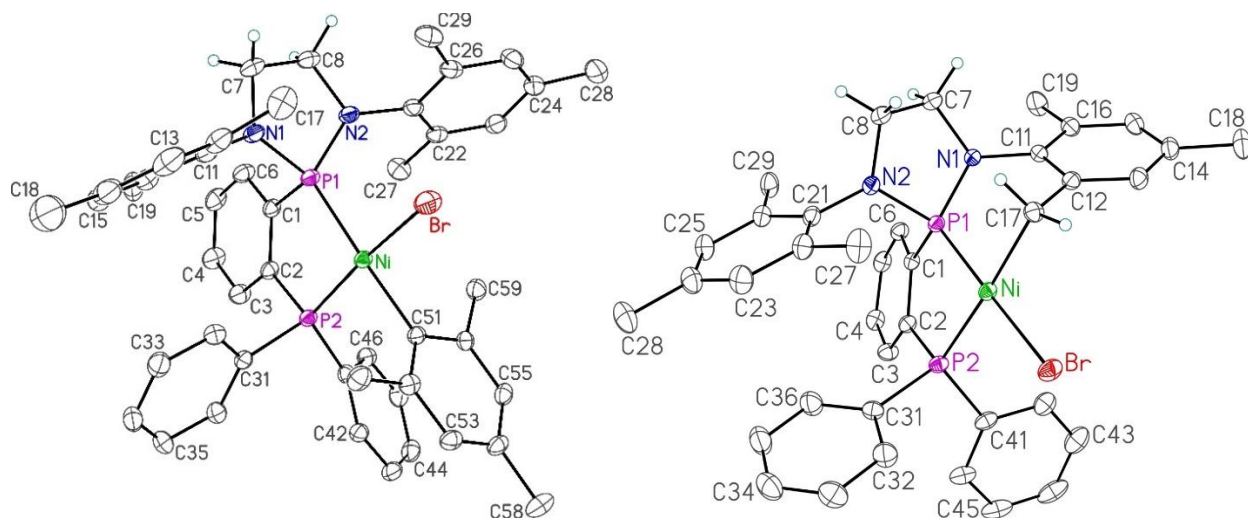
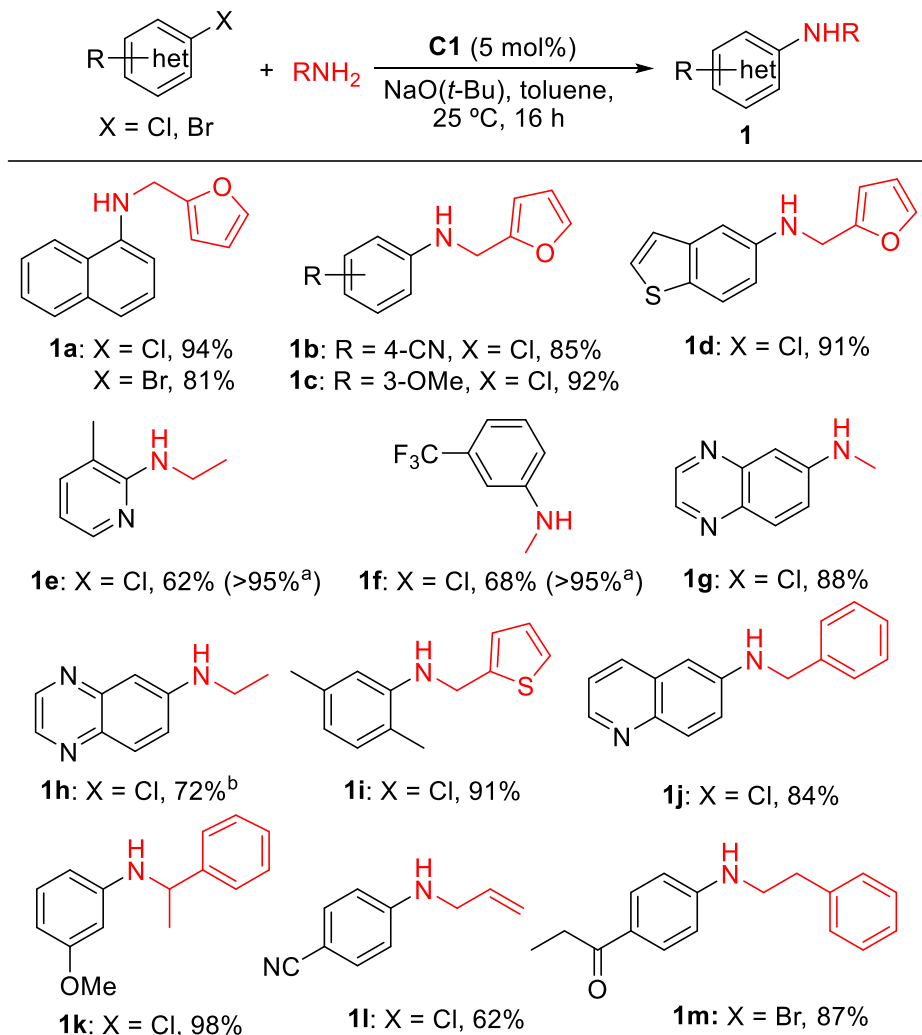


Figure 7: Single-crystal X-ray structures of **C2** (left) and **C3** (right), represented with thermal ellipsoids at the 30% probability level. Selected hydrogen atoms are omitted for clarity. Selected interatomic distances (Å) for **C2**: Ni-P1 2.2220(7); Ni-P2 2.1305(7); Ni-Br 2.3091(4); Ni-C51 1.950(3). Selected interatomic distances (Å) for **C3**: Ni-P1 2.0929(5); Ni-P2 2.1907(5); Ni-Br 2.3668(3); Ni-C17 1.9921(17).

2.3.4 Scope of Reactivity Employing Precatalyst **C1**

Having prepared an appropriate precatalyst, the substrate scope enabled by use of **C1** in the nickel-catalyzed *N*-arylation of primary alkylamines at room temperature was surveyed (**Scheme 5**). In keeping with our preliminary catalytic testing (**Scheme 3**), the cross-coupling of furfurylamine (**N1**) with electrophiles **E1-E4** afforded the targeted monoarylation products **1a-1d** in high isolated yield; 1-bromonaphthalene also proved compatible in this chemistry. In conducting the larger-scale cross-coupling of **E1** and **N1** using **C1** (5.37 mmol **E1**), the desired product **1a** was obtained in excellent yield (1.13 g, 94%).



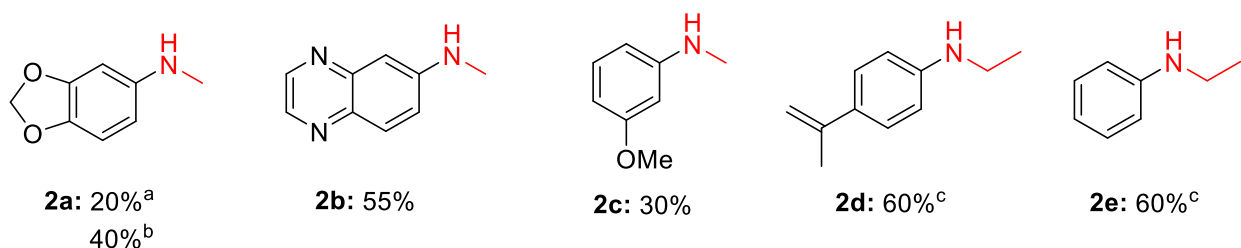
Scheme 5: Substrate scope for the cross-coupling of primary alkylamines and (hetero)aryl halides employing **C1** as a pre-catalyst. Conditions: NaO(*t*-Bu) (1.5-2 equiv), (hetero)aryl halide (1.0 equiv), and amine (1.1 equiv), with isolated yields shown. ^a Estimated yield on the basis of calibrated GC data using dodecane as an internal standard. ^b Conditions: NaO(*t*-Bu) (2.5 equiv), (hetero)aryl halide (1.0 equiv), and ethylammonium chloride (1.2 equiv) at 80 °C.

A range of other (hetero)aryl halides were employed successfully, including those featuring *ortho*-substitution (**1e**, **1i**), trifluoromethyl (**1f**), ether (**1k**), nitrile (**1l**), or ketone (**1m**) functionalities. Heterocyclic electrophiles also proved to be useful coupling partners, including those featuring benzothiophene (**1d**), pyridine (**1e**), quinoxaline (**1g**, **1h**) and quinoline (**1j**) core structures. A diverse array of primary alkylamines were successfully coupled in the course of this reactivity survey, featuring benzylic (**1j**, **1k**), allylic (**1l**), aliphatic (**1m**), and heteroaryl functionalities (**1a-d**, **1i**). In the case of **1l**, no rearrangement of the allylic fragment was seen. Small nucleophilic reagents were also transformed efficiently, using commercially available stock

solutions of methylamine and ethylamine to afford the monoarylated product exclusively (**1e-g**). In the case of **1e** and **1f**, the volatile nature of the cross-coupled product led to material loss while drying *in vacuo*; however, the high conversion achieved in these reactions was confirmed on the basis of GC analysis. The viability of using commercially available ammonium salts, which are more easily handled than their volatile liquid analogues, was also explored briefly. In this vein, the cross-coupling of ethylammonium chloride and 6-chloroquinoxaline leading to **1h** was readily achieved, adding to the few known examples of nickel-catalyzed cross-coupling of alkylammonium salts.^{40b, 42, 54} Throughout the course of these cross-couplings employing **C1** as a pre-catalyst, no undesired polyarylated species were detected as by-products.

2.3.4.1 Challenging Substrates Employing Precatalyst **C1**

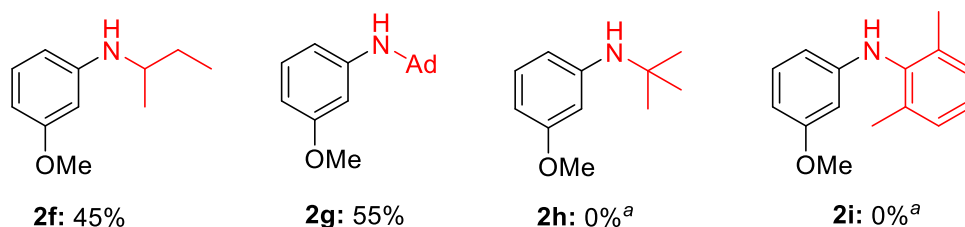
Although the methodology described above was successful in the cross-coupling of many (hetero)aryl halides and amine nucleophiles, there were certain substrate classes which were particularly challenging in this chemistry, resulting in little to none of the desired C(*sp*²)-N cross-coupled product. A selection of these products are shown below in **Schemes 6-8**.



Scheme 6: Challenging small nucleophilic amine substrates employing 5 mol% **C1** as a catalyst. Conditions: NaO(*t*-Bu) (2.5 equiv), (hetero)aryl halide (1.0 equiv), and ammonium salt (1.1 equiv) at 80 °C with estimated GC yields shown. ^a Reaction performed at 25 °C using 1.1 equiv of a methylamine stock solution. ^b Reaction performed at 80 °C using 1.1 equiv of a methylamine stock solution. ^c 2 mol% **C1** used.

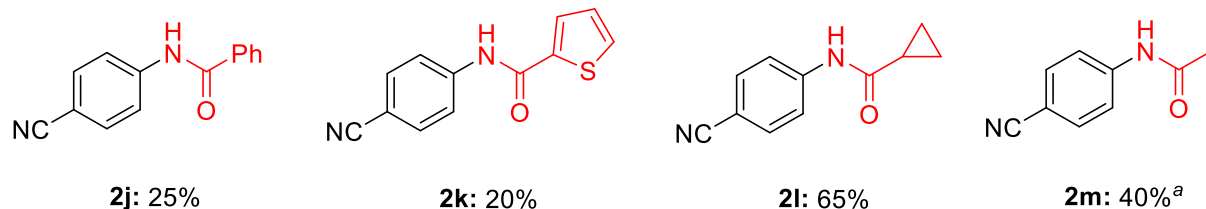
Though ammonium salts were found to be effective substrates in certain cases with **C1** (e.g. **1h**), they were less reactive on average compared to the amine analogues (**Scheme 6**). Furthermore, both (L7)NiCl(*o*-tolyl)^{40b} and (PhPF-*t*Bu)Ni(η^2 -NCPh)⁴² have demonstrated superior reactivity to **C1** with the same substrates under the similar conditions, with **L7** allowing for the conversion of **2b** in 81% isolated yield and the JosiPhos variant affording **2d** in 84% isolated yield. The reduced yields may be a result of inhibition caused by the substrate counter ion, potentially in a similar fashion to the inhibitory effect of tosylate (*vide infra*).

Bulky primary amines were another challenging substrate class when employing **C1**. The current state-of-the-art for the C(*sp*²)-N cross-coupling of bulky amines is still dominated by palladium catalysts,⁷⁴ though some nickel-based examples have appeared in recent years, utilizing both bisphosphine⁷⁵ and NHC⁷⁶ ligand scaffolds. These allow for the cross-coupling of *tert*-butylamine and adamantylamine at elevated temperatures, albeit often in only modest yields (~50%). Conversely, when using **C1**, increasing the steric bulk on the α -carbon or *ortho* position of arylamines led to significant decrease in conversion, with the bulkiest examples affording no product (**2h**, **2i**), as shown in **Scheme 7**. A similar trend is seen with (L7)NiCl(*o*-tolyl). The inversely proportional relationship between reactivity and steric bulk of a substrate is likely due to the inability of the nucleophile to access the metal center, given the steric hindrance enforced by the NHP moiety.



Scheme 7: Challenging bulky primary amine substrates employing 2 mol% **C1** as a catalyst. Conditions: NaO(*t*-Bu) (1.5-2 equiv), (hetero)aryl halide (1.0 equiv), and amine (1.1 equiv), with estimated GC yields shown. ^a Reaction performed at 110 °C with 5 mol% **C1**.

In an attempt to build on the recent success of (L7)NiCl(*o*-tolyl) in the first nickel-catalyzed C(*sp*²)-N cross-coupling of primary amides⁵³ and develop a substrate niche for **C1**, I targeted substrates which had reported yields below 80% in the seminal publication.⁵³ Though **C1** did demonstrate some activity towards primary amides (**Scheme 8**), it was significantly less effective than the **L7** precatalyst for this class of substrates. The most successful substrates (**2l**, **2m**) had less bulky alkyl substituents on the α -carbon, potentially due to rate-limiting steric effects caused by the large NHP-DalPhos ligand. As well, no reactivity was noted with **C1** when employing secondary amides, a challenging reaction for which only palladium variants exist at the time of writing.⁷⁷



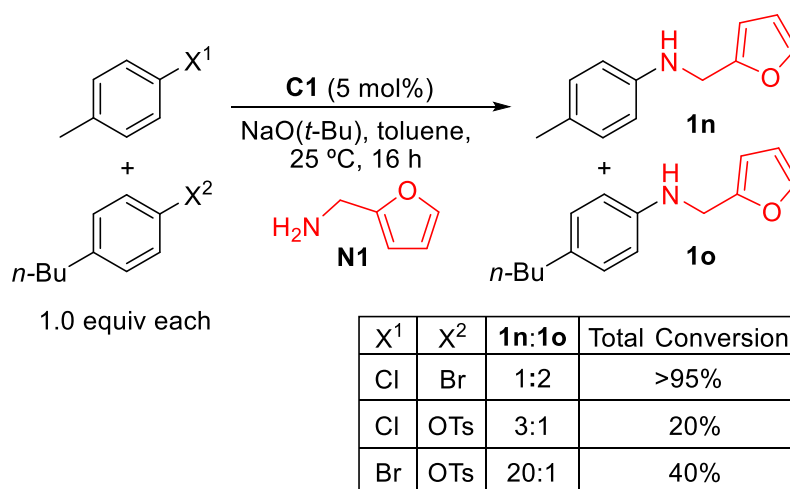
Scheme 8: Challenging primary amide substrates employing 2 mol% **C1** as a catalyst. Conditions: K_3PO_4 (1.5 equiv), (hetero)aryl halide (1.0 equiv), and amide (1.1 equiv) at 90 °C, with estimated GC yields shown. ^a Reaction performed with 5 mol% **C1**.

In addition to the aforementioned substrate classes, a range of other nucleophiles were also unsuccessful when employing **C1**. Most notably the use of ammonia led to polyarylation as the major product instead of exclusive monoarylation observed with **L7**. This difference is potentially due to the nickel metal center being more accessible in the case of **C1** compared to (**L7**)NiCl(*o*-tolyl), allowing for amination of the product aniline to occur more readily. Certain substrates led to no appreciable turnover, such as in the case of hydrazine and related derivatives, a notoriously challenging substrate for which PAd-DalPhos is also ineffective. Indeed, only a handful of examples in palladium $C(sp^2)$ -N cross-coupling can utilize hydrazine and related derivatives.⁷⁸ Similar to secondary amides, Boc-protected amines afforded no turnover product, likely due to the poor nucleophilicity of the substrate. Protic functional groups were poorly tolerated, with the attempted cross-coupling of activated aryl chlorides with hydroxylamine, 4-aminophenol and glycine affording mainly starting material and dehydrohalogenation under forcing conditions. Variation in base, counterion, and base loading had no effect on product distribution. It is possible that an alkoxide forms and preferentially binds to the metal center, preventing turnover or leading to catalyst decomposition. Urea and related derivatives led to no appreciable turnover, potentially limited by the ability of the substrate to form *N,O*-chelated ureates,⁷⁹ limiting productive catalysis. Finally, electron-rich electrophiles were unsuccessful with **C1** in comparison to (**L7**)NiCl(*o*-tolyl), with the $C(sp^2)$ -N cross-coupling of 4-chloroanisole and furfurylamine yielding 45% and 85% product, respectively.

2.3.4.2 Electrophile Selectivity Employing Precatalyst **C1**

To gain some preliminary insights into the electrophile reactivity preferences of **C1**, I conducted a (pseudo)halide competition study using limiting furfurylamine (**N1**). An aryl chloride, bromide, and tosylate were compared under standard reaction conditions, with substituents on the

aryl moiety bearing similar steric and electronic characteristics so as to focus solely on the inherent reactivity behavior of the (pseudo)halide electrophile (**Scheme 9**). In competitions involving an aryl chloride and an aryl bromide, a 2:1 preference for the bromide electrophile was observed, with full conversion of furfurylamine. When an aryl chloride and an aryl tosylate were compared, a 3:1 preference for the chloride was noted, although a significant decrease in overall product formation was found. The same trend was seen in the competition of an aryl bromide and an aryl tosylate, with a 20:1 preference for the bromide. Collectively, these results highlight the potential inhibitory effect of aryl tosylates (and possibly sulfonates more generally) on **C1**, a phenomenon that has been observed in our previous studies involving CyPAD-DalPhos in nickel-catalyzed $C(sp^2)$ -N cross-couplings.⁵⁴



Scheme 9: (Pseudo)halide competition study employing **C1**. Reported product distributions and total conversions to **1n** and **1o** estimated on the basis of calibrated GC data.

2.3.5 Comparison of Different **L2** and **L7** Containing Nickel Precatalyst Systems

Although for convenience I opted to employ 5 mol% **C1** in the substrate scope exploration presented in **Scheme 5**, I became interested in examining if lower loadings, and/or alternative nickel precatalysts featuring **L2**, might be effective in such transformations. Moreover, I sought to learn more about the relative reactivity behavior of (L)NiCl(*o*-tolyl) precatalysts (**L** = **L2**, NHP-DalPhos; **L** = **L7**, PAd-DalPhos). In studying the cross-coupling of 5-chlorobenzo[*b*]thiophene (**E4**, 1 equiv) and furfurylamine (**N1**, 1.1 equiv) to give **1d** as a test reaction (2 equiv NaO(*t*-Bu), toluene, 16 h, 25 °C), quantitative conversion to **1d** was achieved by use of 2 mol% **C1**. In using (TMEDA)NiCl(*o*-tolyl)/**L2** mixtures under analogous room temperature conditions, high (~85%)

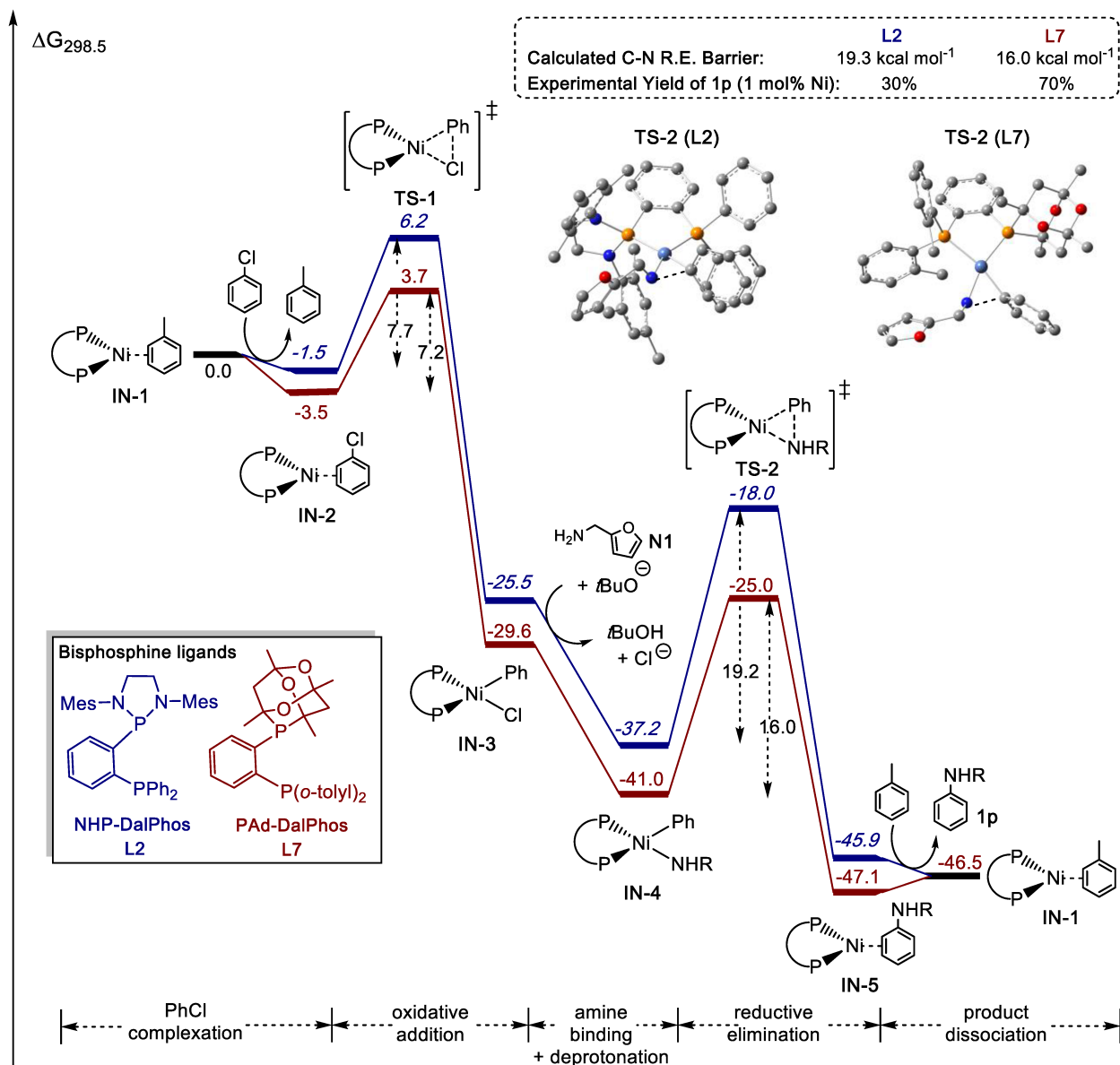
but incomplete conversion to **1d** was detected, and no conversion to product was achieved by use of (TMEDA)NiCl(*o*-tolyl) alone. The finding that the addition of TMEDA (1 equiv) to **C1** did not inhibit room temperature catalysis suggests that the inferior performance of (TMEDA)NiCl(*o*-tolyl)/**L2** mixtures under these conditions is likely attributable to incomplete formation of **C1** *in situ*. While clean conversion to **1d** was also achieved with (**L7**)NiCl(*o*-tolyl) under the test conditions, the use of either (**L2**)NiCl₂ or Ni(COD)₂/**L2** mixtures (2 mol% Ni) in the presence or absence of PhBPIn as an activator⁴⁵ afforded ≤10 % conversion to **1d**, thereby establishing the inferiority of such catalyst systems. Upon lowering the loading of **C1** to the 1 mol% level, only 40% conversion to **1d** (50% in the presence of 1 equiv PhBPIn) was achieved; conversely, >90% conversion to **1d** was achieved by use of (**L7**)NiCl(*o*-tolyl) (1 mol%), in keeping with our previous reports.^{40b, 45} In an effort to learn more about the relative activity of catalysts generated from (**L**)NiCl(*o*-tolyl) (**L** = **L2** or **L7**), I elected to monitor the room temperature cross-coupling of 3-chloroanisole (**E3**, 1 equiv) and furfurylamine (**N1**, 1.1 equiv) to give **1c**. Under the test conditions employed (2 mol% Ni, 2 equiv NaO(*t*-Bu), toluene, 25 °C), quantitative conversion to **1c** was achieved after 0.25 h with (**L7**)NiCl(*o*-tolyl), at which time-point <20% conversion to **1c** was observed when using (**L2**)NiCl(*o*-tolyl) (**C1**); 1.5 h was required in order to achieve full conversion to **1c** when using **C1** under these conditions, in the absence of an observable induction period. Collectively, these experiments reaffirm the particular utility of employing (**L**)NiCl(*o*-tolyl) precatalysts^{40a} in C(*sp*²)-N cross-coupling applications. While in head-to-head reactivity comparisons PAd-DalPhos (**L7**) was found to out-perform NHP-DalPhos (**L2**) to a modest extent, the catalytic performance of **C1** establishes **L2** as being a member of a small subset of ligands (along with PAd-DalPhos^{40b} and CyPAd-DalPhos⁵⁴) that have proven capable of enabling the nickel-catalyzed monoarylation of primary alkylamines with (hetero)aryl chlorides at room temperature with broadly useful scope.

2.3.6 Computational Comparison of NHP-DalPhos (**L2**) and PAd-DalPhos (**L7**)

To understand more fully the behavior of **L2** versus **L7** in nickel-catalyzed C(*sp*²)-N cross-coupling chemistry, one potential reaction pathway within a presumptive Ni⁰/Ni^{II} cycle⁴⁵ for the cross-coupling of chlorobenzene and furfurylamine (**N1**) to yield *N*-phenyl-furanmethanamine (**1p**) was modelled *via* density functional theory (DFT) calculations (**Scheme 10**). The B3LYP-XDM⁸⁰ method and the 6-311+G(2d,2p) basis set were used, which are well-suited for calculating 3d transition metal-ligand binding energies.^{80d} The geometry optimizations and frequency

calculations were performed with a smaller, mixed basis set, and frequencies were used to assign stationary points as either minima (no imaginary frequencies) or transition states (one imaginary frequency). The following steps were modeled: (i) arene exchange between (L)Ni(η^2 -toluene) (**IN-1**) and chlorobenzene to afford (L)Ni(η^2 -PhCl) (**IN-2**); (ii) C-Cl oxidative addition to give (L)Ni(Ph)Cl (**IN-3**) *via* **TS-1**; (iii) reaction with furfurylamine and *tert*-butoxide to give (L)Ni(Ph)(NH(CH₂-furyl)) (**IN-4**); (iv) C-N reductive elimination to afford (L)Ni(η^2 -*N*-phenyl-furanmethanamine) (**IN-5**) *via* **TS-2**; and (v) arene exchange from **IN-5** to regenerate **IN-1** and liberate *N*-phenyl-furanmethanamine product (**1p**).

Exchange of toluene for chlorobenzene in the conversion of **IN-1** to **IN-2** is modestly exergonic for both **L2** (-1.5 kcal mol⁻¹) and **L7** (-3.5 kcal mol⁻¹). Consistent with the view that C-Cl bond oxidative addition of chloroarenes to phosphine supported P₂Ni⁰ complexes is relatively facile,^{26, 30, 33, 45} the free-energy activation barriers for chlorobenzene oxidative addition (*via* **TS-1**) were found to be small (**L2**: 7.7 kcal mol⁻¹, **L7**: 7.2 kcal mol⁻¹), and the formation of **IN-3** from **IN-2** is highly exergonic (**L2**: -24.0 kcal mol⁻¹, **L7**: -26.1 kcal mol⁻¹). Owing to the lack of clarity involving the role of the base, location of a transition state leading to the formation of **IN-4** was not attempted. Nonetheless, the reaction was found to be exergonic for both ligands (**L2**: -11.7 kcal mol⁻¹, **L7**: -11.4 kcal mol⁻¹). The C-N reductive elimination to afford **IN-5** is exergonic for both **L2** (-8.8 kcal mol⁻¹) and **L7** (-6.1 kcal mol⁻¹) pathways. However, it is notable that the **L2** derived pathway (19.2 kcal mol⁻¹) suffers from a comparatively higher barrier to C-N reductive elimination (*via* **TS-2**) versus the **L7** based pathway (16.0 kcal mol⁻¹), which may in part form the basis of the superior reactivity of **L7** versus **L2** in room temperature *N*-arylations of furfurylamine (*vide supra*) within a putative Ni⁰/Ni^{II} cycle.⁴⁵ Indeed, when conducting the cross-coupling of chlorobenzene and furfurylamine (**N1**) using 1 mol% of **C1** or (L7)NiCl(*o*-tolyl) at room temperature under experimental conditions outlined in **Scheme 5**, 70% conversion to *N*-phenyl-furanmethanamine **1p** was observed after only 1 h with (L7)NiCl(*o*-tolyl); conversely, in using **C1** only 30% of the desired product **1p** was obtained under such conditions (with the remainder being unreacted starting materials). To complete the cycle, **IN-1** is regenerated *via* arene exchange of bound **1p** by toluene, the overall reaction of which is approximately thermoneutral (**L1**: -0.6 kcal mol⁻¹, **L2**: 0.6 kcal mol⁻¹).



Scheme 10: Comparative reaction profile (relative free-energies, kcal mol⁻¹) calculated by use of DFT methods for the nickel-catalyzed C(*sp*²)-N cross-coupling of chlorobenzene and furfurylamine (**N1**) involving (**L2/L7**)Ni species (R = CH₂-furyl).

2.3.7 Experimental Investigation into the Reactivity of **C3**

Following characterization of the cyclometallated species **C3**, I performed a brief screen examining the catalytic potential of this complex in the *N*-arylation of primary alkylamines. Surprisingly, **C3** was found to have similar catalytic activity as **C1**, showing excellent reactivity in the C(*sp*²)-N cross-coupling of 1-chloronaphthalene (**E1**) with furfurylamine (**N1**) and 4-

chlorobenzonitrile (**E2**) with allylamine, with both **C1** and **C3** generating the desired product **1a** and **11** in >95% and 70% yield, respectively. Conversely, both precatalysts struggled with 3-chloroanisole (**E3**) and *sec*-butylamine, with < 20% conversion for both systems. Given the structural differences between the two complexes, I became intrigued as to how the cyclometallated species **C3** could activate *in situ*. In an attempt to gain a better understanding of this activation process, I performed a series of stoichiometric studies with **C3**, monitoring three reaction variants using $^{31}\text{P}\{^1\text{H}\}$ NMR. Firstly, only base was added to **C3** (**A**). In the second reaction base and furfurylamine were added (**B**), and in the third reaction base, furfurylamine and 1-chloronaphthalene were added to the reaction vessel (**C**). These reactions were performed with and without COD (**Figure 8** and **Figure 9**, respectively), in an attempt to trap any potential intermediates generated.

For variant **A**, both reactions with and without COD show the same shifts in the $^{31}\text{P}\{^1\text{H}\}$ NMR; residual starting material and a new pair of peaks at 148 ppm and 21 ppm, albeit with different relative intensities. The new shifts at 148/21 ppm are likely due to displacement of the bromide by *tert*-butoxide, generating a nickel alkoxide species consistent with **IN-13** (**Scheme 11**). These do not correspond to a (**L2**)Ni(COD) complex since the $^{31}\text{P}\{^1\text{H}\}$ shifts of a control experiment mixing **L2** and Ni(COD)₂ to generate the putative (**L2**)Ni(COD) were not seen throughout the course of the stoichiometric investigations. In the second set of reactions (**B**) involving amine and base, the presumed nickel alkoxide shifts were once again noted, as were two new pairs of shifts corresponding to a putative amine bound nickel species consistent with **IN-8** (**Scheme 11**), at 151/40 ppm and 153/39 ppm. Only the shifts at 151/40 ppm are seen in the COD containing reaction and as such this is tentatively assign this as the nickel amido species **IN-8**, with 153/39 ppm corresponding to the η^2 -imine species, unseen in the COD reaction due to the potential for displacement by the alkene. In variant **C**, no shifts corresponding to nickel alkoxide, amido or η^2 -imine species are seen. In both cases only new shifts are noted, which likely correspond to intermediates in the catalytic cycle, with significantly more shifts noted in the case of the COD free reaction. As well, the different ratios of product distribution between the two reactions, COD containing and COD free, are likely due to inhibition by COD, though the exact mechanism of this is unclear. As well, the possibility for NMR silent products to be generated cannot be discounted, and any future mechanistic investigations should account for this. Unfortunately, I was unable to isolate and fully characterize any individual species generated throughout the course of the

stoichiometric studies, leading us to undertake alternative methods to probe the activation pathway.

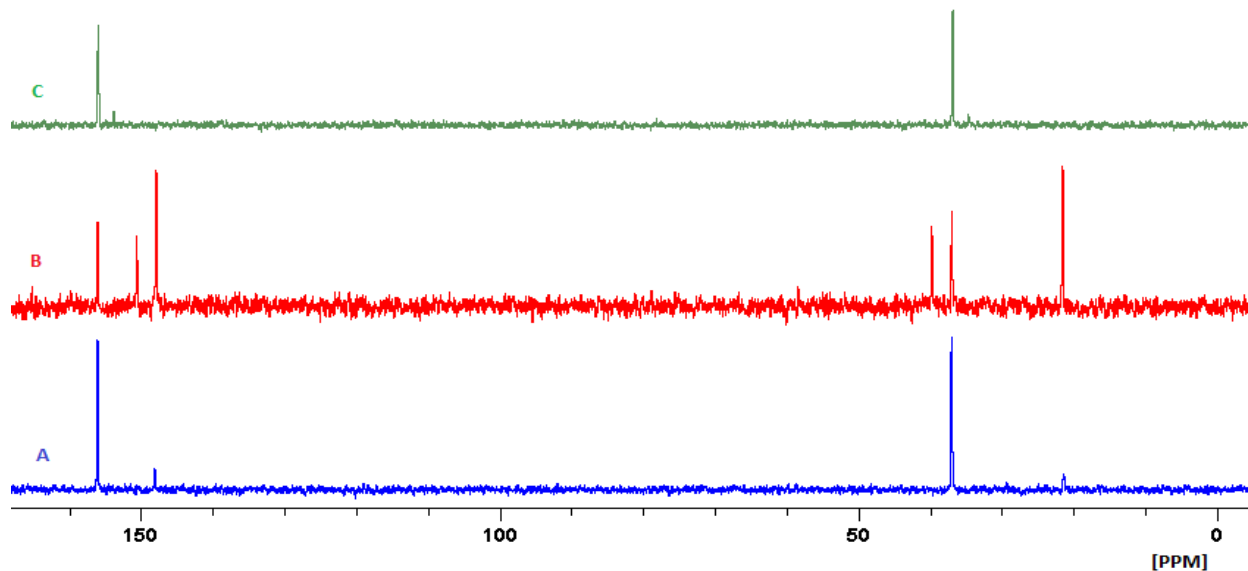


Figure 8: $^{31}\text{P}\{^1\text{H}\}$ NMR data for the stoichiometric experiments on the activation of **C3** employing toluene and 1 equivalent of COD. Reaction **A** performed with 2 equivalents of $\text{NaO}(t\text{-Bu})$. Reaction **B** performed with 2 equiv. $\text{NaO}(t\text{-Bu})$ and 1 equiv furfurylamine. Reaction **C** performed with 2 equiv. $\text{NaO}(t\text{-Bu})$, 1 equiv furfurylamine and 1 equiv 1-chloronaphthalene.

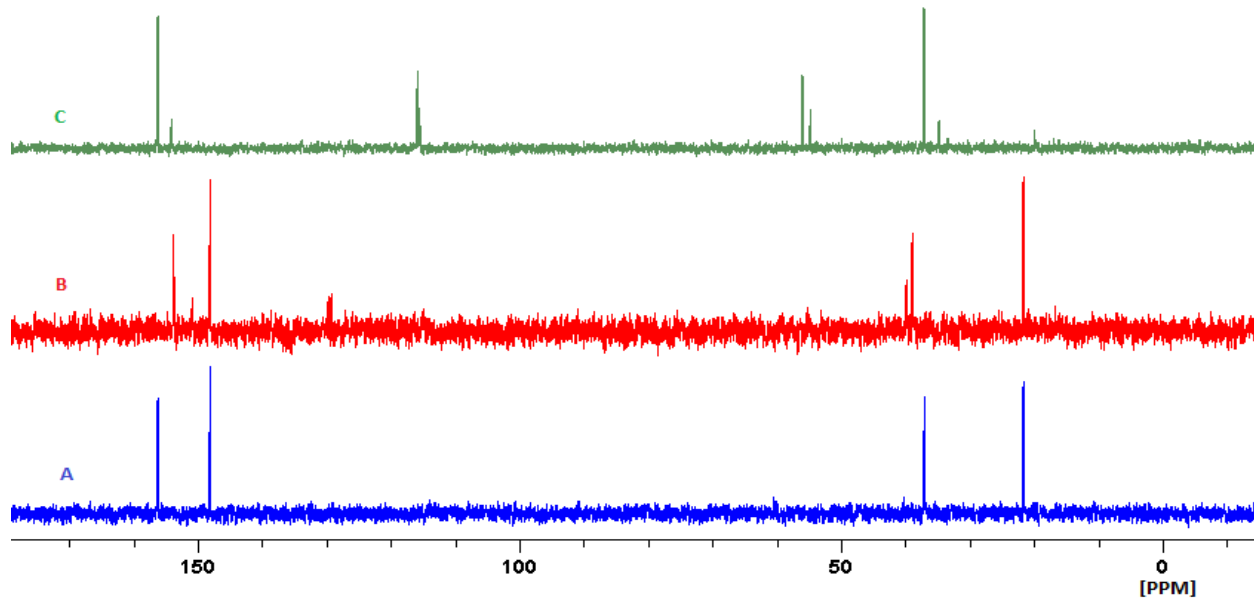
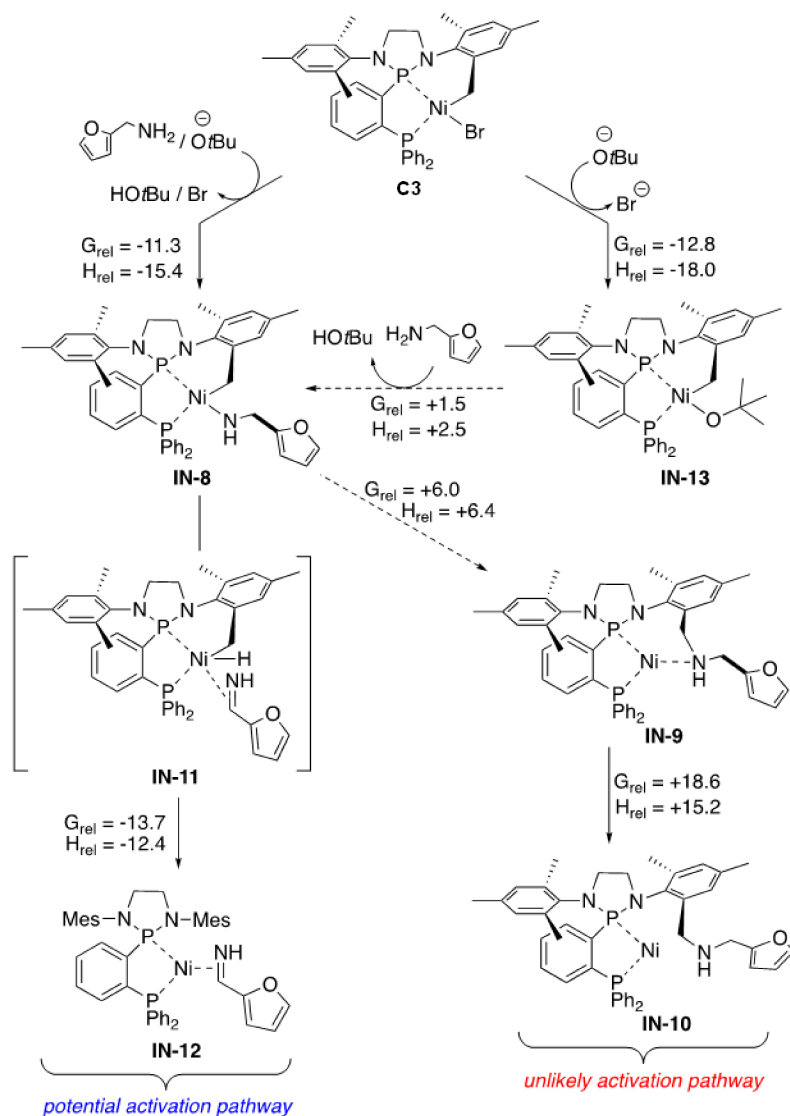


Figure 9: $^{31}\text{P}\{^1\text{H}\}$ NMR data for the stoichiometric experiments on the activation of **C3** employing d_8 -toluene and no COD. Reaction **A** performed with 2 equivalents of $\text{NaO}(t\text{-Bu})$. Reaction **B** performed with 2 equiv. $\text{NaO}(t\text{-Bu})$ and 1 equiv furfurylamine. Reaction **C** performed with 2 equiv. $\text{NaO}(t\text{-Bu})$, 1 equiv furfurylamine and 1 equiv 1-chloronaphthalene.

2.3.8 Computational Investigation into the Reactivity of **C3**

We then undertook computational studies to model the activation of **C3**. Presumably **C3** navigates to a common L_nNi^0 intermediate accessed by **C1**, given their similar reactivity profiles (*vide supra*). The first activation pathway considered involves reaction of furfurylamine and *tert*-butoxide to yield **IN-8**, followed by $C(sp^3)$ -N reductive elimination to form an N-coordinated **IN-9** species. While formation of **IN-8** was calculated to be quite favorable ($G_{rel} = -11.3 \text{ kcal mol}^{-1}$, $H_{rel} = -15.4 \text{ kcal mol}^{-1}$), the C_{sp^3} -N reductive elimination to form **IN-9** was both endergonic ($G_{rel} = +6.0 \text{ kcal mol}^{-1}$) and endothermic ($H_{rel} = +6.4 \text{ kcal mol}^{-1}$). Furthermore, decoordination of the furfurylamine bound mesityl side arm to open up a coordination site (**IN-10**) for starting material complexation is severely disfavored ($G_{rel} = +18.6 \text{ kcal mol}^{-1}$, $H_{rel} = +15.2 \text{ kcal mol}^{-1}$), thus it is unlikely such an activation pathway is responsible for the observed activity of **C3**. Alternatively, **IN-8** could undergo β -hydride elimination to form **IN-11**, followed by $C(sp^3)$ -H reductive elimination to restore the original framework of **L2** and yield an η^2 -furfurylimine Ni species **IN-12**, which could access the same **IN-2** intermediate proposed for the **L2** derived pathway (**Scheme 11**) *via* dissociation of furfurylimine.

Formation of **IN-12** was calculated to be quite favorable relative to **IN-8** ($G_{rel} = -13.7 \text{ kcal mol}^{-1}$, $H_{rel} = -12.4 \text{ kcal mol}^{-1}$), thus an activation pathway involving β -hydride elimination and subsequent $C(sp^3)$ -H reductive elimination may be responsible for the formation of catalytically active species starting from **C3**. Finally, based on spectroscopic analysis of stoichiometric reactions involving **C3**, which implicated the formation of *tert*-butoxy intermediates, we considered the possibility of accessing **IN-8** *via* initial reaction with *tert*-butoxide to form **IN-13**, followed by reaction with furfurylamine. Reaction with base to form **IN-13** is exergonic ($G_{rel} = -18.0 \text{ kcal mol}^{-1}$) and exothermic ($H_{rel} = -12.8 \text{ kcal mol}^{-1}$), and reaction with furfurylamine to form **IN-8** was only slightly disfavored ($G_{rel} = +1.5 \text{ kcal mol}^{-1}$, $H_{rel} = +2.5 \text{ kcal mol}^{-1}$), thus it is possible that **C3** activates *via* multiple pathways that both involve **IN-8**, and avoiding the formation of *tert*-butoxy intermediates such as **IN-13** could lead to more productive catalysis.



Scheme 11: Relative free-energies and enthalpies (kcal mol⁻¹) calculated by DFT for various activation pathways from **C3**.

2.3.9 Conclusions

A series of new *ortho*-phenylene bridged bisphosphine ancillary ligands based on the *N*-heterocyclic phosphine (NHP) structural motif has been prepared and tested in nickel-catalyzed C(*sp*²)-N cross-coupling reactions. In the course of such studies, an ancillary ligand variant featuring a saturated NHP group paired with an adjacent diphenylphosphino donor group (i.e., NHP-DalPhos, **L2**) emerged as being particularly effective in transformations of primary alkylamines. Subsequent application of the derived pre-catalyst (NHP-DalPhos)NiCl(*o*-tolyl) (**C1**) allowed for room-temperature cross-couplings of primary alkylamines with (hetero)aryl chlorides

or bromides to be achieved – a typically challenging class of reactions for which only PAd-DalPhos, **L7**^{40b} and CyPAd-DalPhos⁵⁴ have proven capable with broadly useful scope. In comparing the catalytic behavior of **L2** and **L7** in such transformations, nickel catalysts derived from the latter were found to out-perform the former to a modest extent on the basis of the catalyst turnover number and frequency; this trend can be attributed in part to a larger barrier to C(*sp*²)-N bond reductive elimination in the case of **L2**, as evidenced by the results of our DFT computational studies reported herein. In addition to establishing for the first time the utility of NHP-derived bisphosphines in challenging nickel-catalyzed C(*sp*²)-N cross-couplings, the work presented herein contributes toward advancing our understanding of the key design parameters associated with the rational development of ancillary ligands for such synthetically useful transformations.

2.4 Experimental Section

2.4.1 General Considerations

Unless otherwise indicated, all experimental procedures were conducted in a nitrogen-filled, inert-atmosphere glovebox using oven-dried glassware and purified solvents, with the exception of the workup of catalytic reaction mixtures which was conducted on the bench-top in air using unpurified solvents. Toluene and pentane were purged with nitrogen and passed through a double-column purification system containing alumina and copper-Q5 reactant. Diethyl ether and tetrahydrofuran (THF) were dried over Na/benzophenone and distilled under a nitrogen atmosphere. Dichloromethane (DCM) and acetonitrile were purged with nitrogen, while deuterated NMR solvents were freeze-pump-thaw degassed three times. In all cases, solvents purified as outlined above for use within the glovebox were stored over activated 4 Å molecular sieves in bulbs fitted with Teflon taps for a minimum of 24 h prior to use. 2-Chloro-1,3-dimesityl-1,3,2-diazaphospholidine,⁸¹ 2-bromo-1,3-dimesityl-1,3,2-diazaphospholene,⁸² and 4-butylphenyl tosylate⁵⁴ were prepared according to established literature procedures. Otherwise, all other solvents, reagents, and materials were used as received from commercial sources. Flash chromatography was carried out on silica gel using Silicycle SiliaFlash 60 silica (particle size 40–63 μm; 230–400 mesh), with the exception of the large-scale synthesis of **1a**, where automated flash chromatography was carried out on a Biotage Isolera One automated flash purification system using 100 g Biotage SNAP KP-SIL (particle size 30–90 μm) with a gradient of 2–8–2 column volumes and a flow rate of 40 mL/min. Unless otherwise indicated, NMR spectra were recorded on a Bruker AV 300 MHz or Bruker AV 500 MHz spectrometer at 300 K, with chemical

shifts (in ppm) referenced to residual protio solvent peaks (^1H), deuterated solvent peaks ($^{13}\text{C}\{^1\text{H}\}$), or external 85% H_3PO_4 ($^{31}\text{P}\{^1\text{H}\}$). Splitting patterns are indicated as follows: br, broad; s, singlet; d, doublet; t, triplet; q, quartet; m, multiplet. All coupling constants (J) are reported in hertz (Hz). In some cases, fewer than expected carbon resonances were observed despite prolonged acquisition times. Elemental analyses were performed by Galbraith Laboratories, Inc., Knoxville, TN. Mass spectra were obtained using ion trap electrospray ionization (ESI) instruments operating in positive mode. Gas chromatography (GC) data were obtained on an instrument equipped with a SGE BP-5 column (30 m, 0.25 mm i.d.).

Synthesis of L1. A glass vial was charged with (2-bromophenyl)dicyclohexylphosphine (0.253 g, 0.716 mmol), diethyl ether (4 mL), a magnetic stir bar and was cooled to $-30\text{ }^\circ\text{C}$. Magnetic stirring of the solution was initiated, resulting in a clear and colorless solution. To this mixture was added 2.5 M $n\text{BuLi}$ in hexanes (0.300 mL, 0.752 mmol) leading to the immediate formation of a white opaque solution. The resulting mixture was warmed to room temperature and stirred for 1 h, forming a pale yellow and opaque solution. 2-Chloro-1,3-dimesityl-1,3,2-diazaphospholidine (0.272 g, 0.752 mmol) was added and the resulting solution was stirred for 48 h at room temperature. An opaque orange solution resulted. The solvent was removed *in vacuo*, yielding a pale yellow solid, which was washed with cold ($\sim 0\text{ }^\circ\text{C}$) pentane (3 x 1 mL). The off-white solid was recrystallized *via* slow evaporation of a hexanes solution (initially 5 mL) to afford the title compound as a white solid (0.184 g, 0.308 mmol, 43%). ^1H NMR (500 MHz; C_6D_6): δ 8.27 – 8.19 (m, 1H), 7.34 – 7.24 (m, 2H), 7.14 – 7.10 (m, 1H), 6.76 (br. s, 4H), 3.93 – 3.84 (m, 2H), 3.16 – 3.07 (m, 2H), 2.35 (very br., 12H), 2.15 (s, 6H), 1.84 (br. s, 3H), 1.72 (br. s, 3H), 1.54 (br. s, 2H), 1.45 (br. s, 4H), 1.34 – 1.30 (br. m, 2H), 1.09 (m, 4H), 0.99 – 0.91 (m, 2H), 0.57 (m, 2H). $^{13}\text{C}\{^1\text{H}\}$ NMR (125.8 MHz, C_6D_6): δ 155.7 (d, $J = 23.4$ Hz), 155.3 (d, $J = 23.5$ Hz), 140.8 – 140.4 (overlapping signals), 137.5, 134.4, 132.4, 131.2 (d, $J = 7.5$ Hz), 130.0 (d, $J = 4.0$ Hz), 129.5, 127.9, 127.1, 52.2 (d, $J = 6.0$ Hz), 34.2 – 34.0 (overlapping signals), 30.2 (d, $J = 16.6$ Hz), 28.8 (d, $J = 10.2$ Hz), 27.1 (d, $J = 11.5$ Hz), 27.0 (d, $J = 8.3$ Hz), 26.3, 20.6 – 20.2 (overlapping signals). $^{31}\text{P}\{^1\text{H}\}$ (202.4 MHz, CDCl_3): δ 86.1 (d, $J = 185.7$ Hz, 1P), -13.5 (br. m, 1P). HRMS-ESI (m/z): Calc'd for $\text{C}_{38}\text{H}_{53}\text{N}_2\text{P}_2$ [$\text{M}+\text{H}$] $^+$: 599.3678. Found: 599.3522.

Synthesis of L2 (NHP-DalPhos). A glass vial was charged with (2-bromophenyl)diphenylphosphine (1.00 g, 2.93 mmol), diethyl ether (10 mL), a magnetic stirbar,

and was cooled to -30 °C. Magnetic stirring of the solution was initiated, resulting in a clear and colorless solution. To this solution was added 2.5 M *n*BuLi in hexanes (1.23 mL, 3.08 mmol) leading to the immediate formation of a dark red solution. The resulting mixture was warmed to room temperature and stirred for 1 h, forming a dark red and opaque solution. The solvent was then removed *in vacuo* and the residue was washed with cold (~0 °C) pentane (3 x 8 mL) and subsequently dried *in vacuo*, affording a red residue. 2-Chloro-1,3-dimesityl-1,3,2-diazaphospholidine (1.11 g, 3.08 mmol) and toluene (10 mL) were consecutively added and the resulting solution was stirred for 48 h at room temperature. An opaque brown solution resulted. The mixture was filtered through a Celite/silica plug. The eluent was collected, from which the solvent was removed *in vacuo* to afford an off-white solid. This crude solid was triturated with cold (~0 °C) pentane (4 mL) and dried *in vacuo*, affording the title compound as a white solid (0.687 g, 1.17 mmol, 40%). ¹H NMR (500 MHz; C₆D₆): δ 8.20 (br. s, 1H), 7.24 (br. s, 1H), 7.02 (br. s, 6H), 6.88 (br. s, 6H), 6.71 (br. s, 4H), 3.85 (br. s, 2H), 3.10 (br. s, 2H), 2.29 (br. s, 12H), 2.13 (br. s, 6H). ¹³C{¹H} NMR (125.7 MHz, C₆D₆): δ 153.2 (d, *J* = 25.1 Hz), 152.8 (d, *J* = 25.1 Hz), 143.3 – 143.0 (overlapping signals), 141.1 (d, *J* = 14.9 Hz), 139.0 (d, *J* = 8.6 Hz), 138.9 (d, *J* = 8.6 Hz), 137.7, 135.0, 134.4 – 134.3 (overlapping signals), 131.0 (d, *J* = 7.3 Hz), 130.6, 130.0, 128.7, 128.5, 52.8 (d, *J* = 5.9 Hz), 21.2 – 20.8 (overlapping signals). ³¹P{¹H} (121.4 MHz, CDCl₃): δ 86.8 (d, *J* = 199.0 Hz, 1P), -15.5 (d, *J* = 199.0 Hz, 1P). HRMS-ESI (*m/z*): Calc'd for C₃₈H₄₁N₂P₂ [M+H]⁺ : 587.2739. Found: 587.2739.

Synthesis of L3. A glass vial was charged with (2-bromophenyl)di(*ortho*-tolyl)phosphine (0.400 g, 1.08 mmol), diethyl ether (4 mL), a magnetic stir bar and was cooled to -30 °C. Magnetic stirring of the solution was initiated, resulting in a clear and colorless solution. To this solution was added 2.5 M *n*BuLi in hexanes (0.455 mL, 1.14 mmol) leading to the immediate formation of an off-white and milky solution. The resulting mixture was warmed to room temperature and stirred for 1 h, forming a pale yellow and opaque solution. The solvent was removed *in vacuo* following stirring and the residue was washed with cold (~0 °C) pentane (3 x 3 mL) and subsequently dried *in vacuo*, affording a pale yellow residue. 2-Chloro-1,3-dimesityl-1,3,2-diazaphospholidine (0.410 g, 1.14 mmol) and toluene (4 mL) were added consecutively and the resulting solution was stirred for 48 h at room temperature. An opaque yellow solution resulted. The mixture was cooled to -30 °C and then filtered through a Celite/silica plug. The eluent was collected and the solvent was

removed *in vacuo* to afford an off-white solid. The crude material was dissolved in DCM, cooled to -30 °C and filtered through a Celite/silica plug. The eluent was collected and the solvent was removed *in vacuo* to yield a white solid (0.194g, 0.316 mmol, 29%). ¹H NMR (500 MHz; C₆D₆): δ 8.18 – 8.10 (m, 1H), 7.41 – 7.36 (m, 1H), 7.15 (t, *J* = 7.4 Hz, 1H), 7.09 – 7.04 (m, 2H), 7.04 – 6.99 (m, 2H), 6.80 (t, *J* = 7.3 Hz, 2H), 6.69 (br. s, 5H), 6.52 (dd, *J* = 3.7, 7.4 Hz, 2H), 4.18 – 4.10 (m, 2H), 3.44 – 3.37 (m, 2H), 2.20 (s, 6H), 2.15 (br. s, 12H), 2.03 (s, 6H). ¹³C{¹H} NMR (125.7 MHz, C₆D₆): δ 152.4 (d, *J* = 24.5 Hz), 152.0 (d, *J* = 24.5 Hz), 142.1 (d, *J* = 26.8 Hz), 141.2 (d, *J* = 14.2 Hz), 140.9 (d, *J* = 14.1 Hz), 137.0, 136.2 (d, *J* = 8.9 Hz), 136.1 (d, *J* = 9.0 Hz), 134.2, 133.3, 133.2 (d, *J* = 4.8 Hz), 130.9 (d, *J* = 7.4 Hz), 129.5, 129.4 (d, *J* = 4.9 Hz), 129.2, 128.3, 127.8, 127.7, 125.5, 52.2 (d, *J* = 5.8 Hz), 21.0 – 20.1 (overlapping signals). ³¹P{¹H} (121.4 MHz, CDCl₃): δ 87.6 (d, *J* = 199.6 Hz, 1P), -28.1 (d, *J* = 199.6 Hz, 1P). HRMS-ESI (*m/z*): Calc'd for C₄₀H₄₅N₂P₂ [M+H]⁺ : 615.3052. Found: 615.3052.

Synthesis of L4. A glass vial was charged with (2-bromophenyl)dicyclohexylphosphine (0.288 g, 0.815 mmol), diethyl ether (4 mL), a magnetic stir bar and was cooled to -30 °C. Magnetic stirring of the solution was initiated, resulting in a clear and colorless solution. To this solution was added 2.5 M *n*BuLi in hexanes (0.342 mL, 0.857 mmol) leading to the immediate formation of an opaque and white solution. The resulting mixture was warmed to room temperature and stirred for 1 h, forming a pale yellow and opaque solution. The solvent was then removed *in vacuo* and the residue was washed with cold (~0 °C) pentane (3 x 2 mL) and subsequently dried *in vacuo*, affording a pale yellow residue. 2-Bromo-1,3-dimesityl-1,3,2-diazaphospholene (0.345 g, 0.857 mmol) and toluene (4 mL) were added consecutively and the resulting solution was stirred for 48 h at room temperature. An opaque orange solution resulted. The mixture was filtered through a Celite/silica plug. The eluent was collected and the solvent was removed *in vacuo* to afford an orange solid. The crude solid was recrystallized from acetonitrile (7 mL) to afford the title product as an orange powder (0.185 g, 0.310 mmol, 38%). ¹H NMR (500 MHz; C₆D₆): δ 8.61 – 8.59 (m, 1H), 7.27 – 7.24 (m, 2H), 7.13 – 7.12 (m, 1H), 6.82 (br. s, 2H), 6.66 (br. s, 2H), 5.68 (s, 2H), 2.66 (br. s, 6H), 2.14 (s, 6H), 1.96 (br. s, 6H), 1.86 (br. s, 2H), 1.69 (br. s, 2H), 1.57 (br. s, 2H), 1.51 – 1.47 (m, 4H), 1.28 – 1.25 (m, 2H), 1.10 – 0.95 (m, 8H), 0.47 – 0.46 (m, 2H). ¹³C{¹H} NMR (125.7 MHz, C₆D₆): δ 152.2 (d, *J* = 27.1 Hz), 151.7 (d, *J* = 26.9 Hz), 140.9 (d, *J* = 14.5 Hz), 138.7 (d, *J* = 20.9 Hz), 138.5 (d, *J* = 20.8 Hz), 137.6, 136.8, 135.1, 133.0, 132.4 (d, *J* = 8.8 Hz), 130.4 (d, *J* = 27.1

Hz), 129.8, 120.3 (d, $J = 5.4$ Hz), 35.2 (d, $J = 5.9$ Hz), 35.1 (d, $J = 5.9$ Hz), 31.5 (d, $J = 17.6$ Hz), 29.4 (d, $J = 8.7$ Hz), 28.1, 27.9, 21.3, 20.8, 20.3. $^{31}\text{P}\{^1\text{H}\}$ (202.4 MHz, CDCl_3): δ 81.4 (d, $J = 192.1$ Hz, 1P), -13.9 (br. d, $J = 188.9$ Hz, 1P). HRMS-ESI (m/z): Calc'd for $\text{C}_{38}\text{H}_{51}\text{N}_2\text{P}_2$ $[\text{M}+\text{H}]^+$: 597.3522. Found: 597.3522.

Synthesis of L5. A glass vial was charged with (2-bromophenyl)diphenylphosphine (0.200 g, 0.587 mmol eq), diethyl ether (2 mL), a magnetic stir bar and was cooled to -30 °C. Magnetic stirring of the solution was initiated, resulting in a clear and colorless solution. To this solution was added 2.5 M *n*BuLi in hexanes (0.246 mL, 0.615 mmol) leading to the immediate formation of an opaque and white solution. The resulting mixture was warmed to room temperature and stirred for 1 h, forming a pale yellow and opaque solution. The solvent was then removed *in vacuo* and the residue was washed with cold (~ 0 °C) pentane (3 x 2 mL) and subsequently dried *in vacuo*, affording a pale yellow residue. 2-Bromo-1,3-dimesityl-1,3,2-diazaphospholene (0.248 g, 0.615 mmol) and toluene (2 mL) were consecutively added and the resulting solution was stirred for 48 h at room temperature. An opaque dark orange solution resulted. The mixture was filtered through a Celite/silica plug. The eluent was collected and the solvent was removed *in vacuo* to afford a dark orange residue. The crude material was washed with pentane (3 x 3 mL) and dried *in vacuo* to afford the title compound as an orange solid (0.130 g, 0.222 mmol, 38%). ^1H NMR (500 MHz; C_6D_6): δ 8.51 – 8.47 (m, 1H), 7.21 (doublet of triplets, $J = 7.3, 0.8$ Hz, 1H), 7.05 – 6.93 (overlapping multiplets, 12H), 6.84 – 6.61 (br. m, 4H), 5.70 – 5.68 (m, 2H), 2.58 (br. s, 6H), 2.14 (s, 6H), 1.92 (br. s, 6H). $^{13}\text{C}\{^1\text{H}\}$ NMR (125.7 MHz, C_6D_6): δ 148.4 (d, $J = 27.9$ Hz), 148.0 (d, $J = 28.1$ Hz), 140.4 (d, $J = 14.0$ Hz), 139.8 (d, $J = 14.4$ Hz), 139.6 (d, $J = 14.3$ Hz), 138.5 (d, $J = 7.2$ Hz), 138.4 (d, $J = 7.1$ Hz), 137.2 (d, $J = 12.4$ Hz), 135.3, 134.7, 134.6, 134.4, 131.6 (d, $J = 8.8$ Hz), 130.9, 130.5, 129.4, 128.9 (d, $J = 6.4$ Hz), 120.2 (d, $J = 5.4$ Hz), 21.4, 20.5. $^{31}\text{P}\{^1\text{H}\}$ (202.4 MHz, CDCl_3): δ 82.8 (d, $J = 195.4$ Hz, 1P), -15.4 (d, $J = 195.3$ Hz). HRMS-ESI (m/z): Calc'd for $\text{C}_{38}\text{H}_{39}\text{N}_2\text{P}_2$ $[\text{M}+\text{H}]^+$: 585.2583. Found: 585.2583.

Synthesis of L6. A glass vial was charged with (2-bromophenyl)di(*ortho*-tolyl)phosphine (0.400 g, 1.08 mmol), diethyl ether (4 mL), a magnetic stir bar and was cooled to -30 °C. Magnetic stirring of the solution was initiated, resulting in a clear and colorless solution. To this mixture was added

2.5 M *n*BuLi in hexanes (0.455 mL, 1.14 mmol) leading to the immediate formation of an opaque and white solution. The resulting mixture was warmed to room temperature and stirred for 1 h, forming a pale yellow and opaque solution. The solvent was removed *in vacuo* and the residue was washed with cold (~0 °C) pentane (3 x 2 mL) and subsequently dried *in vacuo*, affording a pale yellow residue. 2-Bromo-1,3-dimesityl-1,3,2-diazaphospholene (0.459 g, 1.14 mmol) and toluene (4 mL) were consecutively added and the resulting solution was stirred for 48 h at room temperature. An opaque orange solution resulted. The mixture was filtered through a Celite/silica plug. The eluent was collected and the solvent was removed *in vacuo* to afford an orange residue. The crude material was washed with pentane (3 x 3 mL) and dried *in vacuo* to afford the title compound as an orange solid (0.094 g, 0.153 mmol, 14%). ¹H NMR (500 MHz; C₆D₆): δ 8.61 – 8.57 (m, 1H), 7.23 – 7.18 (m, 1H), 6.97 – 6.92 (overlapping multiplets, 4H), 6.90 – 6.86 (m, 2H), 6.85 – 6.79 (overlapping multiplets, 4H), 6.76 – 6.53 (br. overlapping multiplets, 4H), 5.69 – 5.68 (m, 2H), 2.54 (br. s, 6H), 2.09 (s, 6H), 2.07 (s, 6H), 1.94 (br. s, 6H). ¹³C{¹H} NMR (125.7 MHz, C₆D₆): δ 149.1 (d, *J* = 26.3 Hz), 148.7 (d, *J* = 26.2 Hz), 143.2 (d, *J* = 26.3 Hz), 140.2 (d, *J* = 14.5 Hz), 138.9 (d, *J* = 13.2 Hz), 138.6 (d, *J* = 13.1 Hz), 136.7 (d, *J* = 7.3 Hz), 136.6 (d, *J* = 7.4 Hz), 135.1, 134.3, 134.1 (d, *J* = 3.6 Hz), 132.4 (d, *J* = 8.1 Hz), 131.1, 130.8 (d, *J* = 4.5 Hz), 130.5, 129.3, 129.2, 128.9, 126.7, 120.5 (d, *J* = 4.2 Hz), 21.7, 21.6, 21.3, 20.8, 20.4 (br. m). ³¹P{¹H} (202.4 MHz, CDCl₃): δ 81.9 (d, *J* = 193.4 Hz, 1P), -28.7 (d, *J* = 193.4 Hz, 1P). HRMS-ESI (*m/z*): Calc'd for C₄₀H₄₃N₂P₂ [M+H]⁺ : 613.2896. Found: 613.2896.

Synthesis of (L2)NiCl₂. A glass vial was charged with NiCl₂(DME) (0.017 g, 0.078 mmol), L2 (0.048 g, 0.082 mmol), THF (0.782 mL) and a magnetic stir bar before being sealed with a cap containing a PTFE septum. The reaction mixture was magnetically stirred at 25 °C for 3 h, affording an opaque orange solution. The solvent was removed *in vacuo*, affording a reddish orange solid which was washed with cold (~0 °C) pentane (3 x 1 mL). The crude residue was dissolved in DCM (1 mL) and quickly filtered through a Celite plug. The solvent was removed *in vacuo* and the dark orange residue washed with pentane (3 x 1 mL) and dried *in vacuo* to afford the title compound as an orange powder (0.047 g, 0.066 mmol, 85%). ³¹P{¹H} (202.4 MHz, 1,1,2,2-Tetrachloroethane-*d*₂): δ 111.6 (d, *J* = 75.5 Hz), 58.0 (d, *J* = 75.2 Hz). Anal. Calc'd for C₃₈H₄₀Cl₂N₂NiP₂ : C, 63.72; H, 5.63; N, 3.91. Found : C, 63.54; H, 5.71; N, 3.88.

Synthesis of (L1)NiCl₂. A glass vial was charged with NiCl₂(DME) (0.018 g, 0.083 mmol), **L1** (0.050 g, 0.084 mmol), THF (0.800 mL) and a magnetic stir bar before being sealed with a cap containing a PTFE septum. The reaction mixture was magnetically stirred at 25 °C for 3 h, affording an opaque dark orange solution. The solvent was removed *in vacuo*, affording an orange solid which was washed with cold (~0 °C) pentane (3 x 1 mL). The crude residue was dissolved in DCM (1 mL) and quickly filtered through a Celite plug. The solvent was removed *in vacuo* and the orange residue washed with pentane (3 x 1 mL) and dried *in vacuo* to afford the title compound as an orange powder (0.057 g, 0.078 mmol, 98%). ³¹P{¹H} (121.4 MHz, CDCl₃): δ 111.6 (d, *J* = 66.8 Hz), 77.2 (d, *J* = 66.8 Hz).

Synthesis of (L4)NiCl₂. A glass vial was charged with NiCl₂(DME) (0.014 g, 0.064 mmol), **L4** (0.040 g, 0.067 mmol), THF (0.638 mL) and a magnetic stir bar before being sealed with a cap containing a PTFE septum. The reaction mixture was magnetically stirred at 25 °C for 3 h, affording an opaque dark red solution. The solvent was removed *in vacuo*, affording a dark purple solid which was washed with cold (~0 °C) pentane (3 x 1 mL). The crude residue was dissolved in DCM (1 mL) and quickly filtered through a Celite plug. The solvent was removed *in vacuo* and the dark purple residue washed with pentane (3 x 1 mL) and dried *in vacuo* to afford the title compound as dark purple powder (0.045 g, 0.062 mmol, 96%). ³¹P{¹H} (202.4 MHz, CDCl₃): δ 110.9 (d, *J* = 48.0 Hz), 80.3 (d, *J* = 48.0 Hz).

Synthesis of (L6)NiCl₂. A glass vial was charged with NiCl₂(DME) (0.0043 g, 0.020 mmol), **L6** (0.0126 g, 0.021 mmol), THF (0.250 mL) and a magnetic stir bar before being sealed with a cap containing a PTFE septum. The reaction mixture was magnetically stirred at 25 °C for 3 h, affording an opaque dark purple solution. The solvent was removed *in vacuo*, affording a dark purple solid which was washed with cold (~0 °C) pentane (3 x 1 mL). The crude residue was dissolved in DCM (1 mL) and quickly filtered through a Celite plug. The solvent was removed *in vacuo* and the dark purple residue washed with pentane (3 x 1 mL) and dried *in vacuo* to afford the title compound as dark purple powder (0.0138 g, 0.018 mmol, 90%). ³¹P{¹H} (202.4 MHz, CDCl₃): δ 104.7, 53.3.

Synthesis of C1. A glass vial was charged with (TMEDA)NiCl(o-tolyl) (0.049 g, 0.162 mmol), **L2** (0.100 g, 0.170 mmol), THF (3.2 mL), and a magnetic stir bar, forming a clear orange solution upon initiation of stirring. The vial was sealed with a cap containing a PTFE septum, magnetic

stirring was initiated, and the mixture was heated to 65 °C for 3 h. A clear amber solution resulted. The reaction mixture was allowed to cool to room temperature and pentane (13 mL) was added, resulting in the immediate formation of an opaque orange solution. The solution was stirred at room temperature for 3 h. An opaque yellow suspension formed while stirring. The solvent was removed *in vacuo* yielding a bright yellow residue, which was washed with cold (~0 °C) pentane (3 x 3 mL) and dried *in vacuo* affording the title compound as a yellow solid (0.123 g, 0.159 mmol, 98%). ¹H NMR (500 MHz; THF-*d*₈): δ 8.27 – 8.21 (m, 1H), 7.61 – 7.52 (overlapping multiplets, 3H), 7.43 – 7.35 (m, 2H), 7.34 – 7.28 (m, 1H), 7.26 – 7.20 (m, 1H), 7.16 – 7.09 (m, 2H), 7.06 (s, 1H), 6.98 – 6.92 (m, 2H), 6.82 (s, 1H), 6.69 (s, 1H), 6.55 (m, 1H), 6.50 (s, 1H), 6.39 (m, 2H), 6.32 (m, 1H), 6.19 (m, 1H), 6.07 (m, 1H), 4.39 – 4.32 (m, 1H), 4.18 – 4.09 (m, 1H), 3.98 – 3.91 (m, 2H), 2.96 (s, 3H), 2.75 (s, 3H), 2.33 (s, 3H), 2.16 (s, 3H), 1.97 (s, 3H), 1.38 (s, 3H), 1.09 (s, 3H). ¹³C{¹H} NMR (125.7 MHz, THF-*d*₈): δ 158.8 (d, *J* = 39.3 Hz), 158.0 (d, *J* = 39.5 Hz), 155.6 (d, *J* = 19.5 Hz), 155.3 (d, *J* = 19.8 Hz), 144.3, 140.3, 139.0 (d, *J* = 10.7 Hz), 138.7 (d, *J* = 38.6 Hz), 138.5, 138.3 (d, *J* = 38.3 Hz), 138.2, 137.3 (d, *J* = 11.6 Hz), 136.0, 135.9, 134.8, 133.6 (d, *J* = 12.0 Hz), 133.2 (d, *J* = 9.1 Hz), 132.0, 131.8 (d, *J* = 14.8 Hz), 131.5, 131.5 (d, *J* = 15.7 Hz), 130.7, 130.5 (d, *J* = 5.2 Hz), 130.2, 129.9 (d, *J* = 1.8 Hz), 129.2, 128.2 (d, *J* = 11.1 Hz), 128.0 (d, *J* = 6.3 Hz), 126.8 (d, *J* = 10.3 Hz), 121.6 (d, *J* = 8.1 Hz), 121.4, 51.4, 50.2, 23.0, 22.0, 21.1, 21.0, 20.0, 19.8, 19.3. ³¹P{¹H} (121.4 MHz, THF-*d*₈): δ 120.3 (d, *J* = 8.8 Hz, 1P), 57.0 (d, *J* = 8.8 Hz, 1P). Anal. Calcd for C₄₅H₄₇ClN₂NiP₂ : C, 70.01; H, 6.14; N, 3.63. Found : C, 70.16; H, 6.08; N, 3.56.

Synthesis of (L2)NiBr₂. A glass vial was charged with NiBr₂ (0.017 g, 0.078 mmol), L2 (0.048 g, 0.082 mmol), THF (0.782 mL) and a magnetic stir bar before being sealed with a cap containing a PTFE septum. The reaction mixture was magnetically stirred and heated to 65 °C for 2 h, and then allowed to stir at room temperature overnight. An opaque red solution formed. The solvent was removed *in vacuo*, affording a dark red solid that was washed with cold (~0 °C) pentane (3 x 1 mL). The crude material was dissolved in DCM (1 mL) and quickly filtered through a Celite plug. The solvent was removed *in vacuo* and the dark red residue washed with pentane (3 x 1 mL) and dried *in vacuo* to afford the title compound as a red powder (0.057 g, 0.071 mmol, 90%). ³¹P{¹H} (202.4 MHz, 1,1,2,2-Tetrachloroethane-*d*₂): δ 122.5 (d, *J* = 63.7 Hz), 63.6 (d, *J* = 62.7 Hz). Anal. Calcd for C₃₈H₄₀Br₂N₂NiP₂ : C, 56.68; H, 5.01; N, 3.48. Found : C, 56.52; H, 5.13; N, 3.32.

Synthesis of C2. A glass vial was charged with (L2)NiBr₂ (0.523 g, 0.653 mmol), THF (4 mL), a magnetic stir bar and cooled to 0 °C. Magnetic stirring was initiated, resulting in an opaque red solution. To this mixture was added 2-mesitylmagnesium bromide (1.0 M in THF; 0.653 mL, 0.653 mmol) dropwise, leading to a clear and dark red solution. The reaction mixture was allowed to warm to room temperature with continued stirring for 18 h. Following this, MeOH (1 mL) was added, the reaction was stirred for 5 minutes, and the solvent was removed *in vacuo*. A rust red residue was obtained. The resulting solid was washed with pentane (3 x 3 mL), diethyl ether (3 x 3 mL) and dried *in vacuo* to afford an orange solid (0.043 g, 0.051 mmol, 77%; ~90% pure C2 with C3 as a contaminant). ¹H NMR (500 MHz; C₆D₆): δ 7.92 – 7.88 (m, 1H), 7.09 (t, *J* = 7.2 Hz, 1H), 7.04 – 6.95 (overlapping multiplets, 9H), 6.87 – 6.81 (overlapping multiplets, 5H), 6.62 (s, 2H), 6.25 (d, *J* = 2.0 Hz, 2H), 3.76 – 3.70 (overlapping multiplets, 4H), 3.13 (s, 6H), 2.12 (s, 6H), 2.10 (s, 3H), 2.07 (s, 6H), 1.65 (s, 6H). ¹³C{¹H} NMR (125.7 MHz, C₆D₆): δ 157.8 (d, *J* = 16.8 Hz), 157.5 (d, *J* = 16.8 Hz), 150.6 (d, *J* = 32.2 Hz), 149.7 (d, *J* = 31.5 Hz), 143.8, 140.6, 139.7 (d, *J* = 36.8 Hz), 139.3 (d, *J* = 36.6 Hz), 139.3 (d, *J* = 11.0 Hz), 137.9, 136.7, 134.8 (d, *J* = 10.3 Hz), 133.2 (d, *J* = 14.1 Hz), 132.4 (d, *J* = 14.4 Hz), 132.2 (d, *J* = 16.3 Hz), 131.8, 131.7, 131.2, 131.0 (d, *J* = 4.9 Hz), 130.4, 130.1, 128.9, 128.2 (d, *J* = 10.2 Hz), 52.0, 25.7, 23.1, 22.5, 21.4, 21.1. ³¹P{¹H} (202.4 MHz, C₆D₆): δ 115.8 (major), 115.4 (minor), 51.3 (major), 50.0 (minor).

Characterization Data for Crystalline C3: ³¹P{¹H} (202.4 MHz, C₆D₆): 156.3 (d, *J* = 14.9 Hz), 37.2 (d, *J* = 14.7 Hz). Anal. Calcd for C₃₈H₃₉BrN₂NiP₂ : C, 63.02; H, 5.43; N, 3.87. Found : C, 63.13; H, 5.29; N, 4.05.

General Procedure for Ancillary Ligand Screening. The following procedure was adapted from the literature.^{13d} In a nitrogen-filled glovebox, bis(cyclooctadiene)nickel(0) (0.0017 g, 0.006 mmol, 5 mol%), L1-L8 (0.006 mmol), base (1.5 – 2 equiv), (hetero)aryl halide (0.12 mmol, 1 equiv), dodecane (0.0273 mL, 0.12 mmol) and toluene or CPME (1 mL) were placed in a screw-capped vial containing a magnetic stir bar, followed by the addition of amine (1.1-1.5 equiv). The vial was sealed with a cap containing a PTFE septum, removed from the glovebox, and placed in a temperature-controlled aluminum heating block set either to 100 °C (CPME) or 110 °C (toluene) for 16 h under the influence of magnetic stirring. After this time, the vial was cooled to room temperature, and then EtOAc (100 μL) was added to the reaction mixture. A 200 μL aliquot of the reaction mixture was filtered through a Celite/silica plug and diluted with EtOAc (1.5 mL) prior

to analysis by use of calibrated gas chromatographic methods using dodecane as an internal standard. Reactions with furfurylamine (1.1 equiv) used toluene and NaO(*t*-Bu) (2 equiv), reactions with morpholine (1.5 equiv) used CPME and LiO(*t*-Bu) (1.5 equiv), and reactions with indole (1.1 equiv) used toluene and NaO(*t*-Bu) (1.5 equiv).

General Procedure for *N*-Arylation of Primary Alkylamines with (Hetero)aryl Halides at Room Temperature. In a nitrogen-filled glovebox, precatalyst **C1** (5 mol%), NaO(*t*-Bu) (1.5 - 2 equiv), (hetero)aryl halide (1.0 equiv), a magnetic stir bar, toluene and amine (1.1 equiv) were consecutively added to a screw-capped 4 dram vial. The vial was sealed with a cap containing a PTFE septum, and the reaction mixture was stirred at 25 °C for 16 h (unoptimized). Following this, the vial was removed from the glovebox, the crude mixture was diluted with EtOAc (30 mL) and washed with a saturated NaCl solution (3 x 30 mL). The organic layer was isolated and dried over anhydrous sodium sulfate. The mixture was filtered, the eluent collected and the solvent removed via rotary evaporation. The resulting residue was purified via flash column chromatography on silica gel. See the Appendix for complete reaction-specific details.

General Procedure for (Pseudo)halide Competition Study. A screw-capped glass vial was charged with **C1** (0.0046 g, 0.006 mmol, 5 mol%), NaO(*t*-Bu) (0.0231 g, 0.24 mmol), aryl halide 1 (0.12 mmol, 1 equiv), aryl (pseudo)halide 2 (0.12 mmol, 1 equiv), toluene (1 mL), dodecane (0.0273 mL, 0.12 mmol), a magnetic stir bar, and furfurylamine (0.0117 mL, 0.132 mmol) consecutively in a nitrogen-filled glovebox. The vial was capped with a cap containing a PTFE septum and the reaction mixture stirred for 16 h at room temperature (unoptimized). After this time, the vial was removed from the glovebox, and then EtOAc (100 µL) was added to the reaction mixture. A 200 µL aliquot of the reaction mixture was filtered through a Celite/silica plug and diluted with EtOAc (1.5 mL) prior to analysis by use of calibrated gas chromatographic methods employing dodecane as an internal standard.

Large-Scale Synthesis of 1a: In a nitrogen-filled glovebox, an oven-dried 100 mL round-bottom flask was charged with **C1** (207.6 mg, 0.269 mmol), NaO(*t*-Bu) (1.033 g, 10.75 mmol), 1-chloronaphthalene (732 µL, 5.37 mmol), toluene (45 mL), and furfurylamine (522 µL, 5.91 mmol), followed by a magnetic stir bar. The flask was sealed with a glass stopcock, and the reaction mixture was stirred at room temperature for 16 h (unoptimized). Following this, the flask was removed from the glovebox, the crude mixture was diluted with EtOAc (200 mL) and washed with

a saturated NaCl solution (3 x 200 mL). The organic layer was isolated and dried over anhydrous sodium sulphate. The mixture was filtered, and the filtrate was concentrated to ~10 mL under reduced pressure. The resulting brown-orange mixture was purified by automated flash chromatography (100 g Biotage SNAP KPSIL cartridge, 0-10% EtOAc in hexanes, 40 mL/min flow rate), affording the title compound as a pale yellow oil (1.128 g, 94%).

General Procedure for Stoichiometric Study of C3. A screw-capped glass vial was charged with **C3** (0.0200 g, 0.028 mmol), NaO(*t*-Bu) (0.0053 g, 0.055 mmol), 1-chloronaphthalene (0.028 mmol, 0.0037 mL, *if required*), toluene (0.750 mL), a magnetic stir bar, and furfurylamine (0.0024 mL, 0.028 mmol, *if required*) consecutively in a nitrogen-filled glovebox. The vial was capped with a cap containing a PTFE septum and the reaction mixture stirred for 45 minutes at room temperature. After this time, COD (0.0034 mL, 0.028 mmol) was added if required and the reaction was stirred a further 15 minutes. Following this, the sample was taken up in an NMR tube, capped and sealed with PTFE tape in the glovebox, and subjected to analysis via $^{31}\text{P}\{^1\text{H}\}$ NMR.

Chapter 3 - Development of 1,1-Bisdiazaphospholenyl Ferrocene Ligands for Nickel-Catalyzed C(*sp*²)-N Cross-Couplings

3.1 Contributions

This chapter describes the development of a new class of bisphosphine ligands containing two neutral NHP fragments for use in the nickel-catalyzed C(*sp*²)-N cross-coupling reactions. This project was initiated by the author, and at the time of writing remains incomplete. The author's contributions consist of the synthesis and characterization of the new ligands. Crystallographic data were collected, solved and refined by Dr. Robert McDonald and Dr. Michael Ferguson.

3.2 Introduction

Given the success of the NHP moiety in nickel-catalyzed C(*sp*²)-N cross-coupling reactions outlined in Chapter 2 (*vide supra*), we became interested in exploring alternate ligand architectures incorporating this fragment and a ferrocene backbone. Bulky bisphosphine ligands have shown excellent activity in nickel-catalyzed cross-coupling reactions (*vide supra*), and the ferrocene backbone is a privileged structural motif present in many bisphosphine ligands (see Chapter 2). It was envisioned that these new bis(NHP) ferrocene ligands might find success in areas where DPPF struggles, such as the C(*sp*²)-N cross-coupling of indoles under mild conditions or the coupling of secondary amides.

Prominent examples of ferrocene-containing phosphine ligands include QPhos, the JosiPhos ligand family (see Chapter 1), and DPPF. The monophosphine ligand QPhos has been used successfully as a general purpose ligand in palladium cross-coupling reactions, enabling Suzuki, BHA and C-O etherification reactions.⁸³ Amination reactions with QPhos have employed aryl bromide and chloride electrophiles alongside with simple primary, secondary aryl and alkyl amines at elevated temperatures. No successful examples of QPhos in analogous nickel-catalyzed amination reactions have been reported at the time of writing. Conversely, DPPF has demonstrated excellent activity in nickel amination reactions, finding particular utility in the cross-coupling of secondary amines and indole.^{39, 47b, c} Varying the PR₂ group of DPPF affords little improvement in performance, with the exception of 3,5-bis(CF₃)phenyl showing slightly better reactivity with challenging indole substrates relative to the parent phenyl structure.^{47c} An excess of steric bulk was found to hinder reactivity, with 1-naphthyl and *tert*-butyl derivatives performing poorly. This is in contrast to palladium-catalyzed aminations, where analogous *tert*-butyl DPPF derivatives

were found to increase reactivity,⁸⁴ further highlighting the importance of striking an appropriate balance of steric and electronic parameters when employing this architecture with nickel.

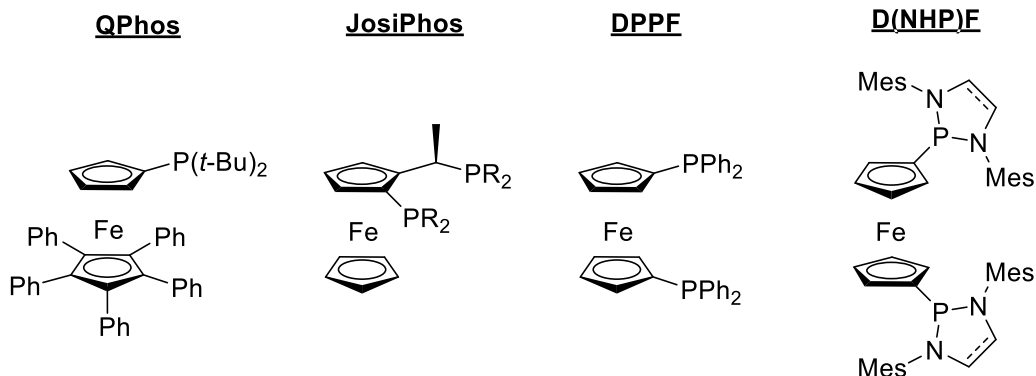


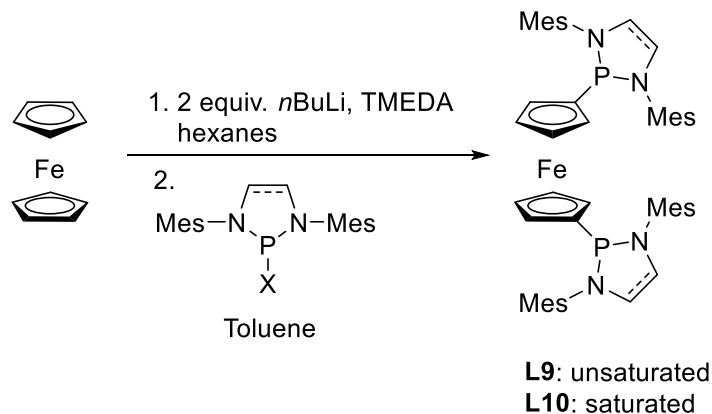
Figure 10: Some previously reported ferrocene containing ancillary ligands, and the new D(NHP)F framework reported

NHP containing variants of the privileged DPPF motif have also been successfully synthesized. Gudat and coworkers reported the synthesis and characterization of an unsaturated version of D(NHP)F shown in **Figure 10**, however no crystallographic data, coordination chemistry or reactivity of this species was reported.⁸⁵ We became intrigued as to how this type of bisphosphine motif would behave as a ligand in nickel-catalyzed $C(sp^2)$ -N cross-coupling reactions. Described below is the synthesis, spectroscopic and crystallographic characterization of two D(NHP)F bisphosphine compounds.

3.2 Results and Discussion

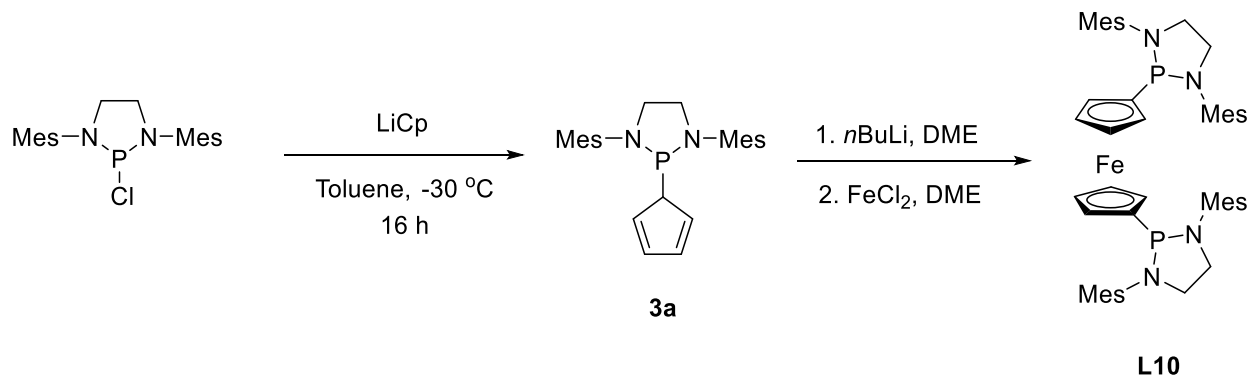
3.2.1 Ligand Synthesis

The synthesis of target ligands **L9** and **L10** was initially attempted via lithiation of ferrocene followed by quenching with an appropriate halo-phosphine fragment (**Scheme 12**). This methodology, though different than literature precedent, was effective in synthesizing the previously reported **L9**. The $^{31}P\{^1H\}$ NMR showed a diagnostic shift at 86 ppm, in keeping with literature values.⁸⁵ The 1H NMR spectrum is consistent with literature, where the C(mesityl) bond rotation is apparently slow on the NMR timescale, as exhibited by broadening of the Ar-H and *ortho*-methyl peaks of the mesityl fragments.



Scheme 12: Synthesis of **L9** and **L10** via lithiation of ferrocene

Conversely, the synthesis of **L10** via this route was unsuccessful, affording a mixture of starting material, alkylated phosphine and product. Purification attempts were hindered by the similar solubilities of the by-products and desired product. As such, an alternate synthetic route was explored to prevent formation of alkylated phosphine by-product, involving the formation of a *P*-cyclopentadienyl-substituted NHP intermediate (**Scheme 13**), as reported by Gudat and coworkers.⁸⁵ This allowed for increased product yields, though residual *P*-cyclopentadienyl-substituted NHP starting material remained challenging to remove fully. ³¹P{¹H} NMR of **L10** showed a diagnostic shift at 88 ppm, and the ¹H NMR spectrum showed similar broadening of the mesityl shifts as **L9**. At the time of writing, I was unable to cleanly isolate pure **L10** for acceptable spectroscopic analysis.



Scheme 13: Synthesis of **L10** via *P*-cyclopentadienyl-substituted 1,3,2-diazaphospholene route

3.2.2 Solid State Structures of Ligands

Though hindered by synthetic challenges, I was fortunate enough to grow high quality crystals for crystallographic assessment of both **L9** and **L10**. Both compounds exhibit a distorted trigonal pyramidal geometry about the phosphorus atoms, consistent with the cyclic nature of the NHP fragment and keeping with literature precedents.⁶⁶ **L10** exhibits a slightly longer average P-N bond than **L9**, whereas both the heterocyclic C-N and C-C bond lengths of the NHP moiety display shorter bond lengths for **L10** compared to **L9**, as expected. This same trend is observed for the NHP containing ligands described in Chapter 2.

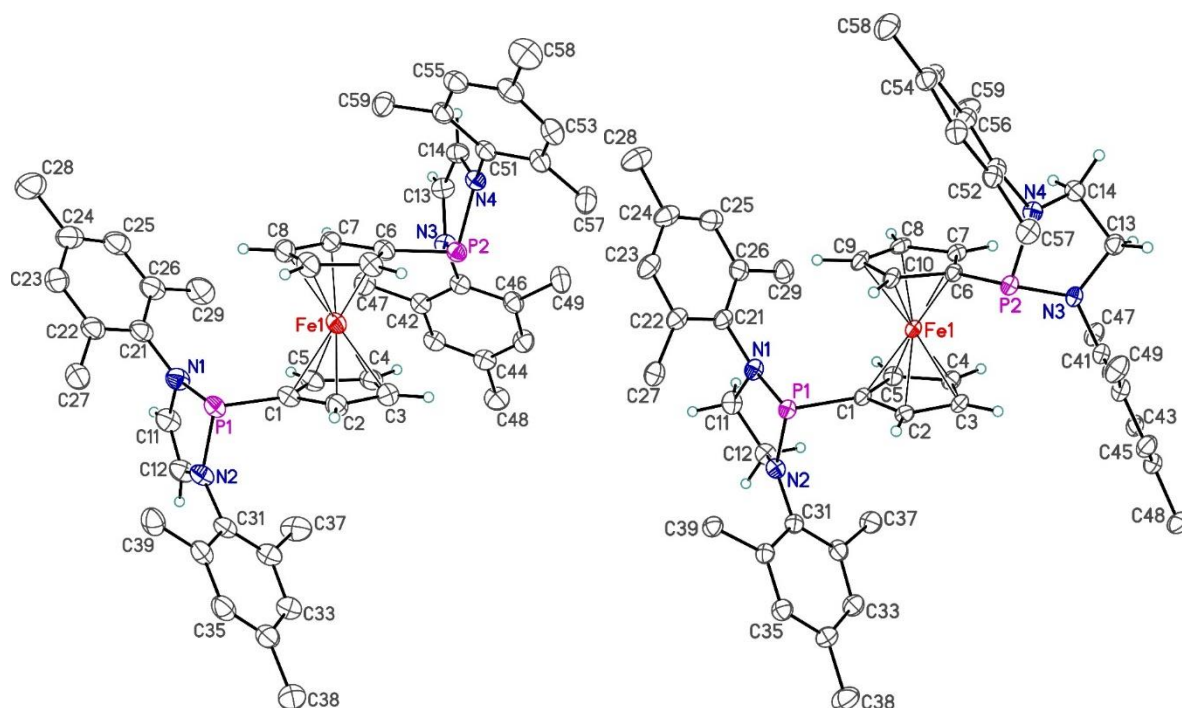


Figure 11: Single-crystal X-ray structures of **L9** (left) and **L10** (right), represented with thermal ellipsoids at the 30% probability level. Selected hydrogen atoms are omitted for clarity. Selected interatomic distances (Å) for **L9**: P2-N4: 1.7292(18); P2-C6: 1.8169(20); C11-C12: 1.324(3); C11-N1: 1.426(3). Selected interatomic distances (Å) for **L10**: P2-N4: 1.7125(20); P2-C6: 1.822(2); C11-C12: 1.510(4); C11-N1: 1.471(3)

3.3 Conclusions

In this chapter I was able to characterize crystallographically for the first time two 1,1-bisdiazaphospholenyl ferrocene species, **L9** and **L10**, which both exhibited distorted trigonal

pyramidal geometry about phosphorous. **L9**, though previously reported in the literature, was synthesized using a new route directly from ferrocene, whereas we were unsuccessful in synthesizing the new compound **L10** in high enough purity for spectroscopic analysis. Future work will need to address this shortcoming, in an effort to continue to build upon our ligand design theme of bulky and moderately electron-rich ligands for use in nickel-catalyzed C(*sp*²)-N cross-coupling catalysis with these ligands and future variants.

3.4 Experimental Section

3.4.1 General Considerations

Unless otherwise indicated, all experimental procedures were conducted in a nitrogen-filled, inert-atmosphere glovebox using oven-dried glassware and purified solvents. Toluene and pentane were purged with nitrogen and passed through a double-column purification system containing alumina and copper-Q5 reactant. Diethyl ether and tetrahydrofuran (THF) were dried over Na/benzophenone and distilled under a nitrogen atmosphere. Dichloromethane (DCM) and acetonitrile were purged with nitrogen, while deuterated NMR solvents and dimethylethoxide (DME) were freeze-pump-thaw degassed three times. In all cases, solvents purified as outlined above for use within the glovebox were stored over activated 4 Å molecular sieves in bulbs fitted with Teflon taps for a minimum of 24 h prior to use. 2-Chloro-1,3-dimesityl-1,3,2-diazaphospholidine⁸¹ and 2-bromo-1,3-dimesityl-1,3,2-diazaphospholene⁸² were prepared according to established literature procedures. The synthesis of **L10** was attempted following literature procedures.⁸⁵ Otherwise, all other solvents, reagents, and materials were used as received from commercial sources. Unless otherwise indicated, NMR spectra were recorded on a Bruker AV 300 MHz or Bruker AV 500 MHz spectrometer at 300 K, with chemical shifts (in ppm) referenced to residual protio solvent peaks (¹H), deuterated solvent peaks (¹³C{¹H}), or external 85% H₃PO₄ (³¹P{¹H}). Splitting patterns are indicated as follows: br, broad; s, singlet; d, doublet; t, triplet; q, quartet; m, multiplet. All coupling constants (*J*) are reported in hertz (Hz). In some cases, fewer than expected carbon resonances were observed despite prolonged acquisition times.

Synthesis of L9: A glass vial was charged with ferrocene (0.200 g, 1.08 mmol), TMEDA (0.338 mL, 2.26 mmol), hexanes (4.5 mL) and a magnetic stir bar. Magnetic stirring of the solution was initiated, resulting in a clear orange solution. To this mixture was added 2.5 M *n*BuLi in hexanes

(0.902 mL, 2.26 mmol) dropwise leading to the formation of an opaque orange solution over 3 hours. The resulting mixture was stirred overnight. A solution of 2-bromo-1,3-dimesityl-1,3,2-diazaphospholene (0.910 g, 2.26 mmol) in toluene (6mL) was cooled to -30 °C and added dropwise. The resulting opaque dark brown solution was stirred for 4 h at room temperature. The solvent was then removed *in vacuo*, yielding a brown residue, which was dissolved in DCM and filtered through a Celite/silica plug. The eluent was collected, from which the solvent was removed *in vacuo* to afford a dark orange solid. The solid was extracted with cold (~ 0 °C) hexanes (3 x 4 mL), and the solvent was removed *in vacuo* to afford an orange solid. The resulting material was recrystallized from hexanes (0.7 mL) at -30 °C to afford the title compound as an orange solid (0.094 g, 0.113 mmol, 10%). ¹H NMR (500 MHz; C₆D₆): δ 6.80 (br. s, 4H), 6.70 (br. s, 4H), 5.62 (s, 4H), 4.02 (m, 4H), 3.97 (m, 4H), 2.63 (br. s, 12H), 2.13 (br. s, 12H), 2.10 (s, 12H). ¹³C{¹H} NMR (125.8 MHz, C₆D₆): δ 138.8 (m, *J* = 7.0 Hz), 136.7, 136.1, 134.9, 130.0, 117.9, 84.0, 83.6, 71.7 (m, *J* = 17.5 Hz), 71.1, 20.8, 19.8. ³¹P{¹H} (202.4 MHz, C₆D₆): δ 86.4. Matches literature precedent.⁸⁵

Chapter 4 – Conclusions and Future Work

4.1 General Conclusions

I have successfully developed a series of NHP containing ligands and nickel complexes for use in nickel-catalyzed $C(sp^2)$ -N cross-coupling reactions. Following the establishment of PAd-DalPhos as the state-of-the-art ligand in challenging nickel-catalyzed amination reactions, we sought to build on this *ortho* phenylene bridged motif and explore new architectures encompassing a bulky, modestly electron-donating bisphosphine framework which would favour reductive elimination, the presumed rate-limiting step in the catalytic cycle. I opted to explore the NHP motif in this context to allow for steric and electronic variation of the ligand set. I developed both NHP-DalPhos and ferrocene bridged bisphosphines ligands (**L9** and **L10**) for use in room-temperature nickel-catalyzed $C(sp^2)$ -N cross-coupling reactions of primary amines and secondary amines, respectively. Notably, NHP-DalPhos joins a handful of ligand frameworks capable of promoting amination reactions with nickel. Though NHP-DalPhos was found to be less active than PAd-DalPhos in head-to-head reactivity comparisons, it does give credence to our idea of rational ligand design for nickel amination reactions; that is, making bulky and more modestly electron-donating bisphosphine ligands to favour reductive elimination. In moving forward, efforts will be directed towards teasing out the relative electronic and steric ligand requirements for particular substrate classes through thoughtful experimental, computational and mechanistic studies (*vide infra*).

From a broader perspective, nickel is still in its infancy relative to palladium for this chemistry, and work on understanding ligand trends and the mechanisms involved, notably off-cycle product formation, remains to be done. This is unfortunately not a simple process, as the current empirical ligand trends for nickel are challenging to rationalize, and the potential for a Ni(I)/Ni(III) cycle complicates the mechanistic picture. Exciting developments in the field of ligand design for nickel, such as Doyle's concept of remote steric hindrance,⁵⁶ Weix's use of pharmaceutical compound libraries for new ligands,⁵⁷ and Balcells' and Nova's computational work studying off-cycle species formation in cross-coupling reactions⁸⁶ have the potential for broad reaching applications in ligand design for nickel-catalyzed amination reactions.

4.2 Future Work

4.2.2 Chapter 2

As discussed in Chapter 2, NHP-DalPhos was less active than PAd-DalPhos in nickel-catalyzed $C(sp^2)$ -N cross-coupling reactions. In a bid to improve this, new and potentially more

active ligand variants could be developed. Notably, a series of electron-donating groups could be incorporated into the NHP backbone to alter the ligand electronic parameters. The rationale behind this is a comparison of Ni-Cl bond lengths in the dichloride complexes. The saturated cyclohexyl variant **L1**NiCl₂ has a longer Ni-Cl bond *trans* to the NHP fragment compared to the unsaturated cyclohexyl version **L4**NiCl₂, with **L1** showing significantly better reactivity than **L4** in the screen reactions (see Section 2.3.2 for screen results and Section 2.3.3.1 for nickel dichloride bond length comparisons). As such, further increasing the donicity of the bisphosphine may yield reactivity improvements. In a bid to save time and synthetic efforts, the rate-limiting reductive elimination step for a series of backbone-modified NHP-DalPhos variants could be modelled computationally, allowing for a broader survey of potential EDG than would be synthetically feasible. As well, EWG could also be modelled to verify if these lead to a higher barrier to reductive elimination.

Due to the similarities in reactivity trends between NHP-DalPhos and PAd-DalPhos, further reactivity screens would likely be unproductive. Modification of the ligand framework is likely to lead to the highest chance of success with regards to reactivity benefits.

Though stoichiometric experiments were unsuccessful in isolating and characterizing any intermediates evolved from **C3**, the use of deuterium labelling experiments coupled with mass spectrometry could yield experimental, instead of computational, insight into this activation pathway. By using deuterated furfurylamine, it could be possible to see a deuterated-methyl group on the mesityl fragment of **L2**, if activation does indeed proceed via the β -hydride elimination pathway outlined in **Scheme 11**. As well, mass spectrometry could be used to identify the furfurylimine species generated from this activation pathway.

4.2.3 Chapter 3

As outlined in Chapter 3, I was able to synthesize and characterize crystallographically for the first time **L9**. Though a solid state structure of **L10** was obtained, we were unsuccessful in obtaining pure material within the allotted timeframe of this project. Moving forward, reaction optimization will be required to establish a reliable synthetic route for **L10**, with efforts focused on the more successful P-cyclopentadienyl-substituted route over the ferrocene lithiation methodology. From here, the coordination chemistry of these ligands with nickel should be established, both via nickel dichlorides for comparison of the ligand electronic parameters, and via L_nNi(Ar)(X) precatalysts for use in substrate scope screens. Both the coordination chemistry and reactivity of these complexes should be compared to analogous DPPF nickel complexes.

Due to the similarities between the architectures of DPPF and **L9/L10**, substrate scope explorations should focus on coupling partners which pose a challenge for DPPF. These may include bulky secondary amines, secondary amides, indole and related derivatives. A particular focus on *N*-heterocyclic nucleophile and electrophile should be made, especially 5-membered *N*-heterocycles, as these represent a gap in the literature for nickel amination reactions. Throughout all reaction screens DPPF should be used as reference to gauge relative success versus the state-of-the-art systems.

References

1. Busacca, C. A.; Fandrick, D. R.; Song, J. J.; Senanayake, C. H., Transition Metal Catalysis in the Pharmaceutical Industry. In *Applications of Transition Metal Catalysis in Drug Discovery and Development*, John Wiley & Sons, Inc.: 2012; pp 1-24.
2. Stradiotto, M.; Lundgren, R. J., Application of Sterically Demanding Phosphine Ligands in Palladium-Catalyzed Cross-Coupling leading to C(sp²)–E Bond Formation (E = NH₂, OH, and F). In *Ligand Design in Metal Chemistry*, John Wiley & Sons, Ltd: 2016; pp 104-133.
3. Ruiz-Castillo, P.; Buchwald, S. L., *Chem. Rev.* **2016**, *116* (19), 12564-12649.
4. Vineyard, B. D.; Knowles, W. S.; Sabacky, M. J.; Bachman, G. L.; Weinkauff, D. J., *J. Am. Chem. Soc.* **1977**, *99* (18), 5946-5952.
5. Surry, D. S.; Buchwald, S. L., *Angew. Chem. Int. Ed.* **2008**, *47* (34), 6338-6361.
6. Lundgren, R. J.; Stradiotto, M., *Chem. Eur. J.* **2012**, *18* (32), 9758-9769.
7. Tolman, C. A., *Chem. Rev.* **1977**, *77* (3), 313-348.
8. Hillier, A. C.; Sommer, W. J.; Yong, B. S.; Petersen, J. L.; Cavallo, L.; Nolan, S. P., *Organometallics* **2003**, *22* (21), 4322-4326.
9. van Leeuwen, P. W. N. M.; Kamer, P. C. J.; Reek, J. N. H.; Dierkes, P., *Chem. Rev.* **2000**, *100* (8), 2741-2770.
10. Alsabeh, P. G.; Lundgren, R. J.; McDonald, R.; Johansson Seechurn, C. C. C.; Colacot, T. J.; Stradiotto, M., *Chem. Eur. J.* **2013**, *19* (6), 2131-2141.
11. Hartwig, J. F.; Shekhar, S.; Shen, Q.; Barrios-landeros, F., Synthesis of Anilines. In *The Chemistry of Anilines*, John Wiley & Sons, Ltd: 2007; pp 455-536.
12. (a) Bhunia, S.; Pawar, G. G.; Kumar, S. V.; Jiang, Y.; Ma, D., *Angew. Chem. Int. Ed.* **2017**, *56* (51), 16136-16179; (b) Monnier, F.; Taillefer, M., Copper-Catalyzed C(aryl)–N Bond Formation. In *Amination and Formation of sp² C–N Bonds*, Taillefer, M.; Ma, D., Eds. Springer Berlin Heidelberg: Berlin, Heidelberg, 2013; pp 173-204.
13. Yin, J., Selected Applications of Pd and Cu Catalyzed Carbon–Heteroatom Cross-Coupling Reactions in the Pharmaceutical Industry. In *Applications of Transition Metal Catalysis in Drug Discovery and Development*, John Wiley & Sons: 2012; pp 97-123.
14. (a) Louie, J.; Hartwig, J. F., *Tetrahedron Lett.* **1995**, *36* (21), 3609-3612; (b) Guram, A. S.; Rennels, R. A.; Buchwald, S. L., *Angew. Chem. Int. Ed.* **1995**, *34* (12), 1348-1350.

15. (a) Wolfe, J. P.; Wagaw, S.; Buchwald, S. L., *J. Am. Chem. Soc.* **1996**, *118* (30), 7215-7216; (b) Driver, M. S.; Hartwig, J. F., *J. Am. Chem. Soc.* **1996**, *118* (30), 7217-7218.
16. (a) Hartwig, J. F.; Kawatsura, M.; Hauck, S. I.; Shaughnessy, K. H.; Alcazar-Roman, L. M., *J. Org. Chem.* **1999**, *64* (15), 5575-5580; (b) Stambuli, J. P.; Kuwano, R.; Hartwig, J. F., *Angew. Chem. Int. Ed.* **2002**, *41* (24), 4746-4748.
17. Old, D. W.; Wolfe, J. P.; Buchwald, S. L., *J. Am. Chem. Soc.* **1998**, *120* (37), 9722-9723.
18. Huang, J.; Grasa, G.; Nolan, S. P., *Org. Lett.* **1999**, *1* (8), 1307-1309.
19. Lundgren, R. J.; Hesp, K. D.; Stradiotto, M., *Synlett* **2011**, *2011* (17), 2443-2458.
20. Crawford, S. M.; Lavery, C. B.; Stradiotto, M., *Chem. Eur. J.* **2013**, *19* (49), 16760-16771.
21. Bruno, N. C.; Buchwald, S. L., *Org. Lett.* **2013**, *15* (11), 2876-2879.
22. Hartwig, J. F., *Acc. Chem. Res.* **2008**, *41* (11), 1534-1544.
23. Beletskaya, I. P.; Cheprakov, A. V., *Organometallics* **2012**, *31* (22), 7753-7808.
24. Kotecki, B. J.; Fernando, D. P.; Haight, A. R.; Lukin, K. A., *Org. Lett.* **2009**, *11* (4), 947-950.
25. (a) Barrios-Landeros, F.; Hartwig, J. F., *J. Am. Chem. Soc.* **2005**, *127* (19), 6944-6945; (b) Barrios-Landeros, F.; Carrow, B. P.; Hartwig, J. F., *J. Am. Chem. Soc.* **2009**, *131* (23), 8141-8154.
26. Tasker, S. Z.; Standley, E. A.; Jamison, T. F., *Nature* **2014**, *509*, 299.
27. Shen, Q.; Hartwig, J. F., *J. Am. Chem. Soc.* **2006**, *128* (31), 10028-10029.
28. Cheung, C. W.; Surry, D. S.; Buchwald, S. L., *Org. Lett.* **2013**, *15* (14), 3734-3737.
29. Bullock, R. M., *Catalysis Without Precious Metals*. Wiley-VCH Weinheim, Germany, 2010; pp. 1-276.
30. Rosen, B. M.; Quasdorf, K. W.; Wilson, D. A.; Zhang, N.; Resmerita, A.-M.; Garg, N. K.; Percec, V., *Chem. Rev.* **2011**, *111* (3), 1346-1416.
31. Grushin, V. V.; Alper, H., *Chem. Rev.* **1994**, *94* (4), 1047-1062.
32. MacQueen, P. M.; Stradiotto, M., *Synlett* **2017**, *28* (13), 1652-1656.
33. Ananikov, V. P., *ACS Catal.* **2015**, *5* (3), 1964-1971.

34. Hu, X., *Chem. Sci.* **2011**, *2* (10), 1867-1886.
35. Tasker, S. Z.; Gutierrez, A. C.; Jamison, T. F., *Angew. Chem. Int. Ed.* **2014**, *53* (7), 1858-1861.
36. Yue, H.; Zhu, C.; Rueping, M., *Angew. Chem. Int. Ed.* **2018**, *57* (5), 1371-1375.
37. Bhawal, B. N.; Morandi, B., *Chem. Eur. J.* **2017**, *23* (50), 12004-12013.
38. Shreve, R. N.; Vriens, G. N.; Vogel, D. A., *Industrial & Engineering Chemistry* **1950**, *42* (5), 791-796.
39. Wolfe, J. P.; Buchwald, S. L., *J. Am. Chem. Soc.* **1997**, *119* (26), 6054-6058.
40. (a) Hazari, N.; Melvin, P. R.; Beromi, M. M., *Nat. Rev. Chem* **2017**, *1*, 0025; (b) Lavoie, C. M.; MacQueen, P. M.; Rotta-Loria, N. L.; Sawatzky, R. S.; Borzenko, A.; Chisholm, A. J.; Hargreaves, B. K. V.; McDonald, R.; Ferguson, M. J.; Stradiotto, M., *Nat. Commun.* **2016**, *7*, 11073; (c) Marín, M.; Rama, R. J.; Nicasio, M. C., *Chem. Rec.* **2016**, *16* (4), 1819-1832.
41. Ge, S.; Green, R. A.; Hartwig, J. F., *J. Am. Chem. Soc.* **2014**, *136* (4), 1617-1627.
42. Green, R. A.; Hartwig, J. F., *Angew. Chem. Int. Ed.* **2015**, *54* (12), 3768-3772.
43. Kampmann, S. S.; Skelton, B. W.; Wild, D. A.; Koutsantonis, G. A.; Stewart, S. G., *Eur. J. Org. Chem.* **2015**, *2015* (27), 5995-6004.
44. Rull, S. G.; Funes-Ardoiz, I.; Maya, C.; Maseras, F.; Fructos, M. R.; Belderrain, T. R.; Nicasio, M. C., *ACS Catal.* **2018**.
45. Lavoie, C. M.; McDonald, R.; Johnson, E. R.; Stradiotto, M., *Adv. Synth. Catal.* **2017**, *359* (17), 2972-2980.
46. Borzenko, A.; Rotta-Loria, N. L.; MacQueen, P. M.; Lavoie, C. M.; McDonald, R.; Stradiotto, M., *Angew. Chem. Int. Ed.* **2015**, *54* (12), 3773-3777.
47. (a) Park, N. H.; Teverovskiy, G.; Buchwald, S. L., *Org. Lett.* **2014**, *16* (1), 220-223; (b) Clark, J. S. K.; Lavoie, C. M.; MacQueen, P. M.; Ferguson, M. J.; Stradiotto, M., *Organometallics* **2016**, *35* (18), 3248-3254; (c) Clark, J. S. K.; Voth, C. N.; Ferguson, M. J.; Stradiotto, M., *Organometallics* **2017**, *36* (3), 679-686.
48. Ritleng, V.; Henrion, M.; Chetcuti, M. J., *ACS Catal.* **2016**, *6* (2), 890-906.
49. Vitaku, E.; Smith, D. T.; Njardarson, J. T., *J. Med. Chem.* **2014**, *57* (24), 10257-10274.

50. Gradel, B. t.; Brenner, E.; Schneider, R.; Fort, Y., *Tetrahedron Lett.* **2001**, 42 (33), 5689-5692.
51. (a) Rull, S. G.; Blandez, J. F.; Fructos, M. R.; Belderrain, T. R.; Nicasio, M. C., *Adv. Synth. Catal.* **2015**, 357 (5), 907-911; (b) Iglesias, M. J.; Blandez, J. F.; Fructos, M. R.; Prieto, A.; Álvarez, E.; Belderrain, T. R.; Nicasio, M. C., *Organometallics* **2012**, 31 (17), 6312-6316; (c) Iglesias, M. J.; Prieto, A.; Nicasio, M. C., *Adv. Synth. Catal.* **2010**, 352 (11-12), 1949-1954.
52. Phosphatrioxa-Adamantane Ligands. In *Phosphorus(III) Ligands in Homogeneous Catalysis: Design and Synthesis*.
53. Lavoie, C. M.; MacQueen, P. M.; Stradiotto, M., *Chem. Eur. J.* **2016**, 22 (52), 18752-18755.
54. Tassone, J. P.; MacQueen, P. M.; Lavoie, C. M.; Ferguson, M. J.; McDonald, R.; Stradiotto, M., *ACS Catal.* **2017**, 7 (9), 6048-6059.
55. Gildner, P. G.; DeAngelis, A.; Colacot, T. J., *Org. Lett.* **2016**, 18 (6), 1442-1445.
56. Wu, K.; Doyle, A. G., *Nat. Chem.* **2017**, 9, 779.
57. Hansen, E. C.; Pedro, D. J.; Wotal, A. C.; Gower, N. J.; Nelson, J. D.; Caron, S.; Weix, D. J., *Nat. Chem.* **2016**, 8, 1126.
58. Yamaguchi, J.; Muto, K.; Itami, K., *Eur. J. Org. Chem.* **2013**, 2013 (1), 19-30.
59. (a) Ackermann, L.; Born, R.; Spatz, J. H.; Meyer, D., *Angew. Chem. Int. Ed.* **2005**, 44 (44), 7216-7219; (b) Ackermann, L.; Kapdi, A. R.; Fenner, S.; Kornhaaß, C.; Schulzke, C., *Chem. Eur. J.* **2011**, 17 (10), 2965-2971.
60. Fantasia, S.; Petersen, J. L.; Jacobsen, H.; Cavallo, L.; Nolan, S. P., *Organometallics* **2007**, 26 (24), 5880-5889.
61. Gudat, D., *Acc. Chem. Res.* **2010**, 43 (10), 1307-1316.
62. Burck, S.; Gudat, D.; Nieger, M., *Organometallics* **2009**, 28 (5), 1447-1452.
63. (a) Arduengo, A. J.; Dias, H. V. R.; Harlow, R. L.; Kline, M., *J. Am. Chem. Soc.* **1992**, 114 (14), 5530-5534; (b) Dorta, R.; Stevens, E. D.; Scott, N. M.; Costabile, C.; Cavallo, L.; Hoff, C. D.; Nolan, S. P., *J. Am. Chem. Soc.* **2005**, 127 (8), 2485-2495; (c) Valente, C.; Çalimsiz, S.; Hoi, K. H.; Mallik, D.; Sayah, M.; Organ, M. G., *Angew. Chem. Int. Ed.* **2012**, 51 (14), 3314-3332.
64. Bezpalko, M. W.; Foxman, B. M.; Thomas, C. M., *Inorg. Chem.* **2015**, 54 (17), 8717-8726.

65. Wucher, P.; Caporaso, L.; Roesle, P.; Ragone, F.; Cavallo, L.; Mecking, S.; Göttker-Schnetmann, I., *Proc. Natl. Acad. Sci. U.S.A.* **2011**, *108* (22), 8955-8959.
66. Adams, M. R.; Tien, C.-H.; Huchenski, B. S. N.; Ferguson, M. J.; Speed, A. W. H., *Angew. Chem. Int. Ed.* **2017**, *56* (22), 6268-6271.
67. Chong, C. C.; Kinjo, R., *Angew. Chem.* **2015**, *127* (41), 12284-12288.
68. Burck, S.; Gudat, D.; Nieger, M.; Du Mont, W.-W., *J. Am. Chem. Soc.* **2006**, *128* (12), 3946-3955.
69. Adams, M. R.; Tien, C. H.; McDonald, R.; Speed, A. W. H., *Angew. Chem. Int. Ed.* **2017**, *56* (52), 16660-16663.
70. Chang, Y.-C.; Lee, Y.-C.; Chang, M.-F.; Hong, F.-E., *J. Organomet. Chem.* **2016**, *808*, 23-33.
71. Standley, E. A.; Jamison, T. F., *J. Am. Chem. Soc.* **2013**, *135* (4), 1585-1592.
72. (a) Standley, E. A.; Smith, S. J.; Müller, P.; Jamison, T. F., *Organometallics* **2014**, *33* (8), 2012-2018; (b) Sawatzky, R. S.; Ferguson, M. J.; Stradiotto, M., *Synlett* **2017**, *28* (13), 1586-1591.
73. (a) Magano, J.; Monfette, S., *ACS Catal.* **2015**, *5* (5), 3120-3123; (b) Shields, J. D.; Gray, E. E.; Doyle, A. G., *Org. Lett.* **2015**, *17* (9), 2166-2169.
74. (a) Ruiz-Castillo, P.; Blackmond, D. G.; Buchwald, S. L., *J. Am. Chem. Soc.* **2015**, *137* (8), 3085-3092; (b) Zhang, Y.; Lavigne, G.; Lugan, N.; César, V., *Chem. Eur. J.* **2017**, *23* (55), 13792-13801.
75. Iwai, T.; Harada, T.; Shimada, H.; Asano, K.; Sawamura, M., *ACS Catal.* **2017**, *7* (3), 1681-1692.
76. Jiang, J.; Zhu, H.; Shen, Y.; Tu, T., *Org. Chem. Front.* **2014**, *1* (10), 1172-1175.
77. Yin, J.; Buchwald, S. L., *Org. Lett.* **2000**, *2* (8), 1101-1104.
78. (a) DeAngelis, A.; Wang, D. H.; Buchwald, S. L., *Angew. Chem. Int. Ed.* **2013**, *52* (12), 3434-3437; (b) Lundgren, R. J.; Stradiotto, M., *Angew. Chem. Int. Ed.* **2010**, *49* (46), 8686-8690.
79. DiPucchio, R. C.; Roşca, S. C.; Schafer, L. L., *Angew. Chem. Int. Ed.* **2018**, *57* (13), 3469-3472.
80. (a) Lee, C.; Yang, W.; Parr, R. G., *Physical Review B* **1988**, *37* (2), 785-789; (b) Becke, A. D., *J. Chem. Phys.* **1993**, *98* (7), 5648-5652; (c) Becke, A. D.; Johnson, E. R., *J. Chem.*

- Phys.* **2007**, *127* (15), 154108; (d) Otero-de-la-Roza, A.; Johnson, E. R., *J. Chem. Phys.* **2013**, *138* (20), 204109.
81. Abrams, M. B.; Scott, B. L.; Baker, R. T., *Organometallics* **2000**, *19* (24), 4944-4956.
 82. Dube, J. W.; Farrar, G. J.; Norton, E. L.; Szekeley, K. L. S.; Cooper, B. F. T.; Macdonald, C. L. B., *Organometallics* **2009**, *28* (15), 4377-4384.
 83. Kataoka, N.; Shelby, Q.; Stambuli, J. P.; Hartwig, J. F., *J. Org. Chem.* **2002**, *67* (16), 5553-5566.
 84. Hamann, B. C.; Hartwig, J. F., *J. Am. Chem. Soc.* **1998**, *120* (29), 7369-7370.
 85. Burck, S.; Gudat, D.; Nieger, M.; Tirree, J., *Dalton Trans.* **2007**, (19), 1891-1897.
 86. Balcells, D.; Nova, A., *ACS Catal.* **2018**, *8* (4), 3499-3515.

Appendix A – Supplementary Information

Catalytic Screening Results

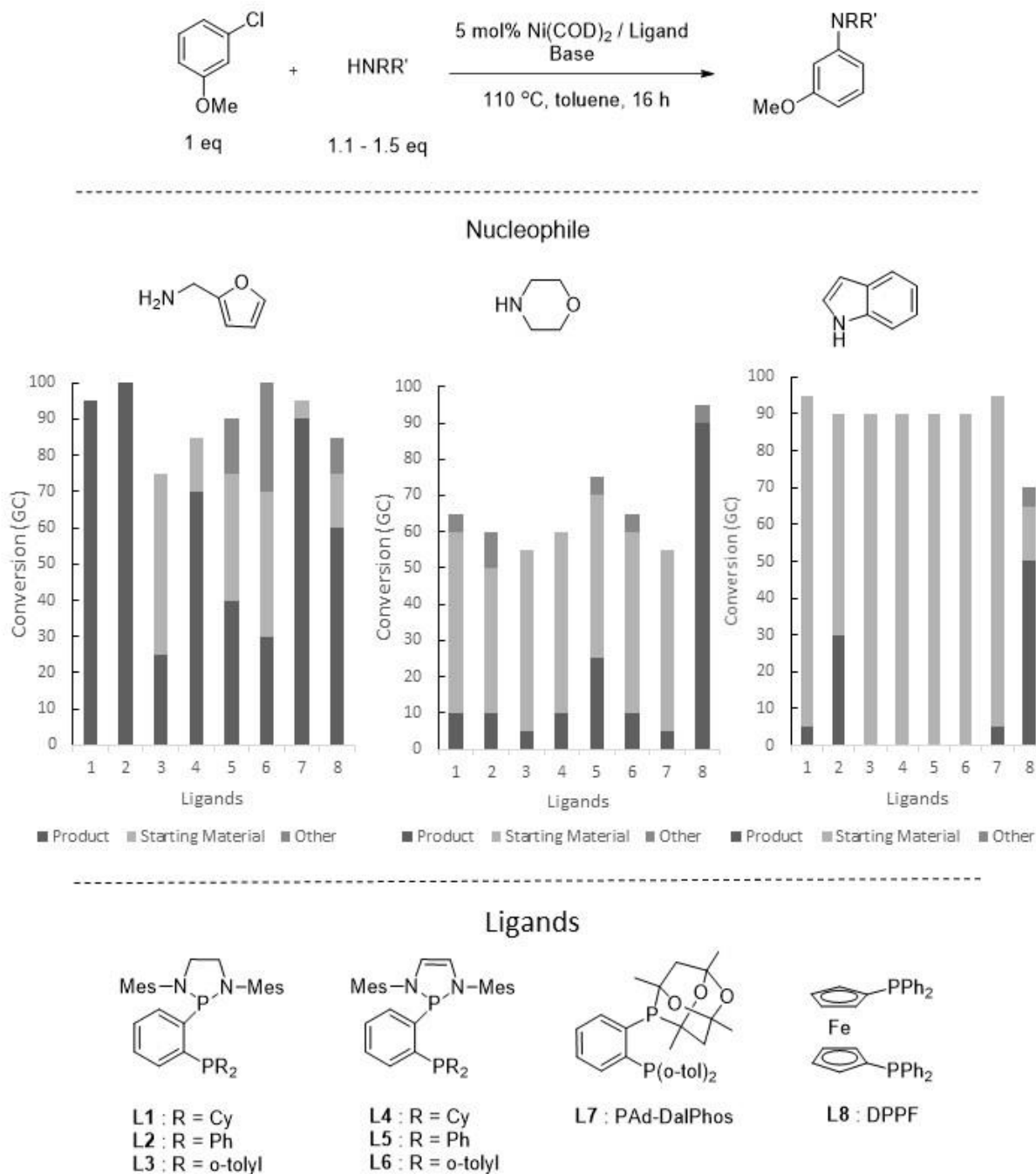


Figure A1. Ligand screen for the *N*-arylation of 3-chloroanisole. Results are estimated from calibrated GC data using dodecane as an internal standard. Mass balance attributed to starting material, polyarylation and unknown by-products on the basis of GC data.

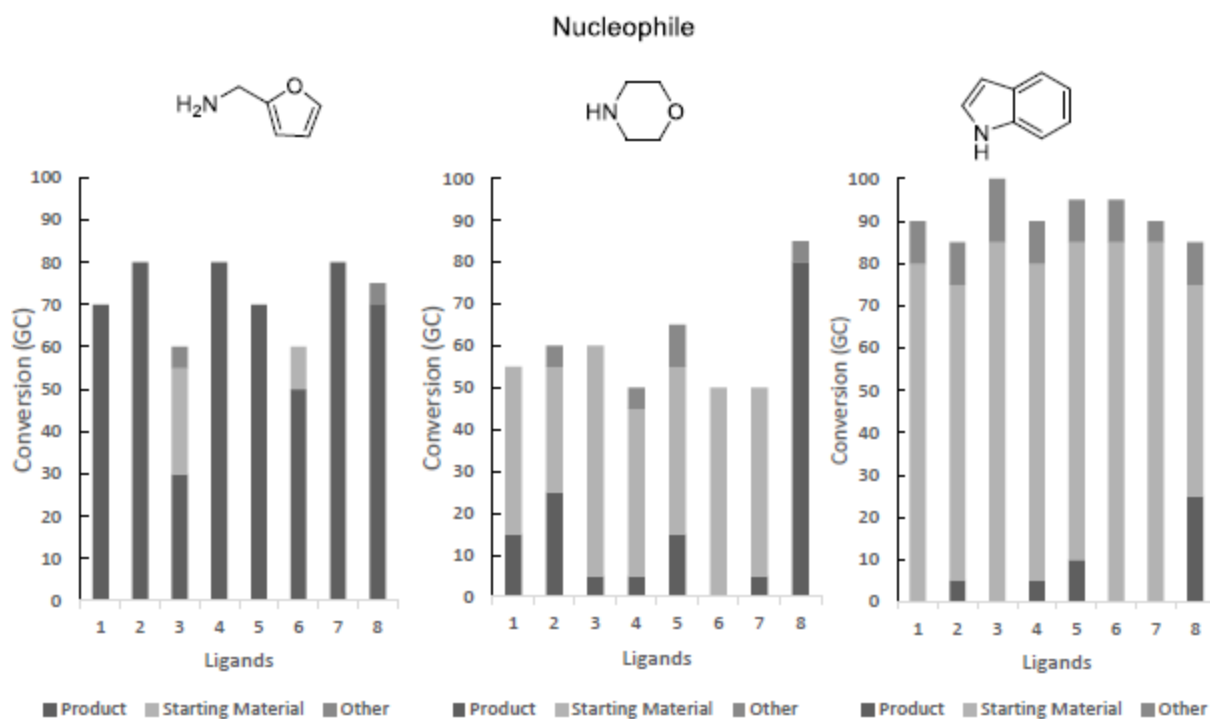
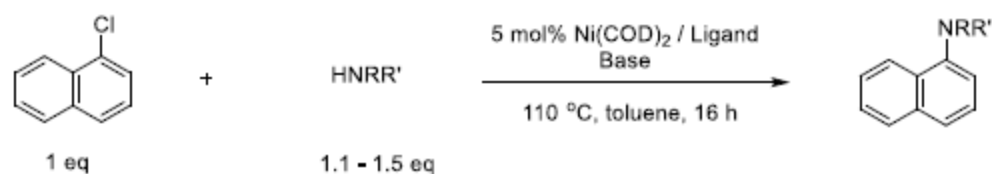


Figure A2: Ligand screen for the *N*-arylation of 1-chloronaphthalene. Results are estimates made using calibrated GC with dodecane as an internal standard. Mass balance attributed to starting material, polyarylation and unknown by-products on the basis of GC data (ligands depicted in Figure A1)

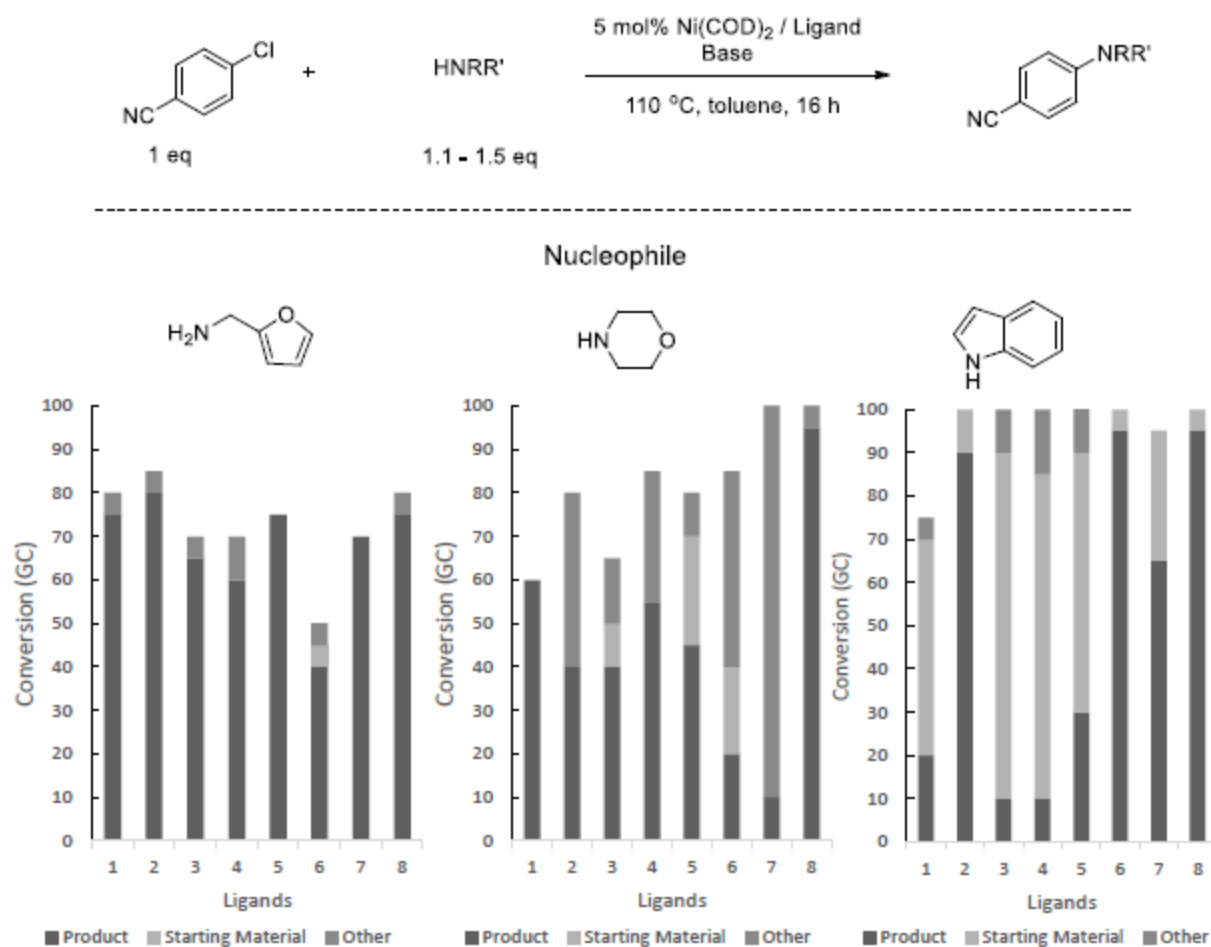


Figure A3: Ligand screen for the *N*-arylation of 4-chlorobenzonitrile. Results are estimates made using calibrated GC with dodecane as an internal standard. Mass balance attributed to starting material, polyarylation and unknown by-products on the basis of GC data (ligands depicted in Figure A1).

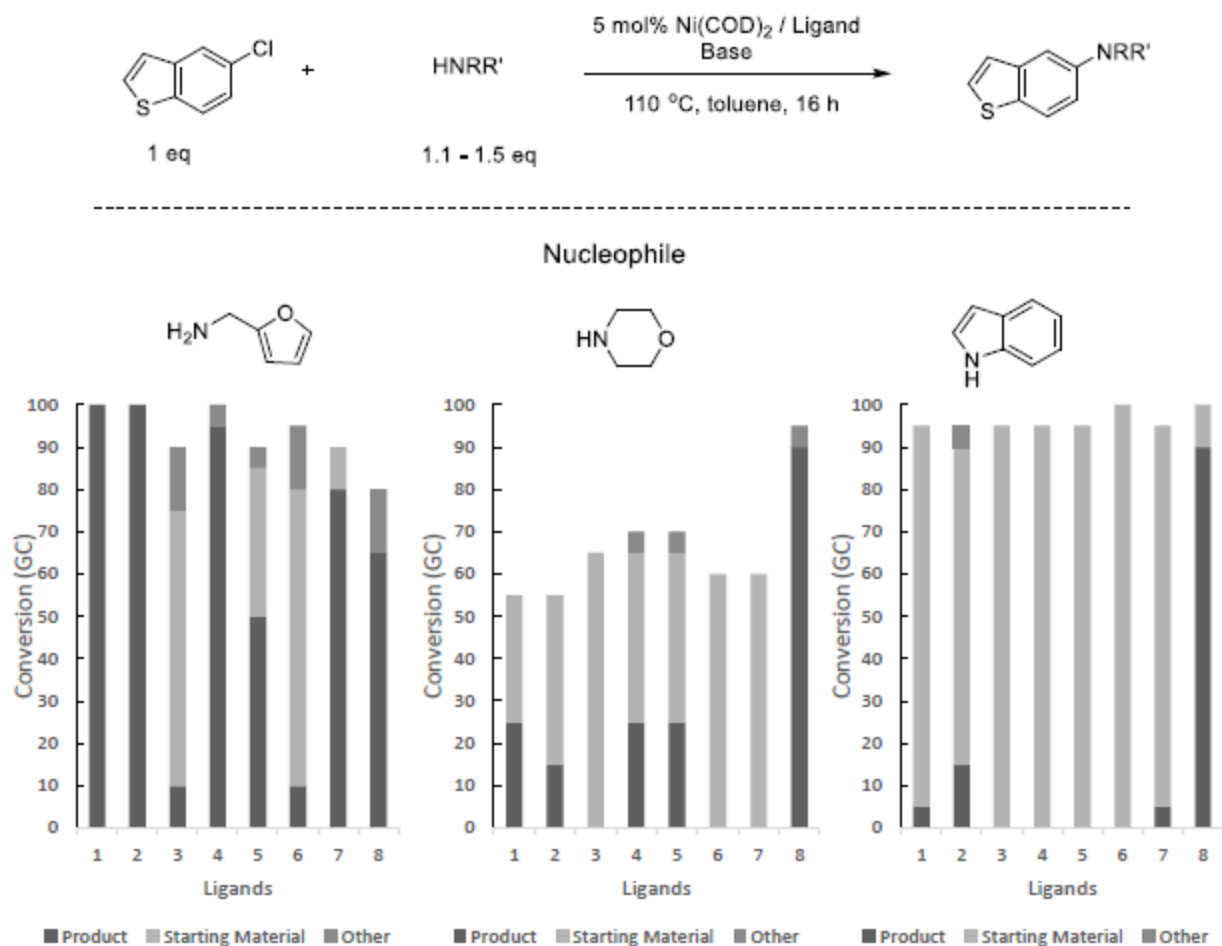
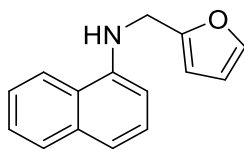
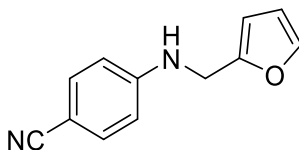


Figure A4: Ligand screen for the *N*-arylation of 5-chloro[*b*]thiophene. Results are estimates made using calibrated GC with dodecane as an internal standard. Mass balance attributed to starting material, polyarylation and unknown by-products on the basis of GC data (ligands depicted in Figure A1).

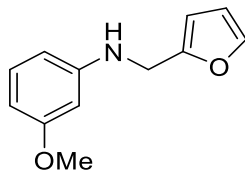
Characterization of Cross-Coupling Products



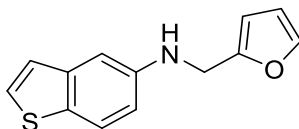
***N*¹-naphthalenyl-2-furanmethanamine (1a):** The general procedure was followed using **C1** (0.023 g, 0.03 mmol, 5 mol %), NaO(*t*-Bu) (0.1153 g, 1.2 mmol), 1-chloronaphthalene (0.082 mL, 0.6 mmol) or 1-bromonaphthalene (0.084 mL, 0.6 mmol), furfurylamine (0.058 mL, 0.66 mmol) and toluene (5 mL). After flash column chromatography on silica gel (10% EtOAc in hexanes) the title compound was isolated as a pale yellow oil (X = Cl; 0.125 g, 94%, X = Br; 0.109 g, 81%). ¹H NMR (500 MHz; CDCl₃): δ 7.90 – 7.84 (m, 2H), 7.50 (m, 2H), 7.47 (d, *J* = 0.9 Hz, 1H), 7.41 (t, *J* = 8.0 Hz, 1H), 7.34 (d, *J* = 8.2 Hz, 1H), 6.76 (d, *J* = 7.5 Hz, 1H), 6.43 – 6.41 (m, 1H), 6.38 (d, *J* = 3.2 Hz, 1H), 4.74 (br. s, 1H), 4.55 (s, 2H). ¹³C {¹H} NMR (125.7 MHz, CDCl₃): δ 152.5, 142.8, 142.1, 134.3, 128.7, 126.5, 125.8, 124.9, 123.6, 120.0, 118.1, 110.4, 107.3, 104.9, 41.8. Spectroscopic data are in agreement with those previously reported (in CDCl₃).¹



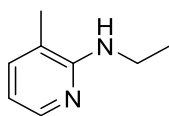
4-[(2-Furanylmethyl)amino]-benzonitrile (1b): The general procedure was followed using **C1** (0.023 g, 0.03 mmol, 5 mol %), NaO(*t*-Bu) (0.1153 g, 1.2 mmol), 4-chlorobenzonitrile (0.0825 g, 0.6 mmol), furfurylamine (0.058 mL, 0.66 mmol) and toluene (5 mL). After flash column chromatography on silica gel (30% EtOAc in hexanes) the title compound was isolated as a pale yellow oil (0.101 g, 0.51 mmol, 85%). ¹H NMR (500 MHz; CDCl₃): δ 7.48 – 7.44 (m, 2H), 7.42 – 7.39 (m, 1H), 6.68 – 6.65 (m, 2H), 6.37 (dd, *J* = 3.2, 1.9 Hz, 1H), 6.29 (dd, *J* = 3.2, 0.5 Hz, 1H), 4.63 (br. s, 1H), 4.39 (d, *J* = 5.8 Hz, 2H). ¹³C {¹H} NMR (125.7 MHz, CDCl₃): δ 151.2, 150.7, 142.3, 133.7, 120.2, 112.5, 110.5, 107.6, 99.6, 40.5. Spectroscopic data are in agreement with those previously reported (in CDCl₃).¹



***N*-(3-Methoxyphenyl)-2-furanmethanamine (1c):** The general procedure was followed using **C1** (0.023 g, 0.03 mmol, 5 mol %), NaO(*t*-Bu) (0.1153 g, 1.2 mmol), 3-chloroanisole (0.074 mL, 0.6 mmol), furfurylamine (0.058 mL, 0.66 mmol) and toluene (5 mL). After flash column chromatography on silica gel (20% EtOAc in hexanes) the title compound was isolated as a pale yellow oil (0.112 g, 0.55 mmol, 92%). ¹H NMR (500 MHz; CDCl₃): δ 7.41 – 7.40 (m, 1H), 7.13 (t, *J* = 8.1 Hz, 1H), 6.38 – 6.32 (overlapping multiplets, 3H), 6.29-6.27 (m, 2H), 4.35 (s, 2H), 4.07 (br. s, 1H), 3.81 (s, 3H). ¹³C{¹H} NMR (125.7 MHz, CDCl₃): δ 160.8, 152.7, 149.0, 141.9, 130.0, 110.3, 107.0, 106.2, 103.2, 99.2, 55.1, 41.4. Spectroscopic data are in agreement with those previously reported (in CDCl₃).¹

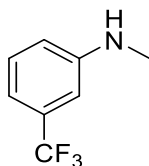


***N*-(2-Furanylmethyl)-benzo[b]thiophen-5-amine (1d):** The general procedure was followed using **C1** (0.023 g, 0.03 mmol, 5 mol %), NaO(*t*-Bu) (0.1153 g, 1.2 mmol), 5-chloro[b]thiophene (0.1012 g, 0.6 mmol), furfurylamine (0.058 mL, 0.66 mmol) and toluene (5 mL). After flash column chromatography on silica gel (20% EtOAc in hexanes) the title compound was isolated as an opaque yellow oil (0.124 g, 0.55 mmol, 91%). ¹H NMR (500 MHz; CDCl₃): δ 7.69 (d, *J* = 8.7 Hz, 1H), 7.44 – 7.41 (m, 2H), 7.22 (d, *J* = 5.4 Hz, 1H), 7.11 (d, *J* = 2.3 Hz, 1H), 6.83 (dd, *J* = 8.6, 2.3 Hz, 1H), 6.39 – 6.37 (m, 1H), 6.31 (d, *J* = 3.0 Hz, 1H), 4.42 (s, 2H), 4.11 (br. s, 1H). ¹³C{¹H} NMR (125.7 MHz, CDCl₃): δ 152.8, 145.2, 141.9, 140.9, 130.0, 126.9, 123.4, 122.9, 114.1, 110.4, 107.0, 105.5, 42.0. Spectroscopic data are in agreement with those previously reported (in CDCl₃).¹

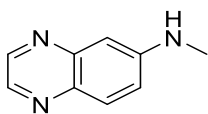


***N*-Ethyl-3-methyl-2-pyridinamine (1e):** The general procedure was followed using **C1** (0.023 g, 0.03 mmol, 5 mol %), NaO(*t*-Bu) (0.0865 g, 0.9 mmol), 2-chloro-3-methylpyridine (0.065

mL, 0.6 mmol), and 2 M ethylamine in THF (2.10 mL, 4.2 mmol). After flash column chromatography on silica gel (50% EtOAc in hexanes) the title compound was isolated as a volatile opaque yellow oil (0.051 g, 0.37 mmol, 62%). ^1H NMR (500 MHz; CDCl_3): δ 8.02 (dd, $J = 5.0, 1.1$ Hz, 1H), 7.20 – 7.18 (m, 1H), 6.49 (dd, $J = 7.1, 5.1$ Hz, 1H), 4.03 (br. s, 1H), 3.53 – 3.47 (m, 2H), 2.07 (s, 3H), 1.27 (t, $J = 7.2$ Hz, 3H). ^{13}C $\{^1\text{H}\}$ NMR (125.7 MHz, CDCl_3): δ 157.1, 145.6, 136.7, 116.5, 112.5, 36.5, 17.1, 15.4. Calc'd for $\text{C}_8\text{H}_{13}\text{N}_2$ $[\text{M}+\text{H}]^+$: 137.1073. Found: 137.1073.

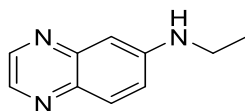


***N*-Methyl-3-(trifluoromethyl)benzenamine (1f):** The general procedure was followed using **C1** (0.023 g, 0.03 mmol, 5 mol %), $\text{NaO}(t\text{-Bu})$ (0.0865 g, 0.9 mmol), 3-chlorobenzotrifluoride (0.081 mL, 0.6 mmol), and 2 M methylamine in THF (2.10 mL, 4.2 mmol). After flash column chromatography on silica gel (40% EtOAc in hexanes) the title compound was isolated as a volatile opaque yellow oil (0.072 g, 0.41 mmol, 68%). ^1H NMR (500 MHz; CDCl_3): δ 7.30 (t, $J = 10.0$ Hz, 1H), 6.98 (d, $J = 7.7$ Hz, 1H), 6.84 (s, 1H), 6.78 (dd, $J = 8.2, 1.6$ Hz, 1H), 3.94 (br. s, 1H), 2.90 (s, 3H). ^{13}C $\{^1\text{H}\}$ NMR (125.7 MHz, CDCl_3): δ 149.4, 131.6 (q, $J = 31.6$ Hz), 129.5, 124.4 (q, $J = 272.2$ Hz), 115.4, 113.5 (q, $J = 3.8$ Hz), 108.3 (q, $J = 3.8$ Hz), 30.4. ^{19}F $\{^1\text{H}\}$ NMR (470.4 MHz, CDCl_3): δ -62.9. Calc'd for $\text{C}_8\text{H}_9\text{F}_3\text{N}$ $[\text{M}+\text{H}]^+$: 176.0682. Found: 176.0682.

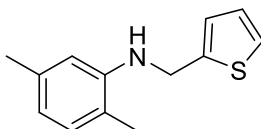


***N*-Methyl-6-quinoxalinamine (1g):** The general procedure was followed using **C1** (0.023 g, 0.03 mmol, 5 mol %), $\text{NaO}(t\text{-Bu})$ (0.0865 g, 0.9 mmol), 6-chloroquinoxaline (0.099 g, 0.6 mmol), and 2.0 M methylamine in THF (2.10 mL, 4.2 mmol). After flash column chromatography on silica gel (60% EtOAc in hexanes) the title compound was isolated as a yellow solid (0.084 g, 0.53 mmol, 88%). ^1H NMR (500 MHz; CDCl_3): δ 8.62 (d, $J = 1.7$ Hz, 1H), 8.48 (d, $J = 1.7$ Hz, 1H), 7.80 (d, $J = 9.1$ Hz, 1H), 7.10 (dd, $J = 9.1, 2.6$ Hz, 1H), 6.93 (d, $J = 2.5$ Hz, 1H), 4.41 (br. s, 1H), 2.96 (d, $J = 5.2$ Hz, 3H). ^{13}C $\{^1\text{H}\}$ NMR (125.7 MHz, CDCl_3): δ

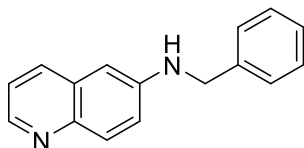
150.3, 145.8, 145.0, 140.4, 138.2, 130.1, 122.2, 103.3, 30.6. Calc'd for C₉H₁₀N₃ [M+H]⁺: 160.0869. Found: 160.0869.



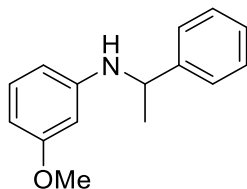
N-Ethyl-6-quinoxalinamine (1h): A modification of the general procedure was followed using **C1** (0.023 g, 0.03 mmol, 5 mol %), NaO(*t*-Bu) (0.1442 g, 1.5 mmol), 6-chloroquinoxaline (0.099 g, 0.6 mmol), ethylamine hydrochloride (0.0587 g, 0.72 mmol) and toluene (3 mL) at 80 °C. After flash column chromatography on silica gel (100% EtOAc) the title compound was isolated as a yellow oil (0.075 g, 0.43 mmol, 72%). ¹H NMR (500 MHz; CDCl₃): δ 8.63 (s, 1H), 8.50 (s, 1H), 7.82 (d, *J* = 9.1 Hz, 1H), 7.10 (dd, *J* = 9.1, 2.5 Hz, 1H), 6.95 (d, *J* = 2.1 Hz, 1H), 4.15 (br. s, 1H), 3.34 – 3.28 (m, 2H), 1.35 (t, *J* = 7.2 Hz, 3H). ¹³C{¹H} NMR (125.7 MHz, CDCl₃): δ 149.4, 145.8, 145.1, 140.4, 138.2, 130.2, 122.3, 103.6, 38.4, 14.6. Calc'd for C₁₀H₁₂N₃ [M+H]⁺: 174.1026. Found: 174.1026.



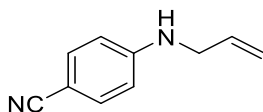
N-(2,5-Dimethylphenyl)-2-thiophenemethanamine (1i): The general procedure was followed using **C1** (0.023 g, 0.03 mmol, 5 mol %), NaO(*t*-Bu) (0.0865 g, 0.9 mmol), 2-chloro-*p*-xylene (0.081 mL, 0.6 mmol), 2-thiophenemethylamine (0.068 mL, 0.66 mmol) and toluene (5 mL). After flash column chromatography on silica gel (8% EtOAc in hexanes) the title compound was isolated as a yellow oil (0.119 g, 0.55 mmol, 91%). ¹H NMR (500 MHz; CDCl₃): δ 7.32 – 7.29 (m, 1H), 7.13 (s, 1H), 7.09 – 7.05 (m, 2H), 6.63 (s, 2H), 4.63 (s, 2H), 3.90 (br. s, 1H), 2.40 (s, 3H), 2.21 (s, 3H). ¹³C{¹H} NMR (125.7 MHz, CDCl₃): δ 145.6, 143.2, 136.8, 130.1, 127.0, 125.1, 124.7, 119.4, 118.4, 111.2, 43.6, 21.6, 17.1. Calc'd for C₁₃H₁₆N [M+H]⁺: 217.0925. Found: 218.0998.



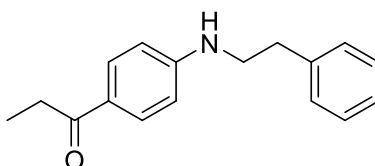
N-(Phenylmethyl)-6-quinolinamine (1j): The general procedure was followed using **C1** (0.023 g, 0.03 mmol, 5 mol %), NaO(*t*-Bu) (0.0865 g, 0.9 mmol), 6-chloroquinoline (0.098 g, 0.6 mmol), benzylamine (0.072 mL, 0.66 mmol) and toluene (5 mL). After flash column chromatography on silica gel (40 - 60% EtOAc in hexanes) the title compound was isolated as an off-white solid (0.118 g, 0.50 mmol, 84%). ¹H NMR (500 MHz; CDCl₃): δ 8.62 (dd, *J* = 4.1, 1.2 Hz, 1H), 7.88 (t, *J* = 8.8 Hz, 2H), 7.43 – 7.39 (overlapping br. s, 2H), 7.37 (t, *J* = 7.3 Hz, 2H), 7.30 (t, *J* = 7.2 Hz, 1H), 7.24 (dd, *J* = 8.3, 4.3 Hz, 1H), 7.13 (dd, *J* = 9.1, 2.5 Hz, 1H), 6.72 (d, *J* = 2.5 Hz, 1H), 4.44 (d, *J* = 5.1 Hz, 2H), 4.41 – 4.37 (br. m, 1H). ¹³C{¹H} NMR (125.7 MHz, CDCl₃): δ 146.3, 146.0, 143.4, 138.7, 133.8, 130.4, 130.1, 128.8, 127.5, 127.4, 121.4, 121.3, 103.3, 48.3. Calc'd for C₁₆H₁₅N₂ [M+H]⁺: 235.1230. Found: 235.1230.



N-(3-Methoxyphenyl)-α-methyl-benzenemethanamine (1k): The general procedure was followed using **C1** (0.023 g, 0.03 mmol, 5 mol %), NaO(*t*-Bu) (0.1153 g, 1.2 mmol), 3-chloroanisole (0.074 mL, 0.6 mmol), α-methyl-benzylamine (0.085 mL, 0.66 mmol) and toluene (5 mL). After flash column chromatography on silica gel (20% EtOAc in hexanes) the title compound was isolated as a pale yellow oil which solidified upon standing (0.133 g, 0.59 mmol, 98%). ¹H NMR (500 MHz; CDCl₃): δ 7.37 (d, *J* = 7.3 Hz, 2H), 7.32 (t, *J* = 7.9 Hz, 2H), 7.24 – 7.21 (m, 1H), 7.00 (t, *J* = 8.2 Hz, 1H), 6.22 (dd, *J* = 7.8, 1.9 Hz, 1H), 6.15 (dd, *J* = 8.1, 1.7 Hz, 1H), 6.08 (t, *J* = 2.3 Hz, 1H), 4.49 (q, *J* = 6.7 Hz, 1H), 4.05 (br. s, 1H), 3.69 (s, 3H), 1.52 (d, *J* = 6.7 Hz, 3H). ¹³C{¹H} NMR (125.7 MHz, CDCl₃): δ 160.7, 148.7, 145.2, 129.8, 128.6, 126.9, 125.8, 106.4, 102.5, 99.4, 55.0, 53.5, 24.9. Calc'd for C₁₅H₁₈N [M+H]⁺: 228.1383. Found: 228.1383.



4-(2-Propen-1-ylamino)benzonitrile (1l): The general procedure was followed using **C1** (0.023 g, 0.03 mmol, 5 mol %), NaO(*t*-Bu) (0.1153 g, 1.2 mmol), 3-chlorobenzonitrile (0.083 g, 0.6 mmol), allylamine (0.050 mL, 0.66 mmol) and toluene (5 mL). After flash column chromatography on silica gel (20% EtOAc in hexanes) the title compound was isolated as a pale yellow oil which solidified upon standing (0.059 g, 0.37 mmol, 62%). ¹H NMR (500 MHz; CDCl₃): δ 7.40 (d, *J* = 8.6, 2H), 6.57 (d, *J* = 8.8 Hz, 2H), 5.94 – 5.85 (m, 1H), 5.27 (dd, *J* = 17.2, 1.3 Hz, 1H), 5.20 (dd, *J* = 10.3, 1.0 Hz, 1H), 4.45 (br. s, 1H), 3.81 (t, *J* = 5.5 Hz, 2H). ¹³C{¹H} NMR (125.7 MHz, CDCl₃): δ 151.2, 133.8, 133.6, 120.5, 116.9, 112.4, 98.7, 45.6. HRMS-ESI (*m/z*): Calc'd for C₁₀H₁₀N₂Na [M+Na]⁺: 181.0736. Found: 181.0736.



1-[4-[(2-Phenylethyl)amino]phenyl]-1-propanone (1m): The general procedure was followed using **C1** (0.023 g, 0.03 mmol, 5 mol %), NaO(*t*-Bu) (0.1153 g, 1.2 mmol), 4-bromophenylethylketone (0.128 g, 0.6 mmol), benzene ethanamine (0.083 mL, 0.66 mmol) and toluene (5 mL). After flash column chromatography on silica gel (20% EtOAc in hexanes) the title compound was isolated as a pale yellow oil which solidified upon standing (0.132 g, 0.52 mmol, 87%). ¹H NMR (500 MHz; CDCl₃): δ 7.89 (d, *J* = 8.7 Hz, 2H), 7.39 – 7.35 (m, 2H), 7.32 – 7.25 (m, 3H), 6.61 (d, *J* = 8.7 Hz, 2H), 4.37 (br. s, 1H), 3.50 (t, *J* = 7.0 Hz, 2H), 2.97 (t, *J* = 7.0 Hz, 2H), 2.94 (q, *J* = 7.3 Hz, 2H), 1.25 (t, *J* = 7.3 Hz, 3H). ¹³C{¹H} NMR (125.7 MHz, CDCl₃): δ 199.1, 151.8, 138.8, 130.5, 128.7 (overlapping singlets), 126.6, 126.4, 111.6, 44.4, 35.3, 31.0, 8.8. HRMS-ESI (*m/z*): Calc'd for C₁₇H₁₉NONa [M+Na]⁺: 276.1359. Found: 276.1363.

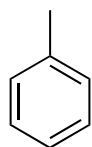
Computational Data

Reference for Gaussian 09 Revision B.01: M. J. Frisch, G. W. Trucks, H. B. Schlegel, G. E. Scuseria, M. A. Robb, J. R. Cheeseman, G. Scalmani, V. Barone, B. Mennucci, G. A. Petersson, H. Nakatsuji, M. Caricato, X. Li, H. P. Hratchian, A. F. Izmaylov, J. Bloino, G. Zheng, J. L. Sonnenberg, M. Hada, M. Ehara, K. Toyota, R. Fukuda, J. Hasegawa, M. Ishida, T. Nakajima, Y. Honda, O. Kitao, H. Nakai, T. Vreven, J. A. Montgomery, Jr., J. E. Peralta, F. Ogliaro, M. Bearpark, J. J. Heyd, E. Brothers, K. N. Kudin, V. N. Staroverov, T. Keith, R. Kobayashi, J. Normand, K. Raghavachari, A. Rendell, J. C. Burant, S. S. Iyengar, J. Tomasi, M. Cossi, N. Rega, J. M. Millam, M. Klene, J. E. Knox, J. B. Cross, V. Bakken, C. Adamo, J. Jaramillo, R. Gomperts, R. E. Stratmann, O. Yazyev, A. J. Austin, R. Cammi, C. Pomelli, J. W. Ochterski, R. L. Martin, K. Morokuma, V. G. Zakrzewski, G. A. Voth, P. Salvador, J. J. Dannenberg, S. Dapprich, A. D. Daniels, O. Farkas, J. B. Foresman, J. V. Ortiz, J. Cioslowski, and D. J. Fox, Gaussian, Inc., Wallingford CT, 2010.

General Computational Details. All density-functional theory (DFT) calculations were performed using the Gaussian 09 software package, revision B.01, along with the postg² program for the dispersion energies. Geometry optimizations and frequency calculations were performed on all species in the gas-phase with the B3LYP functional³ and the exchange-hole dipole moment (XDM)⁴ dispersion correction. A mixed basis set was used, consisting of 6-31G* for C and H, and 6-31+G* for all other elements. Single-point energy calculations on the optimized geometries were carried out using the same B3LYP-XDM method with the 6-311+G(2d,2p) basis set. The XDM damping parameters were $a_1 = 0$, $a_2 = 3.7737 \text{ \AA}$ for the geometry optimizations and $a_1 = 0.4376$, $a_2 = 2.1607 \text{ \AA}$ for the single-point energies.

Thermochemical Energies and Cartesian Coordinates for the Computed Species

Toluene

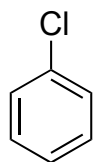


Zero-point correction=	0.128318 (Hartree/Particle)
Thermal correction to Energy=	0.134524

Thermal correction to Enthalpy= 0.135468
 Thermal correction to Gibbs Free Energy= 0.097615
 Sum of electronic and zero-point Energies= -271.443562
 Sum of electronic and thermal Energies= -271.437355
 Sum of electronic and thermal Enthalpies= -271.436411
 Sum of electronic and thermal Free Energies= -271.474264
 Single-point energy (6-311+G(2d,2p)) = -271.668522

C	-1.7827	-4.38255	-0.00067
C	-0.38648	-4.37962	0.01322
C	0.33403	-3.17691	0.01571
C	-0.38622	-1.97395	0.01061
C	-1.78231	-1.97079	-0.00329
C	-2.48671	-3.17663	-0.00967
H	-2.32022	-5.32764	0.00008
H	0.1533	-5.32444	0.02424
H	0.15371	-1.02915	0.0195
H	-2.31963	-1.02559	-0.00471
H	-3.57358	-3.17649	-0.0171
C	1.84666	-3.17674	-0.00051
H	2.23489	-3.16055	-1.02802
H	2.2541	-2.2985	0.51229
H	2.25376	-4.0705	0.48479

Chlorobenzene



Zero-point correction= 0.091230 (Hartree/Particle)
 Thermal correction to Energy= 0.096733
 Thermal correction to Enthalpy= 0.097677
 Thermal correction to Gibbs Free Energy= 0.061441
 Sum of electronic and zero-point Energies= -691.758724
 Sum of electronic and thermal Energies= -691.753221
 Sum of electronic and thermal Enthalpies= -691.752277
 Sum of electronic and thermal Free Energies= -691.788512
 Single-point energy (6-311+G(2d,2p)) = -691.962808

C	-1.25523	1.38798	0.00026
C	0.14021	1.42833	0.00123
C	0.8129	2.65153	0.0006
C	0.06675	3.82944	-0.00106
C	-1.32728	3.81069	-0.00208
C	-1.9839	2.57879	-0.00139
H	-1.77234	0.43305	0.00077

H	0.71403	0.50575	0.00246
H	1.8968	2.69378	0.0013
H	-1.88451	4.74135	-0.0033
H	-3.0701	2.55506	-0.0021
Cl	0.90653	5.37899	-0.0019

***tert*-Butoxide**

Zero-point correction=	0.121461 (Hartree/Particle)
Thermal correction to Energy=	0.127784
Thermal correction to Enthalpy=	0.128728
Thermal correction to Gibbs Free Energy=	0.092817
Sum of electronic and zero-point Energies=	-232.952827
Sum of electronic and thermal Energies=	-232.946504
Sum of electronic and thermal Enthalpies=	-232.945560
Sum of electronic and thermal Free Energies=	-232.981471
Single-point energy (6-311+G(2d,2p)) =	-233.168725

C	1.06553	0.6917	-0.00238
C	1.64319	1.41899	1.2573
H	1.27333	2.45262	1.27595
H	1.27311	0.91851	2.16178
H	2.74715	1.44407	1.301
C	1.64335	1.41885	-1.26207
H	2.74731	1.44392	-1.30563
H	1.27338	0.91827	-2.16654
H	1.27349	2.45248	-1.28088
C	1.64303	-0.76292	-0.00226
H	1.27295	-1.29584	0.88349
H	1.27306	-1.29594	-0.888
H	2.74699	-0.81342	-0.00219
O	-0.2891	0.69185	-0.00247

***tert*-Butanol**

Zero-point correction=	0.136151 (Hartree/Particle)
Thermal correction to Energy=	0.142874
Thermal correction to Enthalpy=	0.143818
Thermal correction to Gibbs Free Energy=	0.107159
Sum of electronic and zero-point Energies=	-233.547294
Sum of electronic and thermal Energies=	-233.540571
Sum of electronic and thermal Enthalpies=	-233.539627
Sum of electronic and thermal Free Energies=	-233.576286
Single-point energy (6-311+G(2d,2p)) =	-233.776853

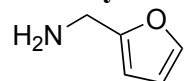
C	1.16699	0.70144	-0.00237
C	1.64481	1.42733	1.26398
H	1.28536	2.46477	1.28012
H	1.26706	0.92096	2.15824
H	2.7394	1.45571	1.31678
C	1.64497	1.42719	-1.26875
H	2.73957	1.45557	-1.32141
H	1.26733	0.92072	-2.163
H	1.28552	2.46462	-1.28505
C	1.6232	-0.75936	-0.00226
H	1.24356	-1.27676	0.88477
H	1.24367	-1.27686	-0.88928
H	2.71672	-0.82454	-0.00219
O	-0.27716	0.63688	-0.00246
H	-0.62655	1.54246	-0.00253

chloride

Zero-point correction=	0.000000 (Hartree/Particle)
Thermal correction to Energy=	0.001416
Thermal correction to Enthalpy=	0.002360
Thermal correction to Gibbs Free Energy=	-0.015023
Sum of electronic and zero-point Energies=	-460.271463
Sum of electronic and thermal Energies=	-460.270047
Sum of electronic and thermal Enthalpies=	-460.269103
Sum of electronic and thermal Free Energies=	-460.286486
Single-point energy (6-311+G(2d,2p)) =	-460.303727

Cl	4.77575	3.37673	-0.48322
----	---------	---------	----------

Furfurylamine



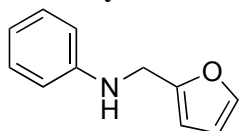
Zero-point correction=	0.115442 (Hartree/Particle)
Thermal correction to Energy=	0.121414
Thermal correction to Enthalpy=	0.122359
Thermal correction to Gibbs Free Energy=	0.085413
Sum of electronic and zero-point Energies=	-324.576109
Sum of electronic and thermal Energies=	-324.570136
Sum of electronic and thermal Enthalpies=	-324.569192
Sum of electronic and thermal Free Energies=	-324.606137

C,0,-0.3654697965,0.2791966128,-0.0000050042
C,0,0.995771008,0.2634244651,0.0003092911
C,0,1.4180556022,1.6372590574,-0.0000338826
C,0,0.2843541298,2.3858704525,-0.0002910015

O,0,-0.8196183481,1.5731448133,0.0001618089
 H,0,1.6099465428,-0.6241847704,0.0005628031
 H,0,2.4331866523,2.0098607943,-0.0000781482
 H,0,0.0818442467,3.4456649032,-0.0005456885
 C,0,-1.4161979548,-0.7897376316,-0.0000070874
 H,0,-2.0685247468,-0.6566608047,0.8743983609
 H,0,-2.0684452151,-0.6567706431,-0.8744879836
 N,0,-0.8027252604,-2.1267983706,0.0000756292
 H,0,-1.0669302358,-2.661969074,0.8205073787
 H,0,-1.0671562244,-2.6621687042,-0.820152776

Single-point energy (6-311+G(2d,2p)) = -3.248081057416E+02

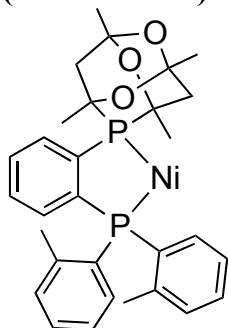
***N*-Phenyl-2-furanmethanamine**



Zero-point correction= 0.196977 (Hartree/Particle)
 Thermal correction to Energy= 0.207759
 Thermal correction to Enthalpy= 0.208703
 Thermal correction to Gibbs Free Energy= 0.158613
 Sum of electronic and zero-point Energies= -555.556142
 Sum of electronic and thermal Energies= -555.545361
 Sum of electronic and thermal Enthalpies= -555.544417
 Sum of electronic and thermal Free Energies= -555.594507
 Single-point energy (6-311+G(2d,2p)) = -5.559443030602E+02
 C,0,-0.2242550117,0.0846961249,0.066119008
 C,0,1.0254382359,-0.4487478472,-0.021108754
 C,0,1.9274765322,0.6563107094,-0.1899771112
 C,0,1.1608767964,1.778214088,-0.1924335015
 O,0,-0.1605371406,1.4491172089,-0.0390357804
 H,0,1.2656711706,-1.5008935447,0.0187090729
 H,0,3.0023234117,0.6122549497,-0.2981967169
 H,0,1.3691689226,2.832443657,-0.2880915516
 C,0,-1.5926093268,-0.4982351239,0.2559652201
 H,0,-1.9627934556,-0.251498382,1.2590980549
 H,0,-2.2913909933,-0.0298334458,-0.4565511681
 N,0,-1.5894157015,-1.9470175709,0.1305128445
 H,0,-2.0798197762,-2.422614027,0.8750336797
 C,0,-1.7206710174,-2.5738452652,-1.1163098928
 C,0,-2.1315416553,-3.91870268,-1.1693880414
 C,0,-1.4279542249,-1.9109096423,-2.3201080772
 C,0,-2.2479578869,-4.5771860455,-2.3889675333
 H,0,-2.3593546946,-4.4439521609,-0.2435837943
 C,0,-1.5507781964,-2.5830833854,-3.536718106
 H,0,-1.0854729136,-0.8823053374,-2.3080577872

C,0,-1.9602191496,-3.9151846879,-3.586002519
H,0,-2.570045987,-5.6152498481,-2.4031310837
H,0,-1.3184776369,-2.0514674608,-4.4559730069
H,0,-2.0524118013,-4.430431383,-4.5373611544

(PAd-DalPhos)Ni



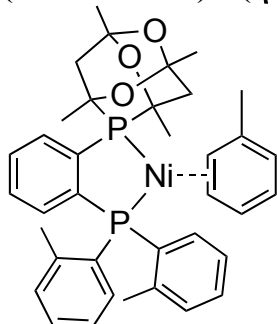
Zero-point correction= 0.575791 (Hartree/Particle)
Thermal correction to Energy= 0.610190
Thermal correction to Enthalpy= 0.611135
Thermal correction to Gibbs Free Energy= 0.511577
Sum of electronic and zero-point Energies= -3579.792858
Sum of electronic and thermal Energies= -3579.758458
Sum of electronic and thermal Enthalpies= -3579.757514
Sum of electronic and thermal Free Energies= -3579.857072
Single-point energy (6-311+G(2d,2p)) = -3581.014408

Ni	0.2736600	0.0216600	-1.7063280
P	-1.3529430	-0.3304910	-0.4509620
P	1.8321280	0.0372710	-0.3084960
C	-0.4498920	-1.0078010	1.0383950
C	0.9607650	-0.8490810	1.0821130
C	-2.9342590	-1.3828100	-0.6143610
C	-2.3393040	1.1896970	0.1496360
C	2.2610960	1.6849250	0.4024540
C	3.4504660	-0.8507400	-0.3731610
O	-3.7491340	-1.4000760	0.5835440
O	-3.2032180	1.5599520	-0.9505150
C	1.6867600	-1.4089360	2.1414400
C	-1.0747250	-1.7299580	2.0687210
C	-3.2117060	0.8605470	1.3629260
C	-3.7415460	-0.7010410	-1.7298720
C	-2.6159360	-2.8337800	-0.9378860
C	-1.4273240	2.3784700	0.3899740
C	2.7385640	2.7007330	-0.4619250
C	2.0374620	1.9846380	1.7545440
C	3.4946940	-2.1513530	-0.9338420
C	4.6419580	-0.2421710	0.0484790

H	2.7670820	-1.2971540	2.1624670
C	1.0478730	-2.1197730	3.1575040
C	-0.3359530	-2.2813080	3.1169600
H	-2.1468210	-1.8816370	2.0358830
C	-4.3076410	-0.1451730	0.9809060
H	-2.6026900	0.4705590	2.1830810
H	-3.7015860	1.7792780	1.7080240
H	-4.5995020	-1.3338000	-1.9871860
H	-3.1237860	-0.5651020	-2.6228660
C	-4.2708140	0.6582610	-1.2466000
H	-3.5461560	-3.3962710	-1.0801180
H	-2.0471380	-3.3038820	-0.1302720
H	-2.0224080	-2.8907960	-1.8563210
H	-2.0277120	3.2610230	0.6411710
H	-0.8363770	2.5936040	-0.5053020
H	-0.7353330	2.1766150	1.2127580
C	2.9799160	3.9728650	0.0700040
C	2.2797130	3.2607910	2.2633390
H	1.6658970	1.2126360	2.4194950
C	2.9919760	2.4522520	-1.9294770
C	4.7353340	-2.7889610	-1.0431540
H	4.6094780	0.7539110	0.4788370
C	2.2493650	-2.8667520	-1.4005130
C	5.8693590	-0.8941250	-0.0755900
O	-5.0687950	0.4236490	-0.0832760
H	1.6296610	-2.5497350	3.9685090
H	-0.8451220	-2.8440520	3.8951070
C	-5.2716150	-0.4462850	2.1109220
C	-5.1512580	1.3577420	-2.2619710
H	3.3484260	4.7542800	-0.5904390
C	2.7541560	4.2602860	1.4162980
H	2.0981430	3.4680840	3.3145200
H	3.7625780	1.6883460	-2.0876560
H	3.3195840	3.3699460	-2.4279170
H	2.0839570	2.0882380	-2.4298870
H	4.7741320	-3.7877800	-1.4719710
H	1.6444860	-2.2298990	-2.0624390
H	1.5988970	-3.1386860	-0.5600420
H	2.5057080	-3.7846980	-1.9388830
C	5.9157950	-2.1747780	-0.6228860
H	6.7796700	-0.4026430	0.2574300
H	-6.0311520	-1.1511440	1.7628840
H	-5.7611810	0.4745460	2.4393620
H	-4.7346500	-0.8878300	2.9558490
H	-5.5134950	2.2991910	-1.8409050
H	-6.0070660	0.7259460	-2.5150770

H	-4.5771580	1.5696800	-3.1684840
H	2.9466210	5.2596230	1.7972710
H	6.8642630	-2.6950740	-0.7261260

(PAd-DalPhos)Ni(η^2 -toluene)



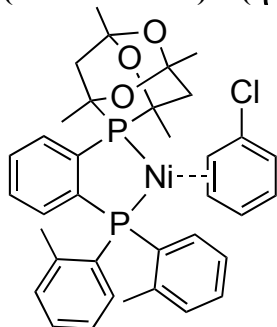
Zero-point correction=	0.706137 (Hartree/Particle)
Thermal correction to Energy=	0.747644
Thermal correction to Enthalpy=	0.748588
Thermal correction to Gibbs Free Energy=	0.635228
Sum of electronic and zero-point Energies=	-3851.279479
Sum of electronic and thermal Energies=	-3851.237972
Sum of electronic and thermal Enthalpies=	-3851.237028
Sum of electronic and thermal Free Energies=	-3851.350388
Single-point energy (6-311+G(2d,2p)) =	-3852.724250

Ni	0.2485680	1.3144450	-0.1226080
P	-1.3183510	-0.1641440	-0.3719960
P	1.7422370	-0.2848330	0.0624600
C	-0.4497540	-1.6581750	-1.0466450
C	0.9531460	-1.6733340	-0.8846580
C	-2.9111240	-0.0086440	-1.3965440
C	-2.2791880	-0.7311550	1.1781100
C	2.1657700	-1.1110690	1.6735530
C	3.3809590	-0.1559260	-0.7889950
O	-3.7113110	-1.2169480	-1.3899580
O	-3.1485790	0.3638850	1.5393830
C	1.7093060	-2.7047440	-1.4567760
C	-1.0577350	-2.6920980	-1.7790980
C	-3.1406260	-1.9599220	0.8761410
C	-3.7201210	1.1040090	-0.7183430
C	-2.6131440	0.3055820	-2.8543170
C	-1.3576720	-0.9374530	2.3653590
C	2.6415260	-0.3397640	2.7612120
C	1.9411610	-2.4837440	1.8674930
C	3.4362350	0.2907880	-2.1327970
C	4.5788870	-0.4129030	-0.1053920
H	2.7891670	-2.7033780	-1.3382880

C	1.0935140	-3.7202540	-2.1868920
C	-0.2930380	-3.7119400	-2.3458030
H	-2.1308440	-2.6809070	-1.9260060
C	-4.2522570	-1.6040160	-0.1227010
H	-2.5271030	-2.7792940	0.4913110
H	-3.6165320	-2.2961000	1.8054300
H	-4.5856190	1.3466500	-1.3472270
H	-3.1107120	2.0008480	-0.5925530
C	-4.2315240	0.6336680	0.6481070
H	-3.5522720	0.4355950	-3.4047130
H	-2.0437570	-0.5000020	-3.3271040
H	-2.0296020	1.2288380	-2.9234820
H	-1.9553560	-1.1591710	3.2573880
H	-0.7667760	-0.0360790	2.5516210
H	-0.6706940	-1.7688650	2.1870980
C	2.8738410	-0.9719350	3.9890870
C	2.1739900	-3.0947400	3.0995450
H	1.5719600	-3.0895700	1.0487740
C	2.9157350	1.1363940	2.6324490
C	4.6909310	0.4799270	-2.7239410
H	4.5438120	-0.7785690	0.9154850
C	2.1959700	0.5315330	-2.9614380
C	5.8188830	-0.2168780	-0.7137420
O	-5.0192590	-0.5428180	0.4422230
H	1.6931850	-4.5096070	-2.6322750
H	-0.7820060	-4.4945840	-2.9200310
C	-5.2047140	-2.7499520	-0.3989710
C	-5.1106720	1.6522610	1.3437080
H	3.2393620	-0.3749420	4.8212550
C	2.6428880	-2.3346940	4.1685950
H	1.9866210	-4.1585950	3.2177950
H	3.7828660	1.3320300	1.9894290
H	3.1174420	1.5846370	3.6103620
H	2.0620600	1.6481930	2.1819690
H	4.7347140	0.8272670	-3.7538250
H	1.3960290	0.9989170	-2.3742440
H	1.7872590	-0.4108670	-3.3470450
H	2.4202780	1.1746320	-3.8187650
C	5.8758620	0.2370780	-2.0297290
H	6.7311070	-0.4219760	-0.1598510
H	-5.9758780	-2.4206710	-1.1002190
H	-5.6806120	-3.0720500	0.5312280
H	-4.6619020	-3.5940960	-0.8349280
H	-5.4580800	1.2436060	2.2962290
H	-5.9760130	1.8904240	0.7190700
H	-4.5374260	2.5641290	1.5327020

H	2.8261600	-2.7951390	5.1356280
H	6.8338580	0.3994120	-2.5162320
C	-0.0529700	3.1659680	-1.0974530
C	0.9598480	3.1985310	-0.0735920
C	0.4788080	3.5412590	1.2363460
C	-0.8246480	3.9452410	1.4669950
C	-1.7341220	4.1096740	0.3937160
C	-1.3425460	3.7255310	-0.8711300
H	0.2601890	3.0273590	-2.1314500
H	1.1862120	3.5542850	2.0620600
H	-1.1326290	4.1991070	2.4780970
H	-2.7239170	4.5196960	0.5731180
H	-2.0176890	3.8403110	-1.7165950
C	2.4250560	3.3832520	-0.4115660
H	3.0732090	3.0014860	0.3829790
H	2.6583400	4.4504300	-0.5435670
H	2.6978350	2.8697380	-1.3370800

(PAd-DalPhos)Ni(η^2 -PhCl)



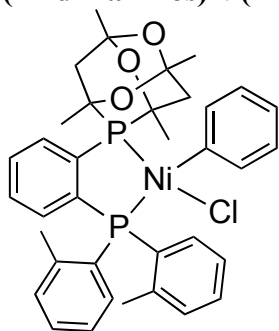
Zero-point correction=	0.668556 (Hartree/Particle)
Thermal correction to Energy=	0.709736
Thermal correction to Enthalpy=	0.710680
Thermal correction to Gibbs Free Energy=	0.597119
Sum of electronic and zero-point Energies=	-4271.600069
Sum of electronic and thermal Energies=	-4271.558889
Sum of electronic and thermal Enthalpies=	-4271.557944
Sum of electronic and thermal Free Energies=	-4271.671505
Single-point energy (6-311+G(2d,2p)) =	-4273.022227

Ni	0.2392290	1.2183100	-0.1290980
P	-1.3972010	-0.2076750	-0.3846030
P	1.6453790	-0.4821740	0.0860850
C	-0.6002800	-1.7368190	-1.0534130
C	0.7977950	-1.8239080	-0.8734540
C	-2.9638270	0.0622000	-1.4161100
C	-2.3917690	-0.7153080	1.1608690
C	1.9950430	-1.3097850	1.7073850

C	3.2992000	-0.4157120	-0.7288600
O	-3.8352010	-1.0936390	-1.4181030
O	-3.1869980	0.4329270	1.5221790
C	1.5065760	-2.8902790	-1.4417890
C	-1.2544320	-2.7346050	-1.7955730
C	-3.3291070	-1.8843850	0.8473750
C	-3.7013750	1.2213040	-0.7332430
C	-2.6365760	0.3645200	-2.8701150
C	-1.4878060	-0.9876000	2.3485510
C	2.4269320	-0.5303070	2.8054940
C	1.7960520	-2.6873790	1.8845160
C	3.3995550	0.0196920	-2.0720570
C	4.4658530	-0.7205130	-0.0135110
H	2.5843710	-2.9413780	-1.3163140
C	0.8461630	-3.8707310	-2.1808740
C	-0.5365120	-3.7914240	-2.3552580
H	-2.3238020	-2.6660910	-1.9553170
C	-4.4094060	-1.4510280	-0.1550950
H	-2.7677760	-2.7400470	0.4617320
H	-3.8304330	-2.1931700	1.7725610
H	-4.5458630	1.5236560	-1.3643830
H	-3.0363400	2.0764490	-0.5983990
C	-4.2482270	0.7769990	0.6282640
H	-3.5622320	0.5564910	-3.4247640
H	-2.1164530	-0.4728370	-3.3442710
H	-1.9958070	1.2496490	-2.9317300
H	-2.1011020	-1.1811040	3.2362940
H	-0.8456730	-0.1247920	2.5470700
H	-0.8509180	-1.8570230	2.1648250
C	2.6540620	-1.1652820	4.0326160
C	2.0166140	-3.2997200	3.1184120
H	1.4585330	-3.2950310	1.0533220
C	2.6236330	0.9596930	2.6957470
C	4.6734190	0.1372840	-2.6389080
H	4.3921390	-1.0630830	1.0131290
C	2.1907340	0.3367890	-2.9187200
C	5.7258910	-0.5913770	-0.5975830
O	-5.1079190	-0.3450740	0.4114770
H	1.4092410	-4.6879880	-2.6233590
H	-1.0577790	-4.5467320	-2.9373810
C	-5.4328450	-2.5303740	-0.4443260
C	-5.0609180	1.8469420	1.3269270
H	2.9914150	-0.5662440	4.8749420
C	2.4505930	-2.5345800	4.1985740
H	1.8507240	-4.3678950	3.2285150
H	3.2923320	1.2379010	1.8736620

H	3.0398580	1.3663680	3.6228380
H	1.6669800	1.4546790	2.5030420
H	4.7559540	0.4789750	-3.6679180
H	1.4363480	0.8938810	-2.3515080
H	1.7055530	-0.5766310	-3.2849050
H	2.4753330	0.9397970	-3.7862380
C	5.8299240	-0.1578990	-1.9173210
H	6.6158660	-0.8289460	-0.0213120
H	-6.1765060	-2.1470090	-1.1477060
H	-5.9345030	-2.8261630	0.4810180
H	-4.9438380	-3.4055540	-0.8826230
H	-5.4371070	1.4568140	2.2762270
H	-5.9069810	2.1441490	0.7012420
H	-4.4296910	2.7183510	1.5222440
H	2.6290260	-2.9970630	5.1655420
H	6.8042990	-0.0469190	-2.3853450
C	-0.0844330	3.0398720	-0.9930530
C	1.0291370	2.9946540	-0.0703830
C	0.8205050	3.5581430	1.2355880
C	-0.3826070	4.1327010	1.5794910
C	-1.4220090	4.2918510	0.6228620
C	-1.2545130	3.7848950	-0.6432460
H	0.1075690	2.8681180	-2.0505270
H	1.6495830	3.5676060	1.9348720
H	-0.5118800	4.5300000	2.5830320
H	-2.3210570	4.8408340	0.8878690
H	-2.0033750	3.9645430	-1.4116960
Cl	2.7263320	3.1619790	-0.7134630

(PAd-DalPhos)Ni(Ph)Cl



Zero-point correction=
Thermal correction to Energy=

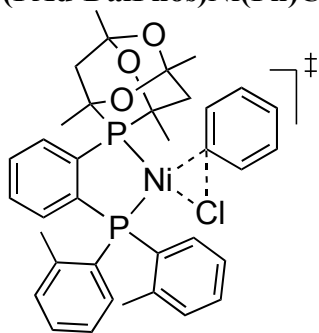
0.669717 (Hartree/Particle)
0.710944

Thermal correction to Enthalpy= 0.711888
 Thermal correction to Gibbs Free Energy= 0.598366
 Sum of electronic and zero-point Energies= -4271.640752
 Sum of electronic and thermal Energies= -4271.599524
 Sum of electronic and thermal Enthalpies= -4271.598580
 Sum of electronic and thermal Free Energies= -4271.712102
 Single-point energy (6-311+G(2d,2p)) = -4273.065005

Ni	0.2294730	1.3238010	-0.0238930
Cl	1.5796940	3.0840710	-0.0861570
P	-1.0733230	-0.4083730	-0.3699090
P	1.9523770	-0.1514150	0.0447110
C	-1.2222190	2.5557740	0.0584700
C	-1.6089680	3.3445740	-1.0342010
C	-1.8751380	2.7528450	1.2828260
C	-0.0040300	-1.7062170	-1.1656490
C	1.3867900	-1.5651200	-0.9803140
C	-2.6618430	-0.3610970	-1.4214430
C	-1.9688990	-1.2172520	1.1124110
C	2.3412400	-0.9214100	1.6775040
C	3.5723840	0.3115180	-0.6720770
C	-2.6428770	4.2784630	-0.9182310
C	-2.8971920	3.7012700	1.4086680
H	-1.6053140	2.1555960	2.1503380
O	-3.2103740	-1.6957620	-1.5369910
O	-3.0126300	-0.3117460	1.5055660
C	2.2772150	-2.4468400	-1.6054010
C	-0.4687010	-2.7533590	-1.9804740
C	-2.5947470	-2.5460570	0.6788920
C	-3.6975320	0.5035730	-0.6978570
C	-2.3807440	0.1263060	-2.8336650
C	-1.0606040	-1.3626890	2.3189290
C	2.3935550	-0.1310480	2.8499620
C	2.5455330	-2.3073280	1.7682090
C	3.6411600	0.8278800	-1.9884630
C	4.7359330	0.2031820	0.1007460
H	-2.9283450	4.8770590	-1.7806590
C	-3.2955070	4.4577980	0.3045530
H	-3.3829370	3.8440830	2.3719100
H	3.3464390	-2.3076240	-1.4735640
C	1.8014680	-3.4771180	-2.4138050
C	0.4264760	-3.6267790	-2.5981190
H	-1.5302320	-2.8646470	-2.1550530
C	-3.7207880	-2.2938350	-0.3343420
H	-1.8395380	-3.2186360	0.2638730
H	-3.0341990	-3.0276940	1.5602470

H	-4.5794460	0.5797400	-1.3447340
H	-3.3169420	1.5041600	-0.5075090
C	-4.1244870	-0.1653930	0.6108310
H	-3.3100460	0.1113800	-3.4139690
H	-1.6462690	-0.5068600	-3.3397720
H	-2.0019810	1.1515100	-2.8009000
H	-1.6434290	-1.7493710	3.1625180
H	-0.6372540	-0.3959990	2.6032060
H	-0.2392260	-2.0535700	2.1117310
C	2.6497300	-0.7737440	4.0689760
C	2.7948670	-2.9244460	2.9929440
H	2.5007190	-2.9189400	0.8745980
C	2.1774250	1.3604280	2.8405080
C	4.8954130	1.2087080	-2.4771210
H	4.6763510	-0.1880490	1.1107810
C	2.4273640	0.9749760	-2.8737050
H	-4.0954480	5.1876010	0.3982910
C	5.9733920	0.5976420	-0.4078130
O	-4.6759000	-1.4463680	0.2884900
H	2.4988370	-4.1512190	-2.9032220
H	0.0443890	-4.4184360	-3.2367860
C	-4.4420270	-3.5552020	-0.7642330
C	-5.1817490	0.6095830	1.3662640
H	2.6911960	-0.1719820	4.9732230
C	2.8452930	-2.1510480	4.1510840
H	2.9467950	-3.9992400	3.0367960
H	2.8353820	1.8778270	2.1361160
H	2.3446840	1.7791700	3.8374340
H	1.1581220	1.6214300	2.5320450
H	4.9605960	1.6110520	-3.4848430
H	1.6420440	1.5454410	-2.3658760
H	2.0091530	0.0024910	-3.1598940
H	2.6872520	1.5096150	-3.7921970
C	6.0514800	1.1015320	-1.7037050
H	6.8640110	0.5121150	0.2082060
H	-5.2358620	-3.2970750	-1.4697310
H	-4.8839940	-4.0455680	0.1072830
H	-3.7437670	-4.2453240	-1.2473630
H	-5.4419970	0.0744570	2.2833510
H	-6.0764850	0.7141620	0.7463670
H	-4.7988800	1.6015390	1.6167340
H	3.0358650	-2.6151860	5.1149060
H	7.0072200	1.4165350	-2.1136260
H	-1.0840820	3.2502400	-1.9820930

(PAd-DalPhos)Ni(Ph)Cl C_{sp2}-Cl oxidative addition transition state (TS-1)



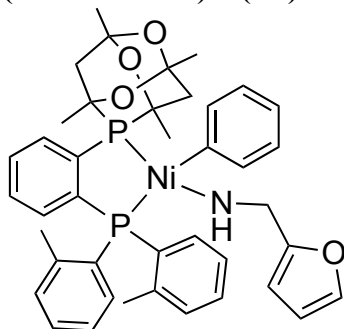
Zero-point correction= 0.667304 (Hartree/Particle)
Thermal correction to Energy= 0.708285
Thermal correction to Enthalpy= 0.709229
Thermal correction to Gibbs Free Energy= 0.596476
Sum of electronic and zero-point Energies= -4271.587154
Sum of electronic and thermal Energies= -4271.546174
Sum of electronic and thermal Enthalpies= -4271.545230
Sum of electronic and thermal Free Energies= -4271.657983
Single-point energy (6-311+G(2d,2p)) = -4273.019837

Ni	-0.2244190	1.0519830	-0.5772420
Cl	-0.1958650	1.9891360	-2.7957450
P	1.4945040	0.0108320	0.2843970
P	-1.5523370	-0.6059400	0.0478810
C	-1.1728060	2.5832420	-1.0892090
C	-0.3040610	3.3735980	-0.2971940
C	-2.5618450	2.8319440	-1.1148080
C	0.7929990	-1.1637610	1.5241200
C	-0.5949250	-1.4103140	1.4227530
C	2.9224420	0.9076840	1.1457700
C	2.6586530	-0.9521670	-0.8693680
C	-1.8080160	-2.0130560	-1.1312240
C	-3.2066240	-0.3718560	0.8324400
C	-0.8717610	4.2813760	0.6200830
C	-3.0831920	3.7383160	-0.2081300
H	-3.2061610	2.2742660	-1.7841640
O	3.9226650	-0.0070260	1.6508890
O	3.3277430	0.0492780	-1.6656330
C	-1.2228120	-2.2264730	2.3727220
C	1.5126180	-1.7374760	2.5855450
C	3.7108730	-1.7326690	-0.0797390
C	3.5664470	1.7760900	0.0542190
C	2.4414550	1.7256570	2.3337390
C	1.8793080	-1.8146330	-1.8448040
C	-2.4251350	-1.7847670	-2.3858100
C	-1.3226080	-3.2968680	-0.8358620

C	-3.3561920	0.5854140	1.8661170
C	-4.3340820	-1.0706510	0.3748830
H	-0.2171270	4.8875160	1.2420930
C	-2.2464640	4.4549820	0.6757750
H	-4.1593920	3.8864220	-0.1687180
H	-2.2908220	-2.4085690	2.2964260
C	-0.4967900	-2.7912500	3.4205020
C	0.8724750	-2.5429310	3.5273050
H	2.5693690	-1.5230820	2.6915310
C	4.6409730	-0.7654340	0.6690760
H	3.2366850	-2.4289650	0.6176180
H	4.3208570	-2.3145390	-0.7811400
H	4.3192900	2.4261970	0.5152890
H	2.8163480	2.4011170	-0.4385350
C	4.2640790	0.8865010	-0.9857790
H	3.2822580	2.2795660	2.7667790
H	2.0159230	1.0809650	3.1082570
H	1.6714800	2.4347120	2.0141120
H	2.5711710	-2.2799310	-2.5565050
H	1.1582810	-1.2074390	-2.3992950
H	1.3338490	-2.6024460	-1.3173840
C	-2.5311510	-2.8534670	-3.2846290
C	-1.4302630	-4.3449760	-1.7499260
H	-0.8499760	-3.4867140	0.1205790
C	-2.9717440	-0.4369480	-2.7841740
C	-4.6380480	0.8151230	2.3799790
H	-4.2202120	-1.8205150	-0.4009360
C	-2.1843790	1.3256200	2.4609450
H	-2.6805080	5.1729320	1.3654540
C	-5.6017630	-0.8255930	0.9023590
O	5.2374680	0.0984550	-0.2943990
H	-1.0000340	-3.4154660	4.1539520
H	1.4429520	-2.9677240	4.3489480
C	5.7658780	-1.4600100	1.4093660
C	4.9905300	1.6706010	-2.0584790
H	-3.0085700	-2.6782580	-4.2455790
C	-2.0373630	-4.1220390	-2.9832440
H	-1.0419460	-5.3269620	-1.4935510
H	-3.4361660	-0.4862700	-3.7738500
H	-2.1755110	0.3116070	-2.8222320
H	-3.7290800	-0.0793230	-2.0771830
H	-4.7567240	1.5523220	3.1706370
H	-1.5138980	1.7168180	1.6895620
H	-1.5847800	0.6670890	3.1021700
H	-2.5267400	2.1669260	3.0700650
C	-5.7552230	0.1276700	1.9071130

H	-6.4590970	-1.3793880	0.5294070
H	6.3957210	-0.7123410	1.8982480
H	6.3739580	-2.0364360	0.7069690
H	5.3578560	-2.1348020	2.1679140
H	5.4901660	0.9766050	-2.7392530
H	5.7377420	2.3266610	-1.6035190
H	4.2743260	2.2724500	-2.6248210
H	-2.1289590	-4.9271000	-3.7072790
H	-6.7369320	0.3340590	2.3250440
H	0.7634490	3.3793020	-0.4822870

(PAd-DalPhos)Ni(Ph)furfurylamido



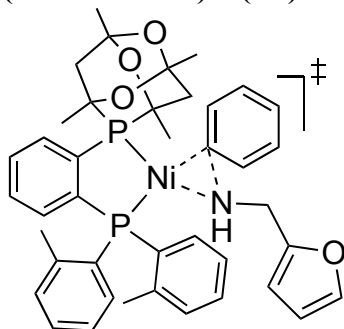
Zero-point correction= 0.772925 (Hartree/Particle)
 Thermal correction to Energy= 0.819678
 Thermal correction to Enthalpy= 0.820622
 Thermal correction to Gibbs Free Energy= 0.693559
 Sum of electronic and zero-point Energies= -4135.381678
 Sum of electronic and thermal Energies= -4135.334926
 Sum of electronic and thermal Enthalpies= -4135.333982
 Sum of electronic and thermal Free Energies= -4135.461045
 Single-point energy (6-311+G(2d,2p)) = -4.136988543490E+03

Ni	0.3120920	0.7322050	-0.1940410
P	-1.7102400	-0.1976020	-0.2985150
P	1.0830730	-1.3907950	-0.0411120
C	-0.2871990	2.5260840	-0.3443070
C	-0.3280540	3.2133750	-1.5689220
C	-0.6707720	3.2363790	0.8069880
C	-1.4715650	-1.9113810	-0.9792170
C	-0.1667080	-2.4417630	-0.8819020
C	-3.1800250	0.5219040	-1.2686780
C	-2.7249190	-0.3486950	1.3095760
C	1.2712290	-2.1669490	1.6237280
C	2.6546680	-1.7366910	-0.9156930
C	-0.7611130	4.5417240	-1.6497000
C	-1.0911040	4.5687440	0.7366670
H	-0.6629730	2.7420440	1.7764120
O	-4.3262570	-0.3594380	-1.1870590

O	-3.1363170	0.9890440	1.6460030
C	0.1363970	-3.6796450	-1.4631090
C	-2.4538240	-2.6617070	-1.6483280
C	-3.9667380	-1.2138720	1.0811490
C	-3.5630330	1.8491750	-0.6080690
C	-2.8540190	0.6838860	-2.7448620
C	-1.8786820	-0.8355350	2.4713030
C	1.7615700	-1.4118590	2.7153340
C	0.8925940	-3.5042990	1.8232740
C	2.7967880	-1.3735000	-2.2764590
C	3.7495770	-2.2608270	-0.2169910
H	-0.7862460	5.0448020	-2.6143030
C	-1.1490210	5.2257060	-0.4954320
H	-1.3760270	5.0935750	1.6466080
H	1.1524920	-4.0608520	-1.4085270
C	-0.8465010	-4.4079120	-2.1308580
C	-2.1423380	-3.8968210	-2.2173430
H	-3.4548220	-2.2628480	-1.7488500
C	-4.9264380	-0.5154850	0.1074280
H	-3.6895060	-2.2045240	0.7105080
H	-4.4872130	-1.3398770	2.0379220
H	-4.3547040	2.3109190	-1.2098440
H	-2.7141400	2.5288050	-0.5650470
C	-4.1189020	1.5985610	0.7966950
H	-3.7309970	1.0815130	-3.2680370
H	-2.5804730	-0.2703180	-3.2045610
H	-2.0248440	1.3867180	-2.8635900
H	-2.4816170	-0.8286150	3.3865130
H	-1.0156540	-0.1816590	2.6190780
H	-1.5180570	-1.8528980	2.2950950
C	1.8657030	-2.0439750	3.9624310
C	0.9956340	-4.1080190	3.0751840
H	0.5036780	-4.0841550	0.9943620
C	2.1474350	0.0395060	2.5972570
C	4.0445840	-1.5582090	-2.8822650
H	3.6403320	-2.5265020	0.8290150
C	1.6584140	-0.8127720	-3.0979370
H	-1.4817140	6.2587590	-0.5534010
C	4.9849180	-2.4340560	-0.8419070
O	-5.2626400	0.7475240	0.6684110
H	-0.6010150	-5.3633410	-2.5862650
H	-2.9139450	-4.4529030	-2.7428450
C	-6.2199970	-1.2726840	-0.1149980
C	-4.5649410	2.8618360	1.5002250
H	2.2460090	-1.4700240	4.8036190
C	1.4887880	-3.3719010	4.1511960

H	0.6942920	-5.1438830	3.2035180
H	2.7783980	0.2419450	1.7266040
H	2.6628550	0.3750550	3.5023450
H	1.2575940	0.6696270	2.4635040
H	4.1656370	-1.2754280	-3.9251010
H	1.1000510	-0.0406250	-2.5540900
H	0.9361150	-1.5917300	-3.3709650
H	2.0356970	-0.3679100	-4.0239050
C	5.1319880	-2.0798350	-2.1810230
H	5.8233390	-2.8366940	-0.2806820
H	-6.8566300	-0.7100980	-0.8026070
H	-6.7449220	-1.3993950	0.8356840
H	-6.0127380	-2.2578340	-0.5437310
H	-4.9537130	2.6113860	2.4908020
H	-5.3516880	3.3510040	0.9193300
H	-3.7165620	3.5428880	1.6014810
H	1.5775520	-3.8264520	5.1342170
H	6.0894560	-2.2014350	-2.6799920
H	-0.0092790	2.7111020	-2.4816000
N	2.1264460	1.3260850	-0.2704420
H	2.3656800	1.3393280	-1.2657710
C	2.5789250	2.5917990	0.2902850
H	2.2088660	2.6744660	1.3223950
H	2.2091460	3.4970000	-0.2217690
C	4.0792890	2.6308400	0.3041010
C	5.0447610	1.6993120	0.0528420
O	4.6699440	3.8269560	0.6324740
C	6.3095620	2.3554420	0.2386170
H	4.8632490	0.6728970	-0.2297360
C	6.0255680	3.6371210	0.5896880
H	7.2951980	1.9250600	0.1228560
H	6.6248150	4.5020730	0.8295470

(PAd-DalPhos)Ni(Ph)furfurylamido C_{sp2}-N reductive elimination transition state (TS-2)



Zero-point correction=

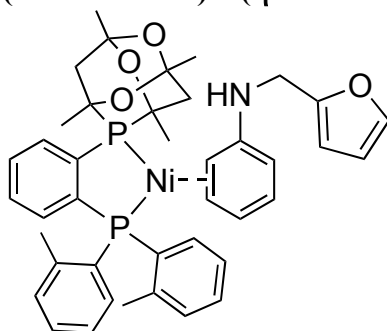
0.772478 (Hartree/Particle)

Thermal correction to Energy=			0.818459
Thermal correction to Enthalpy=			0.819403
Thermal correction to Gibbs Free Energy=			0.695361
Sum of electronic and zero-point Energies=			-4135.358748
Sum of electronic and thermal Energies=			-4135.312767
Sum of electronic and thermal Enthalpies=			-4135.311823
Sum of electronic and thermal Free Energies=			-4135.435866
Single-point energy (6-311+G(2d,2p)) =			-4.136964821056E+03
Ni	0.1762750	0.8382510	-0.2083120
P	-1.6793790	-0.3142260	-0.2881920
P	1.2641500	-1.2023580	-0.0922930
C	-0.3336640	2.6648060	-0.4239100
C	-0.7209890	3.1941770	-1.6908040
C	-0.8055500	3.3608270	0.7259520
C	-1.2506370	-1.9565120	-1.0285770
C	0.1150850	-2.3204120	-0.9959800
C	-3.2611070	0.2527580	-1.1666050
C	-2.5882650	-0.6285290	1.3568460
C	1.5721560	-2.1001540	1.4920010
C	2.8474910	-1.3410800	-1.0121060
C	-1.5269510	4.3230300	-1.7913600
C	-1.6155630	4.4892080	0.6042910
H	-0.5668660	2.9878980	1.7190510
O	-4.3180120	-0.7324810	-1.0583850
O	-3.1116590	0.6485580	1.7678920
C	0.5486680	-3.4741380	-1.6614550
C	-2.1547800	-2.7899820	-1.7092860
C	-3.7500760	-1.6051170	1.1573080
C	-3.7106730	1.5249590	-0.4397780
C	-3.0343840	0.4890390	-2.6510690
C	-1.6397380	-1.0678660	2.4565940
C	2.0537120	-1.3768510	2.6081050
C	1.2842490	-3.4665010	1.6304600
C	2.9306760	-0.8440550	-2.3367940
C	4.0055660	-1.8119970	-0.3766420
H	-1.8024290	4.6880180	-2.7792890
C	-1.9925030	4.9869450	-0.6476530
H	-1.9637630	4.9835560	1.5097890
H	1.6050870	-3.7287870	-1.6550710
C	-0.3586350	-4.2848270	-2.3418900
C	-1.7120530	-3.9427560	-2.3579340
H	-3.2020430	-2.5169180	-1.7525040
C	-4.8254420	-0.9759830	0.2594560
H	-3.3961850	-2.5487630	0.7320370
H	-4.2034750	-1.8175810	2.1329070
H	-4.5576590	1.9548210	-0.9872610

H	-2.9090150	2.2624570	-0.4064730
C	-4.1804160	1.1865700	0.9783420
H	-3.9773160	0.8007290	-3.1148440
H	-2.6833170	-0.4157200	-3.1559630
H	-2.2965610	1.2843350	-2.7869350
H	-2.1909240	-1.1493900	3.4005110
H	-0.8371340	-0.3368390	2.5843840
H	-1.1928270	-2.0386490	2.2249450
C	2.2407160	-2.0580320	3.8171060
C	1.4693510	-4.1245980	2.8460690
H	0.9020900	-4.0251760	0.7838230
C	2.3428210	0.1003800	2.5363020
C	4.1803500	-0.8443460	-2.9682710
H	3.9430090	-2.1877800	0.6392240
C	1.7250430	-0.3395430	-3.0947200
H	-2.6212710	5.8678410	-0.7319150
C	5.2408030	-1.7964630	-1.0238220
O	-5.2469050	0.2365130	0.8741950
H	-0.0110130	-5.1754960	-2.8581690
H	-2.4260240	-4.5667720	-2.8887910
C	-6.0537100	-1.8467760	0.0873430
C	-4.7083310	2.3843540	1.7377590
H	2.6112130	-1.5043300	4.6761880
C	1.9529710	-3.4162890	3.9446340
H	1.2365330	-5.1825960	2.9294030
H	3.0781120	0.3490410	1.7636980
H	2.7230960	0.4711610	3.4930110
H	1.4310320	0.6595320	2.2921410
H	4.2518050	-0.4618690	-3.9837110
H	1.0891320	0.2988970	-2.4678790
H	1.0948820	-1.1659430	-3.4457220
H	2.0340380	0.2406140	-3.9699740
C	5.3287360	-1.3092100	-2.3263320
H	6.1252460	-2.1611870	-0.5090780
H	-6.7785840	-1.3302380	-0.5470450
H	-6.5087740	-2.0460150	1.0613670
H	-5.7804220	-2.7967510	-0.3819290
H	-5.0309770	2.0721260	2.7346030
H	-5.5590210	2.8167650	1.2039890
H	-3.9204060	3.1360110	1.8263920
H	2.1018580	-3.9149850	4.8984870
H	6.2846250	-1.2864210	-2.8424200
H	-0.3769840	2.7027440	-2.6004580
N	1.4665850	2.2174290	-0.4118510
H	1.7064730	2.5333230	-1.3449230
C	2.1750240	2.9829550	0.5921710

H	1.8181430	2.6910880	1.5855770
H	1.9628150	4.0653360	0.5119520
C	3.6531260	2.7547730	0.5186560
C	4.4520390	1.9365140	-0.2247650
O	4.4247550	3.5010950	1.3742470
C	5.8024430	2.1878930	0.1968420
H	4.1182570	1.2357560	-0.9738530
C	5.7289730	3.1389360	1.1640550
H	6.7000770	1.7158220	-0.1776900
H	6.4574630	3.6499100	1.7745300

(PAd-DalPhos)Ni(η^2 - *N*-Phenyl-2-furanmethanamine)

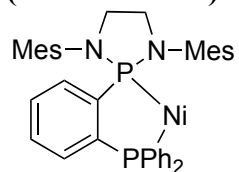


Zero-point correction=			0.774317 (Hartree/Particle)
Thermal correction to Energy=			0.820646
Thermal correction to Enthalpy=			0.821591
Thermal correction to Gibbs Free Energy=			0.694931
Sum of electronic and zero-point Energies=			-4135.393786
Sum of electronic and thermal Energies=			-4135.347457
Sum of electronic and thermal Enthalpies=			-4135.346513
Sum of electronic and thermal Free Energies=			-4135.473173
Single-point energy (6-311+G(2d,2p)) =			-4.136999618103E+03
Ni	-0.0766720	-0.5032230	0.7495800
P	1.7479430	-0.3561820	-0.3996720
P	-0.7322190	1.4201030	-0.0357130
C	1.3445210	0.7853260	-1.8060060
C	0.1774300	1.5643660	-1.6441810
C	2.6601470	-1.8198540	-1.1925410
C	3.3359240	0.2976580	0.4246550
C	-0.2352530	2.9893690	0.8270370
C	-2.4913580	1.7069090	-0.5130380
O	3.8227070	-1.4186330	-1.9582600
O	3.7534090	-0.7366050	1.3451890
C	-0.2692450	2.3759990	-2.6945890
C	2.0380480	0.8505760	-3.0263760
C	4.4527610	0.5211680	-0.5966560
C	3.1397950	-2.6810680	-0.0163560
C	1.7597640	-2.5905650	-2.1453890

C	3.0544230	1.5266050	1.2694050
C	-0.2963690	3.0691430	2.2377820
C	0.2597030	4.0870370	0.1054200
C	-3.1390050	0.8344470	-1.4254490
C	-3.2405270	2.6958180	0.1449390
H	-1.1836720	2.9506810	-2.5732400
C	0.4288980	2.4310540	-3.9000540
C	1.5849090	1.6664640	-4.0632570
H	2.9167310	0.2348010	-3.1748660
C	4.8873850	-0.8157420	-1.2160420
H	4.1326980	1.2198240	-1.3745410
H	5.3208220	0.9543040	-0.0848380
H	3.5597940	-3.6154180	-0.4077030
H	2.3071830	-2.9212940	0.6480520
C	4.2415050	-1.9458630	0.7621610
H	2.2973370	-3.4590540	-2.5435320
H	1.4441930	-1.9638130	-2.9844340
H	0.8637610	-2.9362150	-1.6196520
H	3.9685090	1.8339140	1.7909820
H	2.2824480	1.3089470	2.0122340
H	2.7082380	2.3562300	0.6453580
C	0.1342710	4.2459410	2.8646030
C	0.6873980	5.2485820	0.7474600
H	0.3249030	4.0370240	-0.9746690
C	-0.7938190	1.9277070	3.0838400
C	-4.5167330	0.9918450	-1.6275940
H	-2.7444100	3.3683440	0.8376760
C	-2.4095930	-0.2365210	-2.2054880
C	-4.6112170	2.8314750	-0.0735270
O	5.3053460	-1.6704890	-0.1531640
H	0.0665640	3.0588020	-4.7097700
H	2.1293090	1.6929710	-5.0035460
C	6.0545050	-0.6864310	-2.1739420
C	4.8236890	-2.7612420	1.8984790
H	0.0876500	4.3048100	3.9492810
C	0.6242110	5.3286640	2.1371480
H	1.0679050	6.0809980	0.1617240
H	-1.8237800	1.6494500	2.8372270
H	-0.7605170	2.1863810	4.1468920
H	-0.1933360	1.0240350	2.9314510
H	-5.0195810	0.3149940	-2.3138850
H	-1.6652650	-0.7509690	-1.5907050
H	-1.8959930	0.1872730	-3.0768910
H	-3.1160210	-0.9930270	-2.5591630
C	-5.2536510	1.9716260	-0.9625940
H	-5.1686190	3.6037560	0.4496470

H	6.3205430	-1.6743860	-2.5586150
H	6.9172850	-0.2597300	-1.6552760
H	5.7834720	-0.0375840	-3.0122510
H	5.6226260	-2.1925570	2.3812550
H	5.2327450	-3.7004440	1.5161720
H	4.0458780	-2.9782680	2.6360960
H	0.9565530	6.2252030	2.6536410
H	-6.3224100	2.0598040	-1.1384370
C	0.0405030	-1.9828330	3.9734890
C	0.4583940	-2.4993110	2.7706970
C	-0.3110120	-2.3295340	1.5718890
C	-1.5605350	-1.6112380	1.6533370
C	-1.9993060	-1.1683770	2.9499950
C	-1.2168200	-1.3192840	4.0671000
H	0.6485220	-2.1139470	4.8644490
H	1.3849300	-3.0663200	2.7219310
H	-0.1459660	-3.0115400	0.7387570
H	-2.9809310	-0.7024160	3.0227360
H	-1.5615980	-0.9516570	5.0301940
N	-2.5291880	-1.8040470	0.5975060
H	-3.1114670	-0.9728540	0.5146960
C	-3.4020880	-2.9832510	0.7791360
H	-3.8639360	-3.0108500	1.7809340
H	-2.7846100	-3.8818240	0.6803620
C	-4.4646790	-3.0076670	-0.2628710
C	-4.6073030	-3.6371700	-1.4643750
O	-5.5302700	-2.1644620	-0.0607340
C	-5.8298070	-3.1580040	-2.0424420
H	-3.9164620	-4.3517640	-1.8899740
C	-6.3439140	-2.2668920	-1.1515090
H	-6.2649990	-3.4449820	-2.9897000
H	-7.2369720	-1.6619480	-1.1260960

(NHP-DalPhos)Ni



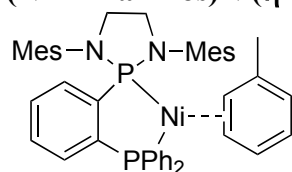
Zero-point correction=	0.684613 (Hartree/Particle)
Thermal correction to Energy=	0.726517
Thermal correction to Enthalpy=	0.727462
Thermal correction to Gibbs Free Energy=	0.606998
Sum of electronic and zero-point Energies=	-3771.998728
Sum of electronic and thermal Energies=	-3771.956824

Sum of electronic and thermal Enthalpies= -3771.955880
 Sum of electronic and thermal Free Energies= -3772.076343
 Single-point energy (6-311+G(2d,2p)) = -3.773393120170E+03

Ni	0.3592090	0.4804080	-1.4331480
P	1.0430060	-0.7652870	0.0738950
P	-1.0918390	1.5911280	-0.4130270
N	0.3663010	-2.3523520	0.3346950
N	2.6015350	-1.3501990	0.5235010
C	0.3706500	0.1633460	1.5512930
C	-0.5485540	1.2138720	1.3351850
C	0.2885590	0.6035010	3.9444650
H	0.6162560	0.3650590	4.9531730
C	0.7698450	-0.1310760	2.8620450
H	1.4744050	-0.9390580	3.0317000
C	1.3669270	-3.4087370	0.4689280
H	1.5987870	-3.8744750	-0.5040670
H	1.0038160	-4.2006820	1.1341390
C	2.6102200	-2.7212600	1.0512300
H	2.5706590	-2.7313660	2.1514920
H	3.5306550	-3.2288420	0.7452750
C	-0.9928400	-2.6824580	0.0486360
C	-1.5048340	-2.6464950	-1.2682550
C	-2.8452010	-2.9771190	-1.4840420
H	-3.2339520	-2.9402550	-2.4998560
C	-3.6916650	-3.3658620	-0.4438410
C	-3.1608740	-3.4149530	0.8459270
H	-3.8002190	-3.7181850	1.6727000
C	-1.8318850	-3.0736960	1.1139080
C	-0.6499300	-2.2676800	-2.4500500
H	-1.0991470	-2.6222040	-3.3834480
H	0.3616120	-2.6739580	-2.3743900
H	-0.5536910	-1.1663260	-2.5333530
C	-5.1345210	-3.7164970	-0.7144430
H	-5.2226880	-4.4777220	-1.4992500
H	-5.6948660	-2.8362720	-1.0525760
H	-5.6278880	-4.1024510	0.1835800
C	-1.3206900	-3.1283380	2.5329440
H	-2.1440400	-3.3041970	3.2325290
H	-0.8228460	-2.1959080	2.8111020
H	-0.5920540	-3.9366890	2.6780270
C	3.7988190	-0.7500240	0.0138950
C	4.6007200	0.0255070	0.8716030
C	5.7686090	0.6100010	0.3686170
C	6.1606060	0.4503350	-0.9610920
C	5.3537700	-0.3324570	-1.7933100
H	5.6449490	-0.4785000	-2.8319890

C	4.1844910	-0.9413550	-1.3316140
C	4.2164510	0.2412780	2.3151230
H	4.0766780	-0.7088210	2.8436490
H	3.2749830	0.7928010	2.4007300
C	3.3596480	-1.7801580	-2.2766320
H	3.8741250	-1.9036950	-3.2347160
H	2.3853250	-1.3128990	-2.4681600
H	3.1599150	-2.7780430	-1.8702790
H	6.3840020	1.2090320	1.0368630
C	-1.0237970	1.9508850	2.4295430
C	-0.6103050	1.6507810	3.7267680
H	-0.9851050	2.2335980	4.5640440
H	-1.7169170	2.7706030	2.2633420
C	-1.3018050	3.4242550	-0.3396510
C	-2.5273510	4.0726950	-0.1327690
C	-0.1449390	4.2005750	-0.5161460
C	-2.5919550	5.4679590	-0.0980560
H	-3.4338230	3.4891710	-0.0037840
C	-0.2080670	5.5918170	-0.4676190
H	0.8062830	3.7033430	-0.6943110
C	-1.4341930	6.2299070	-0.2604010
H	-3.5493430	5.9582540	0.0595320
H	0.6965370	6.1791130	-0.6023940
H	-1.4866400	7.3150030	-0.2324130
C	-2.8265070	0.9742460	-0.4751520
C	-3.4701800	0.3401840	0.5945750
C	-3.5139820	1.1129490	-1.6929380
C	-4.7809080	-0.1230940	0.4572350
H	-2.9495980	0.2008060	1.5354750
C	-4.8262940	0.6648200	-1.8245560
H	-3.0126450	1.5766240	-2.5394190
C	-5.4662030	0.0480060	-0.7451110
H	-5.2635170	-0.6198100	1.2944120
H	-5.3486630	0.7918430	-2.7692060
H	-6.4903820	-0.3016600	-0.8452350
H	4.9917830	0.8072460	2.8409470
C	7.4244880	1.0872210	-1.4881970
H	7.9003180	1.7187470	-0.7313930
H	8.1567060	0.3299570	-1.7966360
H	7.2221020	1.7123650	-2.3663410

(NHP-DalPhos)Ni(η^2 -toluene)



Zero-point correction=	0.815144 (Hartree/Particle)
Thermal correction to Energy=	0.865065
Thermal correction to Enthalpy=	0.866010
Thermal correction to Gibbs Free Energy=	0.728263
Sum of electronic and zero-point Energies=	-4043.489577
Sum of electronic and thermal Energies=	-4043.439655
Sum of electronic and thermal Enthalpies=	-4043.438711
Sum of electronic and thermal Free Energies=	-4043.576458

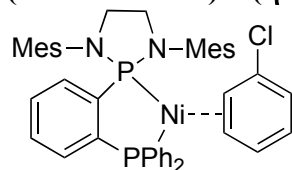
Single-point energy (6-311+G(2d,2p)) = -4.045108349835E+03

Ni	0.5787750	0.5266750	-0.8029620
P	0.7278930	-0.8448420	0.8208830
P	-1.1300830	1.5042550	0.1093970
N	0.0000600	-2.4081000	1.0144510
N	2.2352100	-1.4332150	1.4231740
C	-0.0446570	0.0944950	2.2435930
C	-0.9221590	1.1451470	1.9130480
C	-0.4440900	0.5302710	4.6026430
H	-0.2497090	0.2942240	5.6457700
C	0.1845290	-0.1973830	3.5950440
H	0.8663250	-0.9966330	3.8653760
C	0.8937040	-3.4504300	1.5218700
H	1.1986140	-4.1369770	0.7181310
H	0.3897620	-4.0500030	2.2920360
C	2.1162310	-2.7233780	2.1137120
H	1.9813330	-2.5730240	3.1941300
H	3.0308660	-3.3065070	1.9871060
C	-1.2477280	-2.7834300	0.4213550
C	-1.3006370	-3.1934360	-0.9269090
C	-2.5251850	-3.5927310	-1.4683130
H	-2.5587910	-3.9088780	-2.5091220
C	-3.6993090	-3.6005390	-0.7130290
C	-3.6238820	-3.1929490	0.6199480
H	-4.5258370	-3.1953200	1.2287450
C	-2.4218610	-2.7810370	1.2025960
C	-0.0654490	-3.2004190	-1.7887580
H	-0.3210700	-3.4138650	-2.8309850
H	0.6532680	-3.9632490	-1.4635370
H	0.4449350	-2.2337430	-1.7634880
C	-5.0164810	-4.0141200	-1.3224170
H	-4.8702400	-4.6148380	-2.2262310
H	-5.6114850	-3.1351110	-1.6026890
H	-5.6187720	-4.6003950	-0.6191540
C	-2.4150120	-2.3435670	2.6464860
H	-3.2785380	-2.7574090	3.1776250

H	-2.4652270	-1.2524060	2.7301770
H	-1.5046520	-2.6574330	3.1636790
C	3.4731100	-0.9636640	0.8838080
C	3.9506070	0.3066060	1.2698210
C	5.1332660	0.7930520	0.7041660
C	5.8708380	0.0560050	-0.2240780
C	5.3780420	-1.1967530	-0.5957020
H	5.9184260	-1.7797930	-1.3390330
C	4.1902480	-1.7169330	-0.0733680
C	3.1989900	1.1652680	2.2555960
H	2.8546250	0.5843930	3.1154440
H	2.3054470	1.6116520	1.8017550
C	3.6862860	-3.0390340	-0.5984220
H	4.1780640	-3.2851160	-1.5445790
H	2.6089920	-3.0076480	-0.7762610
H	3.8825380	-3.8717600	0.0893740
H	5.4887000	1.7764060	1.0055810
C	-1.5542140	1.8747360	2.9318940
C	-1.3216590	1.5672740	4.2705800
H	-1.8141020	2.1387420	5.0528850
H	-2.2101360	2.7019400	2.6759480
C	-1.4460760	3.3169840	0.0963190
C	-2.4881200	3.8872470	-0.6496790
C	-0.5269740	4.1714630	0.7307750
C	-2.6141410	5.2749710	-0.7486980
H	-3.2058100	3.2468100	-1.1527160
C	-0.6592310	5.5551050	0.6383710
H	0.2989060	3.7490750	1.2972850
C	-1.7041510	6.1131330	-0.1036920
H	-3.4292820	5.6991280	-1.3293220
H	0.0575780	6.1992890	1.1409700
H	-1.8051580	7.1923100	-0.1795100
C	-2.7660420	0.7936710	-0.3393300
C	-3.8967710	0.8585400	0.4874840
C	-2.8733740	0.1915380	-1.6002990
C	-5.1187880	0.3488020	0.0509560
H	-3.8235130	1.3064030	1.4738250
C	-4.0993710	-0.3115390	-2.0393970
H	-1.9932700	0.1232290	-2.2344490
C	-5.2239850	-0.2263130	-1.2182960
H	-5.9899540	0.4039590	0.6985600
H	-4.1714540	-0.7759370	-3.0188540
H	-6.1803430	-0.6122370	-1.5615130
H	3.8324540	1.9826730	2.6148980
C	1.0976150	-0.5561300	-4.0804870
C	2.0279620	-0.5844040	-3.0705660

C	2.1402550	0.4936080	-2.1320380
C	1.3328080	1.6726060	-2.3138160
C	0.3859810	1.6626300	-3.3954220
C	0.2501200	0.5806370	-4.2324510
H	1.0169860	-1.3858620	-4.7779480
H	2.7047730	-1.4292940	-2.9714080
H	3.0420970	0.5522320	-1.5282320
H	-0.2261050	2.5504190	-3.5470060
H	-0.4828470	0.6029270	-5.0352540
C	1.7901200	3.0042410	-1.7474720
H	2.3006360	2.8765680	-0.7869530
H	2.4997320	3.4918290	-2.4329950
H	0.9505280	3.6888950	-1.5952620
C	7.1652570	0.5854590	-0.7933510
H	7.1726130	1.6802530	-0.8193750
H	8.0263330	0.2679080	-0.1896080
H	7.3322700	0.2214800	-1.8128860

(NHP-DalPhos)Ni(η^2 -PhCl)



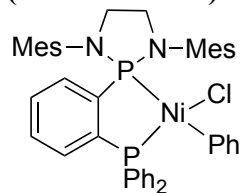
Zero-point correction=	0.778091 (Hartree/Particle)
Thermal correction to Energy=	0.827290
Thermal correction to Enthalpy=	0.828234
Thermal correction to Gibbs Free Energy=	0.693174
Sum of electronic and zero-point Energies=	-4463.810753
Sum of electronic and thermal Energies=	-4463.761554
Sum of electronic and thermal Enthalpies=	-4463.760610
Sum of electronic and thermal Free Energies=	-4463.895670
Single-point energy (6-311+G(2d,2p)) =	-4.465406164609E+03

Ni	0.6786240	0.5441640	-0.6909140
P	0.5772290	-1.1232530	0.6777510
P	-1.0239510	1.4862760	0.2895420
N	-0.2894790	-2.6183730	0.5347370
N	1.9905730	-1.9455480	1.2059310
C	-0.2281430	-0.3864900	2.1915870
C	-1.0132820	0.7648340	1.9929050
C	-0.7564080	-0.3147420	4.5633270
H	-0.6419230	-0.7267270	5.5625970
C	-0.1055540	-0.9114930	3.4855240
H	0.5151280	-1.7854810	3.6557570
C	0.5040730	-3.8155020	0.8237450
H	0.8107090	-4.3140080	-0.1078120

H	-0.0775280	-4.5370760	1.4080170
C	1.7232360	-3.3295090	1.6234290
H	1.5089380	-3.3701630	2.7006470
H	2.6027830	-3.9518950	1.4480350
C	-1.6168530	-2.7406100	0.0231460
C	-1.8868320	-2.4752730	-1.3382830
C	-3.1925750	-2.6214670	-1.8101390
H	-3.3930850	-2.4095220	-2.8580590
C	-4.2395290	-3.0360720	-0.9836590
C	-3.9496950	-3.2990650	0.3550040
H	-4.7499560	-3.6189220	1.0196580
C	-2.6600010	-3.1574050	0.8778100
C	-0.8039490	-2.0368730	-2.2867050
H	-1.1204210	-2.1681910	-3.3259350
H	0.1249210	-2.5948200	-2.1353170
H	-0.5514600	-0.9766530	-2.1526670
C	-5.6355380	-3.2039130	-1.5324440
H	-5.6908220	-4.0440790	-2.2368640
H	-5.9583040	-2.3073870	-2.0743050
H	-6.3595700	-3.3946990	-0.7335510
C	-2.4210370	-3.4664920	2.3354630
H	-3.3600530	-3.4249110	2.8965300
H	-1.7212510	-2.7596810	2.7855110
H	-2.0075810	-4.4747890	2.4773980
C	3.2897760	-1.5105520	0.7914040
C	3.8657260	-0.3890340	1.4227520
C	5.1127440	0.0704350	0.9891860
C	5.8159900	-0.5536920	-0.0431050
C	5.2217510	-1.6568890	-0.6598720
H	5.7352790	-2.1410940	-1.4881440
C	3.9666180	-2.1397210	-0.2770260
C	3.1470740	0.3508110	2.5227730
H	2.6911780	-0.3359240	3.2411800
H	2.3388350	0.9747940	2.1208660
C	3.3521920	-3.2689870	-1.0689530
H	3.8933410	-3.4111770	-2.0092280
H	2.3064110	-3.0569180	-1.3118960
H	3.3776510	-4.2284970	-0.5377660
H	5.5436360	0.9432230	1.4749810
C	-1.6754180	1.3556480	3.0798360
C	-1.5526400	0.8166200	4.3584770
H	-2.0640670	1.2835210	5.1958650
H	-2.2672020	2.2534100	2.9256730
C	-1.1768710	3.2845310	0.6393840
C	-2.2492780	4.0677710	0.1931730
C	-0.1281960	3.9032930	1.3400840

C	-2.2737730	5.4423580	0.4457990
H	-3.0674720	3.6086230	-0.3519580
C	-0.1605930	5.2706180	1.6013790
H	0.7204100	3.3123480	1.6715570
C	-1.2335810	6.0459600	1.1517210
H	-3.1115090	6.0377500	0.0922070
H	0.6581670	5.7341690	2.1450020
H	-1.2543780	7.1144830	1.3479910
C	-2.6524840	1.0519180	-0.4359020
C	-3.7506560	0.6120300	0.3131920
C	-2.7853540	1.2000760	-1.8259140
C	-4.9706980	0.3533550	-0.3133630
H	-3.6538750	0.4663490	1.3841940
C	-4.0089390	0.9533510	-2.4474960
H	-1.9259110	1.5057020	-2.4167530
C	-5.1064670	0.5377740	-1.6902640
H	-5.8151170	0.0072020	0.2761570
H	-4.1032450	1.0807270	-3.5226610
H	-6.0616000	0.3488150	-2.1731160
H	3.8371210	1.0115340	3.0567680
C	1.4230470	-0.0047380	-4.1309790
C	2.2154760	-0.3180670	-3.0560000
C	2.2915940	0.5343400	-1.9027560
C	1.5572950	1.7772290	-1.9415540
C	0.7886930	2.1122050	-3.1085980
C	0.6931140	1.2227660	-4.1487290
H	1.3763180	-0.6673450	-4.9907730
H	2.8318130	-1.2128160	-3.0716460
H	3.1520160	0.4398240	-1.2483600
H	0.2908990	3.0770340	-3.1422570
H	0.0821320	1.4713240	-5.0129460
Cl	2.2511450	3.1826120	-1.0286310
C	7.1768470	-0.0589180	-0.4704510
H	7.9726870	-0.4995250	0.1453450
H	7.3880630	-0.3210320	-1.5124950
H	7.2547220	1.0290730	-0.3726300

(NHP-DalPhos)Ni(Ph)Cl



Zero-point correction=	0.779275 (Hartree/Particle)
Thermal correction to Energy=	0.828723
Thermal correction to Enthalpy=	0.829667

Thermal correction to Gibbs Free Energy= 0.693199
 Sum of electronic and zero-point Energies= -4463.844140
 Sum of electronic and thermal Energies= -4463.794693
 Sum of electronic and thermal Enthalpies= -4463.793749
 Sum of electronic and thermal Free Energies= -4463.930216

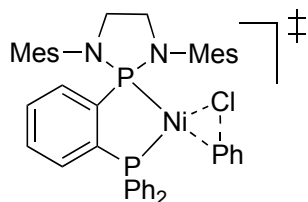
Single-point energy (6-311+G(2d,2p)) = -4.465444433389E+03

Ni	0.3254190	0.4285560	-0.8823470
P	0.7471810	-1.2393980	0.5465940
P	-0.9775960	1.3118820	0.5756190
N	0.0537360	-2.8062140	0.4011900
N	2.3099980	-1.8689510	0.7937040
C	0.1135210	-0.6652000	2.1995310
C	-0.7314480	0.4519820	2.1898340
C	-0.1978760	-0.8550880	4.5997560
H	0.0216370	-1.3567190	5.5383860
C	0.3813950	-1.3062940	3.4187870
H	1.0418300	-2.1659470	3.4448680
C	1.0228680	-3.9006430	0.5465490
H	1.2732960	-4.3354120	-0.4292730
H	0.6025410	-4.6958690	1.1750430
C	2.2685030	-3.2827400	1.2003110
H	2.2166450	-3.3734070	2.2945670
H	3.1810790	-3.7866410	0.8800160
C	-1.2444730	-3.0741510	-0.1503900
C	-1.4106970	-3.2499890	-1.5436290
C	-2.6941930	-3.5006450	-2.0407900
H	-2.8189780	-3.6221190	-3.1147310
C	-3.8085690	-3.6137840	-1.2060460
C	-3.6127690	-3.4692000	0.1677010
H	-4.4628370	-3.5642470	0.8402020
C	-2.3526010	-3.2052300	0.7135890
C	-0.2503770	-3.2034740	-2.5039510
H	-0.6101020	-3.1590280	-3.5362650
H	0.3716360	-4.1042440	-2.4167300
H	0.3950110	-2.3368480	-2.3456200
C	-5.1754520	-3.9235900	-1.7694070
H	-5.2821360	-3.5482460	-2.7928910
H	-5.9707250	-3.4823000	-1.1587150
H	-5.3552810	-5.0065210	-1.8015840
C	-2.2261550	-3.0753330	2.2112420
H	-3.0327790	-3.6229560	2.7094660
H	-2.2908450	-2.0302500	2.5329050
H	-1.2698520	-3.4618800	2.5710370
C	3.5362280	-1.2451680	0.3842140

C	4.0067800	-0.1104560	1.0714150
C	5.2015670	0.4880110	0.6576850
C	5.9497830	-0.0122850	-0.4068170
C	5.4661370	-1.1447200	-1.0658530
H	6.0208330	-1.5431090	-1.9129320
C	4.2678850	-1.7639130	-0.7070600
C	3.2562460	0.4876620	2.2348430
H	2.9086640	-0.2782150	2.9338860
H	2.3706680	1.0434990	1.9034570
C	3.7839340	-2.9350610	-1.5261210
H	4.2388030	-2.9096760	-2.5202310
H	2.7017820	-2.8958920	-1.6617360
H	4.0446600	-3.9032080	-1.0760190
H	5.5572710	1.3659380	1.1930950
C	-1.3384170	0.8889760	3.3780250
C	-1.0741460	0.2373830	4.5780990
H	-1.5404740	0.5813830	5.4970720
H	-2.0027950	1.7476840	3.3653930
C	-0.6926740	3.0734350	0.9835500
C	-1.2839030	4.0817030	0.2069330
C	0.2234300	3.4294910	1.9837350
C	-0.9855770	5.4208250	0.4505950
H	-1.9544700	3.8216920	-0.6045620
C	0.5254330	4.7713630	2.2190670
H	0.7037170	2.6631650	2.5831310
C	-0.0828210	5.7697760	1.4570310
H	-1.4474880	6.1899830	-0.1614900
H	1.2361870	5.0333140	2.9980220
H	0.1523000	6.8146060	1.6406150
C	-2.7731420	1.1498420	0.2592120
C	-3.7258410	1.9869040	0.8578990
C	-3.1995420	0.1078510	-0.5749240
C	-5.0851470	1.7851560	0.6199040
H	-3.4085910	2.8063450	1.4952670
C	-4.5596220	-0.0892400	-0.8130340
H	-2.4684400	-0.5457000	-1.0414300
C	-5.5032730	0.7486870	-0.2180740
H	-5.8162010	2.4421810	1.0831820
H	-4.8747930	-0.8956070	-1.4666240
H	-6.5624690	0.5979570	-0.4083480
H	3.8939510	1.1904240	2.7804460
Cl	1.7478900	-0.2278100	-2.4328740
C	-0.1172610	1.9440980	-1.9807840
C	-1.2832430	2.0207460	-2.7526710
C	0.7954670	3.0079360	-2.0513570
C	-1.5383790	3.1333920	-3.5651850

H	-2.0095210	1.2129870	-2.7314700
C	0.5449100	4.1183140	-2.8585400
H	1.7182930	2.9665330	-1.4775990
C	-0.6291160	4.1901740	-3.6145760
H	-2.4501570	3.1683870	-4.1581310
H	1.2691490	4.9292160	-2.8989590
H	-0.8266280	5.0561310	-4.2416040
C	7.2236820	0.6622540	-0.8561910
H	8.0044820	-0.0694360	-1.0938150
H	7.0551660	1.2603000	-1.7613160
H	7.6138360	1.3352960	-0.0855310

(NHP-DalPhos)Ni(Ph)Cl C_{sp2}-Cl oxidative addition transition state (TS-1)



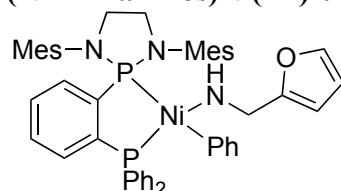
Zero-point correction=	0.776667 (Hartree/Particle)
Thermal correction to Energy=	0.826125
Thermal correction to Enthalpy=	0.827069
Thermal correction to Gibbs Free Energy=	0.690307
Sum of electronic and zero-point Energies=	-4463.794428
Sum of electronic and thermal Energies=	-4463.744970
Sum of electronic and thermal Enthalpies=	-4463.744026
Sum of electronic and thermal Free Energies=	-4463.880788
Single-point energy (6-311+G(2d,2p)) =	-4.465391026979E+03

Ni	0.5240360	0.3233920	-0.8896530
P	0.4070160	-1.2359780	0.6266960
P	-0.9136060	1.5390710	0.2253590
N	-0.6123420	-2.6296190	0.6359110
N	1.7688170	-2.1662730	1.0963800
C	-0.1394250	-0.3162380	2.1510500
C	-0.7136050	0.9549830	1.9679400
C	-0.3791330	-0.0622620	4.5558970
H	-0.2473810	-0.4590980	5.5591040
C	0.0117890	-0.8149970	3.4518030
H	0.4477850	-1.7967650	3.6041600
C	0.0715200	-3.8860310	0.9532760
H	0.2406370	-4.4857200	0.0477450
H	-0.5363990	-4.4881310	1.6412290
C	1.4122760	-3.4986140	1.6039990
H	1.3205670	-3.4903750	2.7000170
H	2.2006220	-4.2135290	1.3528940
C	-1.9181840	-2.6594730	0.0427900

C	-2.0702150	-2.9153490	-1.3366120
C	-3.3570530	-2.9574530	-1.8794040
H	-3.4677720	-3.1535180	-2.9438410
C	-4.4972970	-2.7591180	-1.0984040
C	-4.3235310	-2.5215170	0.2655650
H	-5.1980580	-2.3753220	0.8961470
C	-3.0562650	-2.4668070	0.8532450
C	-0.8800960	-3.1407540	-2.2332260
H	-1.1965510	-3.2411160	-3.2754580
H	-0.3307800	-4.0510910	-1.9652830
H	-0.1832540	-2.3004370	-2.1840000
C	-5.8762620	-2.7831970	-1.7109390
H	-5.8831800	-3.3209080	-2.6647390
H	-6.2365710	-1.7643270	-1.9037870
H	-6.6035390	-3.2619830	-1.0455300
C	-2.9487480	-2.2066580	2.3354280
H	-3.8717200	-2.5038680	2.8441970
H	-2.7852900	-1.1433210	2.5417860
H	-2.1130880	-2.7492260	2.7843100
C	3.1052860	-1.8629280	0.6782790
C	3.8842150	-0.9606460	1.4263590
C	5.1900370	-0.6812660	1.0069050
C	5.7441570	-1.2665620	-0.1320370
C	4.9451980	-2.1461370	-0.8697690
H	5.3461230	-2.5974670	-1.7750640
C	3.6358470	-2.4519080	-0.4910510
C	3.3346270	-0.2706130	2.6488160
H	2.8276310	-0.9728550	3.3161970
H	2.5972770	0.4941490	2.3786010
C	2.8045580	-3.3587800	-1.3638810
H	3.3477380	-3.6166010	-2.2776590
H	1.8689840	-2.8739740	-1.6553600
H	2.5401560	-4.2978510	-0.8635250
H	5.7876670	0.0151810	1.5913650
C	-1.0972390	1.7144190	3.0839570
C	-0.9316030	1.2094430	4.3718310
H	-1.2282500	1.8056030	5.2306270
H	-1.5082630	2.7099740	2.9429120
C	-0.7455060	3.3570050	0.3925530
C	-1.7549160	4.2638650	0.0445640
C	0.5055070	3.8523770	0.7959770
C	-1.5235950	5.6404020	0.1191230
H	-2.7224970	3.8981100	-0.2840830
C	0.7288920	5.2237180	0.8848750
H	1.3107640	3.1585310	1.0232410
C	-0.2863950	6.1231140	0.5460940

H	-2.3152040	6.3333110	-0.1538880
H	1.7014300	5.5913450	1.2008750
H	-0.1094760	7.1936130	0.6062440
C	-2.6982030	1.2780650	-0.1365530
C	-3.7186580	1.4526400	0.8103750
C	-3.0351950	0.9031850	-1.4447460
C	-5.0537160	1.2767270	0.4483770
H	-3.4726150	1.7214310	1.8328880
C	-4.3730340	0.7377710	-1.8071910
H	-2.2464950	0.7323110	-2.1716730
C	-5.3831770	0.9297680	-0.8643620
H	-5.8367120	1.4132710	1.1897780
H	-4.6213440	0.4480610	-2.8243100
H	-6.4249490	0.8014330	-1.1465500
H	4.1368330	0.2221540	3.2070470
Cl	0.2306690	0.1180860	-3.3274740
C	1.3249370	1.4734020	-2.1249330
C	1.2115740	2.8468870	-2.4131380
C	2.5538880	0.8949350	-1.7386250
C	2.2934250	3.6621570	-2.1287050
H	0.2753850	3.2546260	-2.7792340
C	3.6207820	1.7619410	-1.4177040
H	2.7255750	-0.1741440	-1.7944710
C	3.4925740	3.1301460	-1.6055580
H	2.2021120	4.7342870	-2.2833640
H	4.5632450	1.3325380	-1.0910100
H	4.3285470	3.7915350	-1.3960600
C	7.1652760	-0.9746050	-0.5516080
H	7.5411950	-0.0595030	-0.0826610
H	7.8408110	-1.7916100	-0.2650110
H	7.2455750	-0.8565540	-1.6381030

(NHP-DalPhos)Ni(Ph)furfurylamido



Zero-point correction=	0.883899 (Hartree/Particle)
Thermal correction to Energy=	0.938278
Thermal correction to Enthalpy=	0.939222
Thermal correction to Gibbs Free Energy=	0.793005

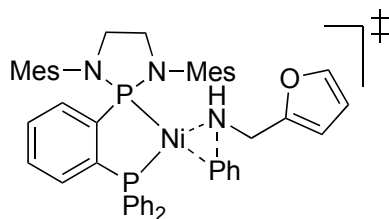
Sum of electronic and zero-point Energies= -4327.589388
 Sum of electronic and thermal Energies= -4327.535009
 Sum of electronic and thermal Enthalpies= -4327.534065
 Sum of electronic and thermal Free Energies= -4327.680282
 Single-point energy (6-311+G(2d,2p)) = -4.329372948997E+03

Ni	0.0172100	0.4360680	-0.5413390
P	0.3087610	-1.2816080	0.8583610
P	-1.5805160	1.1415950	0.7588630
N	-0.3448570	-2.7811920	0.3091760
N	1.7505750	-2.0319170	1.3863040
C	-0.7077470	-0.9416430	2.3801130
C	-1.5958170	0.1408250	2.3106180
C	-1.4974470	-1.4201110	4.6253750
H	-1.4528720	-2.0240390	5.5277990
C	-0.6654840	-1.7144200	3.5504300
H	0.0198400	-2.5520500	3.6201450
C	0.5660730	-3.9212370	0.4578010
H	1.0561350	-4.1649910	-0.4937780
H	0.0102800	-4.8066490	0.7917660
C	1.5994150	-3.4917460	1.5075310
H	1.2565400	-3.7650220	2.5155670
H	2.5641900	-3.9774680	1.3525300
C	-1.4804170	-2.8929870	-0.5584220
C	-1.3299620	-2.7894910	-1.9620120
C	-2.4668390	-2.8996100	-2.7678500
H	-2.3496640	-2.8061830	-3.8457820
C	-3.7370710	-3.1465550	-2.2368450
C	-3.8523040	-3.2823820	-0.8540090
H	-4.8278310	-3.4864120	-0.4178230
C	-2.7481070	-3.1586500	-0.0020780
C	0.0176450	-2.6047050	-2.6117440
H	-0.1023910	-2.3019420	-3.6570010
H	0.5821590	-3.5472470	-2.6123260
H	0.6326050	-1.8490880	-2.1130560
C	-4.9373760	-3.2902290	-3.1427150
H	-4.9835240	-2.4788280	-3.8788950
H	-5.8721780	-3.2854690	-2.5727980
H	-4.9003220	-4.2311410	-3.7070360
C	-2.9547490	-3.3127290	1.4847950
H	-3.8365090	-3.9300860	1.6853390
H	-3.1139720	-2.3435830	1.9705960
H	-2.0891520	-3.7719380	1.9679740
C	3.0494840	-1.4231990	1.3541190
C	3.4030450	-0.4906070	2.3486370
C	4.6634120	0.1142600	2.2944760

C	5.5881070	-0.1920890	1.2960380
C	5.2226660	-1.1380890	0.3356920
H	5.9160790	-1.3708600	-0.4687560
C	3.9674120	-1.7502150	0.3311510
C	2.4568510	-0.1219480	3.4641620
H	2.0066010	-1.0075440	3.9216550
H	1.6291270	0.5037560	3.1106000
C	3.6111970	-2.6801100	-0.8012330
H	4.3634940	-2.6118260	-1.5903210
H	2.6502740	-2.3884430	-1.2333910
H	3.5545220	-3.7310350	-0.4908860
H	4.9274300	0.8402170	3.0607580
C	-2.4463880	0.4261790	3.3898320
C	-2.3983670	-0.3508890	4.5427730
H	-3.0559040	-0.1255250	5.3778360
H	-3.1409310	1.2586080	3.3286660
C	-1.2226940	2.8352090	1.3591790
C	-1.6763930	3.9590280	0.6516360
C	-0.3669650	3.0206660	2.4556250
C	-1.2996680	5.2413210	1.0510300
H	-2.3112430	3.8335420	-0.2180980
C	0.0138730	4.3039690	2.8478120
H	0.0024740	2.1624880	3.0078930
C	-0.4549670	5.4177210	2.1485180
H	-1.6607270	6.1022330	0.4953070
H	0.6763170	4.4314300	3.6995380
H	-0.1600780	6.4176130	2.4547600
C	-3.3336530	1.1617910	0.2348190
C	-4.2894500	2.0275150	0.7881840
C	-3.7324840	0.2235480	-0.7255690
C	-5.6216830	1.9557680	0.3822970
H	-3.9932700	2.7687090	1.5238940
C	-5.0665120	0.1516060	-1.1265610
H	-3.0016210	-0.4506820	-1.1564280
C	-6.0115780	1.0179840	-0.5769110
H	-6.3532360	2.6347160	0.8121540
H	-5.3616820	-0.5788550	-1.8729660
H	-7.0491530	0.9664550	-0.8958690
H	2.9827940	0.4403890	4.2420810
C	-0.5109540	1.7014760	-1.8783350
C	-1.3226170	1.2628190	-2.9410160
C	-0.0712540	3.0345690	-1.9116280
C	-1.6885750	2.1202700	-3.9826470
H	-1.6761550	0.2338720	-2.9641740
C	-0.4308830	3.8970320	-2.9531640
H	0.5604220	3.4173820	-1.1134910

C	-1.2459110	3.4452890	-3.9921220
H	-2.3195990	1.7511420	-4.7890060
H	-0.0725440	4.9246750	-2.9488550
H	-1.5290820	4.1142560	-4.8009340
N	1.5717710	0.0972330	-1.6026720
H	1.3406230	0.3496020	-2.5658140
C	2.6540430	0.9973730	-1.2042180
H	2.9123580	0.8124060	-0.1538620
H	2.3918350	2.0709400	-1.2666880
C	3.8801300	0.7881220	-2.0415470
C	4.1898820	-0.0554980	-3.0674910
O	4.9592030	1.5915580	-1.7689230
C	5.5453560	0.2325620	-3.4472780
H	3.5292880	-0.8000830	-3.4858210
C	5.9632630	1.2337540	-2.6287270
H	6.1233960	-0.2420930	-4.2286590
H	6.8829230	1.7898460	-2.5301200
C	6.9234810	0.5069400	1.2237360
H	7.2030350	0.9411790	2.1895030
H	7.7202080	-0.1790340	0.9148260
H	6.8909770	1.3208880	0.4887590

(NHP-DalPhos)Ni(Ph)furfurylamido C_{sp2}-N reductive elimination transition state (TS-2)



Zero-point correction=	0.882241 (Hartree/Particle)
Thermal correction to Energy=	0.936319
Thermal correction to Enthalpy=	0.937263
Thermal correction to Gibbs Free Energy=	0.791786
Sum of electronic and zero-point Energies=	-4327.559183
Sum of electronic and thermal Energies=	-4327.505105
Sum of electronic and thermal Enthalpies=	-4327.504160
Sum of electronic and thermal Free Energies=	-4327.649637

Single-point energy (6-311+G(2d,2p)) = -4.329341104392E+03

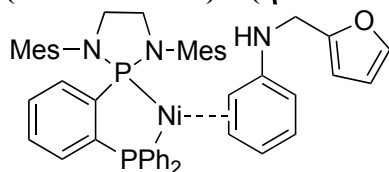
Ni	0.0755920	0.4565630	-0.4711120
P	0.2536020	-1.0742230	1.1599920
P	-1.7799750	1.1374700	0.4056670
N	-0.1618040	-2.7315790	0.9070560
N	1.6772390	-1.5134940	2.0171920
C	-1.0038760	-0.5778170	2.4517560

C	-1.9882520	0.3449800	2.0591980
C	-2.1078990	-0.7982390	4.6076110
H	-2.1427470	-1.2334960	5.6029530
C	-1.0708900	-1.1294640	3.7408230
H	-0.3109680	-1.8284100	4.0711920
C	0.7301280	-3.7017470	1.5471980
H	1.3277840	-4.2332540	0.7929330
H	0.1557850	-4.4560470	2.1023200
C	1.6380630	-2.9001650	2.5032480
H	1.2426230	-2.9388300	3.5270130
H	2.6452520	-3.3167430	2.5397710
C	-1.1021010	-3.1691420	-0.0788260
C	-0.7046580	-3.3048850	-1.4264360
C	-1.6446520	-3.7302600	-2.3702860
H	-1.3360800	-3.8263110	-3.4093760
C	-2.9587240	-4.0460160	-2.0147330
C	-3.3240450	-3.9190080	-0.6732510
H	-4.3426020	-4.1579630	-0.3742870
C	-2.4224390	-3.4844580	0.3031240
C	0.7077940	-3.0050790	-1.8597350
H	0.7955300	-3.0722560	-2.9493080
H	1.4192400	-3.7210420	-1.4299080
H	1.0229880	-2.0022900	-1.5542360
C	-3.9479070	-4.5394660	-3.0440710
H	-4.9579410	-4.1675060	-2.8391570
H	-4.0027520	-5.6363110	-3.0492180
H	-3.6668610	-4.2236620	-4.0543530
C	-2.8908140	-3.3500220	1.7313030
H	-3.7683620	-3.9803990	1.9077540
H	-3.1731580	-2.3169590	1.9617670
H	-2.1119100	-3.6315810	2.4442300
C	2.8961990	-0.7773740	1.8746770
C	2.9851310	0.5111440	2.4431410
C	4.1566660	1.2556910	2.2657870
C	5.2509260	0.7603470	1.5565130
C	5.1457900	-0.5231350	1.0162400
H	5.9738800	-0.9229420	0.4350360
C	3.9890720	-1.2962480	1.1410640
C	1.8429760	1.1150380	3.2228850
H	1.3845660	0.3859370	3.8969920
H	1.0481410	1.4827920	2.5615680
C	3.9466010	-2.6333350	0.4415800
H	4.6624380	-2.6452340	-0.3836020
H	2.9574730	-2.8313970	0.0234700
H	4.2019000	-3.4677000	1.1089890
H	4.2113300	2.2509970	2.7018360

C	-3.0476950	0.6554130	2.9264700
C	-3.1124030	0.0841470	4.1933580
H	-3.9334640	0.3308650	4.8609070
H	-3.8136960	1.3584740	2.6128490
C	-1.9261320	2.9262830	0.7536530
C	-2.2077810	3.7940380	-0.3130000
C	-1.6064060	3.4689770	2.0072750
C	-2.2149250	5.1736770	-0.1149030
H	-2.3994800	3.3954360	-1.3039780
C	-1.6084550	4.8511850	2.2000130
H	-1.3610030	2.8149640	2.8379250
C	-1.9208960	5.7064340	1.1414010
H	-2.4295230	5.8302160	-0.9530780
H	-1.3675690	5.2576380	3.1788210
H	-1.9236920	6.7825910	1.2926760
C	-3.3089980	0.7203450	-0.5160850
C	-4.5292360	1.3869290	-0.3291580
C	-3.2347170	-0.3221590	-1.4495330
C	-5.6561190	1.0097330	-1.0589350
H	-4.5948080	2.2140270	0.3714300
C	-4.3631300	-0.6979450	-2.1791200
H	-2.2909020	-0.8374710	-1.6021130
C	-5.5741590	-0.0331870	-1.9856470
H	-6.5960540	1.5344340	-0.9093640
H	-4.2892890	-1.5047110	-2.9013500
H	-6.4517760	-0.3207340	-2.5585890
H	2.1921770	1.9675000	3.8141530
C	0.2606060	1.7796190	-1.8538080
C	-0.5416410	1.6944680	-3.0335920
C	0.7424790	3.0723670	-1.4980600
C	-0.8123490	2.8191350	-3.8013920
H	-0.9582240	0.7323180	-3.3275020
C	0.4551620	4.1872030	-2.2848280
H	1.3143600	3.2011380	-0.5820940
C	-0.3148620	4.0834500	-3.4452620
H	-1.4314860	2.7116900	-4.6905700
H	0.8331870	5.1583420	-1.9702220
H	-0.5273390	4.9565860	-4.0549480
N	1.4941690	0.4601140	-1.7530290
H	1.4027120	0.1507020	-2.7128960
C	2.8262600	0.9680920	-1.4771210
H	2.9900820	0.9836110	-0.3931910
H	2.9361220	2.0150790	-1.8194390
C	3.8871820	0.1422890	-2.1275690
C	3.9171560	-1.0831820	-2.7273920
O	5.1425800	0.6929890	-2.1515640

C	5.2752470	-1.3100590	-3.1381480
H	3.0784150	-1.7522250	-2.8467520
C	5.9735510	-0.2071530	-2.7605210
H	5.6688020	-2.1777360	-3.6496360
H	7.0044520	0.0979970	-2.8525000
C	6.4913280	1.5917610	1.3374480
H	6.5451720	1.9410700	0.2984970
H	6.5027900	2.4731750	1.9867850
H	7.4026830	1.0147570	1.5338810

(NHP-DalPhos)Ni(η^2 -N- N-Phenyl-2-furanmethanamine)



Zero-point correction=	0.883589 (Hartree/Particle)
Thermal correction to Energy=	0.938268
Thermal correction to Enthalpy=	0.939213
Thermal correction to Gibbs Free Energy=	0.790623
Sum of electronic and zero-point Energies=	-4327.606046
Sum of electronic and thermal Energies=	-4327.551367
Sum of electronic and thermal Enthalpies=	-4327.550423
Sum of electronic and thermal Free Energies=	-4327.699012

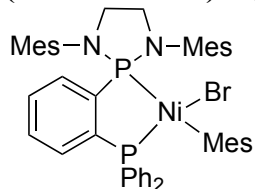
Single-point energy (6-311+G(2d,2p)) = -4.329384518688E+03

Ni	0.2439700	-0.1031390	-0.8147390
P	-0.5484920	-1.4617450	0.6106390
P	-0.6380810	1.5934400	0.1926640
N	-2.0708850	-2.3032400	0.5790120
N	0.2642940	-2.8943480	1.1268780
C	-0.7688160	-0.4004370	2.1336390
C	-0.8647170	0.9890840	1.9290550
C	-1.0045220	-0.0456350	4.5275450
H	-1.0447430	-0.4490550	5.5361960
C	-0.8371200	-0.9016680	3.4409060
H	-0.7440520	-1.9697850	3.6123830
C	-1.9879780	-3.7386950	0.8482080
H	-2.0289530	-4.3175650	-0.0871800
H	-2.8245310	-4.0679230	1.4748380
C	-0.6503780	-3.9535270	1.5761480
H	-0.8001580	-3.8937580	2.6637980
H	-0.2227600	-4.9363790	1.3641060
C	-3.3025380	-1.7028130	0.1799370
C	-3.5047420	-1.3030370	-1.1608000
C	-4.7175320	-0.7085480	-1.5154230

H	-4.8607480	-0.3958370	-2.5474330
C	-5.7470030	-0.5116190	-0.5923420
C	-5.5335050	-0.9281540	0.7215890
H	-6.3207500	-0.7852170	1.4594470
C	-4.3322430	-1.5181540	1.1283720
C	-2.4460660	-1.4996760	-2.2122150
H	-2.8742660	-1.4118510	-3.2156200
H	-1.9625890	-2.4778150	-2.1263420
H	-1.6457020	-0.7515730	-2.1263090
C	-7.0538590	0.1145750	-1.0148730
H	-7.6239530	-0.5534690	-1.6738450
H	-6.8856820	1.0465270	-1.5663880
H	-7.6859120	0.3429480	-0.1503420
C	-4.1792750	-1.9526860	2.5653300
H	-4.8995000	-1.4315690	3.2041400
H	-3.1756580	-1.7459450	2.9413000
H	-4.3620880	-3.0294840	2.6876800
C	1.5761730	-3.1820750	0.6347970
C	2.6845520	-2.5629240	1.2473940
C	3.9667110	-2.8076630	0.7433970
C	4.1881170	-3.6502960	-0.3475350
C	3.0736930	-4.2416950	-0.9483600
H	3.2160410	-4.8770450	-1.8203470
C	1.7727290	-4.0154680	-0.4896210
C	2.5119100	-1.6152310	2.4072060
H	1.7865940	-1.9939270	3.1318770
H	2.1444670	-0.6387740	2.0693000
C	0.6156970	-4.6070550	-1.2574310
H	0.9557080	-4.9878160	-2.2252010
H	-0.1563740	-3.8537430	-1.4425660
H	0.1386540	-5.4431900	-0.7319340
H	4.8177800	-2.3307110	1.2257430
C	-1.0404050	1.8461460	3.0261870
C	-1.1153580	1.3329990	4.3192460
H	-1.2468110	2.0043340	5.1636710
H	-1.0940140	2.9195850	2.8666810
C	0.2955990	3.1564130	0.4629160
C	-0.0889600	4.3880790	-0.0859400
C	1.5252440	3.0741270	1.1431170
C	0.7348110	5.5100660	0.0425050
H	-1.0328450	4.4735210	-0.6152970
C	2.3434490	4.1948640	1.2728990
H	1.8508930	2.1237830	1.5539920
C	1.9514780	5.4178490	0.7192680
H	0.4197570	6.4577670	-0.3867500
H	3.2941770	4.1053470	1.7909700

H	2.5913790	6.2908940	0.8147210
C	-2.2905280	2.1619740	-0.3701280
C	-3.3758400	2.4082390	0.4799630
C	-2.4498730	2.3456160	-1.7534890
C	-4.5903040	2.8574730	-0.0409850
H	-3.2779200	2.2408340	1.5476010
C	-3.6591370	2.8096460	-2.2701930
H	-1.6230340	2.1153820	-2.4210290
C	-4.7301710	3.0728580	-1.4131270
H	-5.4279540	3.0387160	0.6270830
H	-3.7676520	2.9565390	-3.3416190
H	-5.6733310	3.4347180	-1.8141590
H	3.4661080	-1.4530170	2.9193770
C	0.4297650	-0.5875680	-4.3219510
C	0.9447670	-1.4062530	-3.3427420
C	1.5794220	-0.8766610	-2.1747950
C	1.7277290	0.5508750	-2.0717380
C	1.2341520	1.3716000	-3.1390400
C	0.5742290	0.8233550	-4.2150150
H	-0.0604960	-1.0153870	-5.1921890
H	0.8833550	-2.4863410	-3.4486540
H	2.2085700	-1.5347710	-1.5855600
H	1.3933150	2.4468280	-3.0757690
H	0.1889490	1.4683240	-5.0006060
N	2.6282230	1.0801010	-1.0902790
H	2.5606010	2.0932570	-1.0552880
C	4.0391770	0.6640140	-1.1836240
H	4.4564880	0.8310480	-2.1911660
H	4.0992140	-0.4069240	-0.9731060
C	4.8564020	1.3930000	-0.1750670
C	5.2748110	1.1089140	1.0914440
O	5.2407900	2.6699070	-0.5063330
C	5.9586860	2.2732890	1.5750700
H	5.1031780	0.1815940	1.6189310
C	5.9047580	3.1870550	0.5677340
H	6.4296940	2.4053470	2.5393210
H	6.2796470	4.1914650	0.4455420
C	5.5843670	-3.9255710	-0.8523330
H	6.0075660	-4.8247940	-0.3845310
H	5.5930610	-4.0893900	-1.9354050
H	6.2615880	-3.0940700	-0.6301240

(NHP-DalPhos)Ni(mesityl)Br



Zero-point correction=	0.862302 (Hartree/Particle)
Thermal correction to Energy=	0.917048
Thermal correction to Enthalpy=	0.917992
Thermal correction to Gibbs Free Energy=	0.770399
Sum of electronic and zero-point Energies=	-6692.943651
Sum of electronic and thermal Energies=	-6692.888906
Sum of electronic and thermal Enthalpies=	-6692.887962
Sum of electronic and thermal Free Energies=	-6693.035554

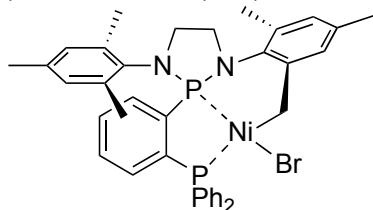
Single-point energy (6-311+G(2d,2p)) = -6.697367605580E+03

Br	1.5677860	-0.8200610	-2.3176550
Ni	0.3778840	0.2288660	-0.5869170
P	-0.6591660	1.3815530	0.9225380
P	0.0364650	-1.6253440	0.6267260
N	1.2937490	-2.7465440	0.8904560
N	-1.0998690	-2.8698480	0.2696070
C	2.9724050	1.9287640	-0.2498790
C	1.7178610	5.6826010	-3.3768760
C	-1.3605190	1.7232040	-2.8936640
C	1.9685760	2.5531190	-1.1888200
C	2.2626150	3.7683750	-1.8098570
C	1.3777470	4.3665500	-2.7160340
C	0.1974110	3.6878500	-3.0174530
C	-0.1185280	2.4518240	-2.4287730
C	0.7492500	1.9034350	-1.4748910
C	0.9020700	2.8018120	2.8063290
C	1.6041890	3.9169290	3.2647180
C	1.5914600	5.1033150	2.5296690
C	0.8825710	5.1666210	1.3291850
C	0.1874090	4.0522440	0.8625240
C	0.1770860	2.8615160	1.6068720
C	-2.9202830	3.1193810	1.0306040
C	-4.2546570	3.4372670	0.7724970
C	-5.0538840	2.5640120	0.0332210
C	-4.5152420	1.3690660	-0.4467160
C	-3.1807010	1.0530940	-0.1982480
C	-2.3704070	1.9271010	0.5393470
C	2.6217390	-4.0998240	-1.3740880

C	6.8613730	-1.6896430	-0.1827880
C	2.7632490	-0.9150080	2.6287930
C	3.3357760	-3.1583850	-0.4354790
C	4.6892640	-2.8973560	-0.6565970
C	5.4153550	-1.9963250	0.1245520
C	4.7510250	-1.3703330	1.1784770
C	3.4031760	-1.6169530	1.4576060
C	2.6856480	-2.5096770	0.6378150
C	-3.5291700	-2.4413780	1.8483420
C	-6.1229080	-1.9678920	-2.4323100
C	-1.2323680	-3.0935740	-2.6751450
C	-3.5233180	-2.4482990	0.3404170
C	-4.7330550	-2.2368030	-0.3320210
C	-4.8168860	-2.2379600	-1.7236480
C	-3.6497700	-2.5001920	-2.4465460
C	-2.4210730	-2.7337530	-1.8229860
C	-2.3490880	-2.6668080	-0.4103030
C	0.7753360	-4.0978930	1.1497340
C	-0.5452450	-4.2269380	0.3737210
C	-0.6479340	-1.8608380	3.4318270
C	-1.1786190	-1.3681130	4.6188560
C	-1.6277970	-0.0433390	4.6890310
C	-1.5027330	0.7880010	3.5812610
C	-0.9265510	0.3030260	2.3958360
C	-0.5282570	-1.0364570	2.3017920
H	2.5169950	1.6640390	0.7114430
H	3.3721950	1.0012660	-0.6747770
H	3.8077520	2.6085950	-0.0469010
H	2.1177790	6.4062650	-2.6558140
H	2.4802600	5.5561080	-4.1574770
H	0.8377430	6.1313370	-3.8501910
H	-2.2824750	2.2611990	-2.6411760
H	-1.3410730	1.5962970	-3.9835520
H	-1.4164590	0.7232550	-2.4560630
H	3.2046620	4.2645410	-1.5782890
H	-0.4910910	4.1151030	-3.7466730
H	0.9254940	1.8859670	3.3864870
H	2.1620510	3.8546750	4.1950140
H	2.1382440	5.9717020	2.8869820
H	0.8833180	6.0784180	0.7392590
H	-0.3285980	4.1058750	-0.0896890
H	-2.3096330	3.8054830	1.6073210
H	-4.6669010	4.3689350	1.1504590
H	-6.0920600	2.8139990	-0.1679880
H	-5.1270810	0.6794300	-1.0188000
H	-2.7705130	0.1261600	-0.5840860

H	2.6167800	-5.1349160	-1.0034900
H	1.5902750	-3.7870660	-1.5410320
H	3.1209010	-4.1083600	-2.3470630
H	6.9439250	-0.9516400	-0.9915510
H	7.3780640	-1.2774800	0.6904670
H	7.4030120	-2.5856400	-0.5062670
H	2.1168620	-0.0901980	2.3074440
H	2.1435310	-1.5938520	3.2215840
H	3.5303640	-0.4868440	3.2817260
H	5.1810220	-3.3912480	-1.4921810
H	5.2950620	-0.6738520	1.8130710
H	-2.8068150	-3.1510220	2.2573920
H	-3.2738430	-1.4550400	2.2508410
H	-4.5242290	-2.7008740	2.2242300
H	-6.2895530	-2.6778320	-3.2504490
H	-6.9729330	-2.0368320	-1.7457950
H	-6.1353490	-0.9628930	-2.8753160
H	-0.3149490	-2.6033940	-2.3464760
H	-1.0621680	-4.1790760	-2.6712510
H	-1.4017960	-2.7976660	-3.7147210
H	-5.6327380	-2.0686080	0.2562090
H	-3.6936440	-2.5380380	-3.5329950
H	1.5021620	-4.8428240	0.8240950
H	0.6131630	-4.2561850	2.2252210
H	-1.2489190	-4.8827990	0.9020080
H	-0.3671440	-4.6526530	-0.6213480
H	-0.3358860	-2.8978340	3.3810430
H	-1.2611020	-2.0166080	5.4869080
H	-2.0672710	0.3367230	5.6070310
H	-1.8389020	1.8192050	3.6379370

(NHP-DalPhos)Ni(CH₂-Mesityl)Br



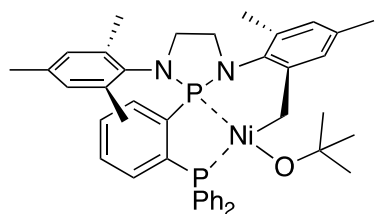
Zero-point correction=	0.676723 (Hartree/Particle)
Thermal correction to Energy=	0.720083
Thermal correction to Enthalpy=	0.721027
Thermal correction to Gibbs Free Energy=	0.598042
Sum of electronic and zero-point Energies=	-6342.920811
Sum of electronic and thermal Energies=	-6342.877451
Sum of electronic and thermal Enthalpies=	-6342.876507
Sum of electronic and thermal Free Energies=	-6342.999491

Single-point energy (6-311+G(2d,2p)) = -6.347033320645E+03

Br	0.9963790	2.2849590	-2.3958680
Ni	0.7774200	0.3921610	-0.9860870
P	-0.5239250	1.4505450	0.4707770
P	0.5366490	-1.3496390	0.1897710
N	-0.5183430	-2.6356220	-0.2026170
N	1.8907110	-2.3704140	0.2697950
C	-1.0430420	4.0741550	1.4187120
C	-0.6428880	5.3376100	1.8586410
C	0.7119870	5.6714350	1.8876330
C	1.6694450	4.7442800	1.4681650
C	1.2743140	3.4849770	1.0208460
C	-0.0849280	3.1403800	1.0041890
C	-3.3104730	0.9877060	0.8341310
C	-4.6441970	1.0740620	0.4300770
C	-4.9722040	1.6923560	-0.7765950
C	-3.9616510	2.2116190	-1.5909500
C	-2.6279640	2.1251850	-1.1963520
C	-2.2971460	1.5238560	0.0299100
C	-2.3563080	-3.7020280	1.7365160
C	-6.1788640	-2.0511420	-1.1099710
C	-1.4661950	-1.3287610	-2.6940470
C	-2.8315650	-2.9933100	0.4910140
C	-4.2033630	-2.8478430	0.2611320
C	-4.6960080	-2.2117590	-0.8790620
C	-3.7751930	-1.7315250	-1.8130940
C	-2.3957200	-1.8574010	-1.6321060
C	-1.9235060	-2.4792050	-0.4556870
C	4.1487820	-2.9195350	1.9798510
C	6.9309660	0.0644860	-1.0118970
C	2.0501180	-0.7101360	-2.0430800
C	4.2726150	-2.0494850	0.7526560
C	5.4897540	-1.4397690	0.4251650
C	5.6079950	-0.5817260	-0.6725910
C	4.4801130	-0.3494910	-1.4661550
C	3.2503390	-0.9667290	-1.2036230
C	3.1661420	-1.8144950	-0.0739940
C	0.2126770	-3.8101230	-0.7005220
C	1.5559790	-3.7880140	0.0467960
C	0.2501850	-1.6434560	3.0232950
C	-0.0699290	-1.1487610	4.2861400
C	-0.5763820	0.1491950	4.4218170
C	-0.7544020	0.9562550	3.2988180
C	-0.4318040	0.4654990	2.0266640

C	0.0677900	-0.8396030	1.8918940
H	-2.0987980	3.8219070	1.3849830
H	-1.3906890	6.0608250	2.1726260
H	1.0213690	6.6567820	2.2254690
H	2.7232780	5.0077370	1.4714780
H	2.0132140	2.7766030	0.6588960
H	-3.0640040	0.4979570	1.7703730
H	-5.4235100	0.6533260	1.0591430
H	-6.0116000	1.7657190	-1.0857690
H	-4.2109520	2.6837170	-2.5372740
H	-1.8377860	2.5146420	-1.8329590
H	-1.6521120	-4.5093640	1.5055880
H	-1.8424110	-3.0168620	2.4173190
H	-3.2025420	-4.1406850	2.2742520
H	-6.7624240	-2.4996670	-0.2996980
H	-6.4528440	-0.9912190	-1.1766510
H	-6.4913560	-2.5234120	-2.0494190
H	-0.9929910	-0.3852170	-2.3926460
H	-0.6563290	-2.0276780	-2.9209160
H	-2.0147840	-1.1337700	-3.6203060
H	-4.9024590	-3.2465880	0.9931770
H	-4.1373850	-1.2430530	-2.7147700
H	3.9976110	-3.9770410	1.7260280
H	5.0507330	-2.8559790	2.5961300
H	3.2916460	-2.6122850	2.5905190
H	7.6122790	0.0572170	-0.1545220
H	7.4328460	-0.4626670	-1.8344840
H	6.7971350	1.1042250	-1.3307010
H	2.2876510	-0.1236290	-2.9299020
H	1.5631640	-1.6424560	-2.3538500
H	6.3566910	-1.6233930	1.0565070
H	4.5511800	0.3184020	-2.3215050
H	-0.3590140	-4.7180200	-0.4791190
H	0.3673110	-3.7630410	-1.7888380
H	2.3512970	-4.2573590	-0.5388000
H	1.4683360	-4.3233470	1.0026510
H	0.6593660	-2.6434710	2.9119380
H	0.0844030	-1.7659540	5.1669330
H	-0.8172370	0.5362680	5.4080210
H	-1.1195590	1.9728880	3.4114300

(NHP-DalPhos)Ni(CH₂-Mesityl)O'Bu



Zero-point correction= 0.801969 (Hartree/Particle)
 Thermal correction to Energy= 0.850456
 Thermal correction to Enthalpy= 0.851400
 Thermal correction to Gibbs Free Energy= 0.719292
 Sum of electronic and zero-point Energies= -4004.407131
 Sum of electronic and thermal Energies= -4004.358644
 Sum of electronic and thermal Enthalpies= -4004.357700
 Sum of electronic and thermal Free Energies= -4004.489807

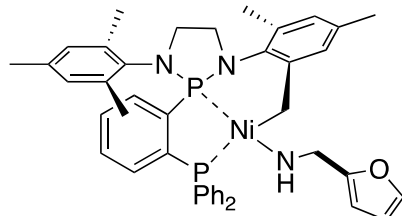
Single-point energy (6-311+G(2d,2p)) = -4.006001794513E+03

Ni	0.8759910	0.3859230	-0.8916600
P	-0.4617810	1.4109220	0.6676690
P	0.3786780	-1.4544470	0.0728580
N	-0.7650100	-2.6258220	-0.4419890
N	1.6338380	-2.6036170	0.1007500
C	-0.7667130	3.8769790	2.0592140
C	-0.2750000	5.0703990	2.5884100
C	1.0626650	5.4233350	2.3927610
C	1.9047620	4.5857520	1.6596630
C	1.4195880	3.3921620	1.1219030
C	0.0794390	3.0281620	1.3284340
C	-3.1728540	0.6381750	1.0191410
C	-4.5493370	0.7634950	0.8259630
C	-5.0618180	1.8243900	0.0802820
C	-4.1875110	2.7606900	-0.4764150
C	-2.8124150	2.6400960	-0.2824470
C	-2.2870270	1.5786860	0.4739420
C	-2.7681780	-3.7447790	1.2752740
C	-6.3129890	-1.6111030	-1.6133220
C	-1.4701360	-0.9971720	-2.8171870
C	-3.1309670	-2.9062210	0.0733730
C	-4.4754600	-2.6723420	-0.2302000
C	-4.8590200	-1.8934730	-1.3238040
C	-3.8551680	-1.3631340	-2.1369640
C	-2.4983800	-1.5821050	-1.8835630
C	-2.1366750	-2.3492200	-0.7556110
C	3.6934960	-3.5860520	1.8946040
C	6.9515800	-0.5235750	-0.4680220
C	2.1308860	-0.7172390	-1.9515000
C	3.9881810	-2.5887470	0.8004820

C	5.2758220	-2.0608940	0.6429820
C	5.5566850	-1.0846810	-0.3174010
C	4.5222850	-0.6499670	-1.1522160
C	3.2289200	-1.1790990	-1.0636940
C	2.9777320	-2.1480290	-0.0648900
C	-0.1145490	-3.8198410	-1.0032250
C	1.1957850	-3.9679630	-0.2179190
C	0.0526300	-2.0118970	2.8592840
C	-0.1583700	-1.6190200	4.1785360
C	-0.4549030	-0.2819700	4.4694400
C	-0.5463840	0.6573820	3.4441000
C	-0.3383260	0.2673180	2.1144220
C	-0.0346660	-1.0722830	1.8235610
H	-1.8102430	3.6136780	2.2042920
H	-0.9360790	5.7236260	3.1518430
H	1.4433690	6.3547040	2.8037380
H	2.9406650	4.8663870	1.4903080
H	2.0479240	2.7671250	0.4952020
H	-2.7963740	-0.1945760	1.6012890
H	-5.2165320	0.0247710	1.2592300
H	-6.1342800	1.9249080	-0.0637720
H	-4.5748810	3.5931880	-1.0575610
H	-2.1482980	3.3814400	-0.7104630
H	-2.1670020	-4.6195000	1.0001000
H	-2.1802580	-3.1722250	1.9992870
H	-3.6701070	-4.1069000	1.7783290
H	-6.9728510	-2.2766520	-1.0474670
H	-6.5703300	-0.5782870	-1.3443820
H	-6.5417240	-1.7322680	-2.6783270
H	-0.9438850	-0.1477100	-2.3600780
H	-0.7004460	-1.7243800	-3.0926870
H	-1.9440290	-0.6383400	-3.7357540
H	-5.2409940	-3.1080610	0.4086250
H	-4.1325140	-0.7648530	-3.0022140
H	3.4814980	-4.5886430	1.5001480
H	4.5432660	-3.6766370	2.5780960
H	2.8169180	-3.2786040	2.4766180
H	7.5662750	-0.7359850	0.4131200
H	7.4646560	-0.9546710	-1.3383330
H	6.9309760	0.5626080	-0.6127660
H	2.4993260	-0.0473870	-2.7222860
H	1.5983980	-1.5592330	-2.4129870
H	6.0685700	-2.4039030	1.3047970
H	4.7176820	0.1129430	-1.9019800
H	-0.7669160	-4.6900920	-0.8720380
H	0.0848050	-3.7040500	-2.0795740

H	1.9670230	-4.4672860	-0.8117380
H	1.0279430	-4.5584450	0.6948480
H	0.3056870	-3.0423670	2.6277470
H	-0.0798750	-2.3457930	4.9825100
H	-0.6070900	0.0277610	5.4997440
H	-0.7651940	1.6948740	3.6766770
O	1.6800090	1.9376600	-1.5529610
C	1.3151650	2.7194320	-2.6591810
C	-0.1140060	3.2772770	-2.5038820
H	-0.1832200	3.8598090	-1.5783130
H	-0.3985410	3.9286270	-3.3407510
H	-0.8371310	2.4543160	-2.4547250
C	2.3116930	3.8953570	-2.7091260
H	3.3332040	3.5097760	-2.7984930
H	2.1143030	4.5647800	-3.5564740
H	2.2480170	4.4782020	-1.7834870
C	1.3928750	1.9351890	-3.9874430
H	1.1023700	2.5632890	-4.8397130
H	2.4122610	1.5746740	-4.1648020
H	0.7245760	1.0663740	-3.9609810

(NHP-DalPhos)Ni(CH₂-Mesityl)furfurylamine



Zero-point correction=	0.780601 (Hartree/Particle)
Thermal correction to Energy=	0.829010
Thermal correction to Enthalpy=	0.829955
Thermal correction to Gibbs Free Energy=	0.695939
Sum of electronic and zero-point Energies=	-4095.432093
Sum of electronic and thermal Energies=	-4095.383683
Sum of electronic and thermal Enthalpies=	-4095.382739
Sum of electronic and thermal Free Energies=	-4095.516754

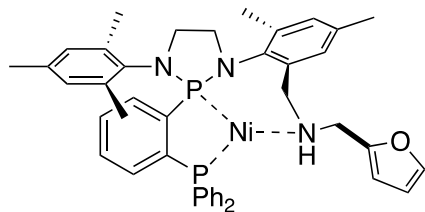
Single-point energy (6-311+G(2d,2p)) = -4.097029017014E+03

Ni	-0.4935200	-0.6331710	-0.9376030
P	0.8775150	-0.5780030	0.8532570
P	-1.4929800	1.0580740	-0.0990510
N	-1.3074010	2.6681400	-0.6725090
N	-3.1770630	1.1015900	-0.3201190
C	2.1480140	-2.5068770	2.5292250
C	2.2080390	-3.7518120	3.1576340

C	1.2011710	-4.6942500	2.9414710
C	0.1350500	-4.3924810	2.0907540
C	0.0786790	-3.1551660	1.4500410
C	1.0836990	-2.2016220	1.6707290
C	2.7346890	1.5267950	1.1328730
C	3.9912850	2.1168470	0.9938530
C	5.0707990	1.3699300	0.5201410
C	4.8878570	0.0269390	0.1815120
C	3.6352840	-0.5693950	0.3222940
C	2.5469640	0.1751420	0.8090250
C	-0.6369850	4.8145470	1.1238880
C	3.8172570	5.2549490	-1.2046570
C	0.5102880	1.8610410	-2.8756980
C	0.3103160	4.3521590	0.0429810
C	1.5561330	4.9747030	-0.0943080
C	2.4652280	4.5945320	-1.0826020
C	2.0881160	3.5794260	-1.9652580
C	0.8527170	2.9334000	-1.8735200
C	-0.0344340	3.3096780	-0.8405520
C	-5.6008620	0.5130100	1.1239560
C	-5.7667650	-3.9357090	-1.2730810
C	-2.0069670	-0.7026510	-2.2223430
C	-5.0257230	-0.4461160	0.1100560
C	-5.6381040	-1.6819180	-0.1298760
C	-5.0874100	-2.6104320	-1.0174560
C	-3.9057050	-2.2751850	-1.6857770
C	-3.2709500	-1.0382320	-1.5077880
C	-3.8532800	-0.1295150	-0.5911100
C	-2.4862380	3.1265720	-1.4196620
C	-3.6774160	2.4114280	-0.7622730
C	-1.9055300	1.8622620	2.6238020
C	-1.5814890	1.8296340	3.9774670
C	-0.4709070	1.0954970	4.4129140
C	0.3026780	0.3837050	3.4988780
C	-0.0244910	0.4042630	2.1359460
C	-1.1255420	1.1556200	1.6984100
H	2.9410810	-1.7838840	2.6936410
H	3.0425260	-3.9841790	3.8138240
H	1.2502730	-5.6637330	3.4301050
H	-0.6453780	-5.1268600	1.9113990
H	-0.7210200	-2.9327530	0.7515990
H	1.9033610	2.1254540	1.4894400
H	4.1199230	3.1629920	1.2551190
H	6.0491910	1.8308850	0.4139350
H	5.7191860	-0.5632010	-0.1935370
H	3.5065160	-1.6137530	0.0557400

H	-1.6355970	5.0282020	0.7270840
H	-0.7612570	4.0556490	1.9021920
H	-0.2614390	5.7266300	1.5981580
H	3.9231820	6.0865240	-0.5006190
H	4.6235210	4.5385040	-1.0030180
H	3.9821080	5.6469160	-2.2154930
H	0.5336630	0.8596730	-2.4246360
H	-0.4938980	1.9896370	-3.2910560
H	1.2238100	1.8694150	-3.7049730
H	1.8173200	5.7800790	0.5890240
H	2.7737000	3.2797500	-2.7550480
H	-6.0339800	1.4060990	0.6544600
H	-6.3924770	0.0340760	1.7082370
H	-4.8240680	0.8602090	1.8152300
H	-6.4423590	-4.2039630	-0.4538600
H	-6.3647920	-3.9072220	-2.1941190
H	-5.0364510	-4.7444650	-1.3885760
H	-1.7811410	-1.4512260	-2.9860050
H	-2.0763920	0.2729440	-2.7212680
H	-6.5520480	-1.9295900	0.4061190
H	-3.4673860	-2.9857300	-2.3839720
H	-2.5740580	4.2159850	-1.3385030
H	-2.4203180	2.8701220	-2.4881400
H	-4.4994740	2.2654770	-1.4688040
H	-4.0531090	3.0003500	0.0868740
H	-2.7674400	2.4262300	2.2786690
H	-2.1917980	2.3688650	4.6969180
H	-0.2191510	1.0688500	5.4695470
H	1.1470860	-0.2040240	3.8459620
N	0.3522780	-2.1375110	-1.6991080
H	-0.2328010	-2.6088360	-2.3844640
C	1.6705560	-1.9343830	-2.2903380
H	1.6480680	-1.8288720	-3.3902950
H	2.1087970	-0.9891580	-1.9352830
C	2.6369990	-3.0320720	-1.9403580
C	2.5861050	-4.0984470	-1.0916140
O	3.8835970	-2.9650390	-2.5194630
C	3.8750540	-4.7324870	-1.1464770
H	1.7310610	-4.3768510	-0.4957830
C	4.6202880	-4.0078910	-2.0220640
H	4.1956190	-5.6118640	-0.6044290
H	5.6280500	-4.0894870	-2.3999790

(NHP-DalPhos)Ni(Mesityl-CH₂-furfurylamine) N-coordinated



Zero-point correction= 0.783647 (Hartree/Particle)
 Thermal correction to Energy= 0.831733
 Thermal correction to Enthalpy= 0.832678
 Thermal correction to Gibbs Free Energy= 0.698074
 Sum of electronic and zero-point Energies= -4095.424134
 Sum of electronic and thermal Energies= -4095.376048
 Sum of electronic and thermal Enthalpies= -4095.375104
 Sum of electronic and thermal Free Energies= -4095.509707

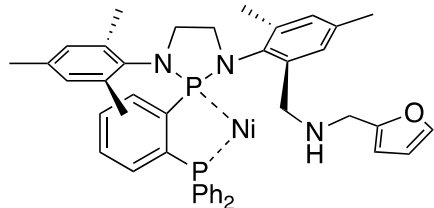
Single-point energy (6-311+G(2d,2p)) = -4.097021577853E+03

Ni	0.6260450	0.5955050	-0.5897620
P	-0.3977620	1.2697070	1.1150450
P	0.3799830	-1.4233460	-0.1325650
N	-0.6603920	-2.7288920	-0.6674690
N	1.7614930	-2.4475380	-0.4175480
C	-1.1719290	3.4104250	2.8956710
C	-0.8843060	4.5113720	3.7072000
C	0.4378980	4.9109060	3.9085840
C	1.4749270	4.2104690	3.2855970
C	1.1854700	3.1240220	2.4617220
C	-0.1392780	2.7015200	2.2644470
C	-3.1467080	0.4690600	1.3335060
C	-4.4935610	0.5416620	0.9695540
C	-4.9229160	1.4978990	0.0495600
C	-3.9959010	2.3766960	-0.5180530
C	-2.6502550	2.2987910	-0.1628090
C	-2.2103730	1.3507610	0.7775370
C	-2.5865050	-4.1941930	0.8682120
C	-6.2738140	-1.8478940	-1.6480230
C	-1.4955760	-0.8263590	-2.8059430
C	-3.0041300	-3.2186780	-0.2052060
C	-4.3630910	-3.0086510	-0.4569570
C	-4.8030740	-2.1013510	-1.4221150
C	-3.8385600	-1.4166390	-2.1630160
C	-2.4693370	-1.6044480	-1.9564710
C	-2.0450450	-2.5049730	-0.9541160
C	3.6169450	-3.4763700	1.5869290
C	7.1180420	-0.3047960	-0.1478010
C	2.6503130	-0.3897770	-2.3975300
C	4.0082690	-2.4213030	0.5814490

C	5.3015030	-1.8948930	0.6207410
C	5.7261770	-0.8819030	-0.2425180
C	4.8106810	-0.4254500	-1.1892100
C	3.5079050	-0.9313540	-1.2786660
C	3.0847050	-1.9372250	-0.3765260
C	0.0606630	-3.7971100	-1.3589370
C	1.4378350	-3.8490210	-0.6875010
C	0.1734830	-2.5542560	2.5347040
C	-0.0193650	-2.4537800	3.9132070
C	-0.3161470	-1.2126770	4.4818930
C	-0.4281890	-0.0821590	3.6708200
C	-0.2383900	-0.1774580	2.2861390
C	0.0802700	-1.4259090	1.7112300
H	-2.2038090	3.1047890	2.7496840
H	-1.6958550	5.0550520	4.1847900
H	0.6594320	5.7671750	4.5402010
H	2.5067560	4.5202070	3.4316120
H	1.9889120	2.5932680	1.9537240
H	-2.8256220	-0.2829490	2.0465700
H	-5.2038650	-0.1566970	1.4033450
H	-5.9719980	1.5566500	-0.2289220
H	-4.3200730	3.1192940	-1.2428110
H	-1.9303260	2.9713590	-0.6226770
H	-1.9734920	-5.0109500	0.4678970
H	-1.9914930	-3.6995100	1.6411010
H	-3.4647720	-4.6425410	1.3436780
H	-6.8914080	-2.6269010	-1.1890180
H	-6.5768520	-0.8856460	-1.2145300
H	-6.5168630	-1.8091420	-2.7163270
H	-1.1080050	0.0443930	-2.2560410
H	-0.6307680	-1.4310970	-3.0964680
H	-1.9846190	-0.4651100	-3.7171490
H	-5.0957710	-3.5638570	0.1255500
H	-4.1574320	-0.7132690	-2.9296460
H	3.4826340	-4.4623240	1.1249050
H	4.3889480	-3.5782150	2.3555800
H	2.6768030	-3.2156700	2.0802930
H	7.1921810	0.4247840	0.6696270
H	7.8639430	-1.0835930	0.0470180
H	7.4012100	0.2103340	-1.0717800
H	3.2871850	-0.2541460	-3.2875120
H	1.8507420	-1.0863700	-2.6554160
H	5.9948660	-2.2809120	1.3656020
H	5.1264630	0.3292070	-1.9090770
H	-0.4708530	-4.7509030	-1.2539370
H	0.1687540	-3.5914500	-2.4385940

H	2.1925840	-4.2883740	-1.3489940
H	1.3855580	-4.4620110	0.2249990
H	0.3938050	-3.5210840	2.0919460
H	0.0596480	-3.3377720	4.5411780
H	-0.4657960	-1.1259910	5.5550520
H	-0.6629460	0.8799980	4.1167480
N	2.0096760	0.9151490	-2.0500610
H	2.7342820	1.5242900	-1.6654880
C	1.4654120	1.5583690	-3.2643160
H	2.2295310	1.6003440	-4.0590430
H	0.6564550	0.9214240	-3.6421210
C	0.9648300	2.9419970	-3.0020300
C	0.7525530	3.7019790	-1.8895210
O	0.6405010	3.6574150	-4.1257440
C	0.2581050	4.9693510	-2.3532610
H	0.8931510	3.3729730	-0.8692240
C	0.2065610	4.8877040	-3.7080780
H	-0.0181580	5.8200600	-1.7460050
H	-0.0917030	5.5648380	-4.4932700

(NHP-DalPhos)Ni(Mesityl-CH₂-furfurylamine)



Zero-point correction=	0.781684 (Hartree/Particle)
Thermal correction to Energy=	0.830751
Thermal correction to Enthalpy=	0.831695
Thermal correction to Gibbs Free Energy=	0.691566
Sum of electronic and zero-point Energies=	-4095.393149
Sum of electronic and thermal Energies=	-4095.344082
Sum of electronic and thermal Enthalpies=	-4095.343138
Sum of electronic and thermal Free Energies=	-4095.483267

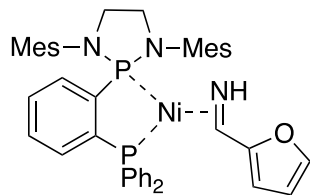
Single-point energy (6-311+G(2d,2p)) = -4.097021577853E+03

Ni	0.0701000	-0.2112520	-1.0418600
P	2.0785200	-0.7531540	-1.2621970
P	-0.1501270	-0.3189520	1.0147160
N	0.0441590	1.0758040	2.0441560
N	-1.4181220	-0.8946340	2.0364000
C	4.1507180	-1.9634290	-2.8537820
C	4.6379120	-2.9651860	-3.6970300
C	3.8209290	-4.0361830	-4.0618190

C	2.5076850	-4.0991000	-3.5878060
C	2.0164360	-3.0928730	-2.7581410
C	2.8348270	-2.0186990	-2.3732760
C	4.1340520	0.9557200	-0.2207980
C	5.0145170	2.0363490	-0.3145330
C	5.0819660	2.7903060	-1.4855480
C	4.2455220	2.4748550	-2.5608430
C	3.3565230	1.4071120	-2.4623340
C	3.3037030	0.6220540	-1.2978530
C	2.2437030	1.5840360	3.8156000
C	3.6368340	5.4208940	0.8513810
C	-0.4360940	2.7478700	-0.3658270
C	1.9975330	2.4293150	2.5896430
C	2.8553930	3.4940930	2.2994880
C	2.6858300	4.2923270	1.1671200
C	1.6093020	4.0101600	0.3238540
C	0.7137900	2.9691820	0.5831720
C	0.9159920	2.1605090	1.7243140
C	-1.6132130	-3.5308550	3.1878310
C	-5.4656580	-4.5067120	0.0840390
C	-3.2760890	0.0312090	-0.0514120
C	-2.5539420	-3.0633330	2.1042090
C	-3.5389470	-3.9268250	1.6196160
C	-4.4056760	-3.5557880	0.5878170
C	-4.2810830	-2.2714770	0.0555710
C	-3.3298950	-1.3641480	0.5344330
C	-2.4397380	-1.7697250	1.5526240
C	-1.0527470	1.2661380	2.9908940
C	-1.5765380	-0.1450660	3.2890670
C	1.5858340	-1.8701920	2.6992100
C	2.7089750	-2.6512400	2.9675180
C	3.6501950	-2.8799190	1.9608210
C	3.4642560	-2.3199310	0.6974960
C	2.3394440	-1.5303320	0.4192270
C	1.3774370	-1.3112550	1.4309290
H	4.7948550	-1.1350370	-2.5749190
H	5.6588910	-2.9082640	-4.0660000
H	4.2020880	-4.8145100	-4.7174620
H	1.8633020	-4.9261020	-3.8744310
H	0.9887140	-3.1314450	-2.4031860
H	4.0932360	0.3774100	0.6955220
H	5.6466730	2.2866950	0.5328810
H	5.7769810	3.6224800	-1.5607900
H	4.2835520	3.0639180	-3.4734740
H	2.6952300	1.1747770	-3.2938990
H	1.4559220	1.7111570	4.5694290

H	2.2747680	0.5205590	3.5633290
H	3.1929790	1.8566800	4.2876040
H	4.3300440	5.6040220	1.6788690
H	4.2333170	5.1914040	-0.0402680
H	3.0992560	6.3552850	0.6497750
H	-0.2072330	1.9329580	-1.0822930
H	-1.3552910	2.4701610	0.1552520
H	-0.6306430	3.6489150	-0.9566450
H	3.6852340	3.6968300	2.9736580
H	1.4514620	4.6250730	-0.5600710
H	-1.6827910	-2.9104210	4.0896080
H	-1.8395950	-4.5616330	3.4773980
H	-0.5726780	-3.4907380	2.8510600
H	-5.1230480	-5.5466370	0.1230710
H	-6.3790510	-4.4437620	0.6911130
H	-5.7461710	-4.2802070	-0.9498390
H	-2.8827780	0.7281300	0.7060890
H	-3.6169390	-4.9241660	2.0483080
H	-4.9385660	-1.9493460	-0.7463410
H	-0.6943400	1.7592840	3.9019190
H	-1.8546250	1.8946240	2.5657950
H	-2.6318230	-0.1309990	3.5796950
H	-1.0031820	-0.5948690	4.1139730
H	0.8556610	-1.6944720	3.4825790
H	2.8487040	-3.0830020	3.9553120
H	4.5253580	-3.4932080	2.1585640
H	4.1967840	-2.5029250	-0.0833480
H	-2.5485020	0.0604960	-0.8785780
N	-4.5645760	0.4692770	-0.5860830
H	-5.2736670	0.4396230	0.1460020
C	-4.4994320	1.8142660	-1.1502420
H	-4.1917530	2.5875740	-0.4213320
H	-3.7215170	1.8048600	-1.9285130
C	-5.8183500	2.2016770	-1.7355280
C	-6.8602710	1.4952950	-2.2595710
O	-6.0879540	3.5440000	-1.8013460
C	-7.8380210	2.4592960	-2.6789620
H	-6.9127350	0.4195060	-2.3416260
C	-7.3197310	3.6803050	-2.3822780
H	-8.7968390	2.2621590	-3.1381670
H	-7.6678350	4.6944740	-2.5016410

(NHP-DalPhos)Ni(η^2 -fufurylimine)



Zero-point correction=	0.779571 (Hartree/Particle)
Thermal correction to Energy=	0.828729
Thermal correction to Enthalpy=	0.829673
Thermal correction to Gibbs Free Energy=	0.693484
Sum of electronic and zero-point Energies=	-4095.453388
Sum of electronic and thermal Energies=	-4095.404230
Sum of electronic and thermal Enthalpies=	-4095.403286
Sum of electronic and thermal Free Energies=	-4095.539476

Single-point energy (6-311+G(2d,2p)) = -4.097048427965E+03

Ni	0.3279680	0.6087090	-0.9472060
P	0.4258790	-1.0011070	0.4683840
P	-1.3420490	1.4973420	0.1402480
N	-0.4592180	-2.4788530	0.2392590
N	1.8021060	-1.8659730	1.0078310
C	-0.3937250	-0.3175000	2.0012870
C	-1.1897170	0.8334530	1.8541730
C	-0.8448720	-0.2995540	4.3889480
H	-0.7062940	-0.7392830	5.3732000
C	-0.2404080	-0.8792190	3.2762070
H	0.3688440	-1.7682730	3.3986620
C	0.3550490	-3.6875110	0.3789640
H	0.7088040	-4.0450130	-0.6003840
H	-0.2326040	-4.4929570	0.8334950
C	1.5303290	-3.2880740	1.2771000
H	1.2730230	-3.4480080	2.3348020
H	2.4259340	-3.8771100	1.0623640
C	-1.7833100	-2.5864800	-0.2888010
C	-2.0434470	-2.3456770	-1.6553810
C	-3.3472920	-2.4936110	-2.1343990
H	-3.5407010	-2.3016230	-3.1879060
C	-4.3986280	-2.9001150	-1.3098780
C	-4.1139000	-3.1611000	0.0310610
H	-4.9149810	-3.4898810	0.6901070
C	-2.8289730	-3.0068470	0.5605090
C	-0.9477240	-1.9450850	-2.6074740
H	-1.2667160	-2.0808420	-3.6458920
H	-0.0344680	-2.5258460	-2.4471490
H	-0.6752950	-0.8889640	-2.4731380
C	-5.7969870	-3.0444370	-1.8583460

H	-5.8072050	-3.6339760	-2.7828230
H	-6.2267300	-2.0631990	-2.0955960
H	-6.4613830	-3.5344410	-1.1391610
C	-2.5906960	-3.3052520	2.0207540
H	-3.5382950	-3.5017970	2.5320830
H	-2.0937070	-2.4735350	2.5254340
H	-1.9556420	-4.1894240	2.1618860
C	3.1574900	-1.4397580	0.8001600
C	3.8211320	-0.7105010	1.8027860
C	5.1713190	-0.3902610	1.6243400
C	5.8775390	-0.7761220	0.4858090
C	5.1906830	-1.4825560	-0.5044870
H	5.7144260	-1.7723950	-1.4124600
C	3.8393270	-1.8073710	-0.3788180
C	3.1142260	-0.2734850	3.0615630
H	2.6474980	-1.1188560	3.5774070
H	2.3168330	0.4471420	2.8507410
C	3.1391920	-2.5314350	-1.5015840
H	3.7577230	-2.5262260	-2.4031530
H	2.1883260	-2.0472590	-1.7437240
H	2.9241700	-3.5785910	-1.2533450
H	5.6835830	0.1691980	2.4043780
C	-1.7930310	1.4172180	2.9776890
C	-1.6208760	0.8548800	4.2404450
H	-2.0850910	1.3161480	5.1078950
H	-2.3852120	2.3203340	2.8658660
C	-1.3482740	3.3211890	0.3407900
C	-2.4792730	4.0408460	0.7570430
C	-0.1573900	4.0093750	0.0674210
C	-2.4094950	5.4236270	0.9261920
H	-3.4187260	3.5235710	0.9312870
C	-0.0904550	5.3926430	0.2417980
H	0.6924890	3.4601100	-0.3235260
C	-1.2125200	6.0999490	0.6760500
H	-3.2901430	5.9735370	1.2477400
H	0.8342900	5.9182170	0.0199630
H	-1.1610700	7.1778600	0.8048650
C	-3.0726640	1.1455050	-0.3609790
C	-3.9939510	0.4586650	0.4368030
C	-3.4688420	1.5886440	-1.6345660
C	-5.2961890	0.2401240	-0.0199430
H	-3.6995240	0.0917820	1.4139890
C	-4.7688030	1.3751150	-2.0855630
H	-2.7571220	2.1140410	-2.2668230
C	-5.6895420	0.7046570	-1.2742040
H	-6.0009610	-0.2962580	0.6091800

H	-5.0650060	1.7326050	-3.0680870
H	-6.7066070	0.5441550	-1.6217350
H	3.8184400	0.1996190	3.7530630
C	7.3272260	-0.4025600	0.3004700
H	7.9068090	-1.2309780	-0.1229520
H	7.4212550	0.4455930	-0.3900820
H	7.7929070	-0.1123130	1.2479600
C	5.1849290	1.1866500	-2.4470300
C	4.9678790	2.0665270	-1.4319460
C	3.5586120	2.0585140	-1.1872470
C	3.0046450	1.1805240	-2.0802560
O	4.0022830	0.6350340	-2.8551260
H	6.0651520	0.8436000	-2.9681100
H	5.7189200	2.6447910	-0.9112120
H	3.0154430	2.6297010	-0.4488890
C	1.6325070	0.8143680	-2.4424560
H	1.5786510	0.0219410	-3.1942790
N	0.6703580	1.7957580	-2.3786800
H	-0.0881580	1.6111330	-3.0415140

Appendix References

1. Clark, J. S. K.; Voth, C. N.; Ferguson, M. J.; Stradiotto, M. *Organometallics* **2017**, *36*, 679-686.
2. The postg program is available at <http://schooner.chem.dal.ca>
3. (a) Lee, C. T.; Yang, W. T.; Parr, R. G. *Phys. Rev. B* **1988**, *37*, 785; (b) Becke, A. D. *J. Chem. Phys.* **1993**, *98*, 5648.
4. (a) Becke, A. D.; Johnson, E. R. *J. Chem. Phys.* **2007**, *127*, 154108; (b) Otero-de-la-Roza, A.; Johnson, E. R. *J. Chem. Phys.* **2013**, *138*, 204109.

Crystallographic Solutions and Refinement Details

L2: Crystallographic data for **L2** were obtained at $-100(\pm 2)$ °C on a Bruker D8/APEX II CCD diffractometer using Cu K α ($\lambda = 1.54178$ Å) microfocus source radiation, employing a sample that was mounted in inert oil and transferred to a cold gas stream on the diffractometer. Programs for diffractometer operation, data collection, data reduction, and absorption correction were supplied by Bruker. Gaussian integration (face-indexed) was employed as the absorption correction method. The structure of **L2** was solved by use of intrinsic phasing methods, and refined by use of full-matrix least-squares procedures (on F^2) with $R1$ based on $F_o2 \geq 2\sigma(F_o2)$ and $wR2$ based on all data. Anisotropic displacement parameters were employed for all the non-hydrogen atoms shown. Non-hydrogen atoms are represented by Gaussian ellipsoids at the 30% probability level.

L1NiCl₂: Crystallographic data for **L1NiCl₂•dichloromethane** were obtained at $-100(\pm 2)$ °C on a Bruker D8/APEX II CCD diffractometer using Cu K α ($\lambda = 1.54178$ Å) microfocus source radiation, employing a sample that was mounted in inert oil and transferred to a cold gas stream on the diffractometer. Programs for diffractometer operation, data collection, data reduction, and absorption correction were supplied by Bruker. Gaussian integration (face-indexed) was employed as the absorption correction method. The structure of **L1NiCl₂** was solved by use of Patterson/structure expansion, and refined by use of full-matrix least-squares procedures (on F^2) with $R1$ based on $F_o2 \geq 2\sigma(F_o2)$ and $wR2$ based on all data. Anisotropic displacement parameters were employed for all the non-hydrogen atoms shown. Non-hydrogen atoms are represented by Gaussian ellipsoids at the 30% probability level.

L2NiCl₂: Crystallographic data for **L2NiCl₂** were obtained at $-100(\pm 2)$ °C on a Bruker D8/APEX II CCD diffractometer using Cu K α ($\lambda = 1.54178$ Å) microfocus source radiation, employing a sample that was mounted in inert oil and transferred to a cold gas stream on the diffractometer. Programs for diffractometer operation, data collection, data reduction, and absorption correction were supplied by Bruker. Gaussian integration (face-indexed) was employed as the absorption correction method. The structure of **L2NiCl₂** was solved by use of intrinsic phasing methods, and refined by use of full-matrix least-squares procedures (on F^2) with $R1$ based on $F_o2 \geq 2\sigma(F_o2)$ and $wR2$ based on all data. Anisotropic displacement parameters

were employed for all the non-hydrogen atoms shown. Non-hydrogen atoms are represented by Gaussian ellipsoids at the 30% probability level.

L4NiCl₂: Crystallographic data for **L4NiCl₂•dichloromethane** were obtained at $-100(\pm 2)$ °C on a Bruker D8/APEX II CCD diffractometer using Cu K α ($\lambda = 1.54178$ Å) microfocus source radiation, employing a sample that was mounted in inert oil and transferred to a cold gas stream on the diffractometer. Programs for diffractometer operation, data collection, data reduction, and absorption correction were supplied by Bruker. Gaussian integration (face-indexed) was employed as the absorption correction method. The structure of **L4NiCl₂** was solved by use of intrinsic phasing, and refined by use of full-matrix least-squares procedures (on F^2) with $R1$ based on $F_o2 \geq 2\sigma(F_o2)$ and $wR2$ based on all data. Anisotropic displacement parameters were employed for all the non-hydrogen atoms shown. Non-hydrogen atoms are represented by Gaussian ellipsoids at the 30% probability level.

L6NiCl₂: Crystallographic data for **L6NiCl₂•dichloromethane** were obtained at $-100(\pm 2)$ °C on a Bruker D8/APEX II CCD diffractometer using Cu K α ($\lambda = 1.54178$ Å) microfocus source radiation, employing a sample that was mounted in inert oil and transferred to a cold gas stream on the diffractometer. Programs for diffractometer operation, data collection, data reduction, and absorption correction were supplied by Bruker. Gaussian integration (face-indexed) was employed as the absorption correction method. The structure of **L6NiCl₂** was solved by use of Patterson/structure expansion, and refined by use of full-matrix least-squares procedures (on F^2) with $R1$ based on $F_o2 \geq 2\sigma(F_o2)$ and $wR2$ based on all data. Anisotropic displacement parameters were employed for all the non-hydrogen atoms shown. Non-hydrogen atoms are represented by Gaussian ellipsoids at the 30% probability level.

C1: Crystallographic data for **C1•THF** were obtained at $-80(\pm 2)$ °C on a Bruker PLATFORM/APEX II CCD diffractometer using graphite-monochromated Mo K α ($\lambda = 0.71073$) radiation, employing a sample that was mounted in inert oil and transferred to a cold gas stream on the diffractometer. Programs for diffractometer operation, data collection, data reduction, and absorption correction were supplied by Bruker. Gaussian integration (face-indexed) was employed as the absorption correction method. The structure of **C1** was solved by use Patterson/structure expansion, and refined by use of full-matrix least-squares procedures (on F^2) with $R1$ based on $F_o2 \geq 2\sigma(F_o2)$ and $wR2$ based on all data. Anisotropic displacement

parameters were employed for all the non-hydrogen atoms shown. Non-hydrogen atoms are represented by Gaussian ellipsoids at the 30% probability level.

C2: Crystallographic data for **C2**•toluene were obtained at $-80(\pm 2)$ °C on a Bruker PLATFORM/APEX II CCD diffractometer using graphite-monochromated Mo $K\alpha$ ($\lambda = 0.71073$) radiation, employing a sample that was mounted in inert oil and transferred to a cold gas stream on the diffractometer. Programs for diffractometer operation, data collection, data reduction, and absorption correction were supplied by Bruker. Gaussian integration (face-indexed) was employed as the absorption correction method. The structure of **C2** was solved by use Patterson/structure expansion, and refined by use of full-matrix least-squares procedures (on F^2) with $R1$ based on $F_o2 \geq 2\sigma(F_o2)$ and $wR2$ based on all data. Anisotropic displacement parameters were employed for all the non-hydrogen atoms shown. Non-hydrogen atoms are represented by Gaussian ellipsoids at the 30% probability level.

C3: Crystallographic data for **C3**•1,1,2,2-tetrachloroethane•0.5 hexanes were obtained on a Bruker D8/APEX II CCD diffractometer using Cu $K\alpha$ ($\lambda = 1.54178$ Å) microfocus source radiation, employing a sample that was mounted in inert oil and transferred to a cold gas stream on the diffractometer. Programs for diffractometer operation, data collection, data reduction, and absorption correction were supplied by Bruker. Gaussian integration (face-indexed) was employed as the absorption correction method. The structure of **C3** was solved by use of intrinsic phasing methods, and refined by use of full-matrix least-squares procedures (on F^2) with $R1$ based on $F_o2 \geq 2\sigma(F_o2)$ and $wR2$ based on all data. Anisotropic displacement parameters were employed for all the non-hydrogen atoms shown. Non-hydrogen atoms are represented by Gaussian ellipsoids at the 30% probability level.

L9: Crystallographic data for **L9** were obtained at $-100(\pm 2)$ °C on a Bruker D8/APEX II CCD diffractometer using Cu $K\alpha$ ($\lambda = 1.54178$ Å) microfocus source radiation, employing a sample that was mounted in inert oil and transferred to a cold gas stream on the diffractometer. Programs for diffractometer operation, data collection, data reduction, and absorption correction were supplied by Bruker. Gaussian integration (face-indexed) was employed as the absorption correction method. The structure of **L9** was solved by use of intrinsic phasing methods, and refined by use of full-matrix least-squares procedures (on F^2) with $R1$ based on $F_o2 \geq 2\sigma(F_o2)$ and $wR2$ based on all data. Anisotropic displacement parameters were employed for all the non-

hydrogen atoms shown. Non-hydrogen atoms are represented by Gaussian ellipsoids at the 30% probability level.

L10: Crystallographic data for **L10**•benzene were obtained at $-100(\pm 2)$ °C on a Bruker D8/APEX II CCD diffractometer using Cu K α ($\lambda = 1.54178$ Å) microfocus source radiation, employing a sample that was mounted in inert oil and transferred to a cold gas stream on the diffractometer. Programs for diffractometer operation, data collection, data reduction, and absorption correction were supplied by Bruker. Gaussian integration (face-indexed) was employed as the absorption correction method. The structure of **L10** was solved by use of intrinsic phasing methods, and refined by use of full-matrix least-squares procedures (on F^2) with $R1$ based on $F_o2 \geq 2\sigma(F_o2)$ and $wR2$ based on all data. Anisotropic displacement parameters were employed for all the non-hydrogen atoms shown. Non-hydrogen atoms are represented by Gaussian ellipsoids at the 30% probability level.

Crystallographic experimental details for **L2**

A. Crystal Data

formula	C ₃₈ H ₄₀ N ₂ P ₂
formula weight	586.66
crystal dimensions (mm)	0.24 × 0.14 × 0.04
crystal system	triclinic
space group	$P\bar{1}$ (No. 2)
unit cell parameters ^a	
<i>a</i> (Å)	10.8029 (2)
<i>b</i> (Å)	11.0466 (2)
<i>c</i> (Å)	15.1847 (3)
α (deg)	96.8689 (9)
β (deg)	103.7648 (11)
γ (deg)	110.2858 (9)
<i>V</i> (Å ³)	1609.73 (5)
<i>Z</i>	2
ρ_{calcd} (g cm ⁻³)	1.210
μ (mm ⁻¹)	1.435

B. Data Collection and Refinement Conditions

diffractometer	Bruker D8/APEX II CCD ^b
----------------	------------------------------------

radiation (λ [Å])	Cu K α (1.54178) (microfocus source)
temperature (°C)	–100
scan type	ω and ϕ scans (1.0°) (5 s exposures)
data collection 2θ limit (deg)	148.34
total data collected	11630 ($-13 \leq h \leq 13$, $-13 \leq k \leq 13$, $-18 \leq l \leq 18$)
independent reflections	6302 ($R_{\text{int}} = 0.0277$)
number of observed reflections (NO)	5524 [$F_o^2 \geq 2\sigma(F_o^2)$]
structure solution method	intrinsic phasing (<i>SHELXT-2014^c</i>)
refinement method	full-matrix least-squares on F^2 (<i>SHELXL-2014^d</i>)
absorption correction method	Gaussian integration (face-indexed)
range of transmission factors	0.9964–0.7585
data/restraints/parameters	6302 / 0 / 385
goodness-of-fit (S) ^e [all data]	1.035
final R indices ^f	
R_1 [$F_o^2 \geq 2\sigma(F_o^2)$]	0.0364
wR_2 [all data]	0.1036
largest difference peak and hole	0.399 and –0.310 e Å ⁻³

Crystallographic experimental details for **L1NiCl₂•dichloromethane**

A. Crystal Data

formula	C ₃₉ H ₅₄ Cl ₄ N ₂ NiP ₂
formula weight	813.29
crystal dimensions (mm)	0.41 × 0.18 × 0.06
crystal system	triclinic
space group	$P\bar{1}$ (No. 2)
unit cell parameters ^a	
a (Å)	10.30453 (18)
b (Å)	10.82298 (19)
c (Å)	19.0988 (3)
α (deg)	90.5905 (6)
β (deg)	93.6539 (6)
γ (deg)	110.7544 (8)
V (Å ³)	1986.50 (6)
Z	2
ρ_{calcd} (g cm ⁻³)	1.360
μ (mm ⁻¹)	4.165

B. Data Collection and Refinement Conditions

diffractometer	Bruker D8/APEX II CCD ^b
----------------	------------------------------------

radiation (λ [Å])	Cu K α (1.54178) (microfocus source)
temperature (°C)	-100
scan type	ω and ϕ scans (1.0°) (5 s exposures)
data collection 2θ limit (deg)	147.84
total data collected	14264 ($-12 \leq h \leq 12$, $-13 \leq k \leq 13$, $-23 \leq l \leq 23$)
independent reflections	7740 ($R_{\text{int}} = 0.0212$)
number of observed reflections (NO)	7496 [$F_o^2 \geq 2\sigma(F_o^2)$]
structure solution method	Patterson/structure expansion (<i>DIRDIF-2008</i> ^c)
refinement method	full-matrix least-squares on F^2 (<i>SHELXL-2014</i> ^d)
absorption correction method	Gaussian integration (face-indexed)
range of transmission factors	0.8598–0.3644
data/restraints/parameters	7740 / 0 / 460
goodness-of-fit (S) ^e [all data]	1.015
final R indices ^f	
R_1 [$F_o^2 \geq 2\sigma(F_o^2)$]	0.0399
wR_2 [all data]	0.1089
largest difference peak and hole	0.925 and -0.621 e Å ⁻³

Crystallographic experimental details for L2NiCl₂

A. Crystal Data

formula	C _{42.50} H ₄₈ Cl ₆ N ₂ NiP ₂
formula weight	920.18
crystal dimensions (mm)	0.16 × 0.14 × 0.05
crystal system	monoclinic
space group	$P2_1/n$ (an alternate setting of $P2_1/c$ [No. 14])
unit cell parameters ^a	
a (Å)	12.8219(3)
b (Å)	17.6158(5)
c (Å)	19.8760(5)
β (deg)	107.4462(17)
V (Å ³)	4282.84(19)
Z	4
ρ_{calcd} (g cm ⁻³)	1.427
μ (mm ⁻¹)	5.058

B. Data Collection and Refinement Conditions

diffractometer	Bruker D8/APEX II CCD ^b
radiation (λ [Å])	Cu K α (1.54178) (microfocus source)
temperature (°C)	-100
scan type	ω and ϕ scans (1.0°) (5-10-15 s exposures) ^c
data collection 2θ limit (deg)	144.52

total data collected	25857 ($-15 \leq h \leq 15$, $-21 \leq k \leq 21$, $-24 \leq l \leq 24$)
independent reflections	8372 ($R_{\text{int}} = 0.0813$)
number of observed reflections (NO)	5881 [$F_o^2 \geq 2\sigma(F_o^2)$]
structure solution method	intrinsic phasing (<i>SHELXT-2014^d</i>)
refinement method	full-matrix least-squares on F^2 (<i>SHELXL-2016^{e,f}</i>)
absorption correction method	Gaussian integration (face-indexed)
range of transmission factors	0.8594–0.4951
data/restraints/parameters	8372 / 0 / 466
goodness-of-fit (S) ^g [all data]	1.059
final R indices ^h	
R_1 [$F_o^2 \geq 2\sigma(F_o^2)$]	0.0582
wR_2 [all data]	0.1672
largest difference peak and hole	0.915 and $-0.714 \text{ e } \text{\AA}^{-3}$

Crystallographic experimental details for **L4NiCl₂•dichloromethane**

A. Crystal Data

formula	C ₃₉ H ₅₂ Cl ₄ N ₂ NiP ₂
formula weight	811.27
crystal dimensions (mm)	0.25 × 0.05 × 0.04
crystal system	orthorhombic
space group	<i>Pbca</i> (No. 61)
unit cell parameters ^a	
a (Å)	21.9326 (7)
b (Å)	16.0004 (5)
c (Å)	23.0088 (8)
V (Å ³)	8074.5 (5)
Z	8
ρ_{calcd} (g cm ⁻³)	1.335
μ (mm ⁻¹)	4.098

B. Data Collection and Refinement Conditions

diffractometer	Bruker D8/APEX II CCD ^b
radiation (λ [Å])	Cu K α (1.54178) (microfocus source)
temperature (°C)	–100
scan type	ω and ϕ scans (1.0°) (30 s exposures)
data collection 2θ limit (deg)	141.03
total data collected	51657 ($-26 \leq h \leq 26$, $-19 \leq k \leq 19$, $-24 \leq l \leq 27$)
independent reflections	7617 ($R_{\text{int}} = 0.1842$)

number of observed reflections (<i>NO</i>)	4969 [$F_o^2 \geq 2\sigma(F_o^2)$]
structure solution method	intrinsic phasing (<i>SHELXT-2014^c</i>)
refinement method	full-matrix least-squares on F^2 (<i>SHELXL-2014^d</i>)
absorption correction method	Gaussian integration (face-indexed)
range of transmission factors	0.8213–0.4269
data/restraints/parameters	7617 / 0 / 439
goodness-of-fit (<i>S</i>) ^e [all data]	1.038
final <i>R</i> indices ^f	
R_1 [$F_o^2 \geq 2\sigma(F_o^2)$]	0.0708
wR_2 [all data]	0.1932
largest difference peak and hole	1.115 and $-0.535 \text{ e } \text{\AA}^{-3}$

Crystallographic experimental details for **L6NiCl₂•dichloromethane**

A. Crystal Data

formula	C _{41.75} H _{45.5} Cl _{5.5} N ₂ NiP ₂
formula weight	890.92
crystal dimensions (mm)	0.34 × 0.27 × 0.27
crystal system	monoclinic
space group	<i>P</i> 2 ₁ / <i>c</i> (No. 14)
unit cell parameters ^a	
<i>a</i> (Å)	16.9518 (3)
<i>b</i> (Å)	10.14114 (19)
<i>c</i> (Å)	26.5298 (5)
β (deg)	105.3206 (12)
<i>V</i> (Å ³)	4398.67 (14)
<i>Z</i>	4
ρ_{calcd} (g cm ⁻³)	1.345
μ (mm ⁻¹)	4.635

B. Data Collection and Refinement Conditions

diffractometer	Bruker D8/APEX II CCD ^b
radiation (λ [Å])	Cu K α (1.54178) (microfocus source)
temperature (°C)	–100
scan type	ω and ϕ scans (1.0°) (5 s exposures)
data collection 2θ limit (deg)	148.10
total data collected	30641 ($-21 \leq h \leq 21$, $-12 \leq k \leq 12$, $-32 \leq l \leq 33$)
independent reflections	8871 ($R_{\text{int}} = 0.0255$)
number of observed reflections (<i>NO</i>)	8348 [$F_o^2 \geq 2\sigma(F_o^2)$]
structure solution method	Patterson/structure expansion (<i>DIRDIF-2008^c</i>)
refinement method	full-matrix least-squares on F^2 (<i>SHELXL-2014^d</i>)

absorption correction method	Gaussian integration (face-indexed)
range of transmission factors	0.4898–0.3233
data/restraints/parameters	8871 / 0 / 488
goodness-of-fit (S) ^e [all data]	1.084
final R indices ^f	
R_1 [$F_o^2 \geq 2\sigma(F_o^2)$]	0.0654
wR_2 [all data]	0.2007
largest difference peak and hole	1.617 and -1.203 e \AA^{-3}

Crystallographic experimental details for **C1•THF**

A. Crystal Data

formula	$\text{C}_{49}\text{H}_{55}\text{ClN}_2\text{NiOP}_2$
formula weight	844.05
crystal dimensions (mm)	$0.21 \times 0.13 \times 0.06$
crystal system	triclinic
space group	$P\bar{1}$ (No. 2)
unit cell parameters ^a	
a (\AA)	10.7807 (9)
b (\AA)	11.7173 (10)
c (\AA)	18.7445 (16)
α (deg)	86.5087 (13)
β (deg)	88.8545 (13)
γ (deg)	66.8194 (12)
V (\AA^3)	2172.6 (3)
Z	2

ρ_{calcd} (g cm^{-3}) 1.290

μ (mm^{-1}) 0.620

B. Data Collection and Refinement Conditions

diffractometer	Bruker PLATFORM/APEX II CCD ^b
radiation (λ [\AA])	graphite-monochromated Mo $K\alpha$ (0.71073)
temperature ($^\circ\text{C}$)	-80
scan type	ω scans (0.3°) (20 s exposures)
data collection 2θ limit (deg)	55.29
total data collected	19297 ($-14 \leq h \leq 14$, $-15 \leq k \leq 15$, $-24 \leq l \leq 24$)
independent reflections	10070 ($R_{\text{int}} = 0.0449$)
number of observed reflections (NO)	6690 [$F_o^2 \geq 2\sigma(F_o^2)$]
structure solution method	Patterson/structure expansion (<i>DIRDIF-2008</i> ^c)
refinement method	full-matrix least-squares on F^2 (<i>SHELXL-2014</i> ^e)
absorption correction method	Gaussian integration (face-indexed)
range of transmission factors	1.0000–0.8649

data/restraints/parameters	10070 / 0 / 512
goodness-of-fit (S) ^e [all data]	1.031
final R indices ^f	
R_1 [$F_o^2 \geq 2\sigma(F_o^2)$]	0.0468
wR_2 [all data]	0.1230
largest difference peak and hole	0.623 and -0.337 e \AA^{-3}

Crystallographic experimental details for C2•toluene

A. Crystal Data

formula	C ₄₅ H ₄₇ BrN ₂ NiP ₂
formula weight	816.40
crystal dimensions (mm)	0.64 × 0.16 × 0.08
crystal system	monoclinic
space group	$P2_1/n$ (an alternate setting of $P2_1/c$ [No. 14])
unit cell parameters ^a	
a (\AA)	10.1048 (5)
b (\AA)	16.6355 (9)
c (\AA)	23.9617 (13)
β (deg)	100.9528 (7)
V (\AA^3)	3954.6 (4)
Z	4
ρ_{calcd} (g cm ⁻³)	1.371
μ (mm ⁻¹)	1.616

B. Data Collection and Refinement Conditions

diffractometer	Bruker PLATFORM/APEX II CCD ^b
radiation (λ [\AA])	graphite-monochromated Mo K α (0.71073)
temperature ($^{\circ}\text{C}$)	-80
scan type	ω scans (0.3°) (15 s exposures)
data collection 2θ limit (deg)	56.60
total data collected	37269 ($-13 \leq h \leq 13$, $-22 \leq k \leq 22$, $-31 \leq l \leq 31$)
independent reflections	9764 ($R_{\text{int}} = 0.0295$)
number of observed reflections (NO)	7950 [$F_o^2 \geq 2\sigma(F_o^2)$]
structure solution method	Patterson/structure expansion (<i>DIRDIF-2008</i> ^c)
refinement method	full-matrix least-squares on F^2 (<i>SHELXL-2014</i> ^d)
absorption correction method	Gaussian integration (face-indexed)
range of transmission factors	0.9039–0.5197
data/restraints/parameters	9764 / 0 / 466
goodness-of-fit (S) ^e [all data]	1.039
final R indices ^f	
R_1 [$F_o^2 \geq 2\sigma(F_o^2)$]	0.0312

wR_2 [all data]	0.0858
largest difference peak and hole	0.586 and $-0.215 \text{ e } \text{\AA}^{-3}$

Crystallographic experimental details for **C3•1,1,2,2-tetrachloroethane•0.5 hexanes**

A. Crystal Data

formula	$\text{C}_{42.50}\text{H}_{48}\text{Cl}_6\text{N}_2\text{NiP}_2$
formula weight	920.18
crystal dimensions (mm)	$0.16 \times 0.14 \times 0.05$
crystal system	monoclinic
space group	$P2_1/n$ (an alternate setting of $P2_1/c$ [No. 14])
unit cell parameters ^a	
a (Å)	12.8219(3)
b (Å)	17.6158(5)
c (Å)	19.8760(5)
β (deg)	107.4462(17)
V (Å ³)	4282.84(19)
Z	4

ρ_{calcd} (g cm⁻³) 1.427

μ (mm⁻¹) 5.058

B. Data Collection and Refinement Conditions

diffractometer	Bruker D8/APEX II CCD ^b
radiation (λ [Å])	Cu K α (1.54178) (microfocus source)
temperature (°C)	-100
scan type	ω and ϕ scans (1.0°) (5-10-15 s exposures) ^c
data collection 2θ limit (deg)	144.52
total data collected	25857 ($-15 \leq h \leq 15$, $-21 \leq k \leq 21$, $-24 \leq l \leq 24$)
independent reflections	8372 ($R_{\text{int}} = 0.0813$)
number of observed reflections (NO)	5881 [$F_o^2 \geq 2\sigma(F_o^2)$]
structure solution method	intrinsic phasing (<i>SHELXT-2014^d</i>)
refinement method	full-matrix least-squares on F^2 (<i>SHELXL-2016^{e,f}</i>)
absorption correction method	Gaussian integration (face-indexed)
range of transmission factors	0.8594–0.4951
data/restraints/parameters	8372 / 0 / 466
goodness-of-fit (S) ^g [all data]	1.059
final R indices ^h	
R_1 [$F_o^2 \geq 2\sigma(F_o^2)$]	0.0582
wR_2 [all data]	0.1672
largest difference peak and hole	0.915 and $-0.714 \text{ e } \text{\AA}^{-3}$

Crystallographic experimental details for L9

A. Crystal Data

formula	$C_{52.25}H_{61.25}FeN_4P_2$
formula weight	863.09
crystal dimensions (mm)	$0.34 \times 0.08 \times 0.06$
crystal system	monoclinic
space group	$C2/c$ (No. 15)
unit cell parameters ^a	
a (Å)	24.4360(5)
b (Å)	20.0370(4)
c (Å)	19.4486(4)
β (deg)	95.3765(12)
V (Å ³)	9480.6(3)
Z	8
ρ_{calcd} (g cm ⁻³)	1.209
μ (mm ⁻¹)	3.476

B. Data Collection and Refinement Conditions

diffractometer	Bruker D8/APEX II CCD ^b
radiation (λ [Å])	Cu K α (1.54178) (microfocus source)
temperature (°C)	-100
scan type	ω and ϕ scans (1.0°) (5-10-15 s exposures) ^c
data collection 2θ limit (deg)	144.85
total data collected	32765 ($-30 \leq h \leq 30$, $-24 \leq k \leq 24$, $-24 \leq l \leq 23$)
independent reflections	9380 ($R_{\text{int}} = 0.0419$)
number of observed reflections (NO)	7818 [$F_o^2 \geq 2\sigma(F_o^2)$]
structure solution method	intrinsic phasing (<i>SHELXT-2014^d</i>)
refinement method	full-matrix least-squares on F^2 (<i>SHELXL-2016^{e,f}</i>)
absorption correction method	Gaussian integration (face-indexed)
range of transmission factors	0.8732–0.4595
data/restraints/parameters	9380 / 0 / 526
goodness-of-fit (S) ^g [all data]	1.037
final R indices ^h	
R_1 [$F_o^2 \geq 2\sigma(F_o^2)$]	0.0374
wR_2 [all data]	0.1098
largest difference peak and hole	0.253 and -0.320 e Å ⁻³

Crystallographic experimental details for **L10•benzene**

A. Crystal Data

formula	C ₅₆ H ₆₆ FeN ₄ P ₂
formula weight	912.91
crystal dimensions (mm)	0.19 × 0.13 × 0.04
crystal system	triclinic
space group	<i>P</i> $\bar{1}$ (No. 2)
unit cell parameters ^a	
<i>a</i> (Å)	12.4322(3)
<i>b</i> (Å)	13.9428(3)
<i>c</i> (Å)	15.0464(4)
α (deg)	71.8732(16)
β (deg)	79.7521(15)
γ (deg)	88.0432(16)
<i>V</i> (Å ³)	2438.53(10)
<i>Z</i>	2

ρ_{calcd} (g cm⁻³) 1.243

μ (mm⁻¹) 3.406

B. Data Collection and Refinement Conditions

diffractometer	Bruker D8 /APEX II CCD ^b
radiation (λ [Å])	Cu K α (1.54178) (microfocus source)
temperature (°C)	-100
scan type	ω and ϕ scans (1.0°) (5-5-10 s exposures) ^c
data collection 2θ limit (deg)	145.48
total data collected	16329 ($-15 \leq h \leq 15$, $-17 \leq k \leq 16$, $-18 \leq l \leq 18$)
independent reflections	9240 ($R_{\text{int}} = 0.0483$)
number of observed reflections (<i>NO</i>)	7312 [$F_o^2 \geq 2\sigma(F_o^2)$]
structure solution method	intrinsic phasing (<i>SHELXT-2014</i> ^d)
refinement method	full-matrix least-squares on F^2 (<i>SHELXL-2016</i> ^e)
absorption correction method	Gaussian integration (face-indexed)
range of transmission factors	0.9703--0.5646
data/restraints/parameters	9240 / 0 / 580
goodness-of-fit (<i>S</i>) ^f [all data]	1.054
final <i>R</i> indices ^g	
<i>R</i> ₁ [$F_o^2 \geq 2\sigma(F_o^2)$]	0.0434
<i>wR</i> ₂ [all data]	0.1179
largest difference peak and hole	0.535 and -0.452 e Å ⁻³

NMR Spectra

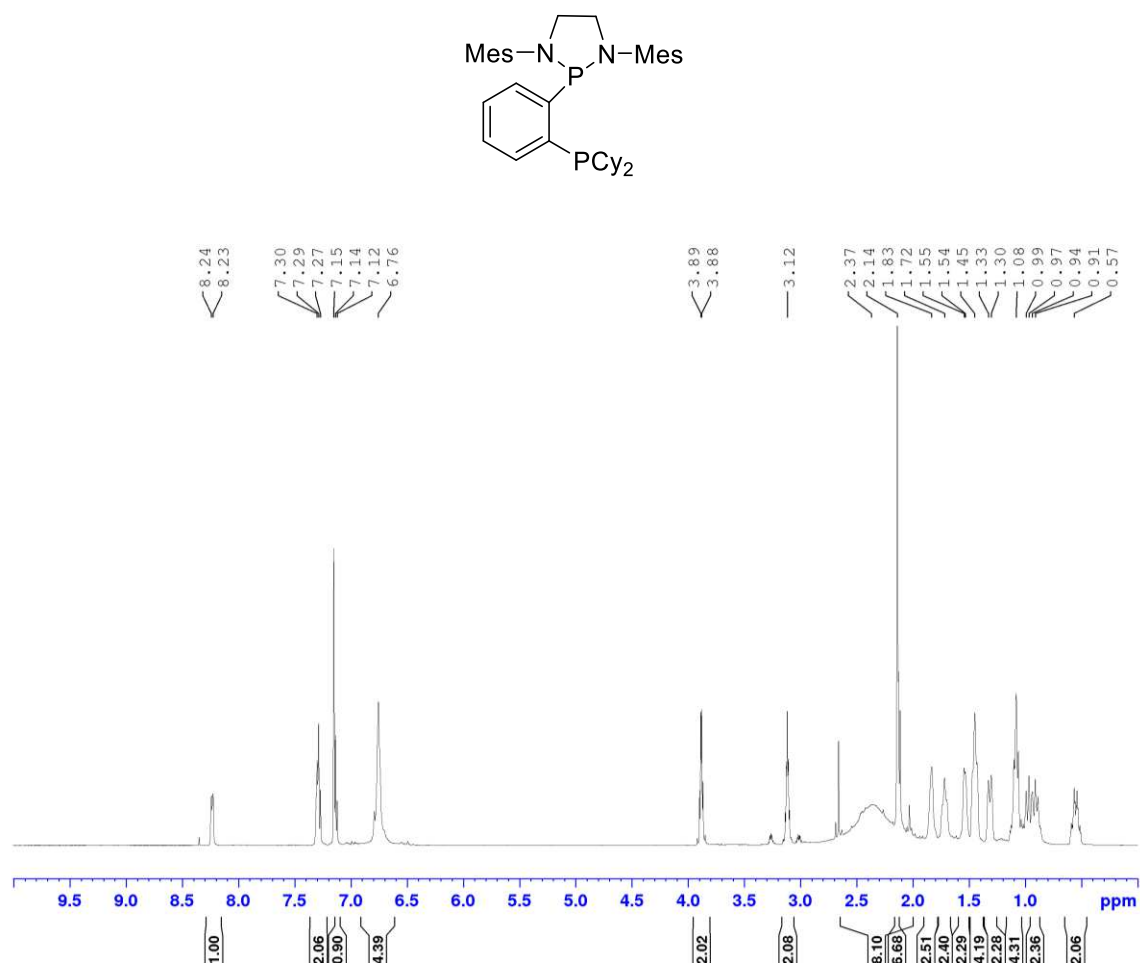


Figure A5. ¹H NMR spectrum of L1 (C₆D₆, 500.1 MHz)

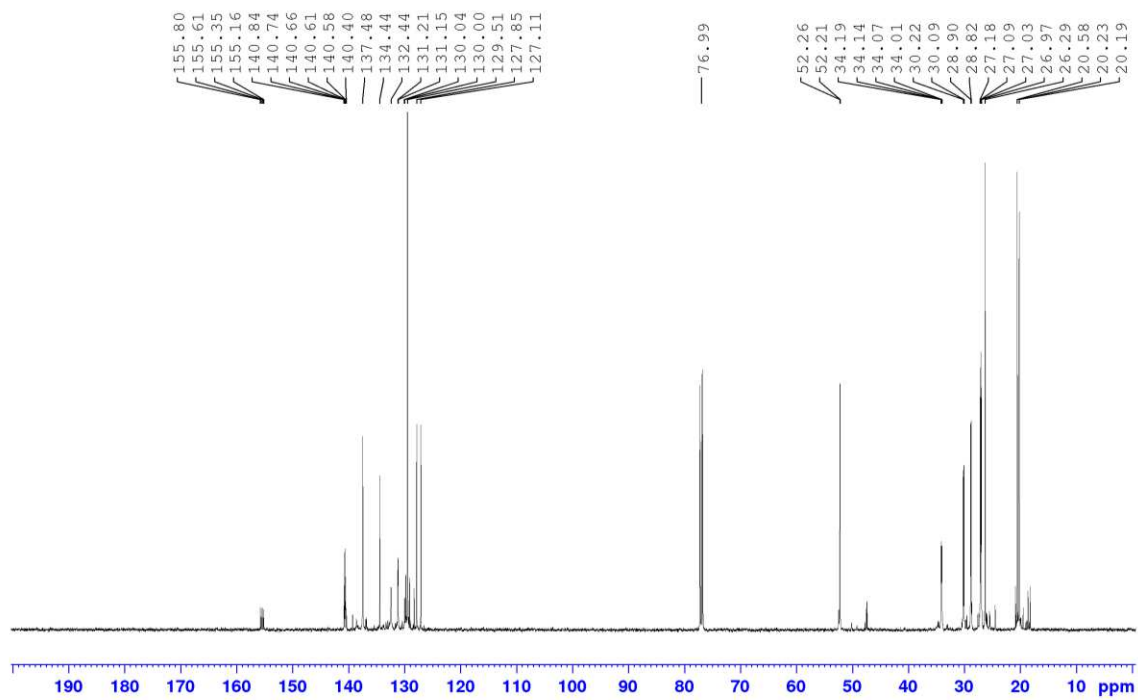


Figure A6. $^{13}\text{C}\{^1\text{H}\}$ NMR spectrum of **L1** (C_6D_6 , 125.8 MHz)

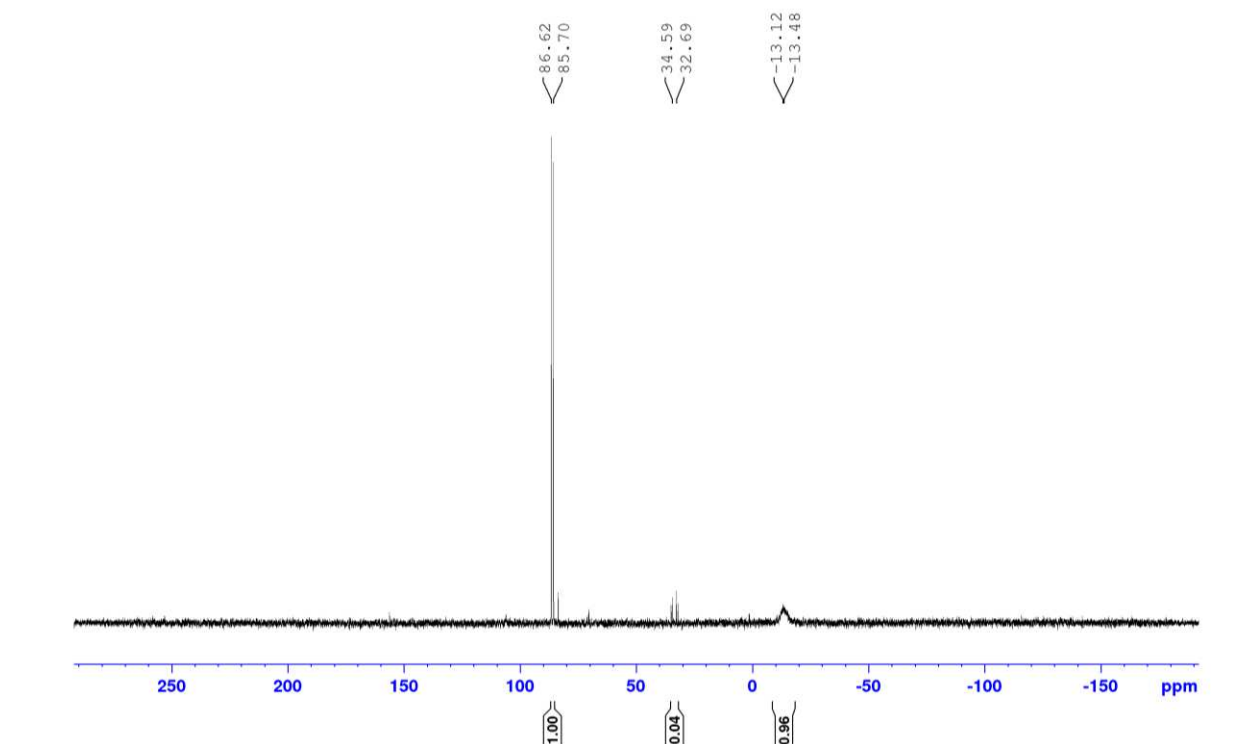
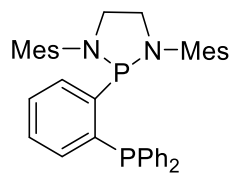


Figure A7. $^{31}\text{P}\{^1\text{H}\}$ NMR spectrum of **L1** (CDCl_3 , 202.4 MHz)



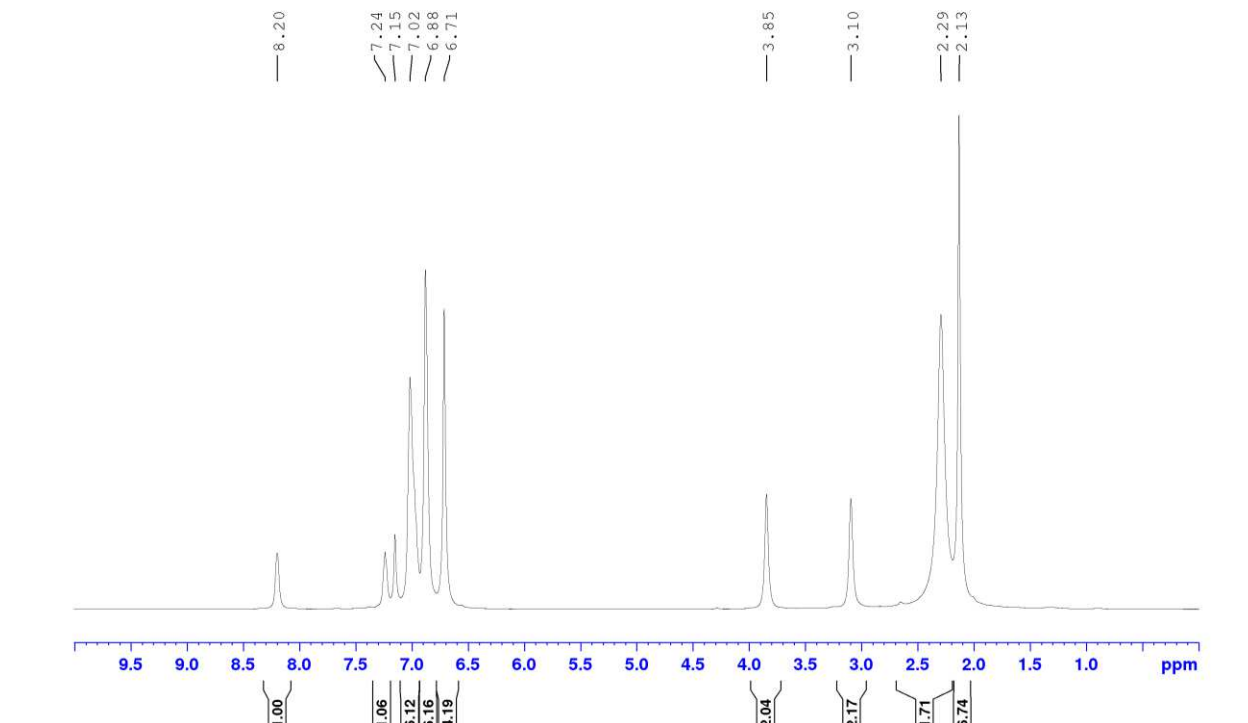


Figure A8. ^1H NMR spectrum of **L2** (C_6D_6 , 500.1 MHz)

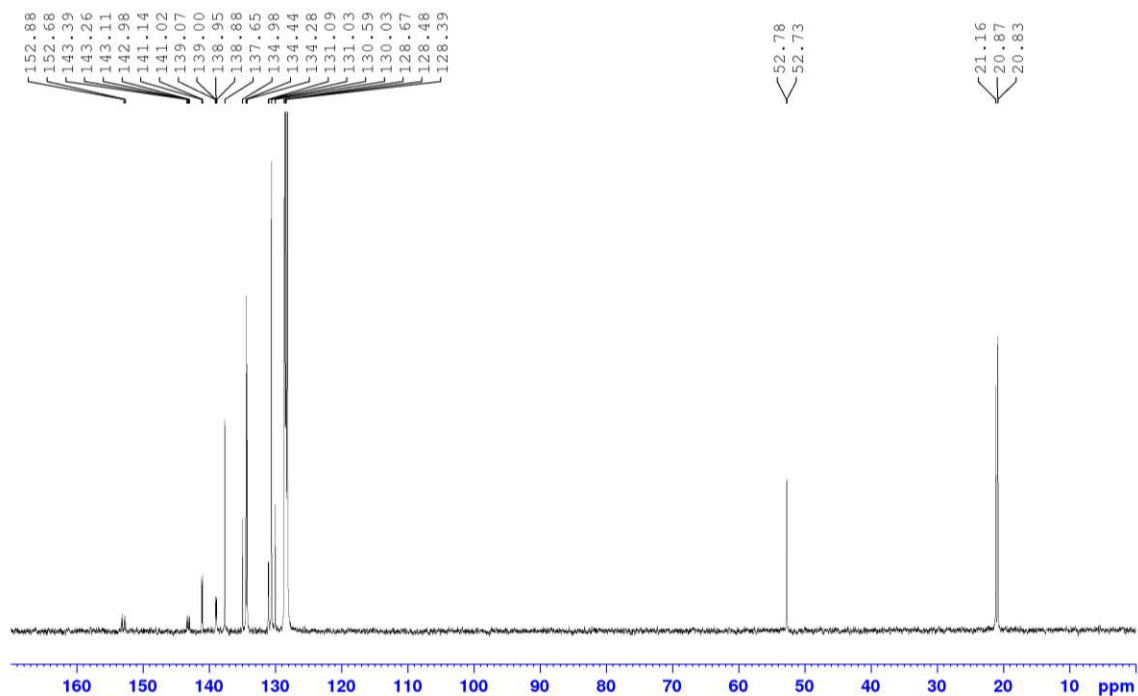


Figure A9. $^{13}\text{C}\{^1\text{H}\}$ NMR spectrum of **L2** (C_6D_6 , 125.7 MHz)

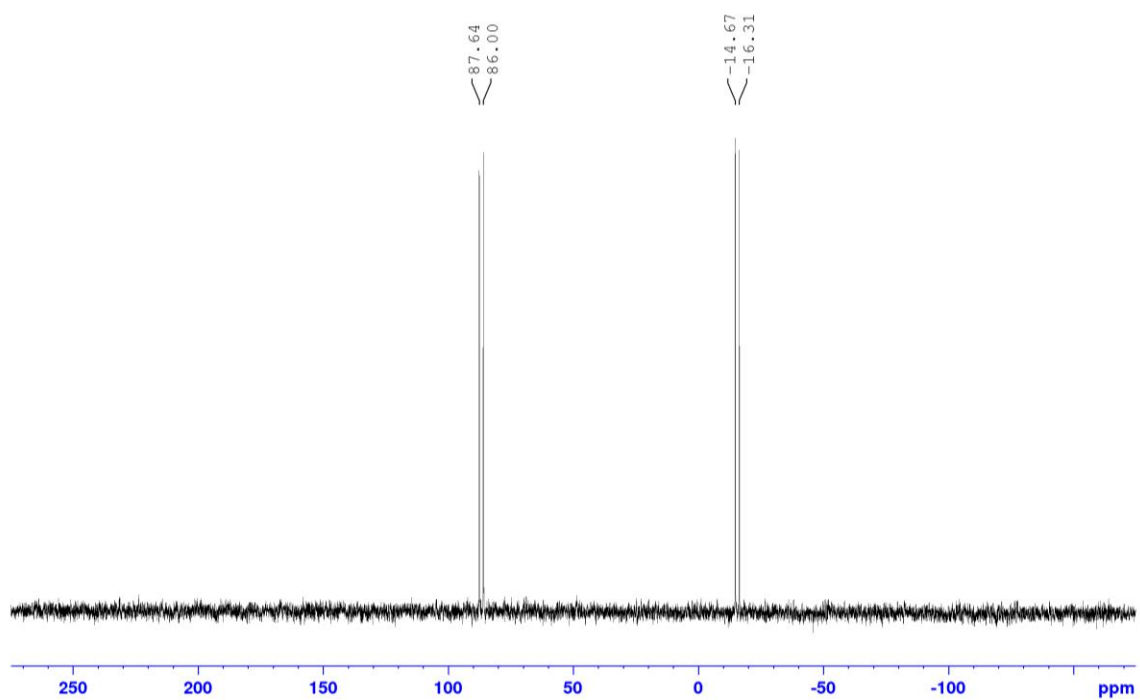
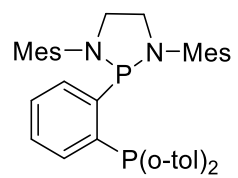


Figure A10. $^{31}\text{P}\{^1\text{H}\}$ NMR spectrum of **L2** (CDCl_3 , 121.4 MHz)



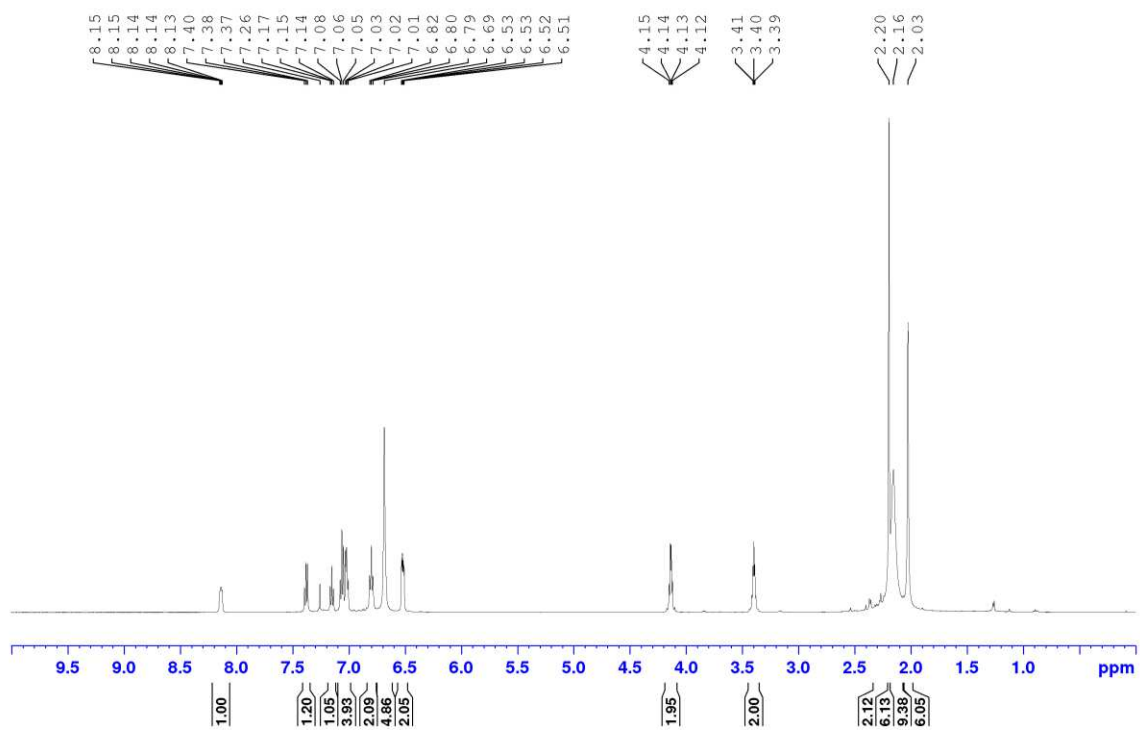


Figure A11. ^1H NMR of **L3** (C_6D_6 , 121.4 MHz)

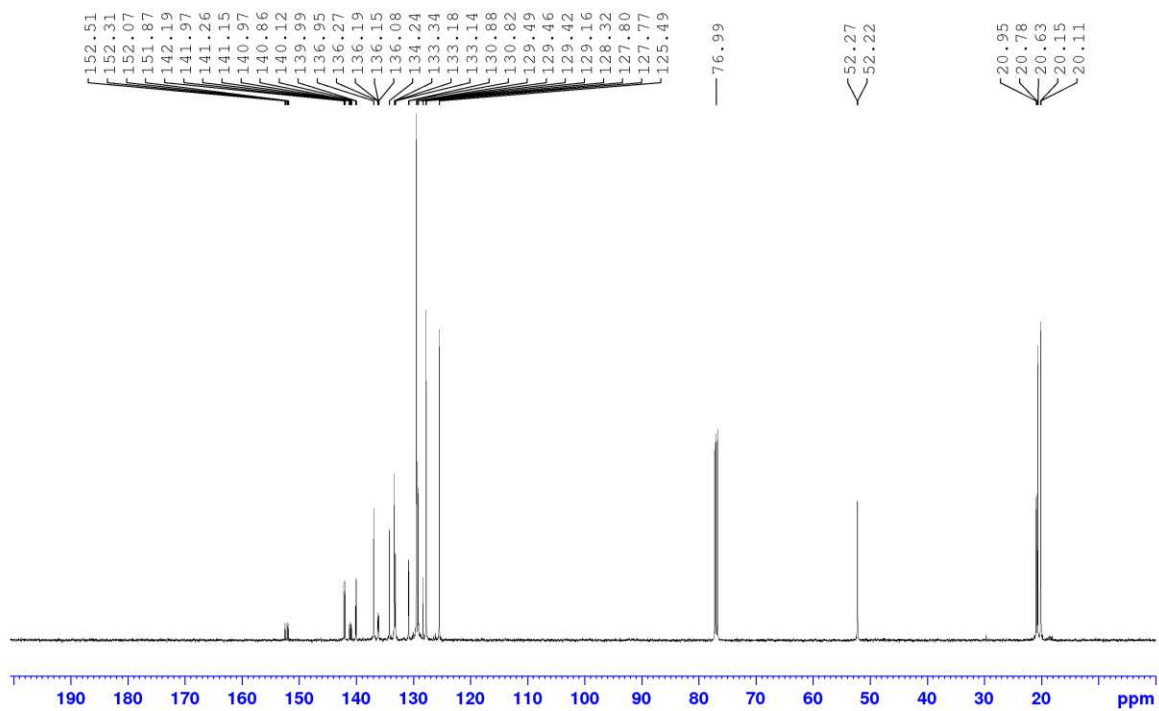


Figure A12. $^{13}\text{C}\{^1\text{H}\}$ NMR spectrum of **L3** (C_6D_6 , 125.7 MHz)

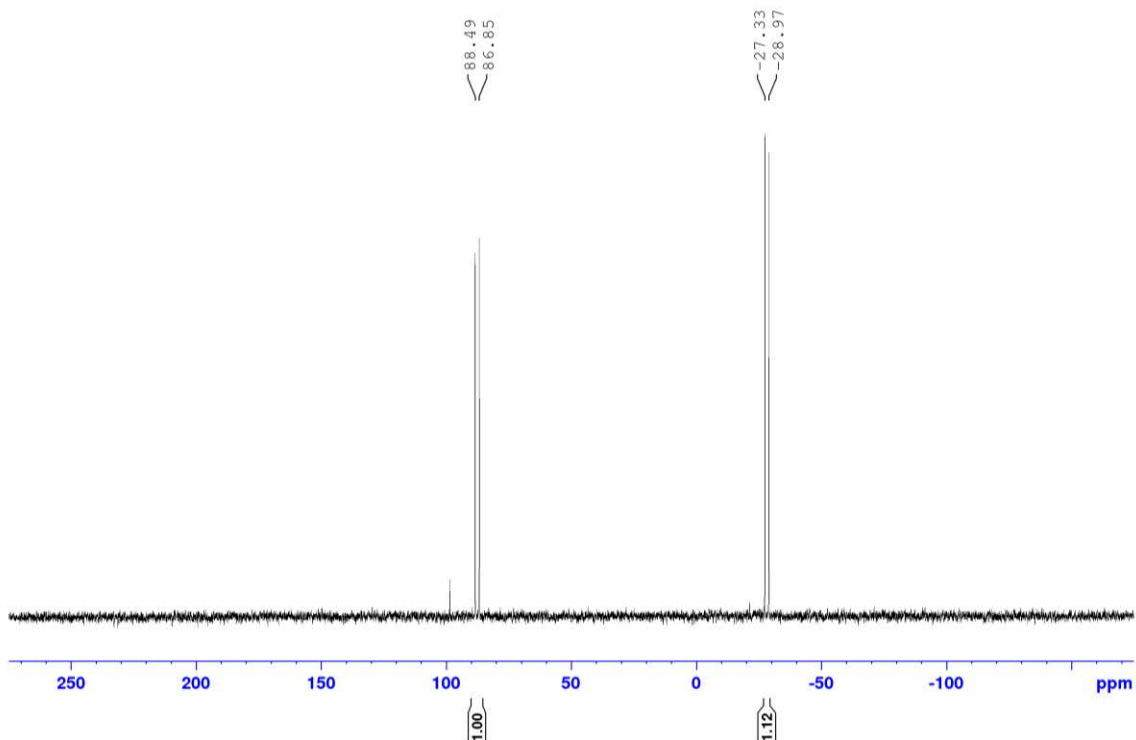


Figure A13. $^{31}\text{P}\{^1\text{H}\}$ NMR spectrum of **L3** (CDCl_3 , 121.4 MHz)

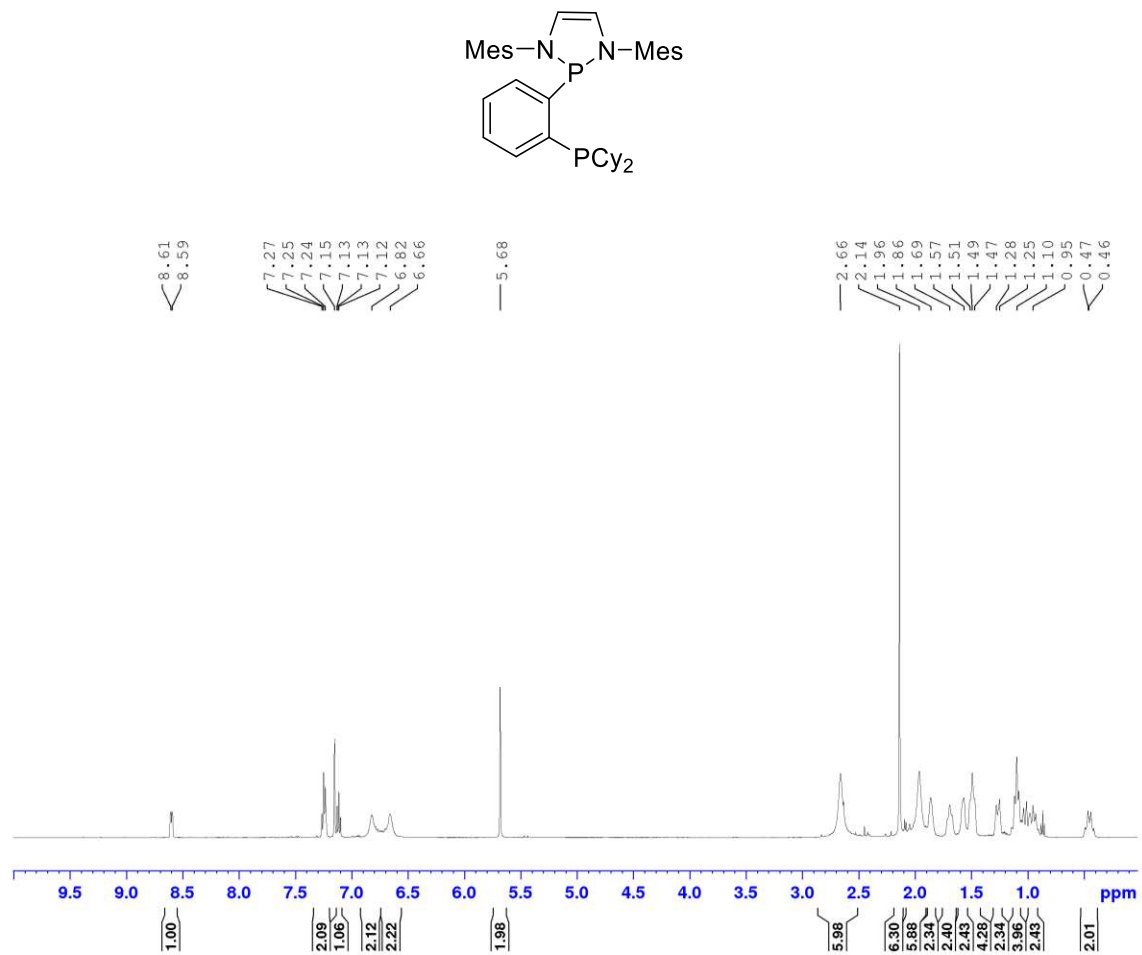


Figure A124. ¹H NMR spectrum of L4 (C₆D₆, 500.1 MHz)

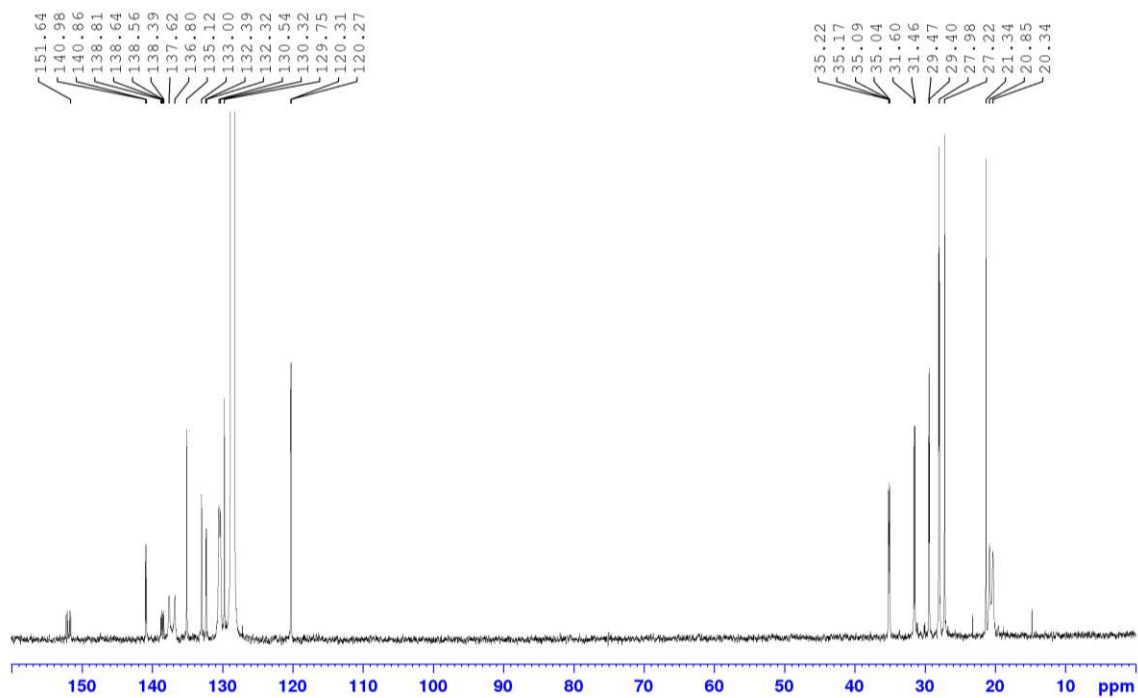


Figure A15. $^{13}\text{C}\{^1\text{H}\}$ NMR spectrum of **L4** (C_6D_6 , 125.7 MHz)

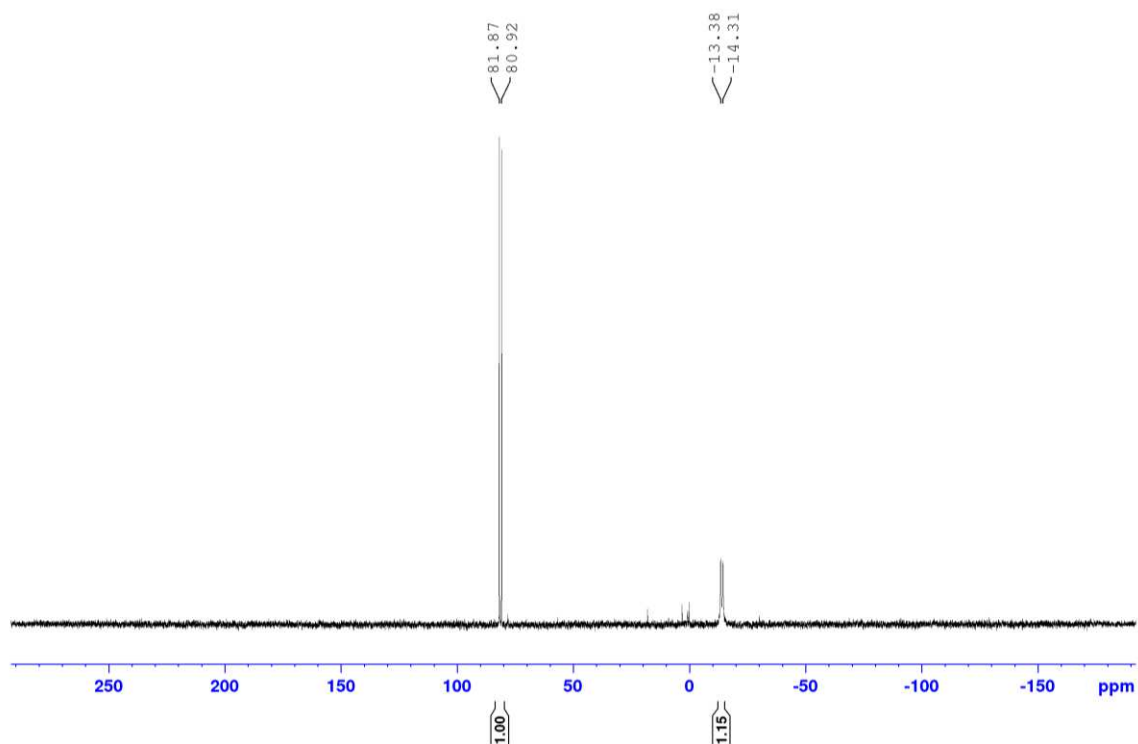


Figure A16. $^{31}\text{P}\{^1\text{H}\}$ NMR spectrum of **L4** (CDCl_3 , 202.4 MHz)

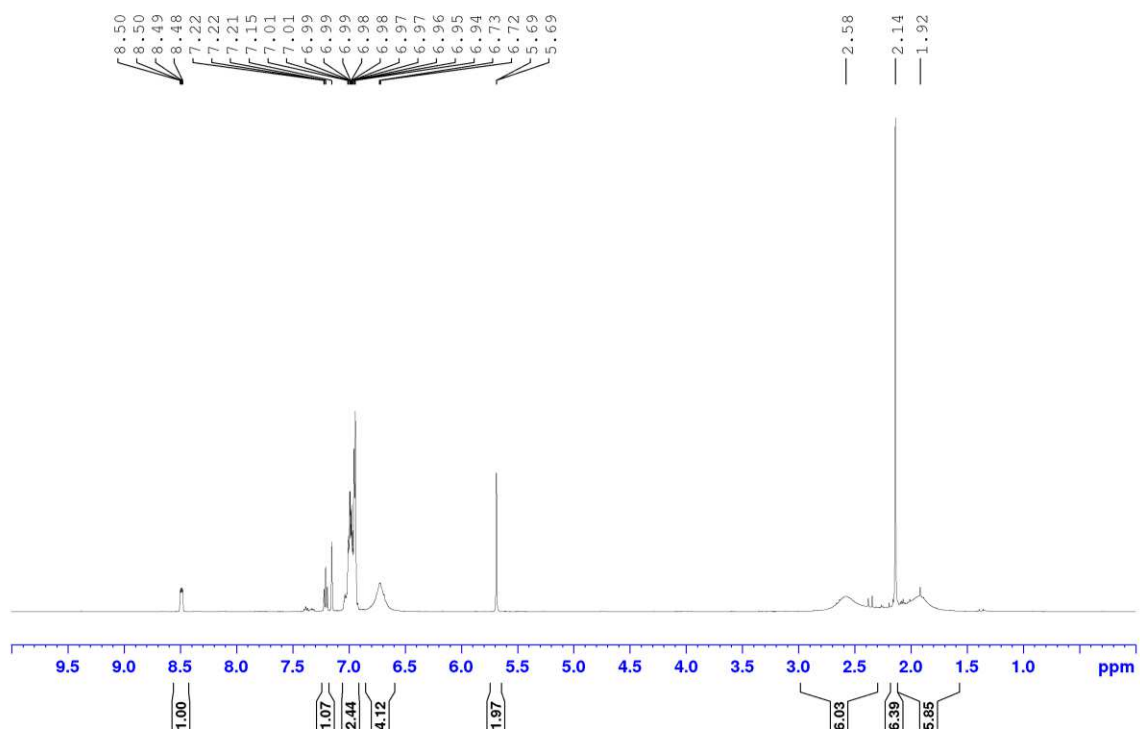
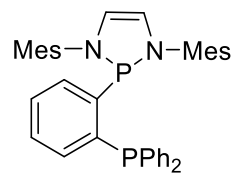


Figure A17. ¹H NMR spectrum of L5 (C₆D₆, 500.1 MHz)

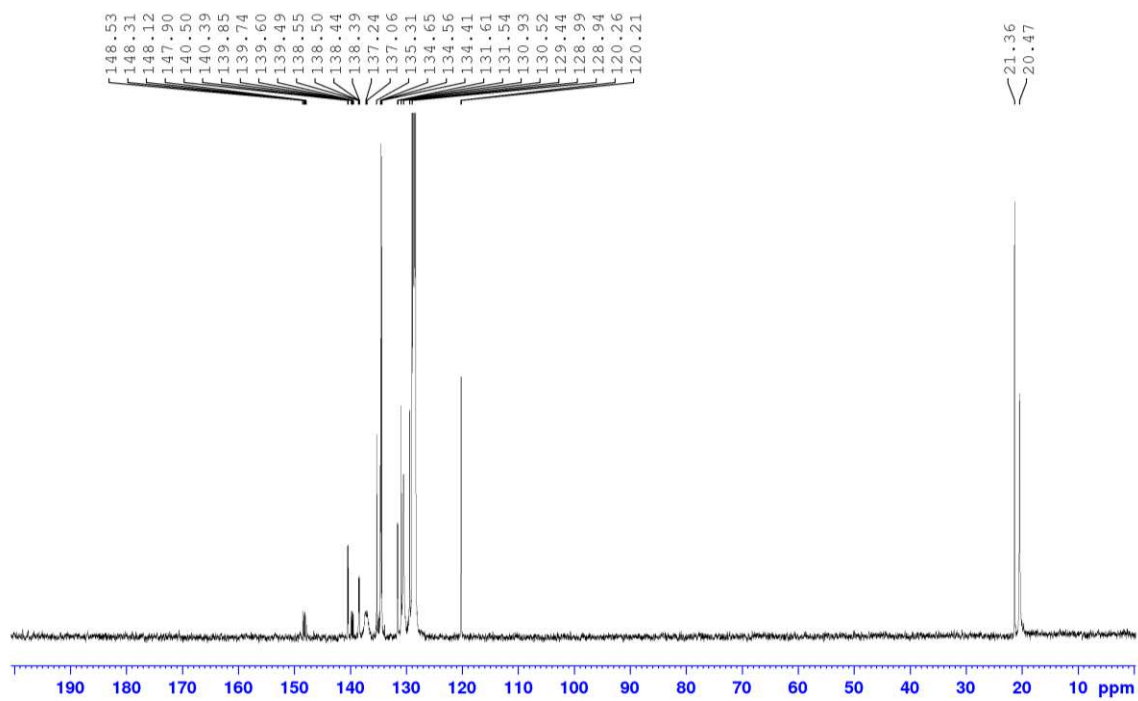


Figure A18. $^{13}\text{C}\{^1\text{H}\}$ NMR spectrum of **L5** (C_6D_6 , 125.7 MHz)

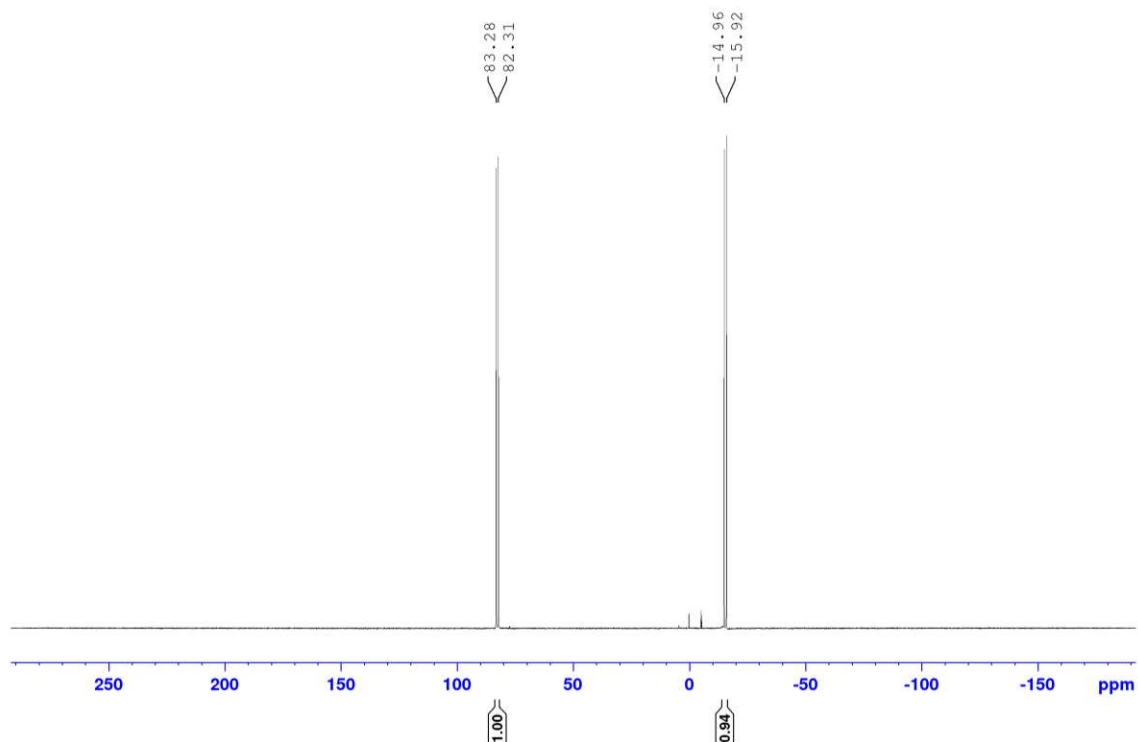


Figure A19. $^{31}\text{P}\{^1\text{H}\}$ NMR spectrum of **L5** (CDCl_3 , 202.4 MHz)

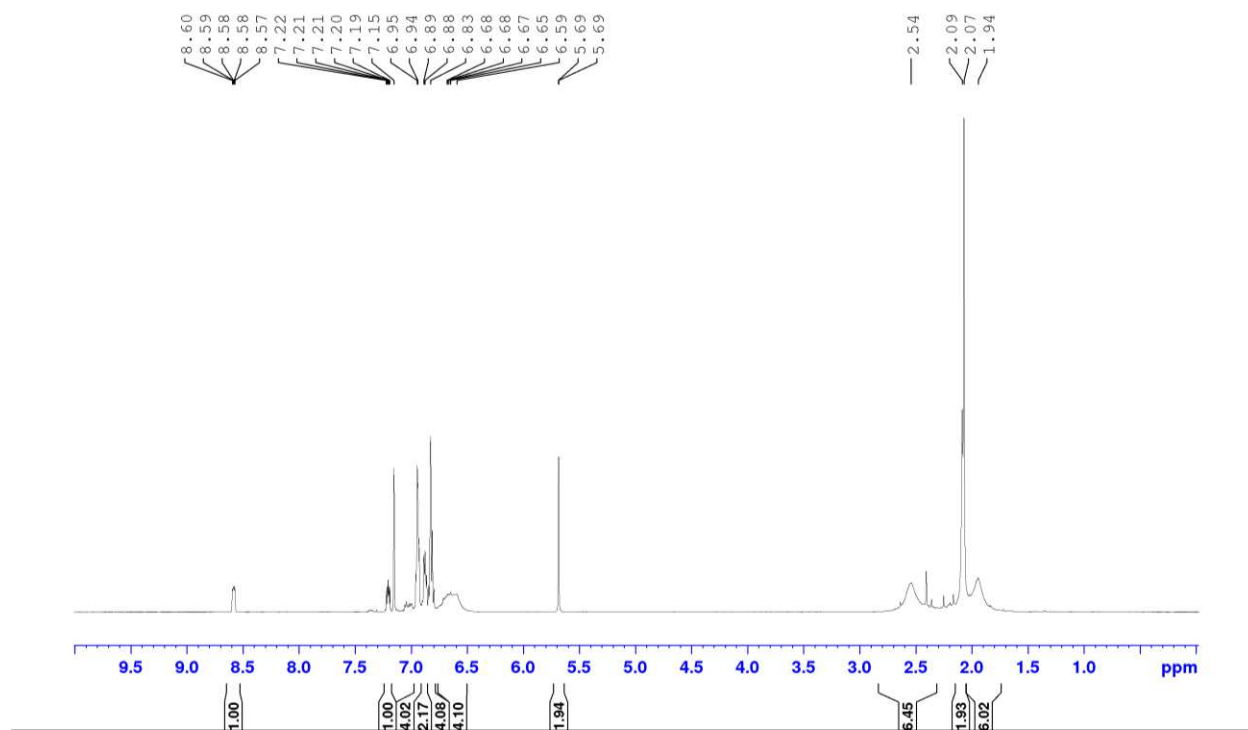
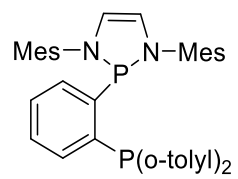


Figure A20. ¹H NMR spectrum of L6 (C₆D₆, 500.1 MHz)

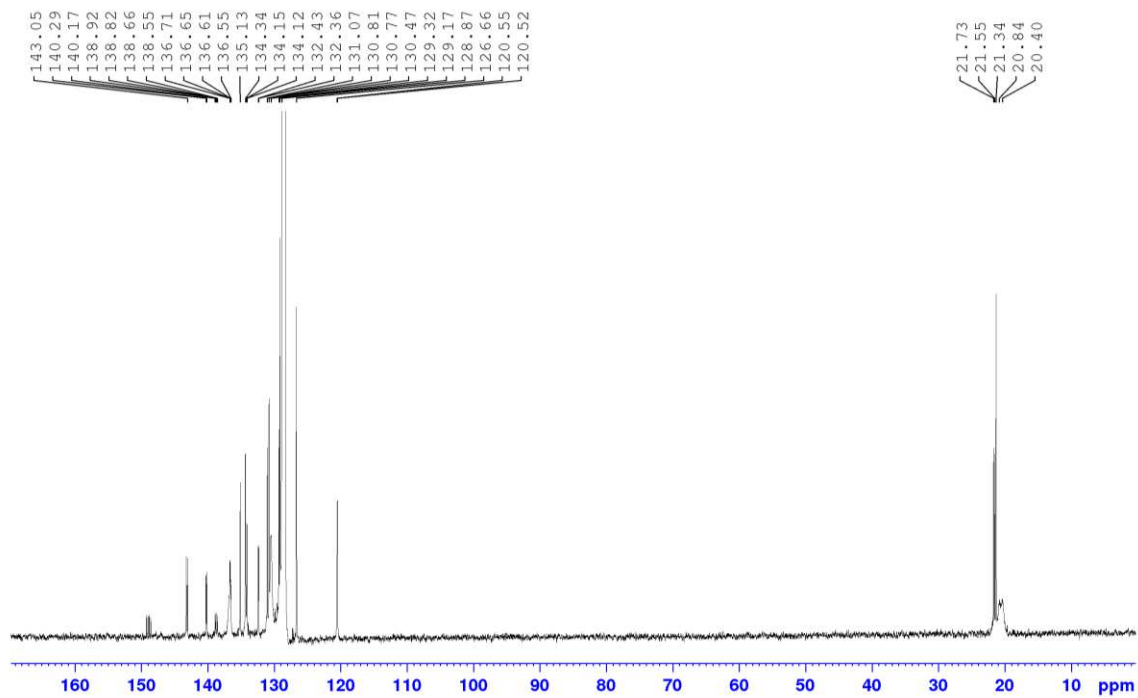


Figure A21. $^{13}\text{C}\{^1\text{H}\}$ NMR spectrum of L6 (C_6D_6 , 125.7 MHz)

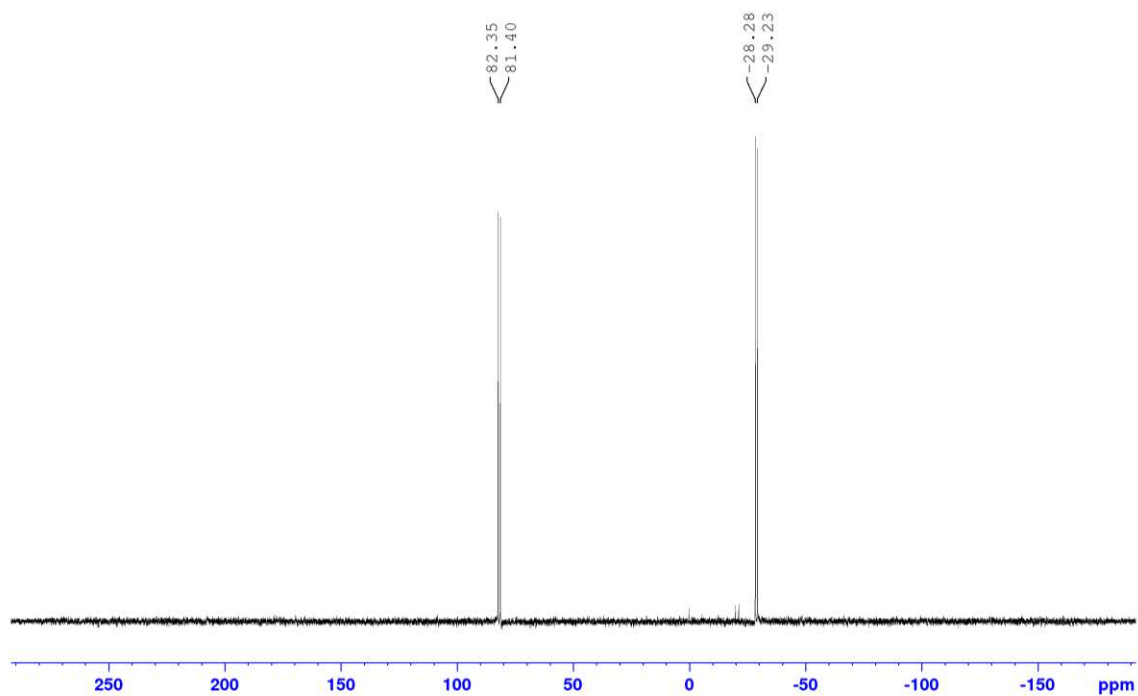


Figure A22. $^{31}\text{P}\{^1\text{H}\}$ NMR spectrum of L6 (CDCl_3 , 202.4 MHz)

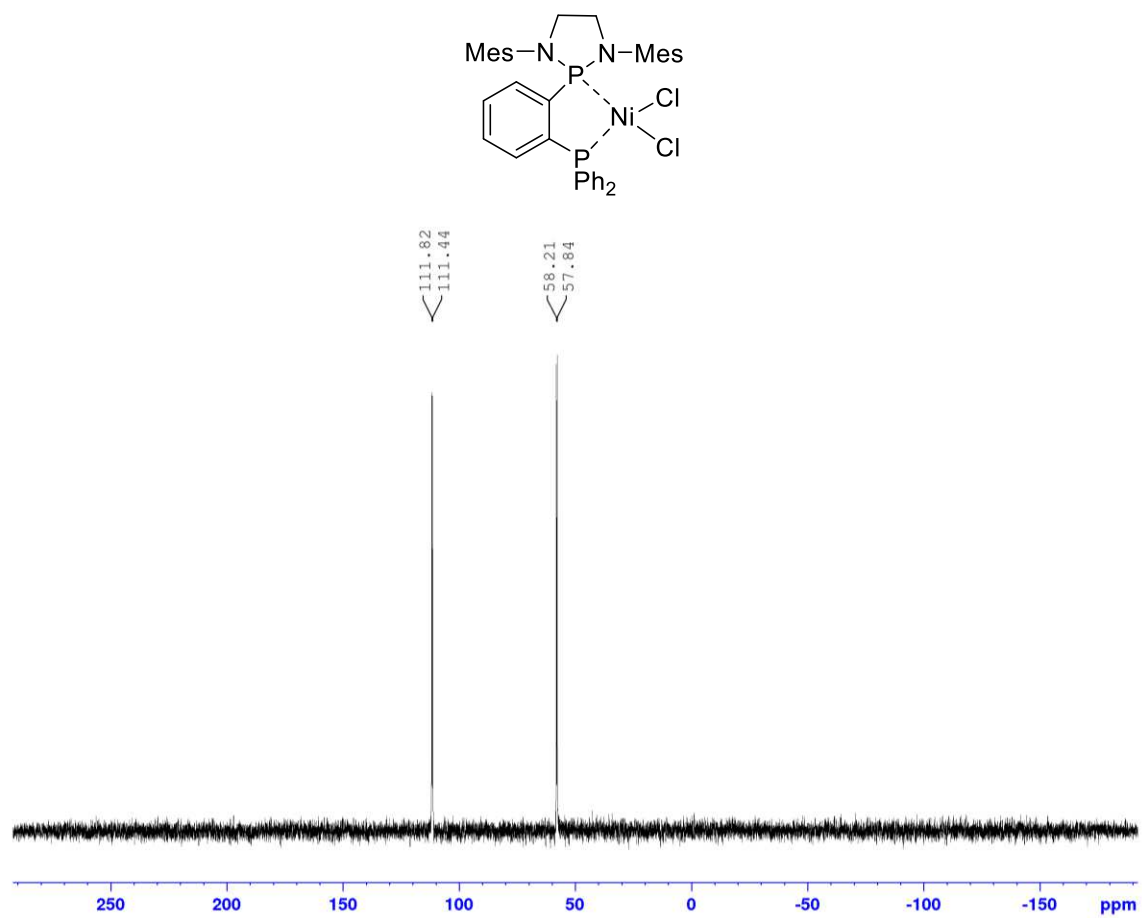
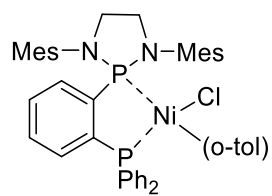


Figure A23. $^{31}P\{^1H\}$ NMR spectrum of $(L2)NiCl_2$ (1,1,2,2-Tetrachloroethane- d_2 , 202.4 MHz)



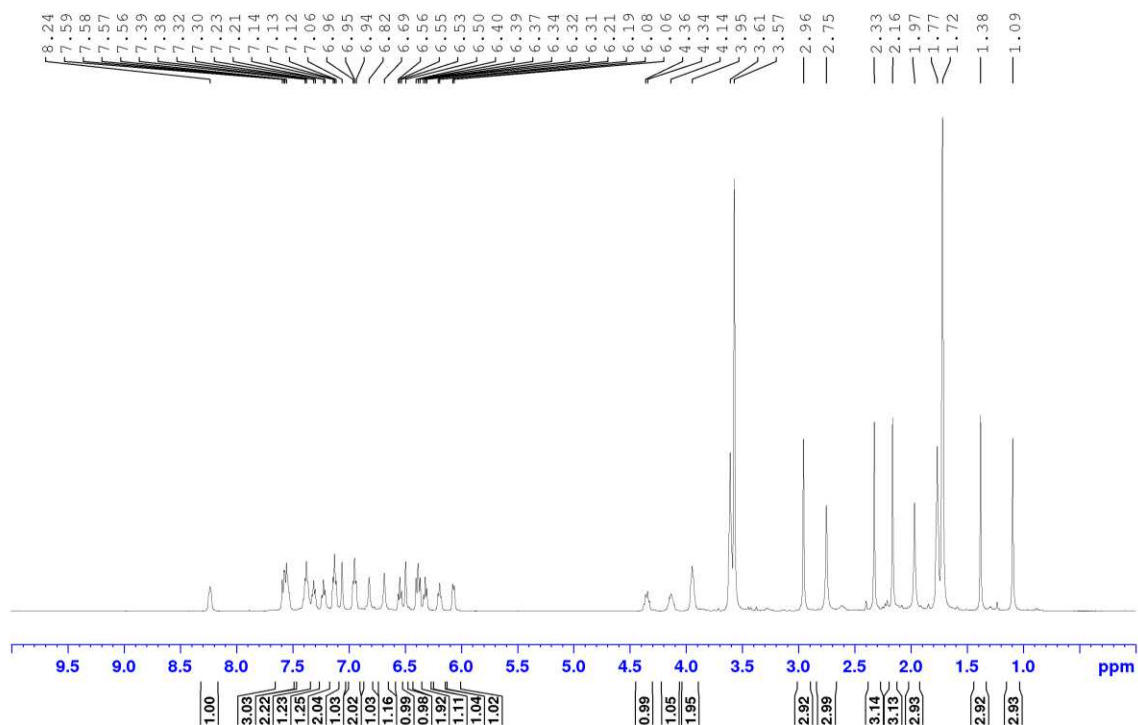


Figure A24. ^1H NMR spectrum of C1 (THF- d_8 , 500.1 MHz)

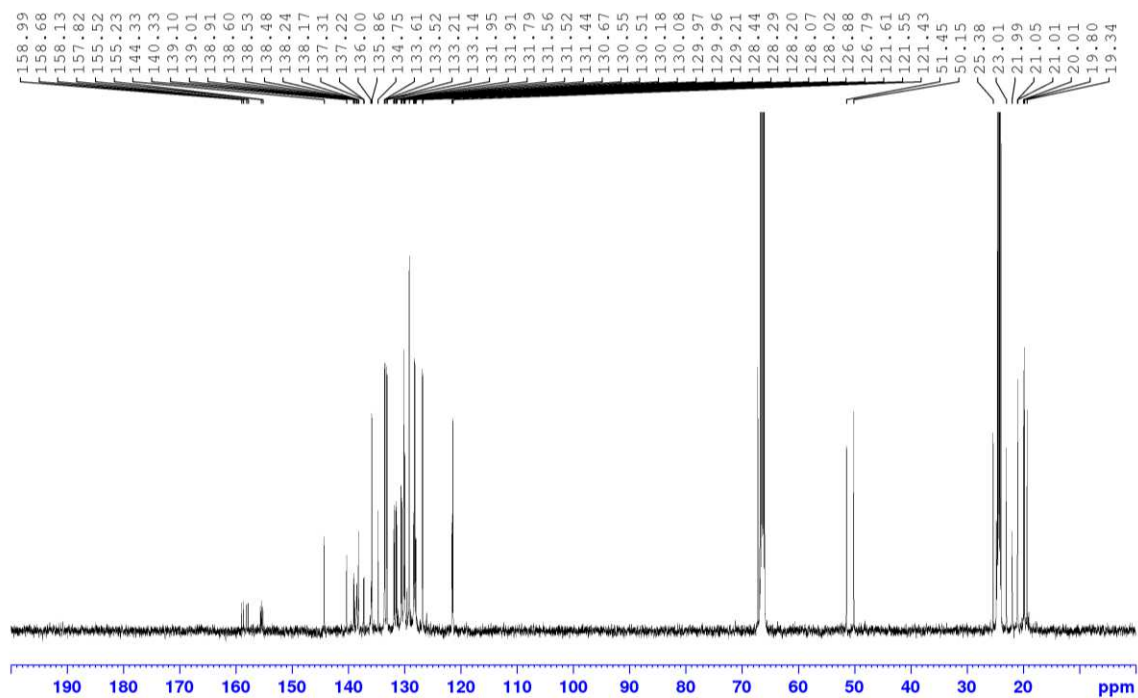


Figure A25. $^{13}\text{C}\{^1\text{H}\}$ NMR spectrum of C1 (THF- d_8 , 125.7 MHz)

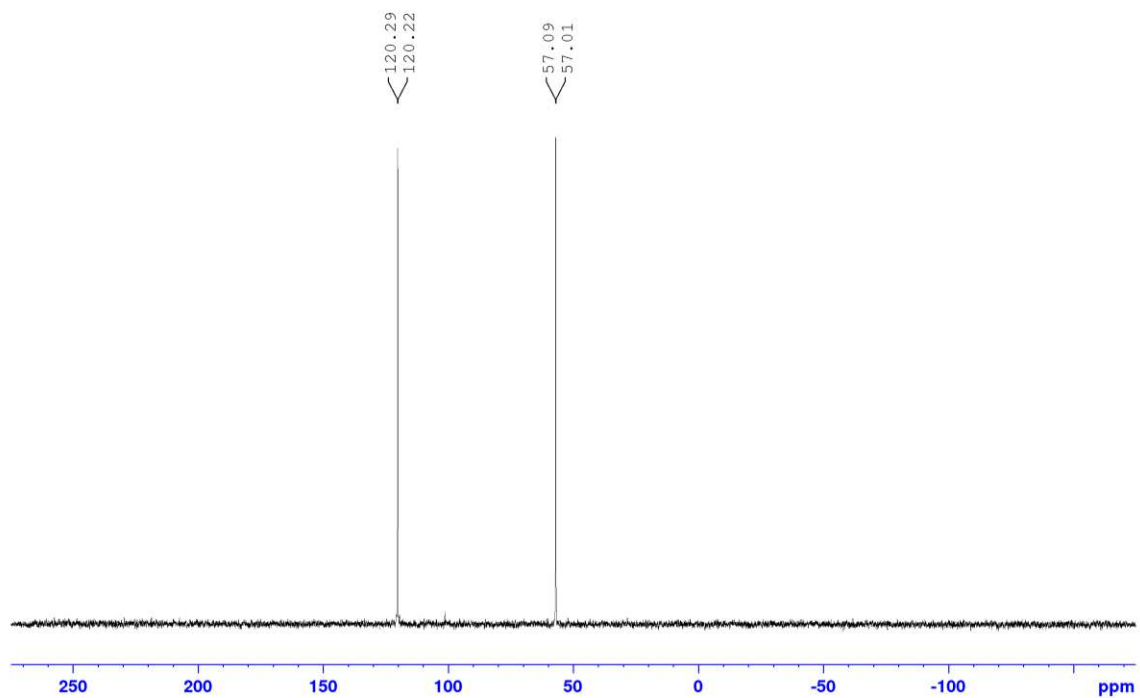
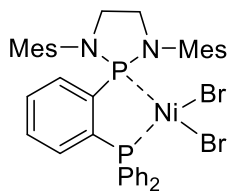


Figure A26. $^{31}\text{P}\{^1\text{H}\}$ NMR spectrum of **C1** (THF, 202.4 MHz)



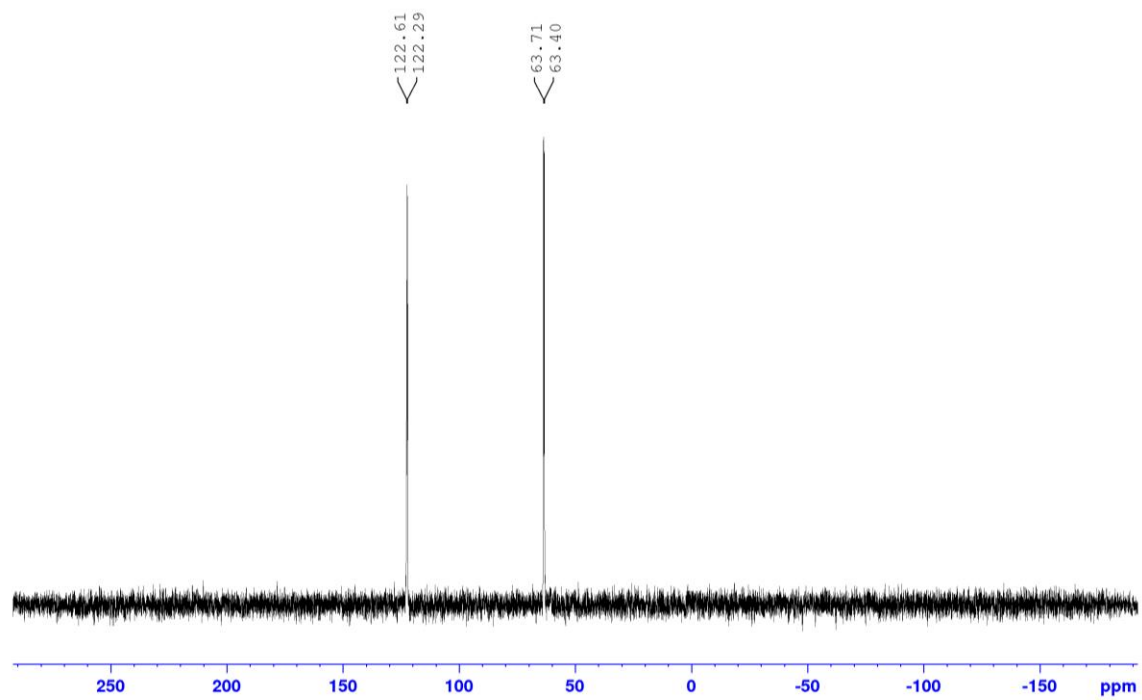


Figure A27. $^{31}\text{P}\{^1\text{H}\}$ NMR spectrum of $(\text{L}2)\text{NiBr}_2$ (1,1,2,2-Tetrachloroethane- d_2 , 202.4 MHz)

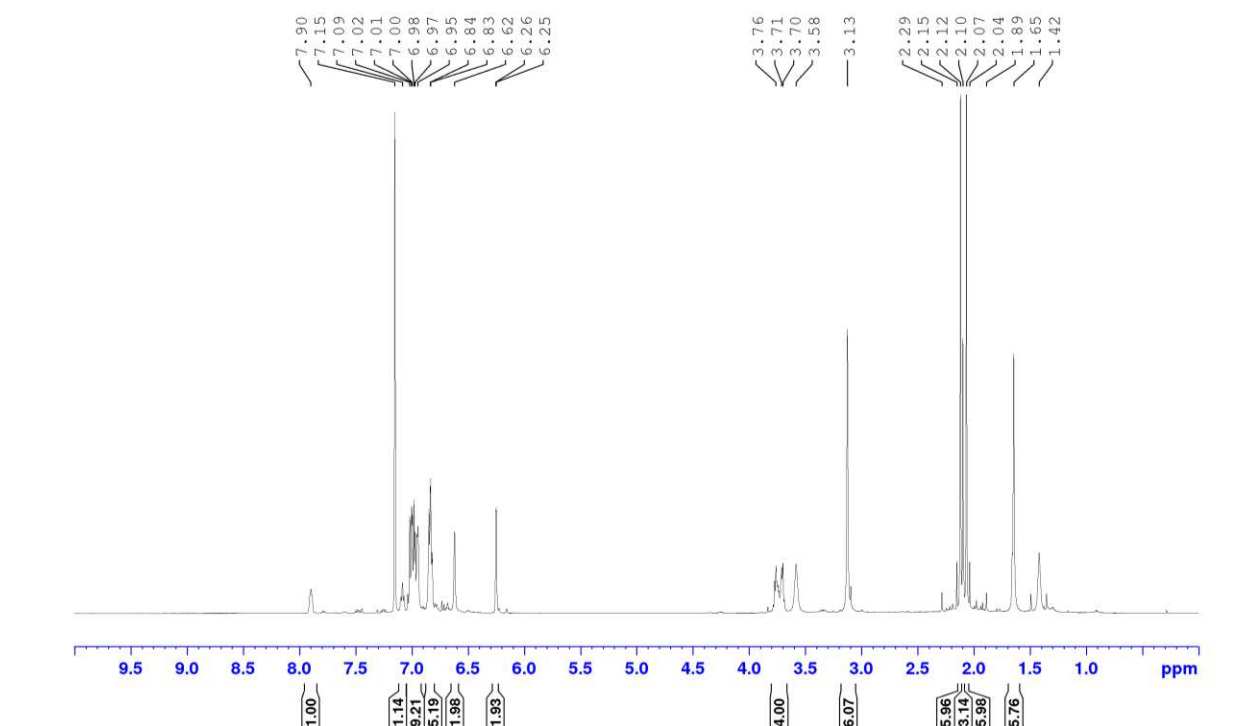
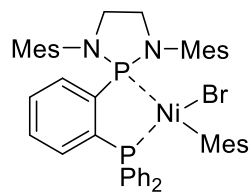


Figure A28. ¹H NMR spectrum of C2 (C₆D₆, 500.1 MHz)

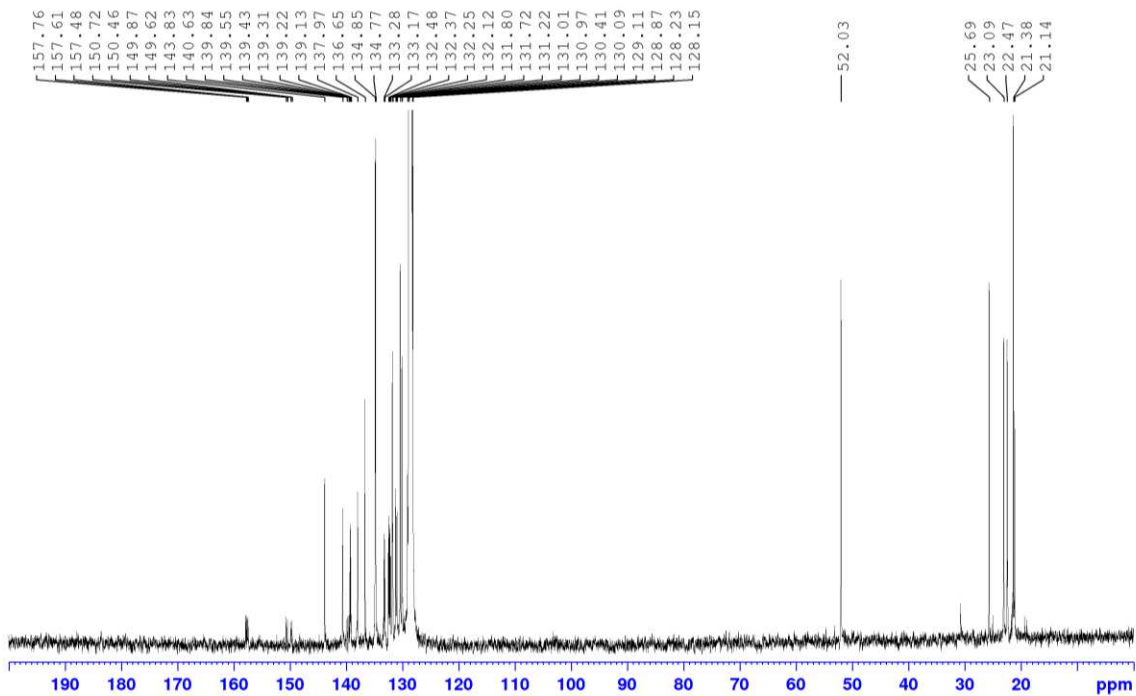


Figure A29. $^{13}\text{C}\{^1\text{H}\}$ NMR spectrum of **C2** (C_6D_6 , 125.7 MHz)

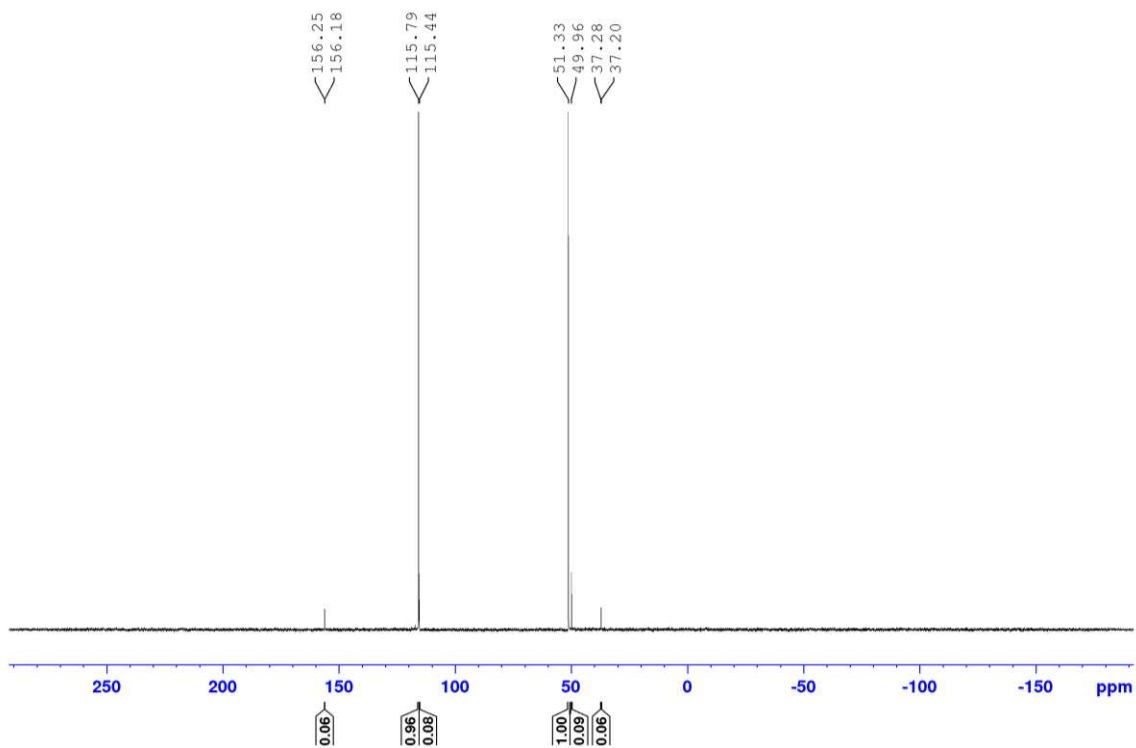


Figure A30. $^{31}\text{P}\{^1\text{H}\}$ NMR spectrum of **C2** (C_6D_6 , 202.4 MHz)

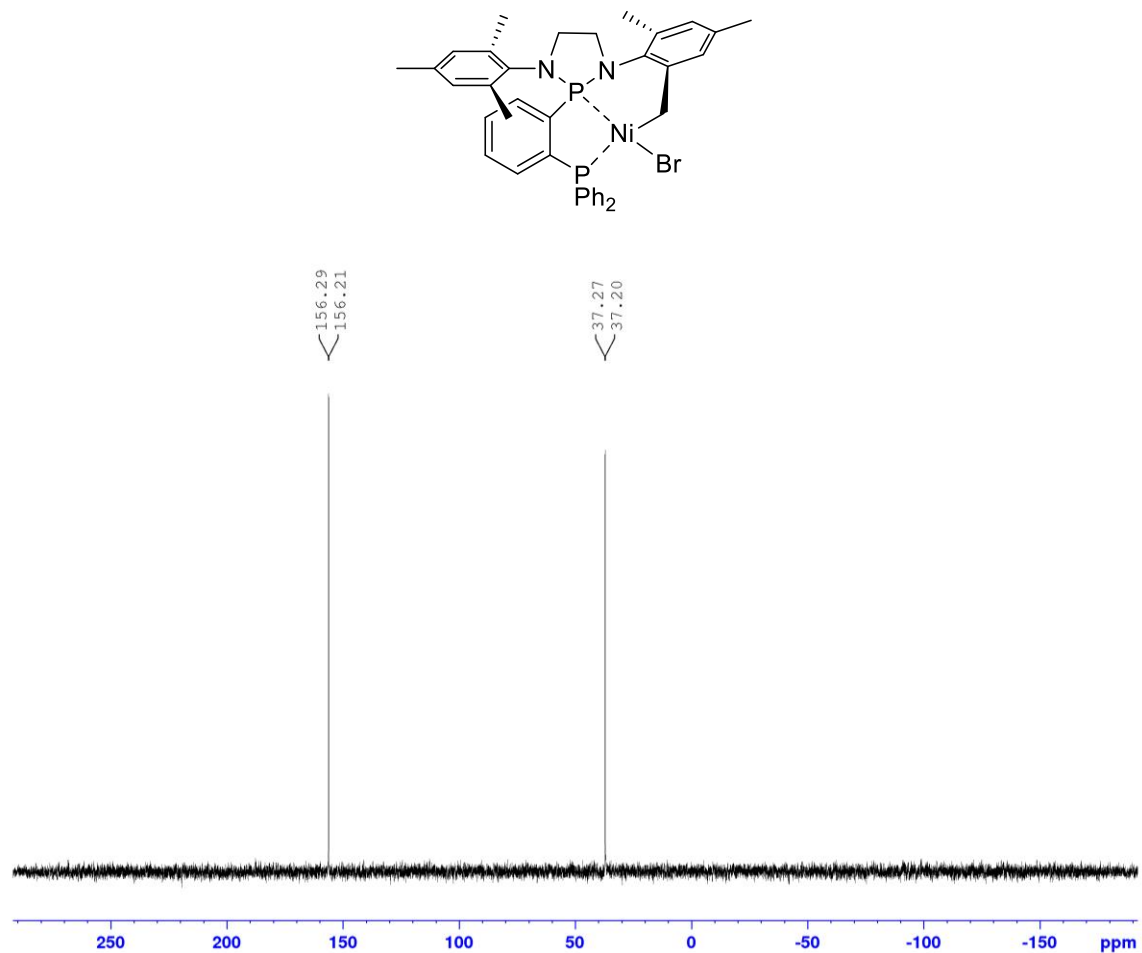


Figure A31. $^{31}\text{P}\{^1\text{H}\}$ NMR spectrum of C3 (C_6D_6 , 202.4 MHz)

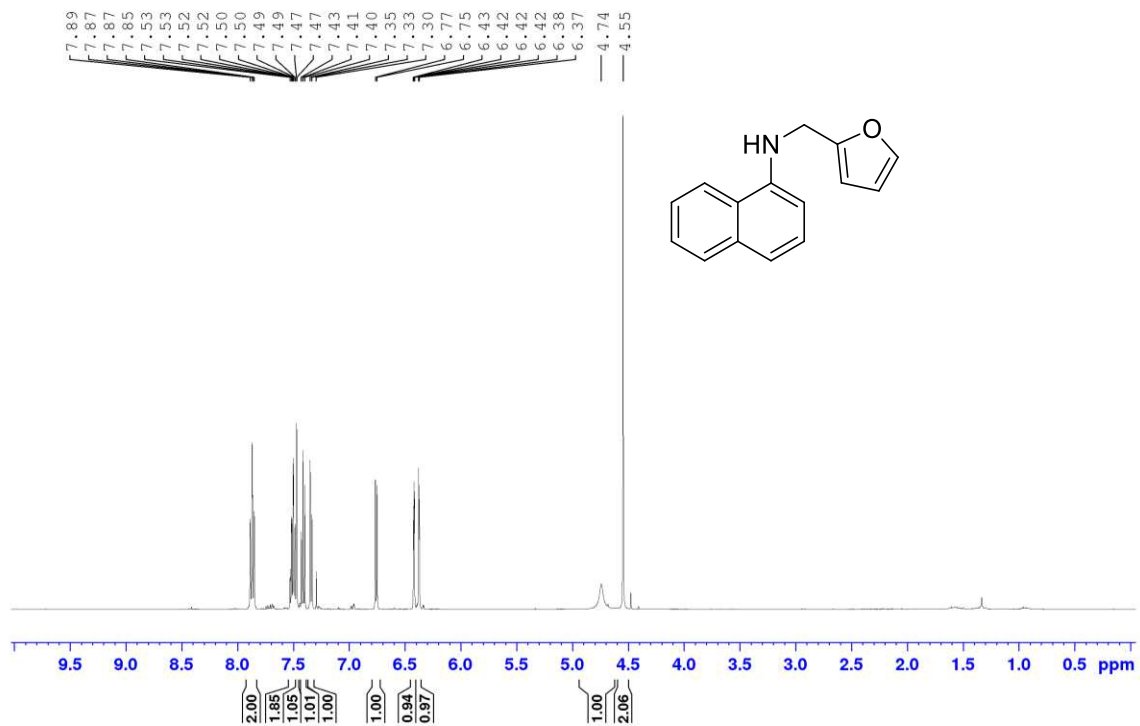


Figure A32. ¹H NMR spectrum of *N*¹-naphthalenyl-2-furanmethanamine **1a** (CDCl₃, 500.1MHz)

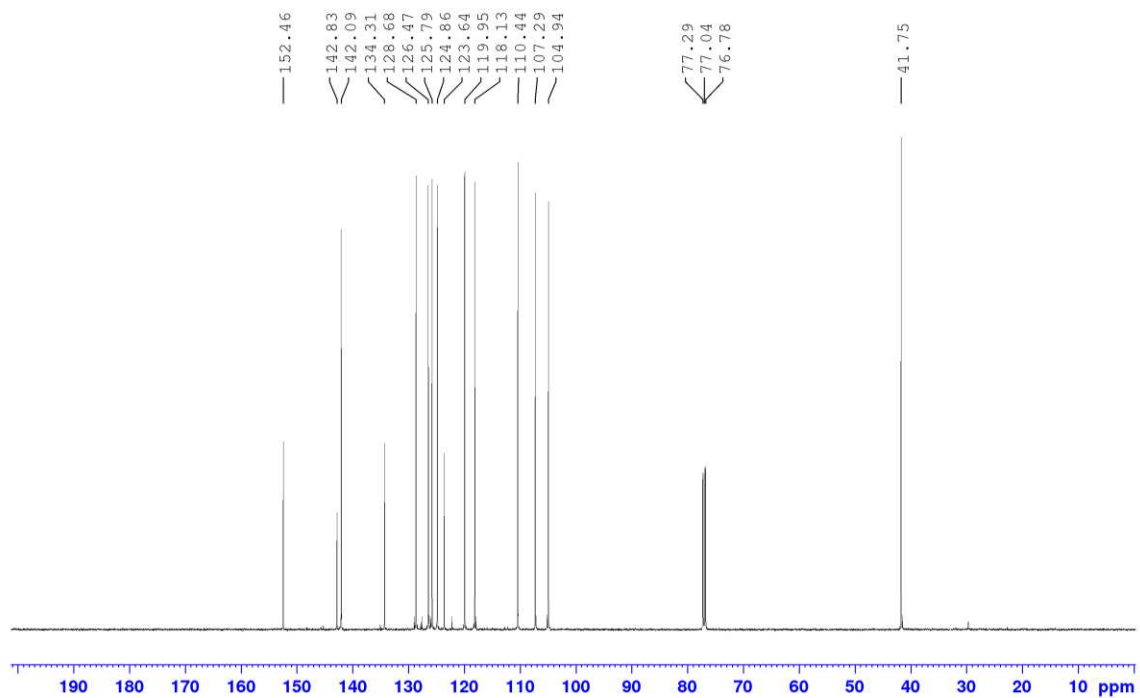


Figure A33. $^{13}\text{C}\{^1\text{H}\}$ NMR spectrum of *N*¹-naphthalenyl-2-furanmethanamine **1a** (CDCl_3 , 125.7 MHz)

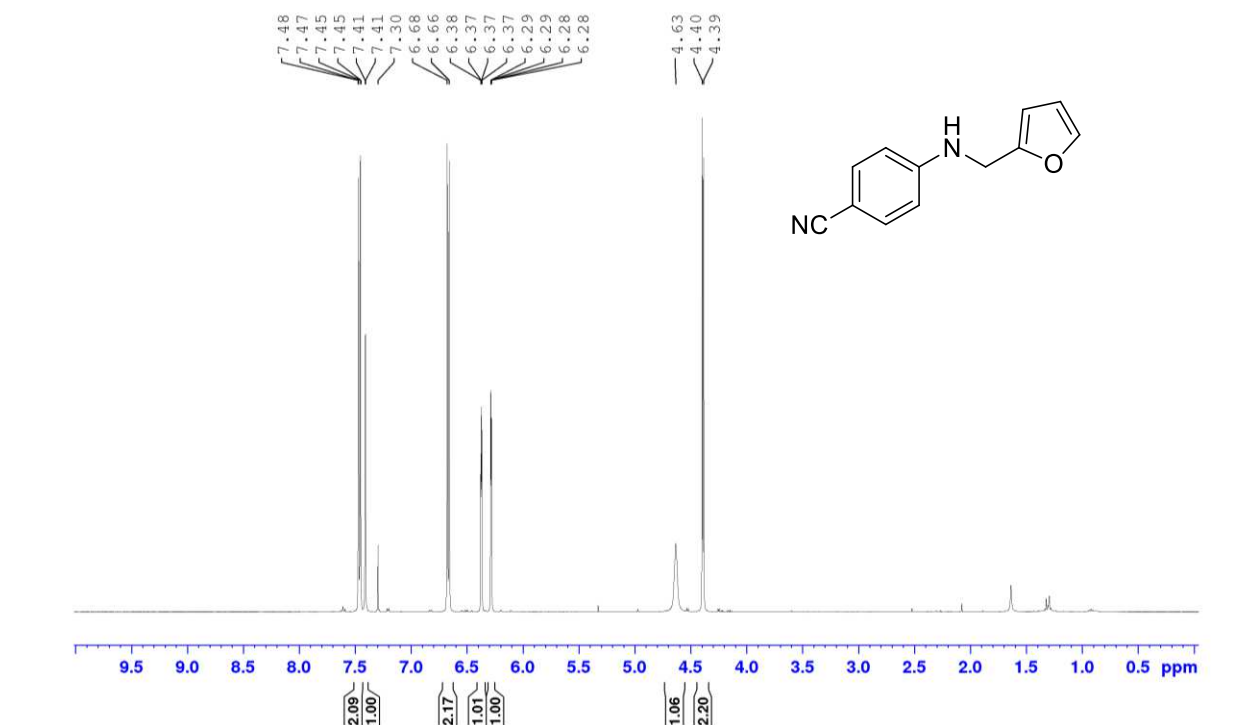


Figure A34. ¹H NMR spectrum of 4-[(2-furanylmethyl)amino]-benzonitrile **1b** (CDCl₃, 500.1 MHz)

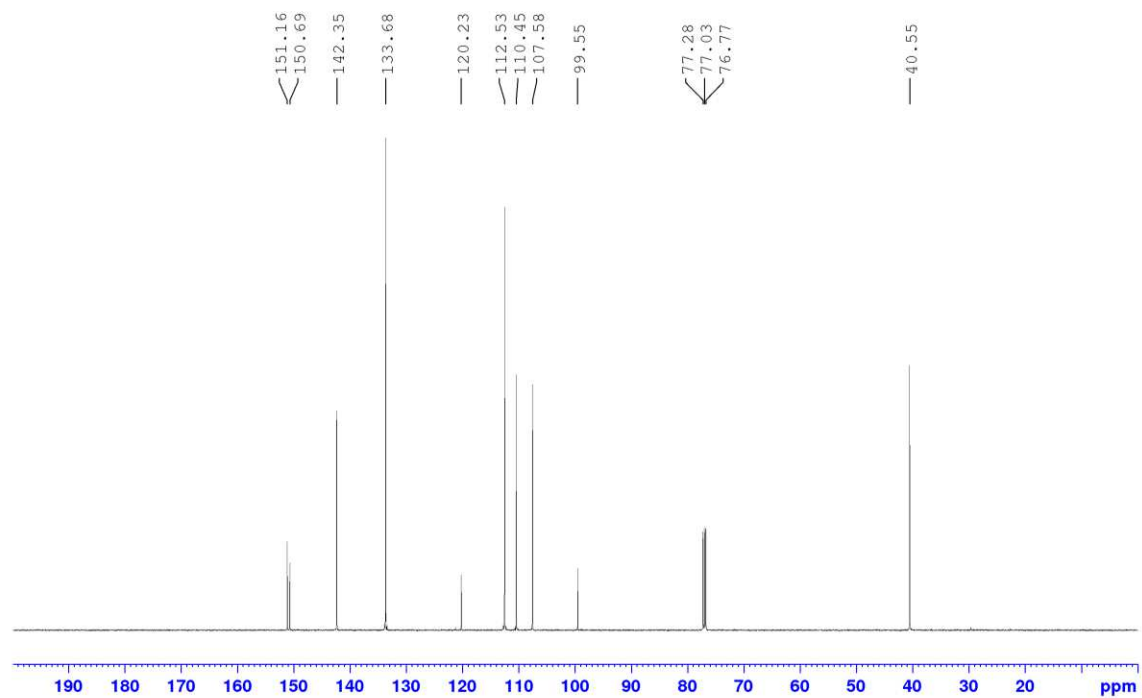


Figure A35. $^{13}\text{C}\{^1\text{H}\}$ NMR spectrum of 4-[(2-furanylmethyl)amino]-benzonitrile **1b** (CDCl_3 , 125.7 MHz)

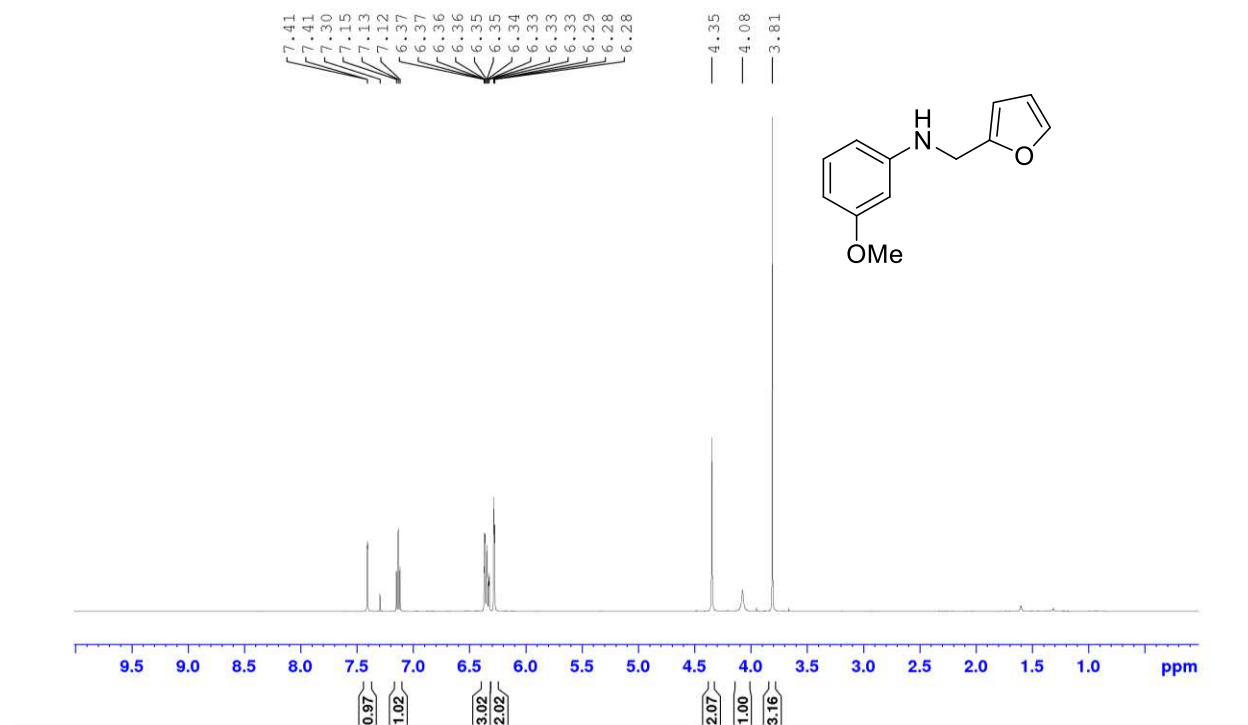


Figure A36. ¹H NMR spectrum of *N*-(3-methoxyphenyl)-2-furanmethanamine **1c** (CDCl₃, 500.1 MHz)

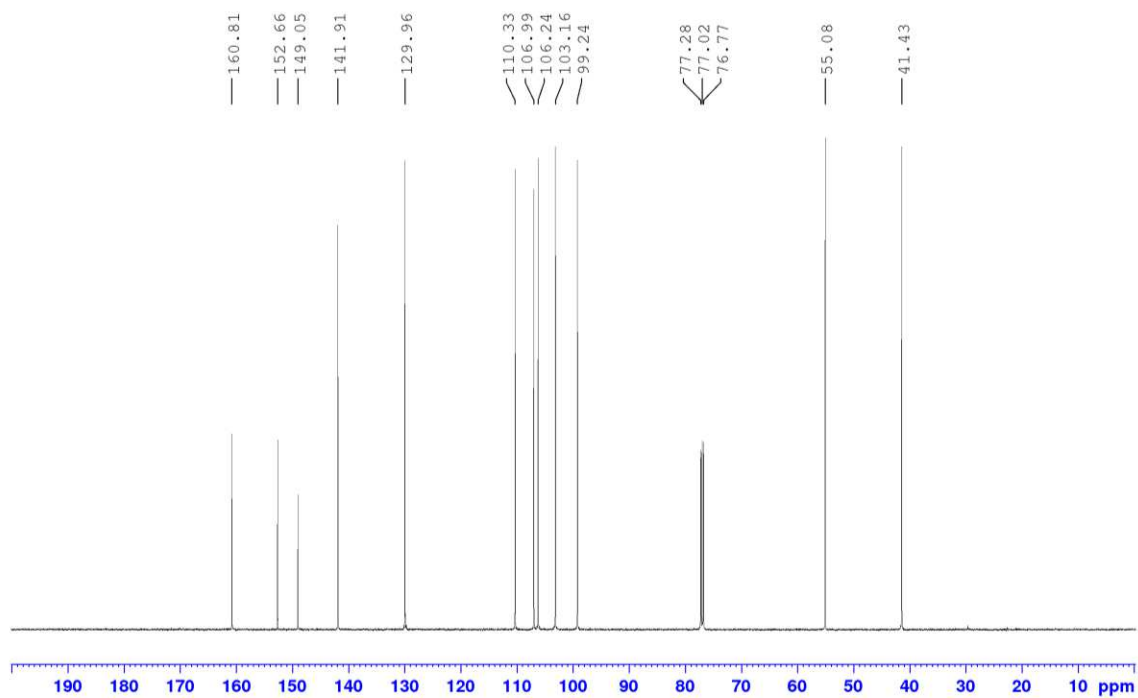


Figure A37. $^{13}\text{C}\{^1\text{H}\}$ NMR spectrum of N-(3-methoxyphenyl)-2-furanmethanamine **1c** (CDCl_3 , 125.7 MHz)

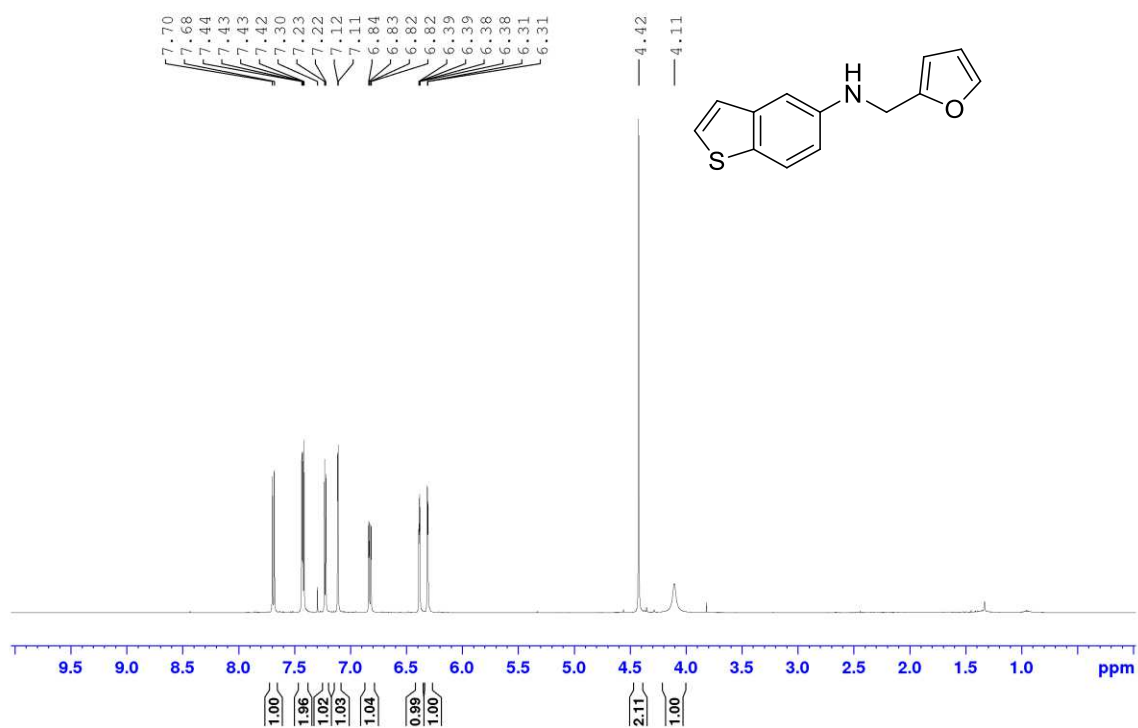


Figure A38. ^1H NMR spectrum of *N*-(2-furanylmethyl)-benzo[*b*]thiophen-5-amine **1d** (CDCl_3 , 500.1 MHz)

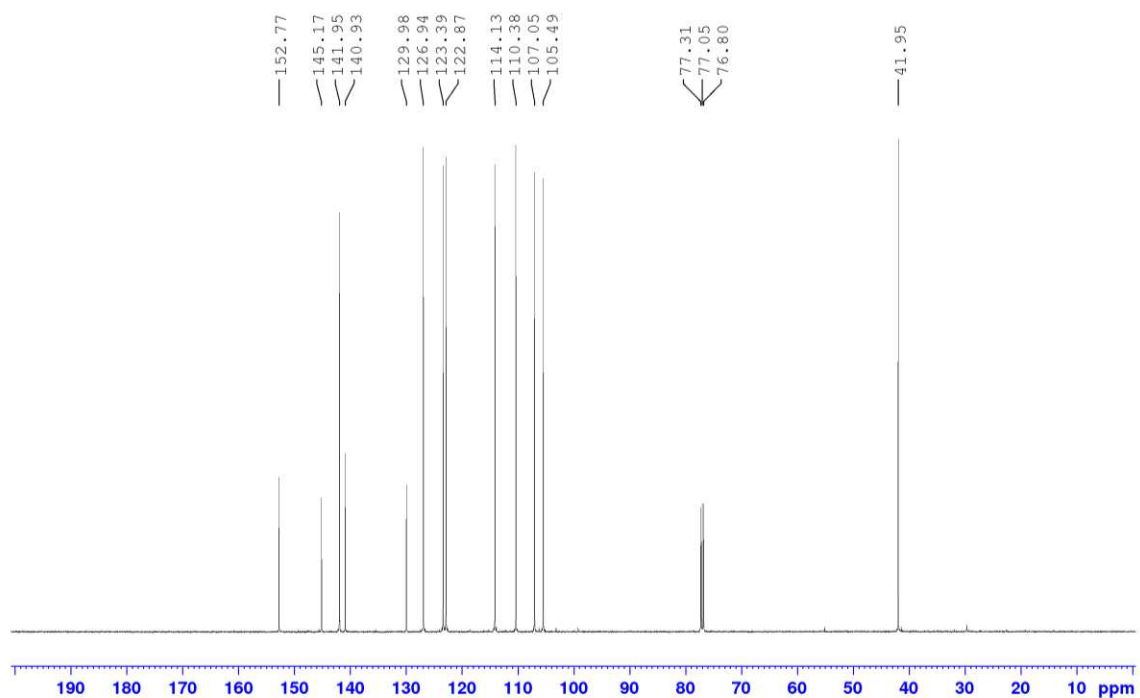


Figure A39. $^{13}\text{C}\{^1\text{H}\}$ NMR spectrum of *N*-(2-furanylmethyl)-benzo[*b*]thiophen-5-amine **1d** (CDCl_3 , 125.7 MHz)

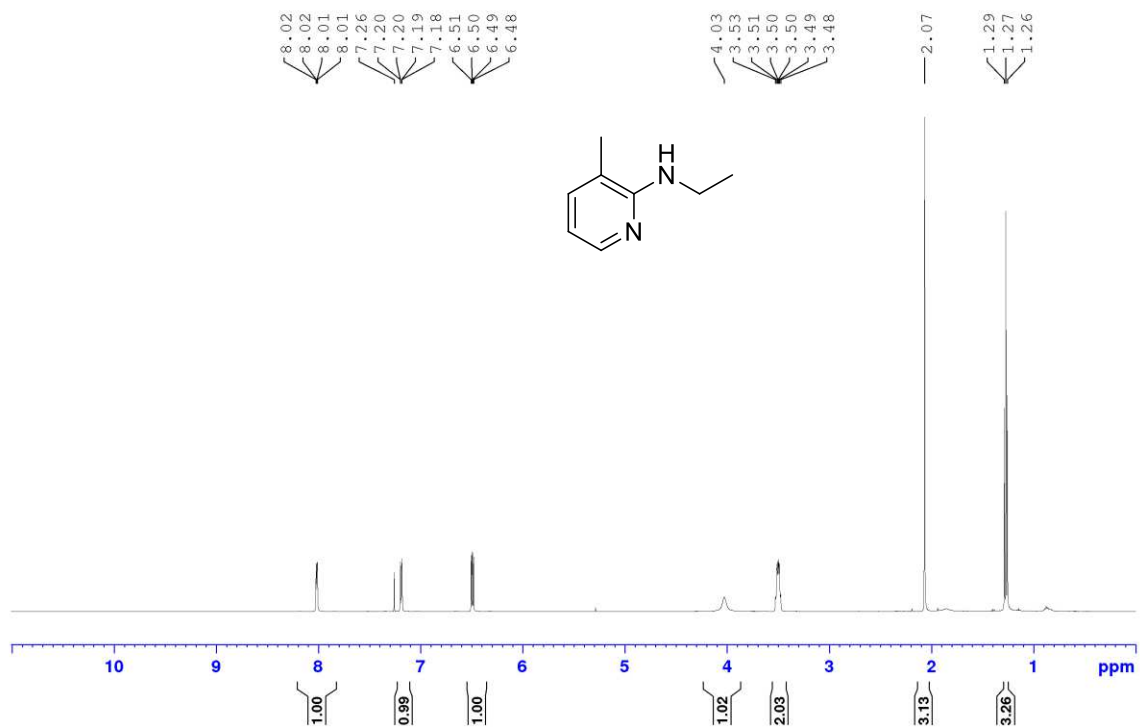


Figure A40. ^1H NMR spectrum of *N*-ethyl-3-methyl-2-pyridinamine **1e** (CDCl_3 , 500.1 MHz)

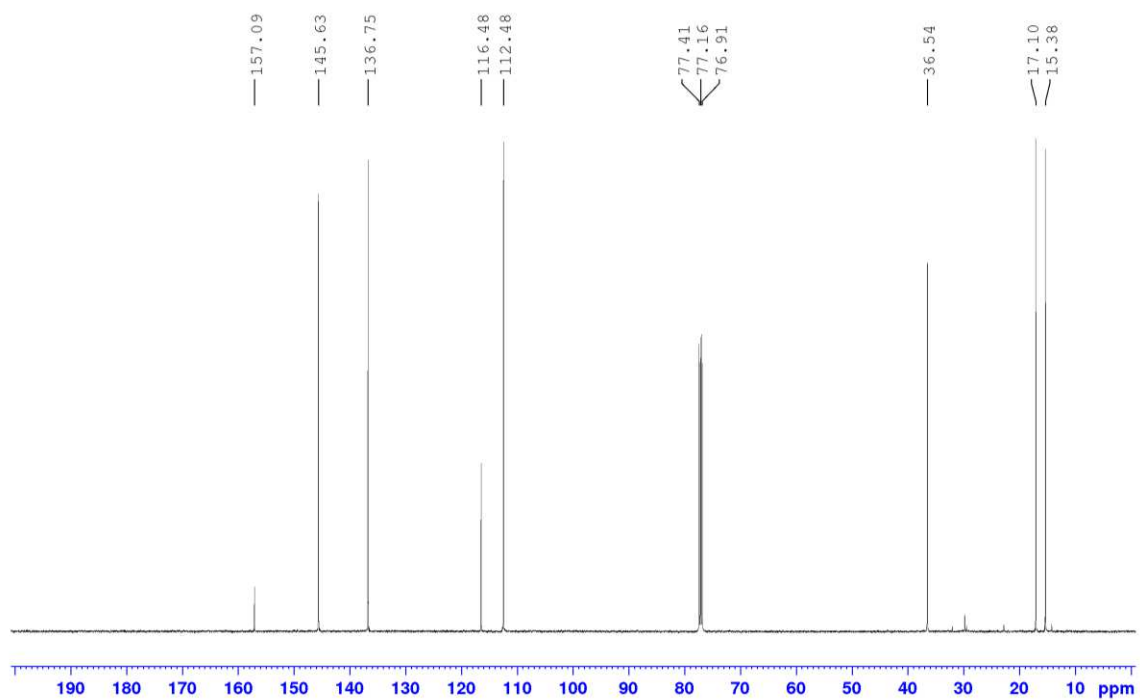


Figure A41. $^{13}\text{C}\{^1\text{H}\}$ NMR spectrum of *N*-ethyl-3-methyl-2-pyridinamine **1e** (CDCl_3 , 125.7 MHz)

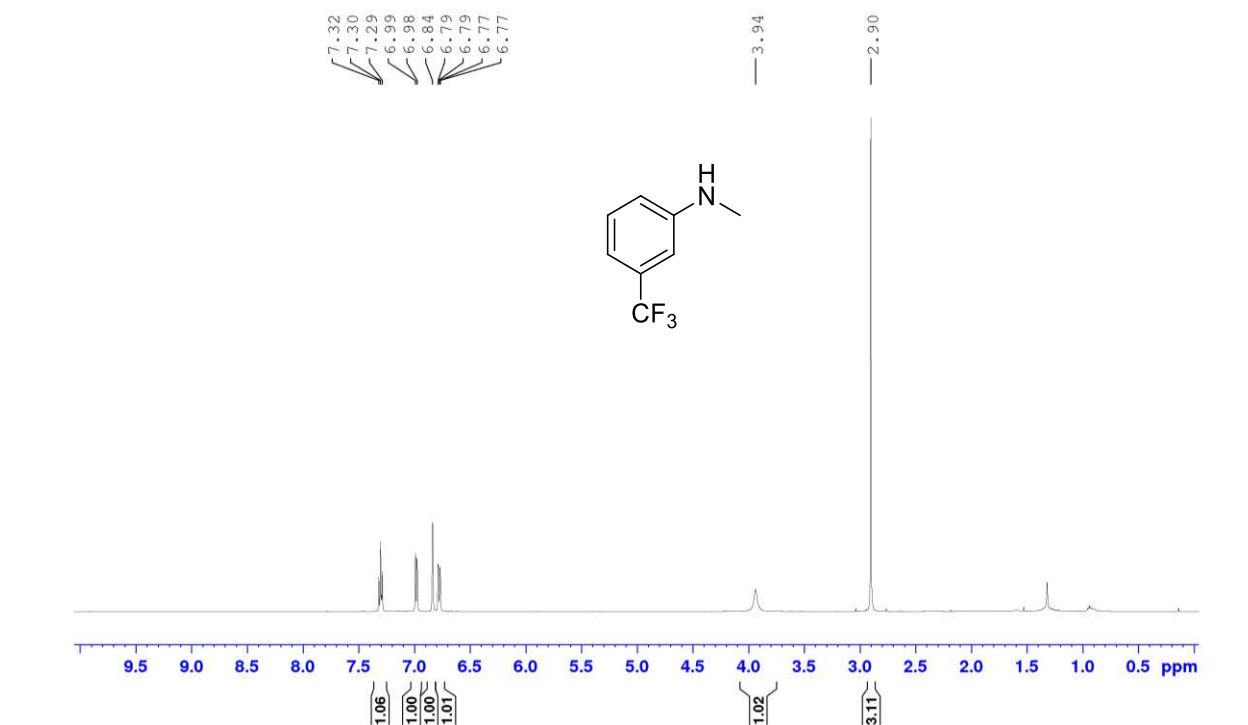


Figure A42. ^1H NMR spectrum of *N*-methyl-3-(trifluoromethyl)-benzenamine **1f** (CDCl_3 , 500.1 MHz)

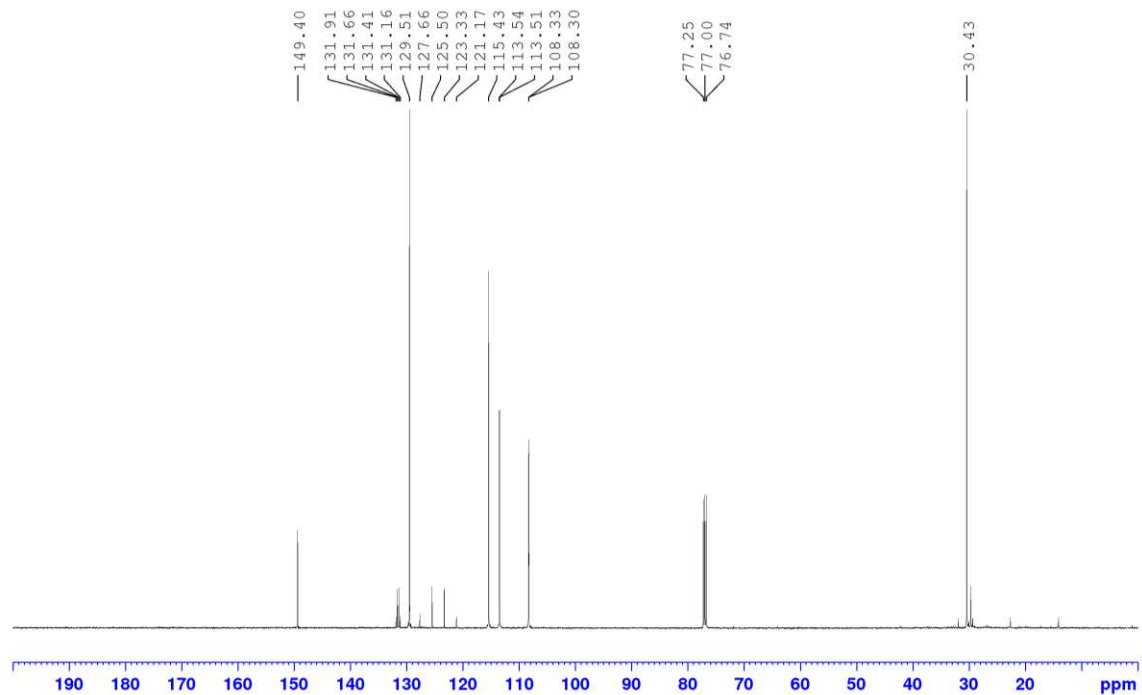


Figure A43. $^{13}\text{C}\{^1\text{H}\}$ NMR spectrum of *N*-methyl-3-(trifluoromethyl)-benzenamine **1f** (CDCl_3 , 125.7 MHz)

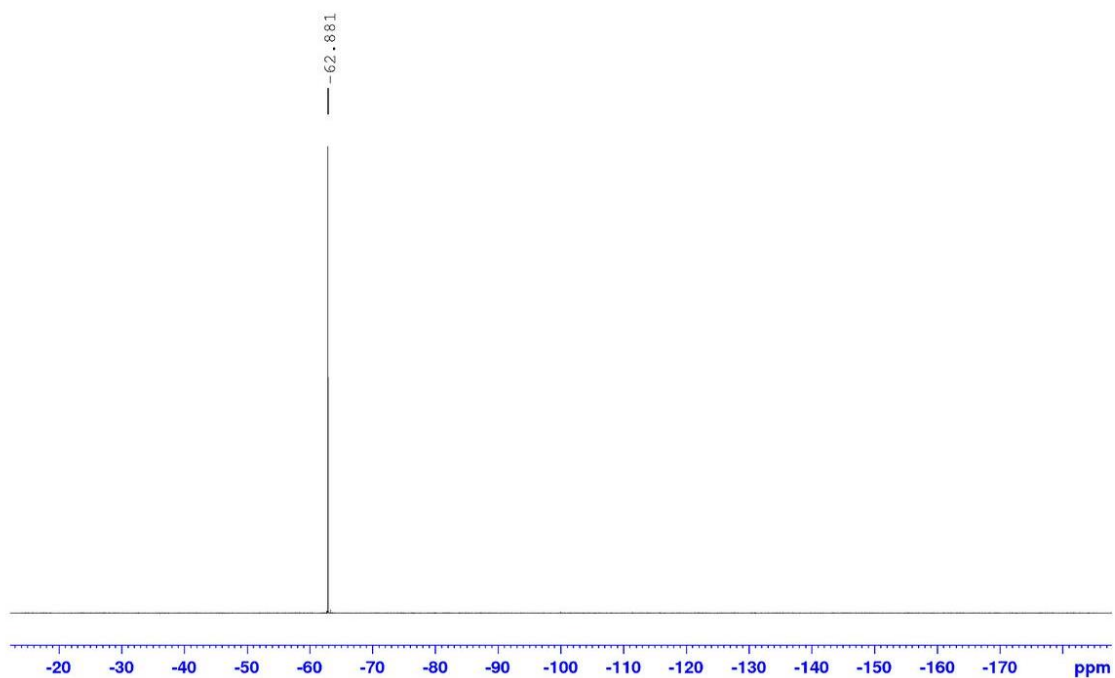


Figure A44. $^{19}\text{F}\{^1\text{H}\}$ NMR of *N*-methyl-3-(trifluoromethyl)-benzenamine **1f** (CDCl_3 , 470.4 MHz)

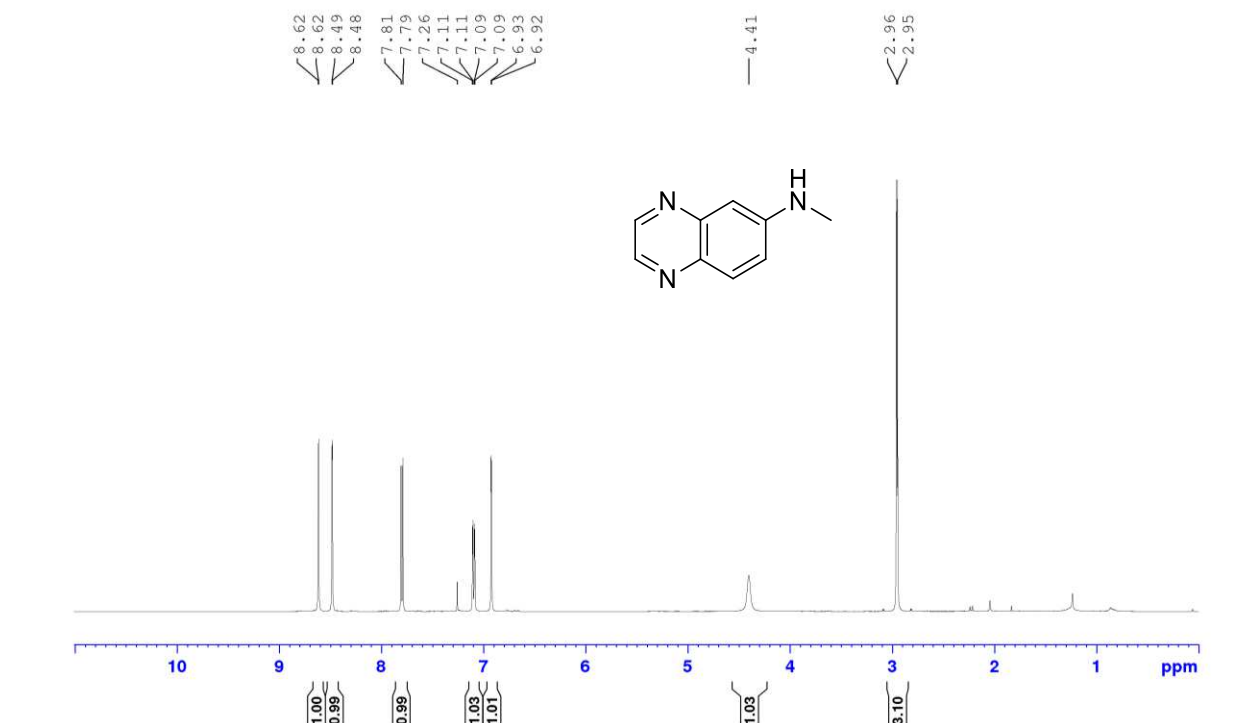


Figure A45. ¹H NMR spectrum of *N*-methyl-6-quinoxalinamine **1g** (CDCl₃, 500.1 MHz)

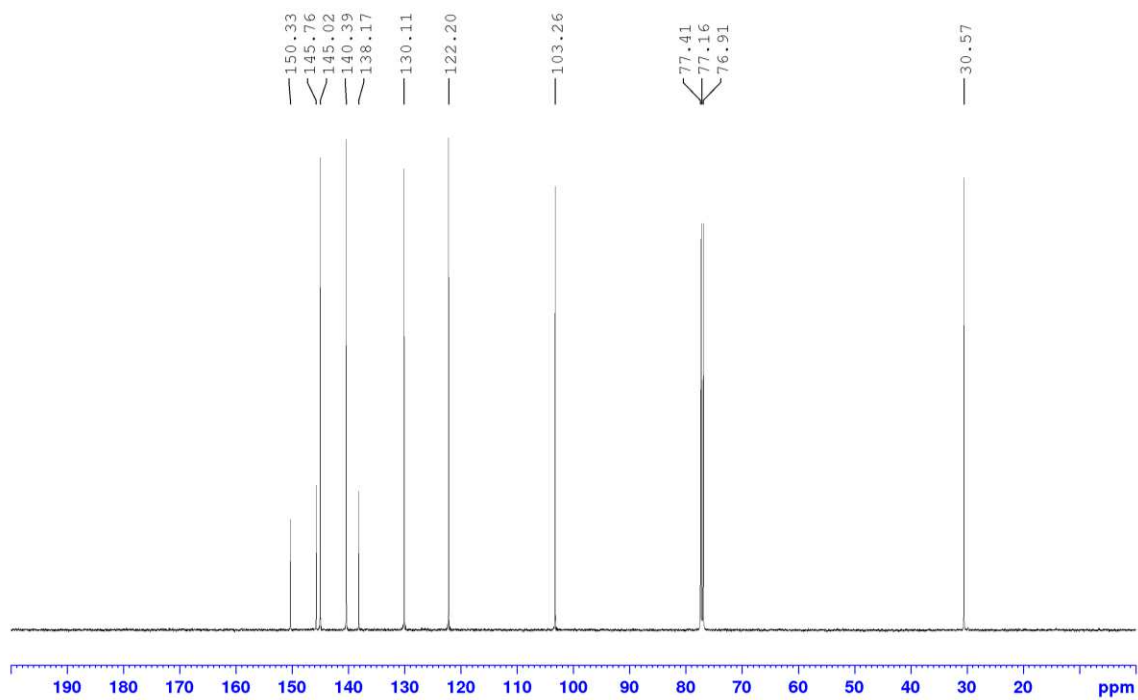


Figure A46. ¹³C{¹H} NMR spectrum of *N*-methyl-6-quinoxalinamine **1g** (CDCl₃, 125.7 MHz)

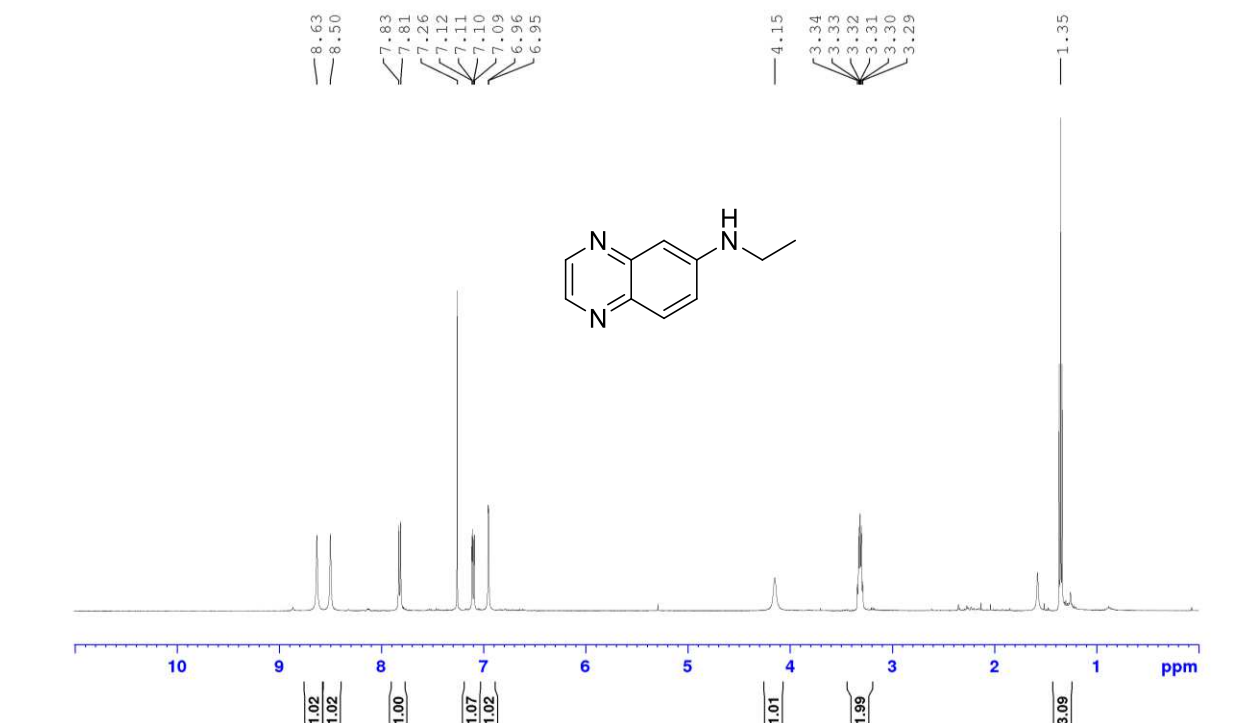


Figure A47. ^1H NMR spectrum of *N*-ethyl-6-quinoxalinamine **1h** (CDCl_3 , 500.1 MHz)

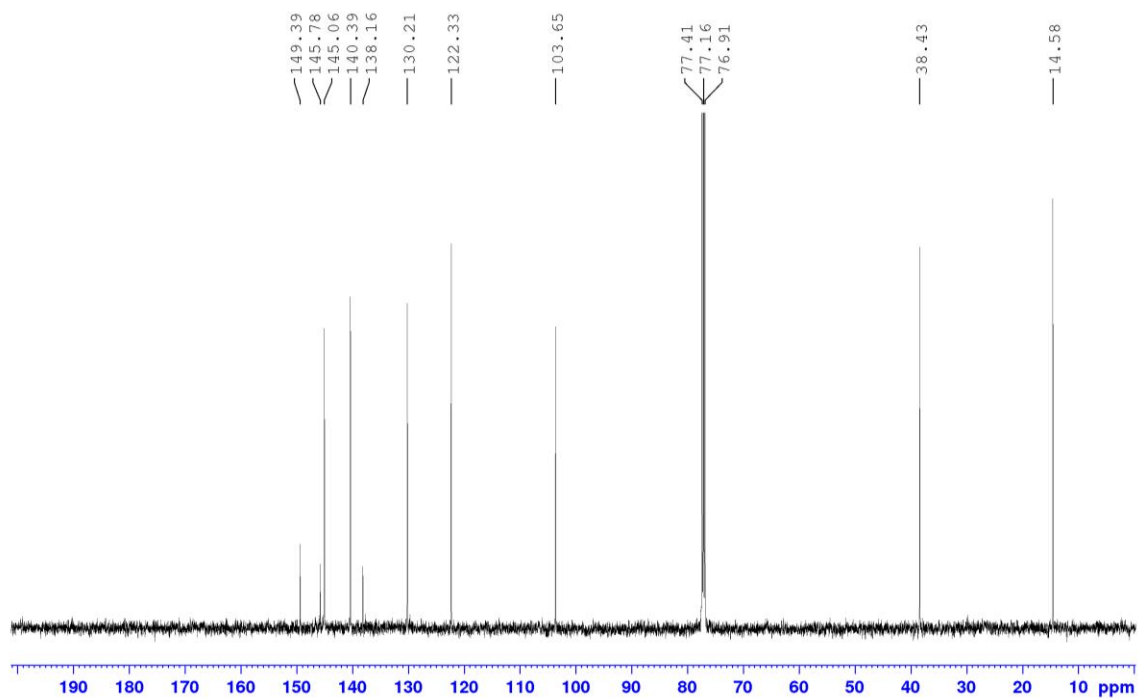


Figure A48. $^{13}\text{C}\{^1\text{H}\}$ NMR spectrum of *N*-ethyl-6-quinoxalinamine **1h** (CDCl_3 , 125.7 MHz)

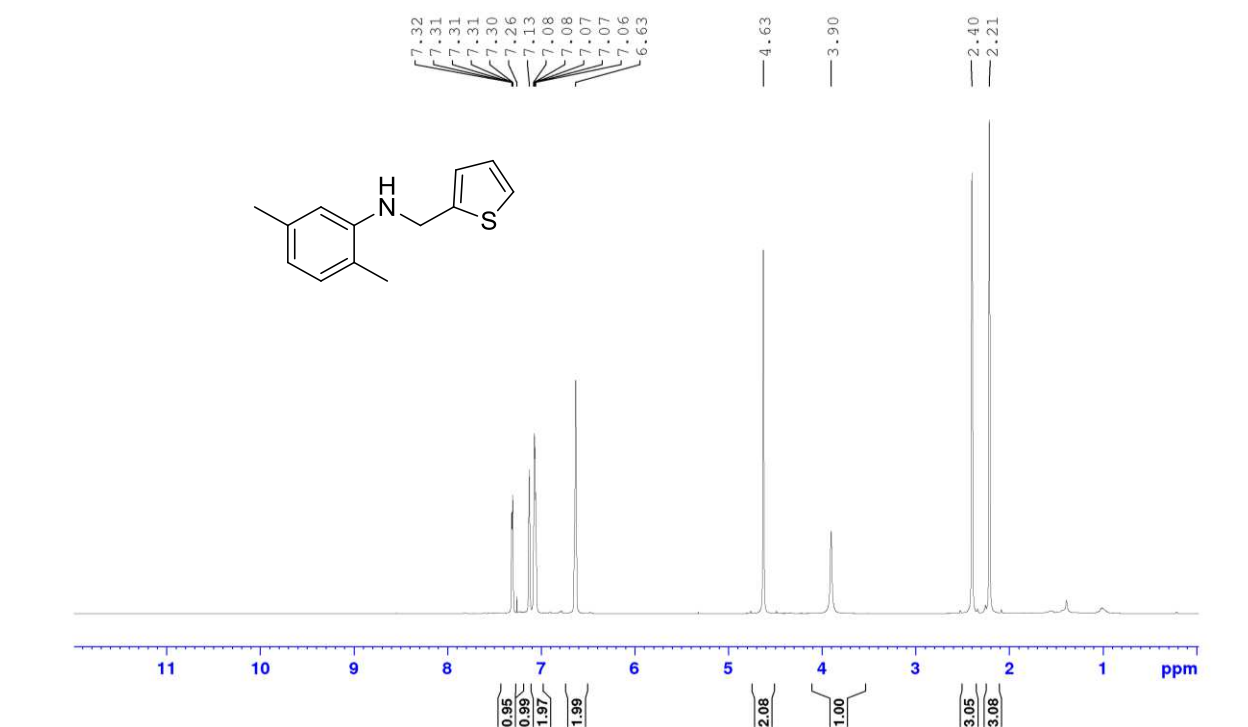


Figure A49. ¹H NMR spectrum of *N*-(2,5-dimethylphenyl)-2-thiophenemethanamine **1i** (CDCl₃, 500.1 MHz)

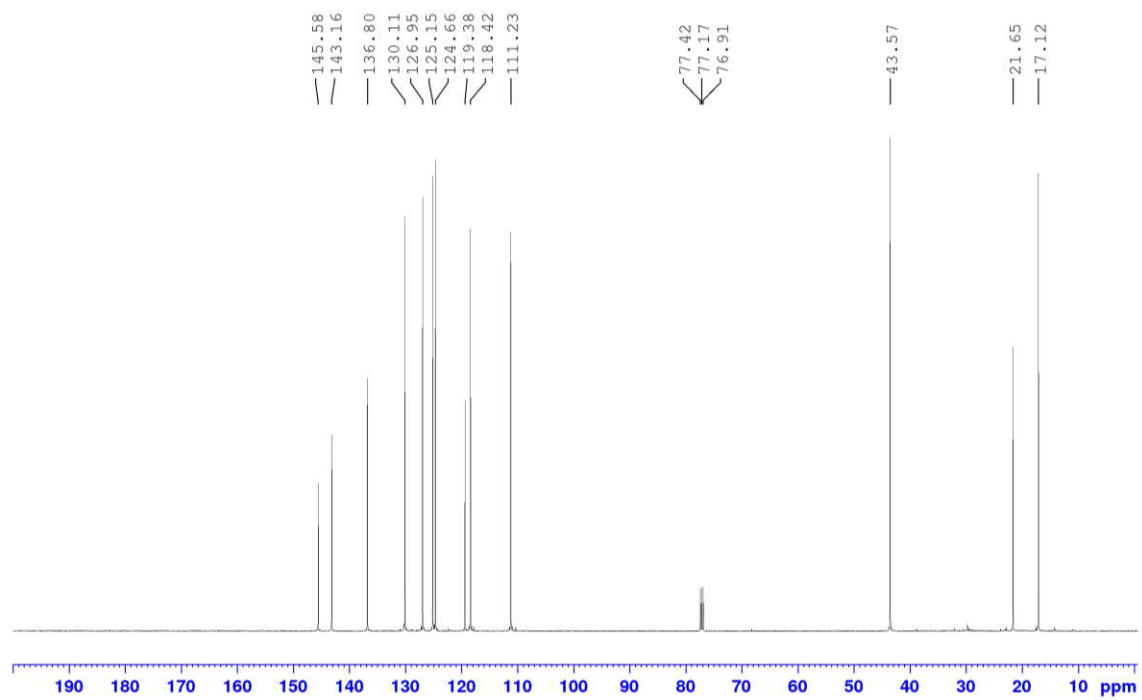


Figure A50. $^{13}\text{C}\{^1\text{H}\}$ NMR spectrum of *N*-(2,5-dimethylphenyl)-2-thiophenemethanamine **1i** (CDCl_3 , 125.7 MHz)

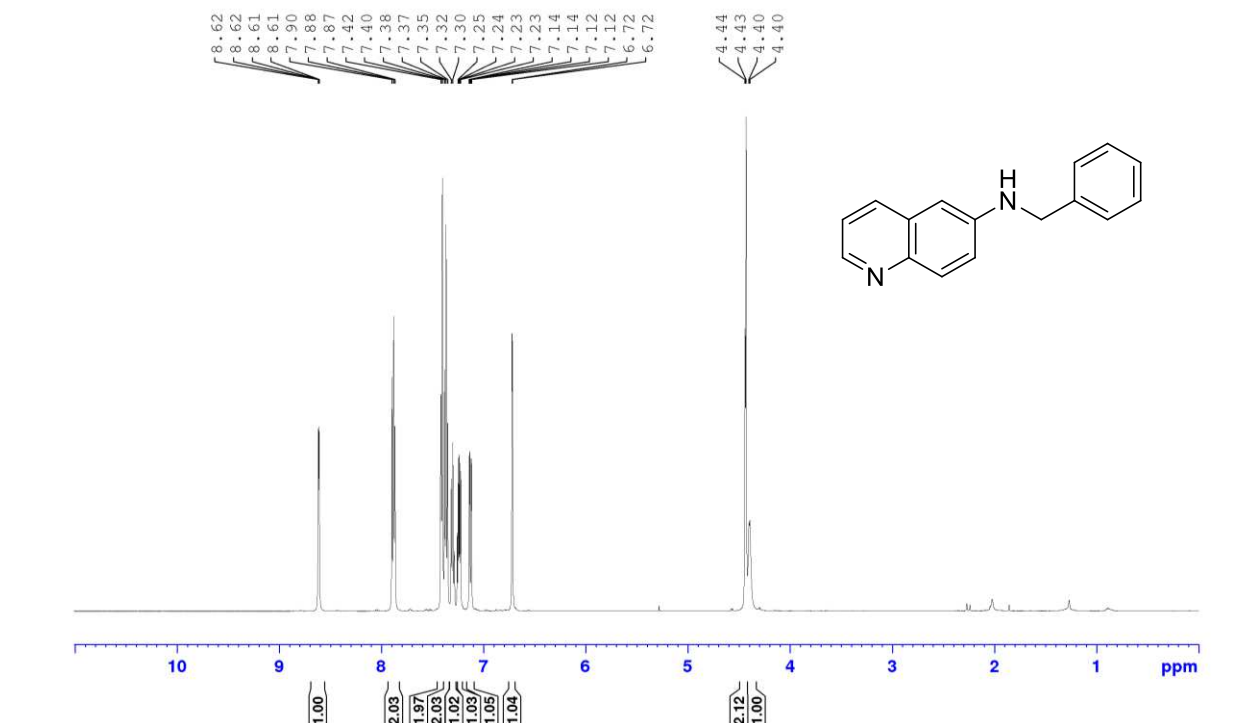


Figure A51. ^1H NMR spectrum of *N*-(phenylmethyl)-6-quinolinamine **1j** (CDCl_3 , 500.1 MHz)

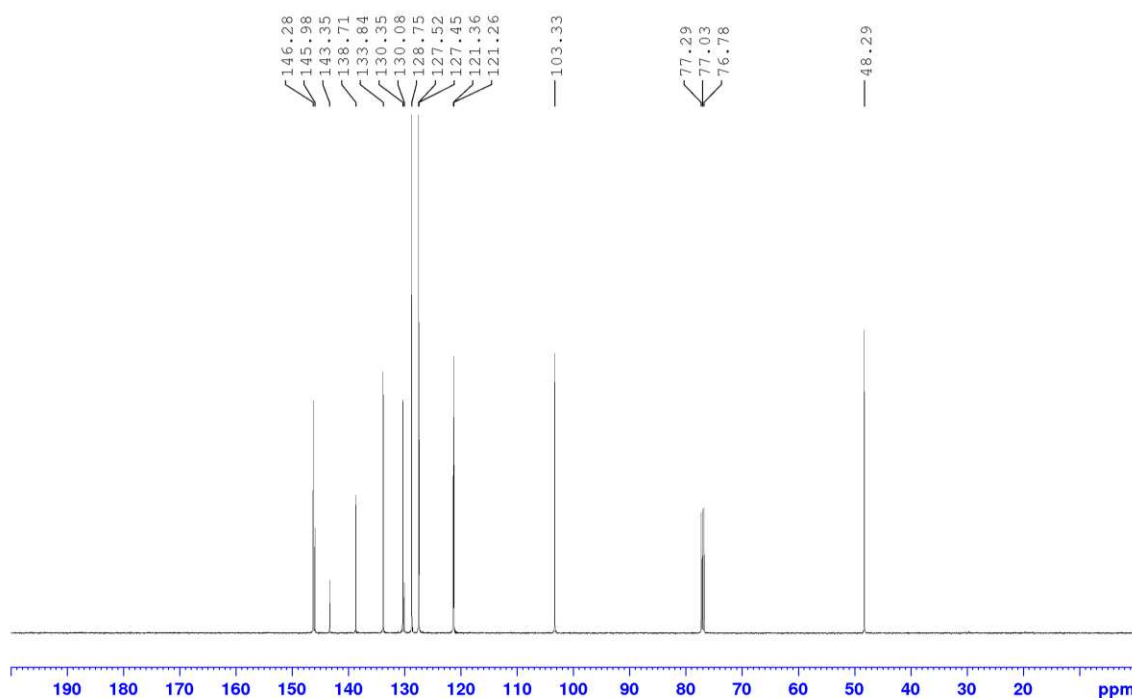


Figure A52. $^{13}\text{C}\{^1\text{H}\}$ NMR spectrum of *N*-(phenylmethyl)-6-quinolinamine **1j** (CDCl_3 , 125.7 MHz)

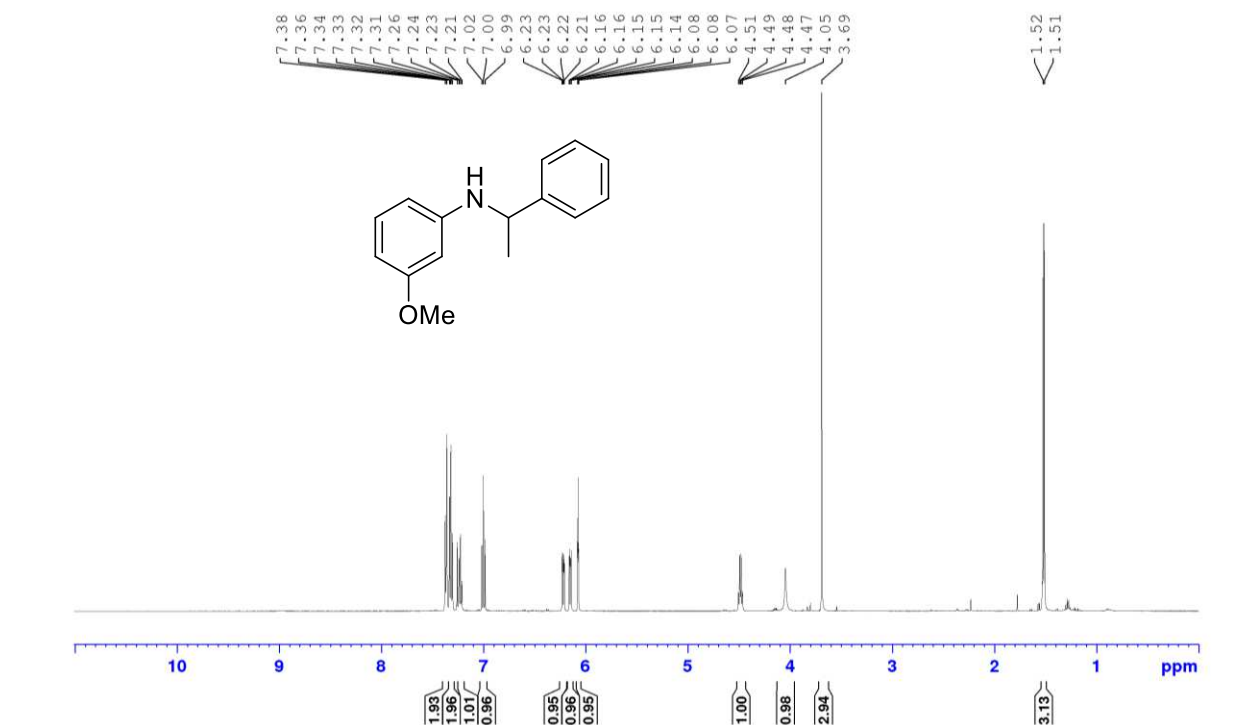


Figure A53. ¹H NMR spectrum of *N*-(3-methoxyphenyl)- α -methyl-benzenemethanamine **1k** (CDCl₃, 500.1 MHz)

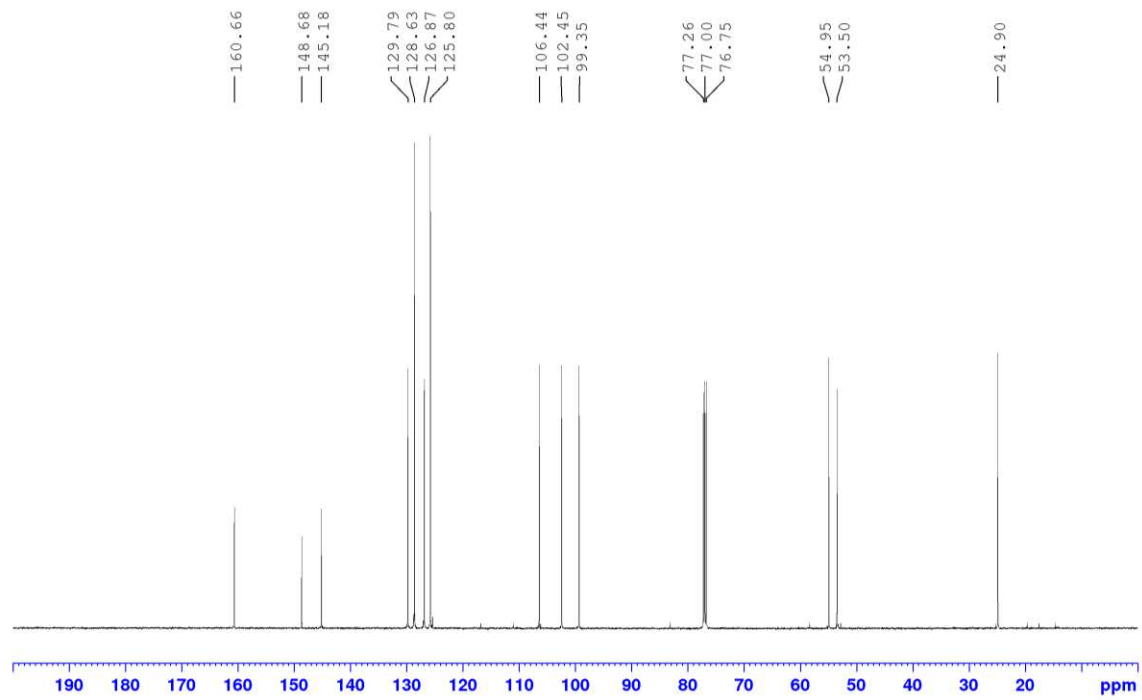


Figure A54. $^{13}\text{C}\{^1\text{H}\}$ NMR spectrum of *N*-(3-methoxyphenyl)- α -methyl-benzenemethanamine **1k** (CDCl_3 , 125.7 MHz)

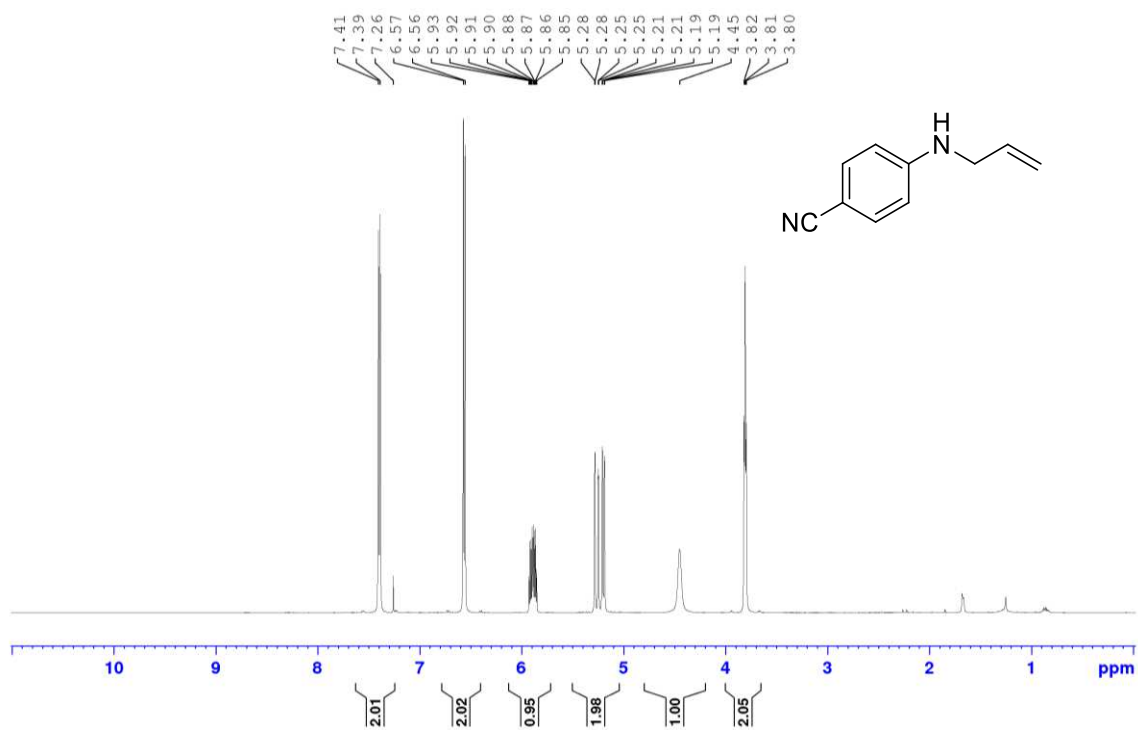


Figure A55. ^1H NMR spectrum of 4-(2-propen-1-ylamino)-benzonitrile **11** (CDCl_3 , 500.1 MHz)

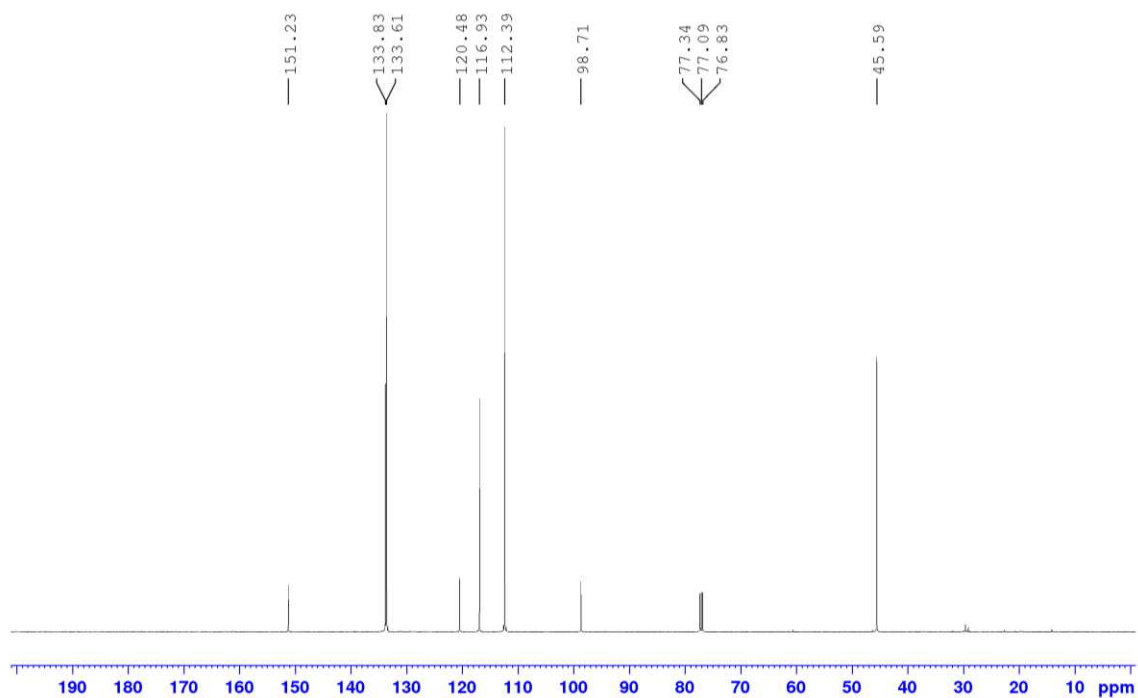


Figure A56. $^{13}\text{C}\{^1\text{H}\}$ NMR spectrum of 4-(2-propen-1-ylamino)-benzonitrile **11** (CDCl_3 , 125.7 MHz)

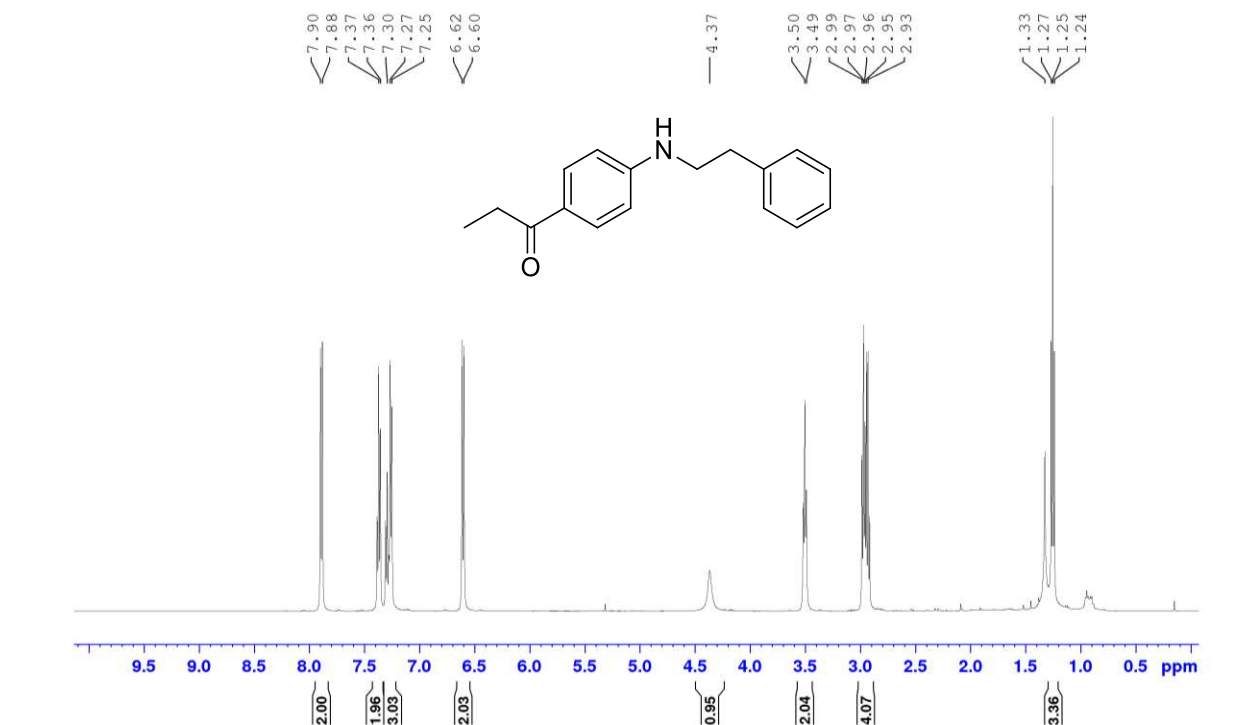


Figure A57. ¹H NMR spectrum of 1-[4-[(2-Phenylethyl)amino]phenyl]-1-propanone **1m** (CDCl₃, 500.1 MHz)

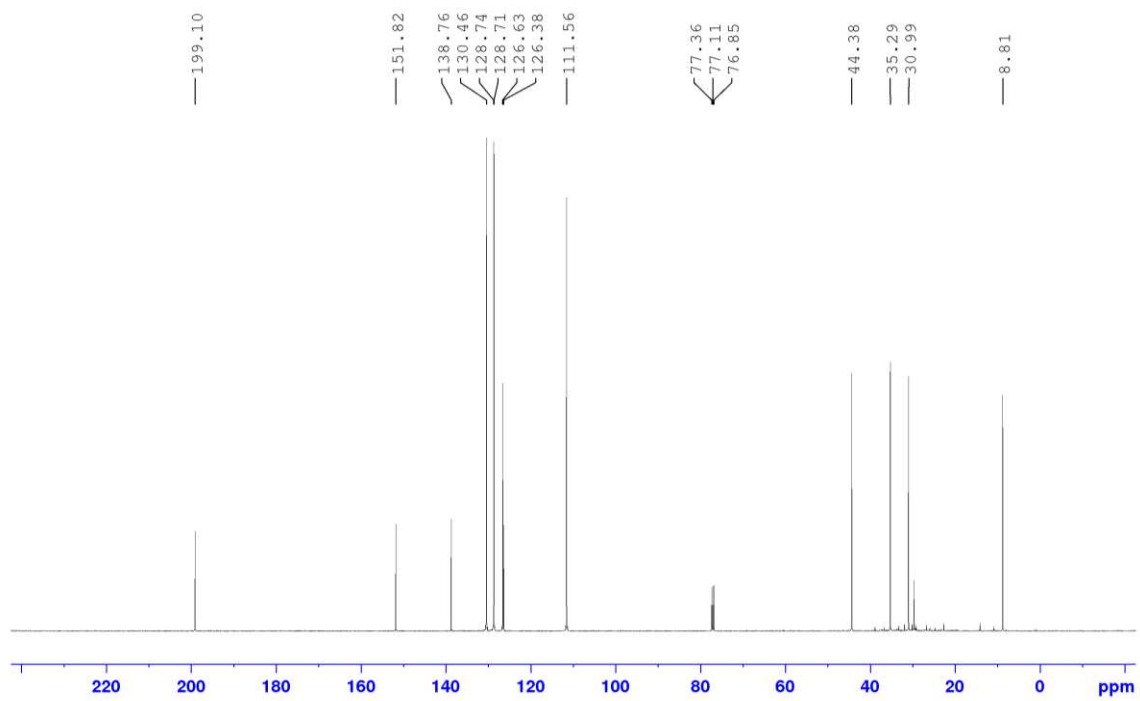
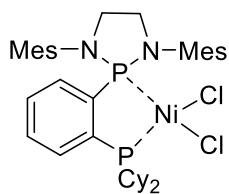


Figure A58. $^{13}\text{C}\{^1\text{H}\}$ NMR spectrum of 1-[4-[(2-Phenylethyl)amino]phenyl]-1-propanone **1m** (CDCl_3 , 125.7 MHz)



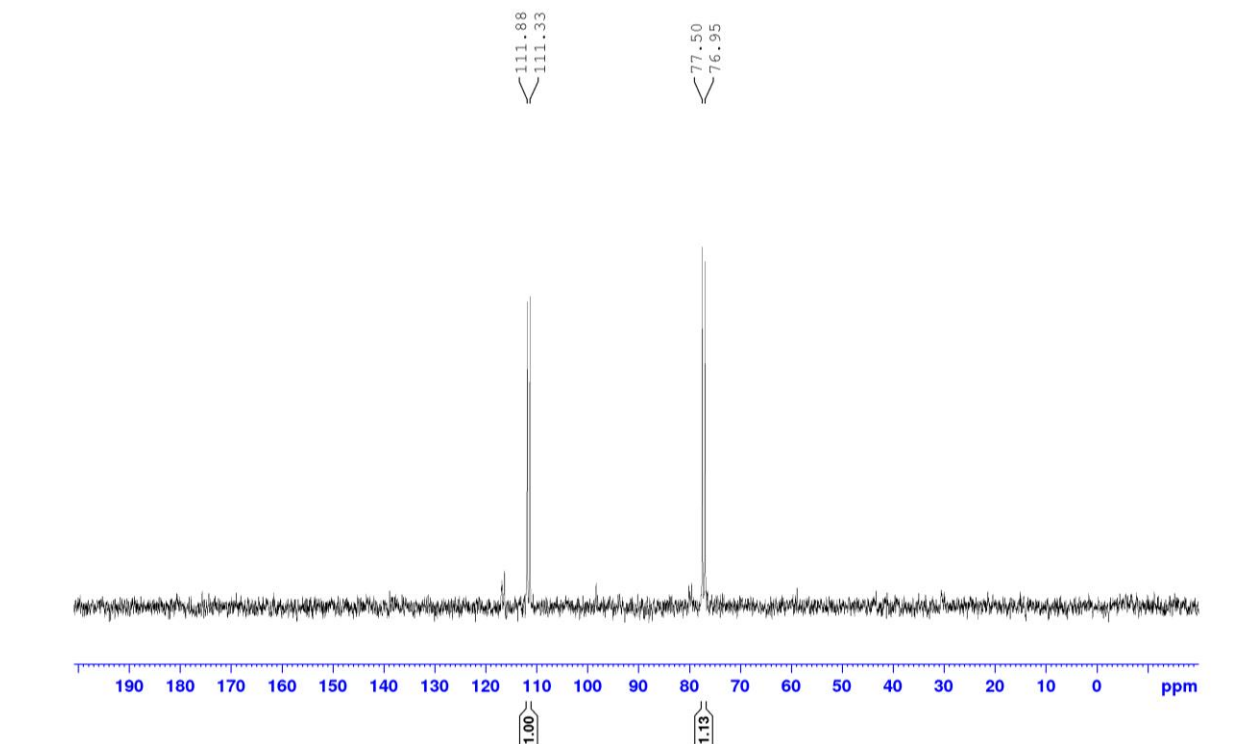
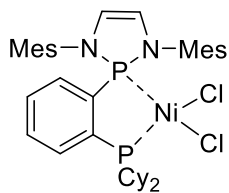


Figure A59. $^{31}\text{P}\{^1\text{H}\}$ NMR spectrum of **L1NiCl₂** (CDCl_3 , 121.4 MHz)



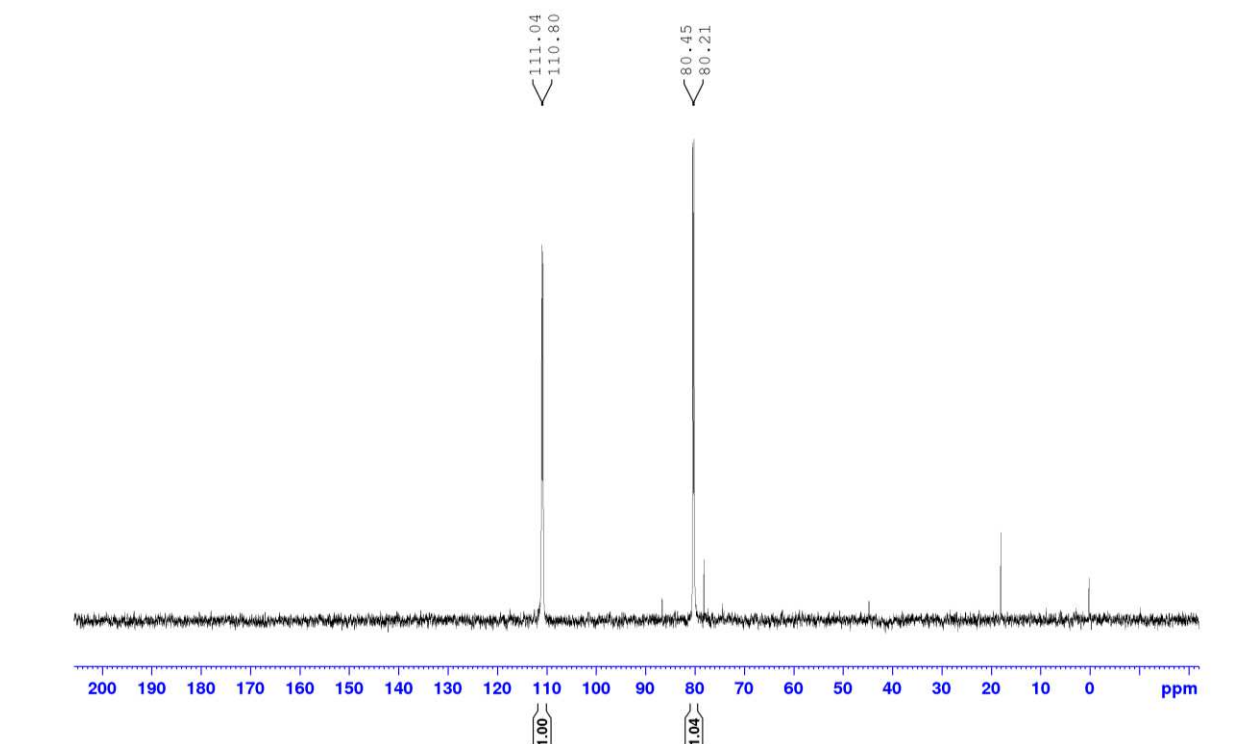
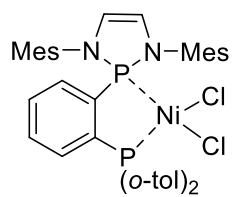


Figure A60. $^{31}\text{P}\{^1\text{H}\}$ NMR spectrum of **L4NiCl₂** (CDCl₃, 202.4 MHz)



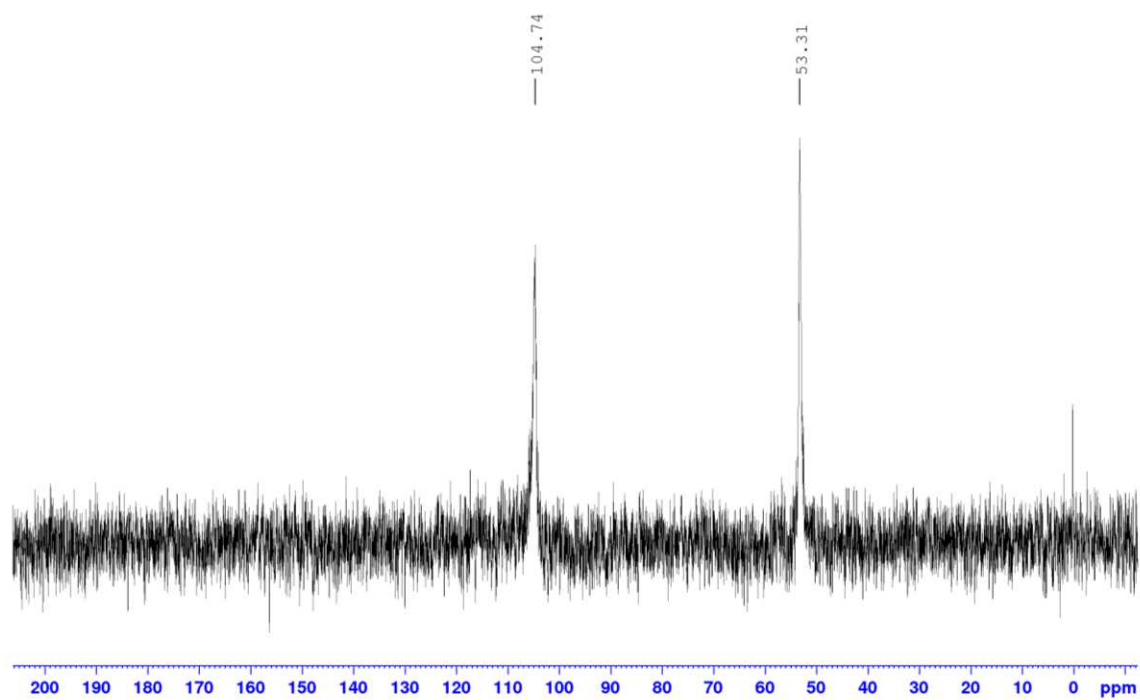


Figure A61. $^{31}\text{P}\{^1\text{H}\}$ NMR spectrum of L6NiCl_2 (CDCl_3 , 202.4 MHz)

Appendix B

Copyright Permission

11/05/2018

Rightslink® by Copyright Clearance Center



RightsLink®

Home

Create Account

Help



ACS Publications
Most Trusted. Most Cited. Most Read.

Title: Application of Diazaphospholidine/Diazaphospholene-Based Bisphosphines in Room-Temperature Nickel-Catalyzed C(sp²)-N Cross-Couplings of Primary Alkylamines with (Hetero)aryl Chlorides and Bromides

Author: Alexandre V. Gatién, Christopher M. Lavoie, Raymond N. Bennett, et al

Publication: ACS Catalysis

Publisher: American Chemical Society

Date: May 1, 2018

Copyright © 2018, American Chemical Society

LOGIN

If you're a [copyright.com](#) user, you can login to RightsLink using your [copyright.com](#) credentials.

Already a RightsLink user or want to [learn more?](#)

PERMISSION/LICENSE IS GRANTED FOR YOUR ORDER AT NO CHARGE

This type of permission/license, instead of the standard Terms & Conditions, is sent to you because no fee is being charged for your order. Please note the following:

- Permission is granted for your request in both print and electronic formats, and translations.
- If figures and/or tables were requested, they may be adapted or used in part.
- Please print this page for your records and send a copy of it to your publisher/graduate school.
- Appropriate credit for the requested material should be given as follows: "Reprinted (adapted) with permission from (COMPLETE REFERENCE CITATION). Copyright (YEAR) American Chemical Society." Insert appropriate information in place of the capitalized words.
- One-time permission is granted only for the use specified in your request. No additional uses are granted (such as derivative works or other editions). For any other uses, please submit a new request.

BACK

CLOSE WINDOW

Copyright © 2018 [Copyright Clearance Center, Inc.](#) All Rights Reserved. [Privacy statement](#). [Terms and Conditions](#). Comments? We would like to hear from you. E-mail us at customer@copyright.com